Keele University

Exploring the impact of hypoxia mimetic agents on multipotent stem cell biology

Muhammad A. Ahmed

Thesis submitted to Keele University for the Degree of Doctor of Philosophy

March 2018

Keele University

SUBMISSION OF THESIS FOR A RESEARCH DEGREE

Part I. DECLARATION by the candidate for a research degree. To be bound in the thesis

Degree for which thesis being submitted Doctor of Philosophy

Title of thesis Exploring the impact of hypoxia mimetic agents on multipotent stem cell biology

This thesis contains confidential information and is subject to the protocol set down for the submission and examination of such a thesis. NO

Date of submission Original registration date 09.12.2013

(Date of submission must comply with Regulation 2D)

Name of candidate Muhammad A. Ahmed

Research Institute Institute for Science and Technology in Medicine

Name of Lead Supervisor Professor Nicholas R Forsyth

I certify that:

(a) The thesis being submitted for examination is my own account of my own research
(b) My research has been conducted ethically. Where relevant a letter from the approving body confirming that ethical approval has been given has been bound in the thesis as an Annex
(c) The data and results presented are the genuine data and results actually obtained by me during the conduct of the research
(d) Where I have drawn on the work, ideas and results of others this has been appropriately acknowledged in the thesis
(e) Where any collaboration has taken place with one or more other researchers, I have included within an 'Acknowledgments' section in the thesis a clear statement of their contributions, in line with the relevant statement in the Code of Practice (see Note overleaf).
(f) The greater portion of the work described in the thesis has been undertaken subsequent to my registration for the higher degree for which I am submitting for examination
(g) Where part of the work described in the thesis has previously been incorporated in another thesis submitted by me for a higher degree (if any), this has been identified and acknowledged in the thesis
(h) The thesis submitted is within the required word limit as specified in the Regulations

Total words in submitted thesis (including text and footnotes, but excluding references and appendices) 50041.

Signature of candidate …… Date ……

Abstract

Oxygen is an important molecule in life and is essential for a broad spectrum of physiological reactions that include, but are not restricted to, cell metabolism, respiration and growth. Under physiological conditions, oxygen levels vary from one tissue to another ranging from 0.002% to 10% and substantially lower than the atmospheric level of 21 % O_2. Hypoxia is defined as a state of reduced O_2 supplied to cells or tissues when compared to their normal physiological levels. Hypoxia mimetic agents (HMAs) are chemical used to induce pharmacological hypoxia without affecting environmental oxygen levels *per se*. The name HMA is routinely applied as these agents will activate the family of transcription factors which respond to reduced oxygen availability, Hypoxia Inducible Factors (HIF), which is taken as a surrogate indicator for hypoxia. These agents have been proposed as a cheaper alternative to engineered oxygen control measures including tri-gas incubators and workstation approaches. Multipotent stem cells (e.g. neuronal PC12 and human mesenchymal stem cells (hMSCs)) due their ability to differentiate into various cell types provide a means to develop better understanding of tissue development, repair, and protection. In addition, they provide better therapeutic perspectives and opportunities for the treatment of many diseases. Physiological oxygen plays a key role in the maintenance of cellular proliferation, behaviour and biology both *in vivo* and when mimiced *in vitro*. Physiological oxygen and hypoxia are routinely confused creating additional complexity in defining the role of oxygen in cell behaviours. This work has therefore evaluated the role of a panel of well-established HMAs ($CoCl_2$, DFO, DMOG) and new agent (IOX2) vs. different reduced oxygen culture conditions. PC12 and hMSCs were both used to examinine the roles of HMAs on proliferation, metabolic activity, HIFs expression, nitroreductase activity, oxidative stress, apoptosis, death/necrosis and mitochondrial dynamic (burden, action potential and genome copy number) in comparison to physiological normoxia and intermittent hypoxia. HMAs induced HIF expression, apoptosis, trapped cell at G0/G1 phase and induced both ROS formation and

nitroreductase activity in a manner that was not consistent with a reduced oxygen culture condition alone. Mitochondrial burden, mitochondrial action potential, and mitochondrial genome number also changed in response to HMA exposure in a manner that was indenependent of the oxygen culture conditions tested. In summary, HMAs do not provide an accurate replication of engineered oxygen control measures in PC12 and hMSC biology. This is reflected in biological alterations impacting on cell yield, behaviour and biology.

Key words: Hypoxia, hypoxia mimetic agents, PC12, hMSCs, HIF, apoptosis, cell cycle and ROS.

Table of contents

Table of Figures

List of Tables

List of Abbreviations

Abbreviation	Definition
ABCB7	ATP-binding cassette sub-family B member 7
ACTB	β-ACTIN
ADP	Adenosine Di-Phosphate
AKAP121	mitochondrial A kinase anchor protein 121
AKAPs	A-kinase-anchor-proteins
Akt	Protein kinase B (PKB)
ALS	Amyotrophic lateral sclerosis
AMP	Adenosine Mono-Phosphate
AMPK	AMP-activated protein kinase
ANGPT2	Angiopoietin-2
ANOVA	Analysis of variance
ANT	Adenine nucleotide translocator
AO	Air oxygen
AP-1	activator protein-1
Apaf-1	Apoptosome-containing adaptor-1
APC	Annexin-phosphatidylserine complex
ARD-1	Acetyl-transferase-arrest-defective-1
ATM	Ataxia telangiectasia mutated
ATP	Adenosine Tri-Phosphate
ATR	Ataxia telangiectasia and Rad3 related
AV	Atrio-Ventricular (Cardiac)
Bad	Bcl-2-associated death promoter
Bak	Bcl-2 homologous antagonist/killer
Bax	Apoptosis regulator X
Bcl-2	B-cell lymphoma 2
Bcl-xL	B-cell lymphoma-extra large
BH3	Bcl2 homolgy-3
b-HLH	Basic helix-loop-helix
Bid	BH3 interacting-domain death agonist

Abbreviation	Definition
BM-hMSC	Bone marrow human mesenchymal stem cells
BNIP-3	BCL2/adenovirus E1B 19 kDa protein-interacting protein 3
BSA	Bovine serum albumin
cAMP	Cyclic adenosine monophosphate
CD105	Cluster of differentiation 105
CD14	Cluster of differentiation 14
CD19	Cluster of differentiation 19
CD34	Cluster of differentiation 34
CD44	Cluster of differentiation 44
CD45	Cluster of differentiation 45
CD73	Cluster of differentiation 73
CD90	Cluster of differentiation 90
CD95	Cluster of differentiation 95
CDK	Cyclin-dependent kinases
Cep192	centrosome component
CFU-F	Colony-forming unit-fibroblasts
CN	Continuous normoxia
CO_2	Carbon dioxide
CoA	Acetyl Co-A
$CoCl_2$	$CoCl_2$
COX	Cytochrome c oxidase
CP	Cytoplasm processes
C-TAD	C-terminal transcriptional activation domain
DAG	Diacylglycerol
DAPI	4',6-diamidino-2-phenylindole
DFO	Deferoxamine
DMEM	Dulbecco's Modified Eagle's Medium
DMOG	Dimethyloxalylglycine
DMSO	Dimethyl sulfoxide
DNA	Deoxyribonucleic Acid
DPSCs	Dental pulp stem cells

Abbreviation	Definition
DRAM	Damage-regulated autophagy modulator
Drp1	Dynamin-related protein 1
DW	Distilled water
DynA	dynamin-like protein DynA
E-box	Enhancer box
EDTA	Ethylene diamine tetra-acetic acid
EGF	Epidermal growth factor
EGLN	Egl nine homolog
EPAS1	Endothelial PAS domain protein 1
EPO	Erythropoietin
ER	Endoplasmic reticulum
ERK	Extracellular signal–regulated kinase
ERRs	Estrogen-related receptors
ETC	Electron transport chain
FABP4	Fatty acid-binding protein 4
FACS	Fluorescence-activated cell sorting
FAD	Flavin adenine dinucleotide
FasL	Fas ligand
FBS	Fasting Blood Sugar
FACS	Flow Cytometry
FH	Fumarate hydratase
FIH	Factor inhibiting hypoxia inducible factor
FMN	Flavin mononucleotide
Foxo	Fork head box O
FS	Forward scatter
GAP-43	Growth Associated Protein 43
GAPDH	Glyceraldehyde 3-phosphate dehydrogenase
GCN5	Histone acetyl-transferase
GDAP-1	Ganglioside-induced differentiation associated protein-1
GLUT-1	Glucose transporter 1
Grx5	Glutathione-dependent oxidoreductase

Abbreviation	Definition
GSK3	Glycogen synthase kinase 3
GTP	Guanosine triphosphate
H_2O_2	Hydrogen peroxide
Hydrogen peroxide	Hydrogen peroxide
Hydrogen peroxide	Hydrogen peroxide
HCl	hydrochloric acid
HEPES	4-(2-hydroxyethyl)-1-piperazineethanesulfonic acid
hFis-1	fission-1 homolog protein
HIF-1a	Hypoxia-inducible factor 1-alpha
HIF-β	Hypoxia-inducible factor 1-beta
HLA-DR	Human leukocyte antigen
HMAs	Hypoxia mimetic agents
HNF4	Hepatic nuclear factor 4
HRE	Hypoxia response elements
HSCs	Hematopoietic stem cells
IC50	Half maximal inhibitory concentration
IDH1	Isocitrate dehydrogenase-1
IH	Intermittent hypoxia
IKK	IκB kinase
IL-8	Interleukin 8
IMM	Inner mitochondrial membrane
IOX2	2-[(1-benzyl-4-hydroxy-2-oxoquinoline-3-carbonyl)amino]acetic acid
ISU1/2	Cluster assembly protein 1 and 2
IκB	Nuclear factor of kappa light polypeptide gene enhancer in B-cells inhibitor
JAK-2	Janus kinase 2
JIP1	JNK interacting protein 1
JNK	c-Jun N-terminal kinases
KH	K homology
LONP1	Lon protease homolog

Abbreviation	Definition
MAP	Mitogen activated protein
MAPK	Mitogen activated protein kinase
MARCH5	Membrane-associated ring finger (C3HC4) 5
MDM2	Modulating mouse double minute 2 homolog
MEK	Mitogen-activated protein kinase kinase 1
Mfn-1	Mitofusin-1
mRNA	Messenger RNA
MSCs	Mesenchymal stem cells
mt-AP	Mitochondrial action potential
mtDNA	Mitochondrial DNA
mt-ND1	Mitochondrial NADH-ubiquinone oxidoreductase chain 1
mTOR	Mammalian target of rapamycin
MTP18	Mitochondrial protein 18
NAD	Nicotinamide adenine dinucleotide
NADP	Nicotinamide adenine dinucleotide phosphate
nDNA	Nuclear DNA
NDUFS4	NADH dehydrogenase [ubiquinone] iron-sulfur protein 4
NEMO	Nuclear factor-kappa B Essential Modulator
NF-κB	Nuclear factor kappa-light-chain-enhancer of activated B cells
NGF	Nerve growth factor
NOX2	NADPH oxidase-2
NOX4	NADPH oxidase-4
NOXA	Phorbol-12-myristate-13-acetate-induced protein 1
NRF1	Nuclear respiratory factor 1
NRF2	Nuclear respiratory factor 2
Nrf2	Nuclear factor (erythroid-derived 2)-like 2
NSC-34	Spinal cord × Neuroblastoma hybrid cell line
NT2	NTERA-2 cell line
O_2	Oxygen
O_3	Ozone

Abbreviation	Definition
ODD	Oxygen degradation dependent
ODDD	Oxygen degradation dependent domain
OMM	Outer mitochondrial membrane
OPA-1	Optic atrophy gene-1
OXPHOS	Oxidative phosphorylation
p21	Cyclin-dependent kinase inhibitor 1
p27	Cyclin-dependent kinase inhibitor 1B
p38	p38 mitogen-activated protein kinases
p53	p53 upregulated modulator of apoptosis
PCR	Polymerase Chain Reaction
PDC	pyruvate dehydrogenase complex
PDK1	3-phosphoinositide-dependent protein kinase-1
PGC-1	Peroxisome proliferator-activated receptor-gamma co-activator
PHD	prolyl-4-hydroxylase domain
PI3K	Phosphatidylinositol-4,5-bisphosphate 3-kinase
PKA	protein kinase A
PK-M2	pyruvate kinase 2
pO2	Partial pressure of O_2
PP2A	protein phosphatase 2A
PPARs	peroxisome proliferator activated receptors
PUMA	p53 upregulated modulator of apoptosis
p-VHL	Von Hippel–Lindau tumor suppressor
qPCR	Quantitative polymerase chain reaction
Rab32	Ras-related protein Rab-32
Rad3	Protein kinase rad3
RAF	RAF kinases
RNA	Ribonucleic acid
RNAi	RNA interference
RNS	Reactive nitrogen species
ROS	Reactive oxygen species

Abbreviation	Definition
rRNA	Ribosomal ribonucleic acid
RUNX2	Runt-related transcription factor 2
SAPK	Stress-activated protein kinases
SD	Standard deviation
SDH	Succinate dehydrogenase
SIRT1	Sirtuin 1
SIRT3	Sirtuin 3
Smad3	Mothers against decapentaplegic homolog 3
SOD	Superoxide dismutase
SS	Side scatter
StAR	Steroidogenic acute regulatory protein
STAT3	Signal transducer and activator of transcription 3
SUMO-1	Ubiquitin-related modifier 1
TAC	Tricarboxylic acid cycle
TAD-C	C-terminal transactivation domain
TAD-N	N-terminal transactivation domain
TEM	Transmission electron microscopy
TFAM	Mitochondrial transcription factor A
TGF-β3	Transforming growth factor beta
tRNAs	transfer RNA
UCP-1	Proton uncoupling protein
VDAC	Mitochondrial voltage dependent anion channels
VEGF	Vascular endothelial growth factor

Presentation

- Effects of hypoxia mimetic agents on human mesenchymal stem cell culture. ISTM Postgraduate Symposium MAY 2nd 2014.
- 9th Meeting of the Canadian Oxidative Stress Consortium University of Guelph, Guelph, Ontario, June 1st – June 3rd, 2016.
- Ukmsc-2016, Do hypoxia mimetic agents accurately reflect the role of hypoxia in hMSC biology-1? Muhammad A. Ahmed, Rouli Chen PhD, Nicholas R. Forsyth PhD. 9th UK Mesenchymal Stem Cell Meeting.
- 7th Annual Scientific Meeting & YI Workshop Monday 12 - Tuesday 13 December 2016 Manchester Conference Centre.
- The role of hypoxia and hypoxia-mimetic agents on oxidative stress level in bone marrow derived mesenchymal stem cells. 10th Annual UK MSC Meeting held at the University of York on Monday 5th December 2016.
- Participate in paper (Reactive oxygen species formation in the brain at different oxygen levels: the role of hypoxia inducible factors), BJP.
- Participate in Chapter 9 of (Cell Culture Techniques), 2016.
- Do hypoxia mimetic agents accurately reflect the role of hypoxia in hMSC biology? Regenerative Medicine PhD WebEx Forum 31st March 2017.

Acknowledgments

I would like to sincerely thank Iraqi people and Iraqi government represent by Ministry of Higher Education and Scientific Research to support me over all the study years and I want to extend my thanks to the Keele University especially my supervisor Prof. Nicholas Forsyth for all help, support, advises during my work. He also helps me to develop my skills independently but provide all possible support when I need, and the most important thing was his support during the difficult time when ISIS occupied my city and kidnapped my brother but his support was vital for me. I would also like to thank my co-supervisor Dr. Ruoli Chen and my advisor Prof. Paul Horrocks for their supportive comments. Many thanks for Prof. David Furness and Ms Karen Walker for advice in electron microscope experiment. Mr. Joshua Price, Mr. Mark Kitchen and Ms. Tina Dale.

I'd like to thank Prof. Trevor J Greenhough for all his helps and support he provide and Dr Alan Richardson for help in flow cytometry work and Prof. Ying Yang for help with fluorescent microscope. The work described in this Thesis was principally funded by Ministry of Higher Education and Scientific Research – Iraq, but Keele university support make it done. I'd like to thank my dear colleague Mohammed Al-Zubaidi, Dr Buthainah Al-Azzawi, and Ajile Alzamily for providing supporting. Moreover, I would thank all Guy Hilton staff who work through my study interval to provide me with all possible support especially John Misra, Katy Cressy, Pam Brannigan, Pauline Pursglove and Amy Chell.

My thanks and appreciation to my dear mother who played the major role in my life and my brothers and sisters. Finally, thank you Saraa my love and my daughters Sama and Maryam who make the house a great place to live, even when things aren't going so well you are here to support me, encouraging me to continue.

Keele University

Chapter 1 : Introduction

1.1. Oxygen, hypoxia and hypoxia mimetic agents

Oxygen can be thought of as the molecule of life. It is a vital molecule for all forms of life, excepting where prevalent conditions differed i.e. anaerobic bacteria, which evolved during a period when oxygen levels were very low on Earth. With increased availability of atmospheric O_2 the evolution of the extraordinarily efficient mechanism of oxidative phosphorylation (OXPHOS) was seen; mitochondria generating energy that is stored as adenosine triphosphate (ATP) molecules. Oxygen itself is produced by plants, algae and cyanobacteria as a by-product from a reaction between carbon dioxide and water and is used by animals for a more efficient energy production. Oxygen is available in nature in different forms, gaseous diatomic oxygen (O_2) is found in the atmosphere at a concentration of 21.1% and it can also exist as a triatomic molecule called ozone (O_3). Water contains oxygen in the form of O_2 with a concentration of 1-13 mg/L O_2 depending on water temperature and salinity (Kildea & Andreacchio, 2012). Normoxia is defined as the oxygen partial pressure (pO_2) that an organism can live healthily on. Any reduction in bioavailability of O_2 due to partial lack of oxygen is called hypoxia (Loiacono *et al.,* 2010) while a total lack of oxygen is called anoxia. Restricted oxygen supply to tissues due to blocked blood flow is called ischemia (Barnabas *et al.,* 2013). Insufficient blood flow to the brain is collectively known as stroke or ischemic stroke. Adaptability to changes in oxygen supply varies markedly among organisms and the borders of hypoxia and normoxia are species or even population-specific (Das *et al.,* 2010).

Oxygen is essential for a broad spectrum of physiological reactions that include, but are not restricted to cell metabolism, respiration and growth (Loiacono *et al.,* 2010). All multi-cellular organisms have mechanisms that regulate oxygen homeostasis which is very important to maintain cell viability (Semenza, 1999). Under physiological conditions, oxygen levels vary from one tissue to another, ranging from 0.002% to 10%, which is lower than the atmospheric oxygen level of 21 % (Stamati *et al.,* 2011). Hypoxia is defined as a state of reduced O_2 supply to cells or tissue that results in reduction of ATP

production in one state or condition compared with another. As such, the highly relative term “hypoxic status” differs from one cell type to another (Prabhakar & Semenza, 2012).

Hypoxic cells depend on anaerobic glycolysis for ATP generation, and the low residual oxygen will participate in some level of ATP production through the tri-carboxylic acid cycle (TCA) and electron transport chain (ETC) (Duke, 1999). Mitochondria are the major consumer of oxygen (some 85–90%) in cells as they are responsible for oxidative phosphorylation (OXPHOS), the main metabolic pathway for ATP production (Clanton, 2007). During hypoxia, there is increased reactive oxygen species (ROS) production, related to the excess electrons leaking from the mitochondrial ETC (Prabhakar & Semenza, 2012). ROS causes oxidative stress, which is defined as an imbalance between pro-oxidants and antioxidant substances (Griendling & Fitzgerald, 2003). ROS impairs cell function and results in decreased cell viability (Peterson *et al.,* 2011).

Many underlying pathogeneses of diseases include hypoxia as a feature, such as cancer, infections and inflammation-related conditions. Cancerous tissue has hypoxic regions due to abnormal cell proliferation, increased distances to vascular supply, and angiogenesis. Low oxygen levels in diagnostic tumour biopsies indicate a higher risk of mortality in cancers of the bladder, brain, breast, colon, cervix, endometrium, head/neck, lung, ovary, pancreas, prostate, rectum, and stomach (Semenza, 2010).

Hypoxia plays a critical role in cancer biology by activating the transcription of genes that are included in glucose metabolism (Liu *et al.,* 2009), genetic instability (Huang *et al.,* 2007), vascularisation (Liao & Johnson, 2007), stem cell maintenance (Spees *et al.,* 2015), cell immortalisation, epithelial-mesenchymal transition (Mak *et al.,* 2010), pH regulation (Swietach *et al.,* 2007), immune evasion (Lukashev *et al.,* 2007), metastasis and invasion (Chan & Giaccia, 2007), and radiation resistance (Moeller *et al.,* 2007). Hypoxia plays a role in infectious conditions such as bacillary angiomatosis that is caused by *Bartonella henselae* (Kempf *et al.,* 2005), chronic hepatitis C (Ripoli *et al.,* 2010) and cutaneous infections caused by *Staphylococcus aureus*, varicella-zoster virus, human

herpesvirus, or *Candida albicans* (Werth *et al.,* 2010). In inflammatory conditions, it is associated with cellular hyperproliferation and infiltration by cells derived from the circulation, such as T cells and monocytes (Feldmann, 2002). The increase in tissue mass lead to an increase in oxygen consumption by inflamed tissue (Lee *et al.,* 2007).

1.2. Molecular response to hypoxia

Hypoxic conditions can occur under several physiological conditions - for example during normal embryonic development and pathological conditions, including inflammation-related settings like solid tumours, healing wounds, atherosclerotic plaque formation and rheumatoid arthritis. Cells respond by initiating adaptive mechanisms to maintain cell survival through the AMP-activated protein kinase (AMPK) pathway (Viollet *et al.,* 2009) which shifts metabolism to glycolysis by increasing catalytic activity of a number of enzymes, including phosphofructokinase-1 and pyruvate kinase, but this is unsustainable for longer periods of time (Duke, 1999). The three phases theory for cell responses to hypoxia was postulated by Connett and colleagues in 1990 (Connett *et al.,* 1990) where they described three phases in response to hypoxia. The first phase starts when oxygen decreases inside the cell, but ATP production is still sufficient to fulfil the energy demand. The second phase is where ATP is maintained by anaerobic glycolysis via the Embden-Meyerhof pathway which generates only 2 molecules of ATP per 1 molecule of glucose metabolized. This pathway is not sufficient to satisfy the ATP demands of highly metabolic tissues such as the kidney, liver, and brain and these organs will develop ATP depletion rapidly under hypoxic conditions. The third and the last phase initiates when glycolysis becomes insufficient to produce enough ATP to maintain cell function and structural integrity (Connett *et al.,* 1990).

Many tissues develop ATP depletion after phase two and these tissues i.e. brain nerve cells, require high levels of ATP to operate the sodium-potassium 1 pump. If ATP

depletion reaches 50-60% of the demands, membrane depolarization and sodium and water retention occur (Loiacono *et al.,* 2010). Due to membrane depolarization calcium influx occurs through voltage-gated calcium channels leading to glutamate neurotransmitter release and which initiate a glutamate cascade (Dendorfer *et al.,* 2004; Cook, 2010). Death of neurons from these insults can follow quickly by swelling and lysing, or through a complex process resembling apoptosis (Dendorfer *et al.,* 2004). However, many studies have shown that some neuronal cells under hypoxic conditions do survive (Cook, 2010). These surviving cells develop adaptive responses and express high levels of hypoxia inducible factor-1α (HIF-1α) (Chavez *et al.,* 2006), which is a transcription factor and a major regulator of the cellular response to hypoxia (Semenza, 2000).

1.3. Hypoxia inducible factor (HIF)

In 1992, Semenza and Wang investigated the promoter region of the erythropoietin (EPO) gene. Erythropoietin (EPO) is a glycoprotein hormone, which regulates red blood cell production; in hypoxia, the expression of this protein significantly increases to facilitate tissue re-oxygenation. They use electrophoretic mobility shift assay to determine a DNA /protein complex with reduced mobility. This identified a nuclear factor that was bound to the EPO promoter and the DNA-binding activity of this factor was tightly regulated by oxygen, therefore the protein was designated hypoxia-inducible factor (HIF-1) (Semenza & Wang, 1992). Further work revealed that the HIF protein has transcriptional activity and the ability to recognize and bind specific DNA sequence known as hypoxia response elements (HRE) (RCGTG) in target gene promoters (Wiesener *et al.,* 1998). HIF consists of two subunits, α– and β- subunits, which show high structural similarity and both subunits contain three acting domains; N-terminal domain which is a basic helix-loop-helix (b-HLH) domain for DNA binding; the second domain is the central region which is PER-

ARNT-SIM (PAS) domain, which facilitates hetero-dimerization of sub-units and the third one is the C-terminus which is responsible for recruiting transcriptional co-regulatory proteins (Zhulin *et al.,* 1997). There are three HIF-α subunits isoforms.

1.3.1. HIF-1α

HIF-1α is a 826-amino acid protein encoded by the *HIF-1A* gene (Ponting & Aravind, 1997) with a molecular weight of 120 k Da. HIF-1α is ubiquitously expressed in the body and is the main regulator of the cellular response to hypoxia (Ke & Costa, 2006). HIF-1α levels are significantly elevated at O_2 concentrations below 6% (or 42 mmHg), and is rapidly degraded by re-oxygenation to 21% O_2 (140 mmHg) with a half-life of about 5 min (Prabhakar & Semenza, 2012). HIF-1α mRNA is transiently expressed with high protein stability (Jiang *et al.,* 1996; Ema *et al.,* 1997; Makino *et al.,* 2001). HIF-1α needs specific co-factors; hepatic nuclear factor 4 (HNF4), mothers against decapentaplegic homolog 3 (Smad3), signal transducer and activator of transcription 3 (STAT3), and c-Myc (Aprelikova *et al.,* 2006; Warnecke *et al.,* 2008). The Lyer and Kotch groups determined that the knockout of HIF-1α is lethal for mice and the knockout mice had a specific phenotype that was characterized by cardiac malformation and vascular regression (Kotch *et al.,* 1999). HIF-1α and 2α share common target genes such as Vascular endothelial growth factor (VEGF) and EPO, suggesting they may have a similar role in regulating processes including angiogenesis and erythropoiesis (Semenza *et al.,* 1994; Warnecke *et al.,* 2003; Raval *et al.,* 2005; Zhu *et al.,* 2006). In addition, HIF-1α has specific target genes like Glucose transporter 1 (GLUT-1), Bcl-2/adenovirus E1B 19d-interacting protein (BNIP-3), and carbonic anhydrase 9 (CA9) thus HIF-1α plays a vital role in metabolism, apoptosis, angiogenesis (Zhong *et al.*, 1999; Greijer & van der Wall, 2004) and its associated with a majority of cancers (Zhong *et al.,* 1999, Semenza, 2010). The structure of HIF-1α is showed in Figure 1.1A.

1.3.2. HIF-2α

HIF-2α is an 870-amino acid protein with a molecular weight of 115 kDa. It shares 48% amino acid homology with HIF-1α, with high identity in the b-HLH (85%), PER-ARNT-SIM (PAS)-A (68%), and (PAS)-B (73%) domains (Tian *et al.,* 1997). HIF-2α is more tissue-specific and is included in developing blood vessels and lung (Tian *et al.,* 1997). It plays a vital role in embryonic heart development and it is essential for catecholamine homeostasis (Comino-Méndez *et al.,* 2013). HIF-2α mRNA is more stable than HIF-1α mRNA and HIF-2α protein levels significantly increase in hypoxia. HIF-2α needs specific co-factors like NEMO, NFκB essential modulator, and CITED-2-CBP/p300-interacting modulator. Tian *et al.,* (1997) and Scortegagna *et al.,* (2003) identified that knockout of HIF-2α is lethal for mice and the knockout mice have a specific phenotype that is characterized by heart failure bradycardia, and impaired Reactive oxygen species (ROS) metabolism. In addition, HIF-2α has specific target genes like cyclin D, TGF-β, ANGPT2, and VEGFR1 (Raval *et al.,* 2005; Aprelikova *et al.,* 2006; Kasuya *et al.,* 2011), thus HIF-2α plays a role in vascular remodelling, haematopoiesis and cancer genesis and HIF-2α associates with renal cell carcinoma, and polycythaemia (Ang *et al.,* 2002; Raval *et al.,* 2005). The structure of HIF-2α is showed in Figure 1.1B.

1.3.3. HIF-3α

HIF-3α is 662 amino-acids long with a molecular weight of 73K Da and has a transactivation domain (TAD-N) and oxygen dependent domain (ODD), but no TAD-C in its C terminus (Ravenna *et al.,* 2016). It is involved in the negative control of HIF-1α-mediated transcription by reducing the binding of HIF-1 to HRE, thus inhibiting HIF-1 downstream gene transcription. Hypoxia induces the down-regulation of HIF-3α, leading to the activation of HIF-1 in hypoxia (Hu *et al.,* 2013). While in re-oxygenation states, HIF-3α expression is increased to promote the inhibition of HIF-1α activity. The sub-isoform HIF-3α 4 lacks ODD, TAD-N, and TAD-C and has a dominant-negative function of inactivating HIF-1-mediated transcription and is considered a new path for feedback mechanisms that control HIF-1 (Maynard *et al.,* 2005). HIF-3α is mainly found in the

cornea, retina, brain, heart and lung (Makino *et al.,* 2001; Kant *et al.,* 2013; Ravenna *et al.,* 2016). The novel hypoxia-inducible product of the HIF-3α gene is expressed predominantly during embryonic and neonatal stages and thereby designated NEPAS (neonatal and embryonic PAS) (Yamashita, 2008). The structure of HIF-3α is showed in Figure 1.1C.

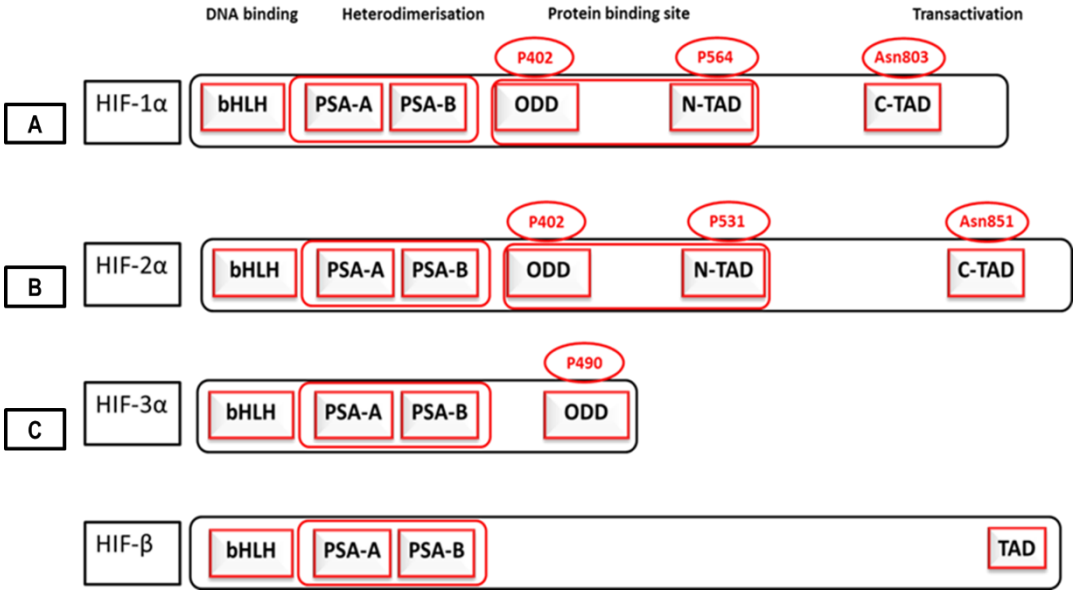

Figure 1.1. HIF structure

The three human HIF-1α, HIF-2α and HIF-3α isoforms and binding partner HIF-β all contain the basic helix-loop-helix (b-HLH) domain that acts as a HRE binding site. The central region – Per-ARNT-Sim (PAS) domain, facilitates heterodimerization of HIFs. HIF-1α (A), HIF-2α (B) and HIF-3α (C) contain an oxygen dependent domain (ODDD) which is responsible for protein stability as it contains Pro 402 and Pro 564 in HIF-1α, Pro 531 in HIF-2α and Por490 in HIF-3α (all indicated by red circles) which are the target for PHDs. The C-terminal recruit's transcriptional coregulatory proteins via the Asparginyl residue in C-TAD (Asp813 in HIF-1 α and Asp 851 in HIF-2 α) (Red circles) represent the site of action of FIH and a revital for HIF-1α, HIF-2α transactivation (Prabhakar & Semenza, 2012).

In normoxia conditions, HIF-α subunits are destabilized by hydroxylation of the two proline residues located in the ODDD region by prolyl-4-hydroxylase domain (PHD) (Ivan *et al.,* 2001), and acylation of lysine (Lys532) by the acetyl-transferase-arrest-defective-1 (ARD-

1) enzyme activity (Masson *et al.,* 2001). After hydroxylation and acetylation, HIF-α is recognized by von-Hippel-Lindau (p-VHL) tumour suppressor leading to poly-ubiquitination by the action of E3 ubiquitin-ligase and this complex is subjected to degradation by proteasome 26S (Lando *et al.,* 2002). There is another hydroxylation process that occurs on Asparagine 803 on the C-terminal domain of HIF-α. The hydroxylation is caused by factor inhibiting HIF (FIH) that inhibits the co-activation with p300, thus inhibits HIF transcriptional activation (Lando *et al.,* 2002). Both prolyl-hydroxylase and asparagine hydroxylase belong to oxygen dependent hydroxylase families that rely on oxygen to possess their catalytic activity, and are considered to be the cellular sensors for oxygen level (Schofield & Ratcliffe, 2004) (Figure1.2).

In hypoxic conditions, the lack of oxygen, the substrate for PHDs and FIH, causes a cease of the hydroxylation process, resulting in no binding of HIF-α to the p-VHL. This results in the accumulation of HIF-1α in its stable form, translocation into the nucleus and binding to the β- subunit to form the active HIF dimer. This in turn binds to co-activators such as CREB-binding protein CBP/p300, transcription intermediary factor 2 and steroid–receptor activator activators to up regulate gene transcription (Kumar *et al.,* 2003; Ke & Costa, 2006; Luo *et al.,* 2011) (Figure 1.2).

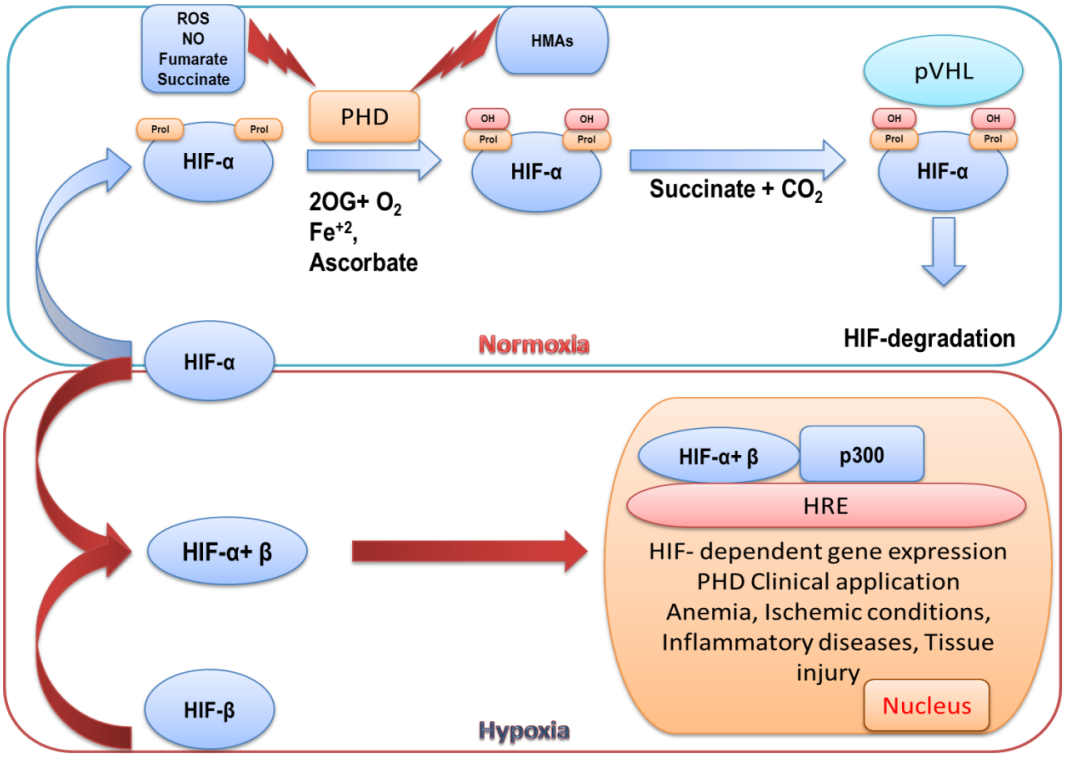

Figure 1.2. Hypoxia inducible factor pathway

HIF-1α contains oxygen degradation dependent domain (ODDD) that contains two proline residues (402 and 564) (yellow rectangle). Under air oxygen culture condition these ODDD are hydroxylated in the presence of oxygen (pink rectangle) by PHD enzyme (yellow rectangle) activity leading to the binding of the von Hippel-Lindau (p-VHL) E3 ubiquitin ligase component (blue circle) that earmarks HIF-α with polyubiquitin chains that are recognized by the 26S proteasome leading to HIF-α degradation. Many factors can inhibit PHDs enzyme activity as (ROS, NO, Fumarate, succinate and HMAs). Under hypoxia, PHD activity inhibited and HIF-1α accumulated in cytoplasm and bind to HIF-β both subunit enter the nucleus attached to CBP/p300 and bind HRE leading to upregulation of hundreds of genes responsible for hypoxia adaption.

1.4. HIF hydroxylases: the cellular oxygen sensor

Prolyl hydroxylase domain enzyme activity is the connects oxygen sensing and energy production by the TCA cycle (Figure 1.3). Intermediates of the TCA cycle are essential to the PHDs activity while end products of the TCA cycle such as succinate and fumarate inhibit enzymatic activity of PHDs (Isaacs *et al.,* 2005; Lee *et al.,* 2005; Koivunen *et al.,* 2007). Mutations of metabolic genes such as fumarate hydratase (*FH*) and the subunits of succinate dehydrogenase (*SDH*) as well as isocitrate dehydrogenase (*IDH1* and *IDH2*)

can produce a condition called pseudo hypoxia by production of a reduced form of 2-OG, (R)-2HG, as an oncometabolite, where HIF-1 is activated despite normal oxygen conditions (Chowdhury *et al.,* 2011; Xu *et al.,* 2011; Koivunen *et al.,* 2012). The APC/C-Cdh1 E3 ubiquitin ligase link between glycolysis and gutaminolysis regulation and cell cycle as APC/C-Cdh1 E3 ubiquitin ligase modulate 6-phosphofructo-2-kinase/fructose-2,6-biphosphatase 3 (PFKFB3) and Glutaminase (GLS1) proteins thus affecting utilization of glucose and glutamine (Xu *et al.,* 2011; Koivunen *et al.,* 2012).

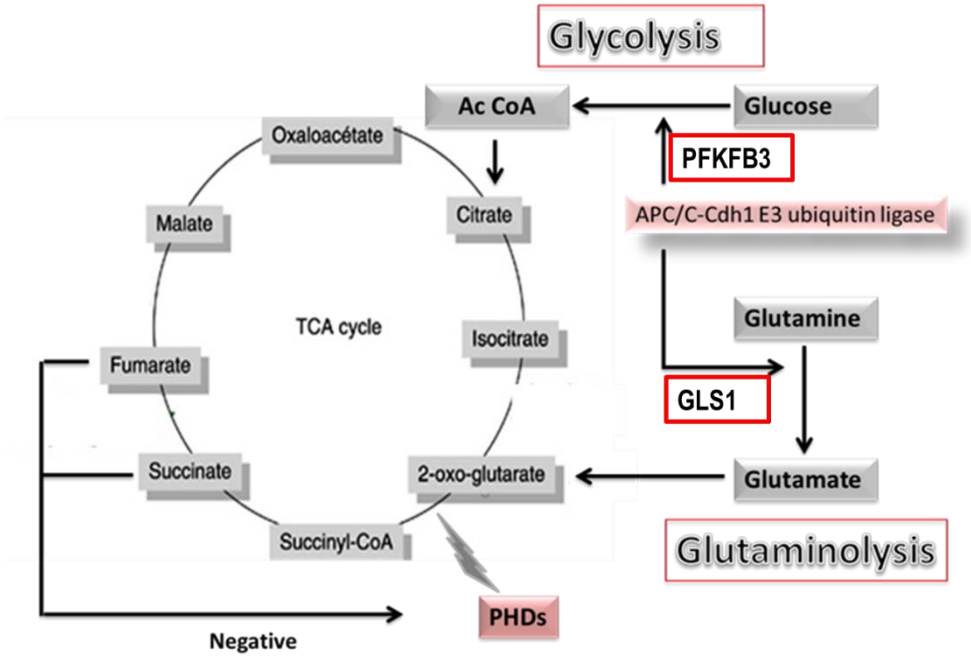

Figure 1.3. 2-OG at the crossroads of metabolic pathways

The TCA cycle intermediate 2-OG acts as a cofactor of PHD enzymes, the intermediates succinate and fumarate are known to inhibit enzymatic functions of PHDs (red box). The APC/C-Cdh1 E3 ubiquitin ligase link between glycolysis and gutaminolysis regulation and cell cycle by modulate PFKFB3 and GLS1.

1.4.1. HIF hydroxylases discovery

Since the discovery of HIF transcription factors it was believed that they played the major role in oxygen sensing in response to hypoxia. Subsequent investigation changed this idea by focusing on a group of oxygen-dependent hydroxylases. Prior to this Hutton et al

(1967) reported on a prolyl-hydroxylase-catalysed reaction that requires 2-OG. Further work revealed that prolyl-hydroxylase mediated a wide variety of roles in plants and animals that include oxygen sensing (Jaakkola *et al.,* 2001; Masson *et al.,* 2001), DNA repair (Ringvoll *et al.,* 2006; Sedgwick *et al.,* 2007), biosynthesis (Jenkins & Raines, 2002; Myllyharju & Kivirikko, 2004), and metabolism (Snell *et al.,* 2014). In the mid-1990s, Jiang *et al.,* (1996) suggested a potential role for HIF as an oxygen sensor as HIF-1α protein concentration dramatically changes over a physiological oxygen range. Further work identified that prolyl-hydroxylase accelerated the process of HIF protein ubiquitylation and degradation by production of hydroxyprolines (Ivan *et al.,* 2001; Jaakkola *et al.,* 2001; Masson *et al.,* 2001) which were approximately 100-fold more tightly bound by p-VHL than non-hydroxylated prolines (Chan *et al.,* 2002). Post-translational modification of HIFs by oxygen-dependent HIF hydroxylases was clearly defined in 2002 (Bruick & Mc Knight, 2001; Epstein *et al.,* 2001; Lando *et al.,* 2002). These enzymes catalysed the transfer of two electrons from an oxygen atom to 2-OG forming succinate and carbon dioxide and the other atom of oxygen being directly incorporated into the HIF-α unit as shown in Figure 1.4.

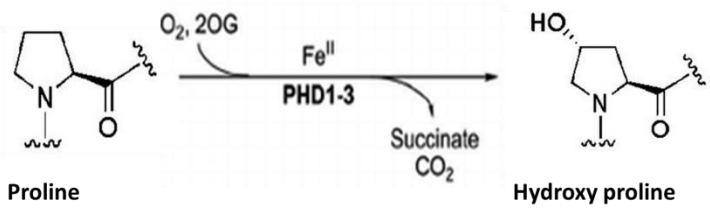

Figure 1.4. Prolyl-4 hydroxylase domain activity

The catalytic activity of the PHD used proline as substrate. In addition, PHD activity need O_2 and 2-oxoglutarate as co-substrates, Fe^{2+} and ascorbate as co-factors. The hydroxylation reaction produces hydroxyproline and succinate.

Now there is the general acceptance that prolyl hydroxylases are the primary oxygen sensors as they are the main regulators of HIFs which respond to changes in oxygen levels. HIF-α is subjected to hydroxylation in prolyl residues Pro- 402 and Pro-564 in the

case of HIF-1α and Pro-405 and Pro-531 in the case of HIF-2α located within the ODD domain (Snell *et al.,* 2014) This reaction also requires ferrous iron (from Fenton reaction) as a cofactor, and 2-OG and molecular oxygen as co-substrates (Gaber *et al.,* 2005) (Figure 1.5).

In mammalian cells, at least 4 isoforms of the prolyl hydroxyls domain (PHD1-4) have been discovered to date. The PHDs share a common motif of a double strand β-helix core fold, also known as jelly roll folds (Karuppagounder & Ratan, 2012). According to their high Km values (Hirsila *et al.,* 2003), PHDs respond fairly linearly to the wide range of physiological oxygen levels and this make it well fitted to be the cellular oxygen sensors (Appelhoff *et al.,* 2004). All the isoforms can hydroxylate the LXXLAP motif in HIF-α subunits and this sequence is also found in other substances such as IκBα, RNA polymerase and β-adrenergic receptor (Fong & Takeda, 2008). The HIF pathway is inactivated in normoxia by the inhibitory effect of PHD, while in hypoxia, the PHDs are not active so the HIF pathway is activated (Fong & Takeda, 2008).

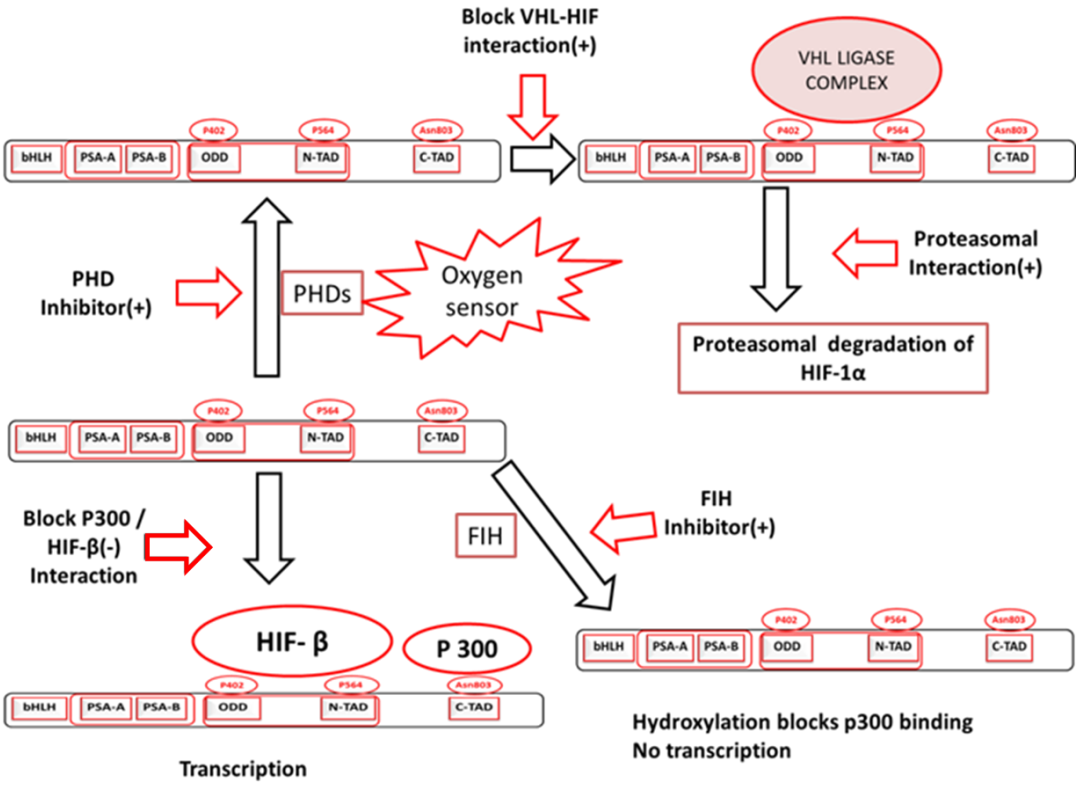

Figure 1.5. PHDs act as oxygen sensors

In the presence of oxygen, HIF pathway is inactivated by PHD inhibition, while in hypoxia, the PHDs are not active so the HIF pathway is activated. Both PHD and FIH inhibitors act as HIF-α stabilisers and increase HIF activity. On the contrary, blocking p300 and HIF interaction decreases HIF activity. Red arrows (+) ve indicate factors that could increase HIF activity. Red arrow (-) ve represents sites of inhibition, while black arrows point out factors that could decrease HIF activity. Red circle sits of hydroxylation.

1.4.1.1. PHD-1 (EGLN-2)

Prolyl hydroxylase domain-1 is found principally in the nucleus, with highest concentrations in the testis, moderate concentration in the liver and lower concentrations in heart, kidney and brain (Kant *et al.,* 2013). PHD-1 is a constitutively expressed 407 amino acid long protein with a molecular weight of 43 kDa (Erez *et al.,* 2003). In normoxia, PHD-1 shows a higher affinity to HIF-2α than HIF-1α while in hypoxic conditions it possesses equal affinity to both HIF isoforms (Corcoran *et al.,* 2013). Explorations of physiological PHD-1 functions have revealed that PHD-1 plays a role in the energy metabolism of muscle and liver as directing metabolism towards the TCA cycle (Aragones *et al.,* 2008; Schneider *et al.,* 2010), cell cycle progression as it regulates the abundance of cyclin D1 which is needed for proper cell cycle progression (Zhang *et al.,* 2016), and control of the stability of centrosome component Cep192 (Moser *et al.,* 2013). From previous work, PHD-1 affects centrosome duplication and maturation in G2 phase which allows cell cycle progression through cyclin D1 induction (Zeng *et al.,* 2010) and hydroxylation of IκB kinase (IKK) (Cummins *et al.,* 2006).

1.4.1.2. PHD-2 (EGLN-1)

Prolyl hydroxylase domain-2 is found predominately in the cytoplasm with features of nucleus shuttling. It consists of 426 amino acids with a molecular weight of 46 kDa (Fong & Takeda, 2008). The highest expression of PHD-2 is found in the heart and testis and is moderately expressed in the brain, kidney and liver (Fong & Takeda, 2008). Both mRNA and protein expression are up regulated by hypoxia, and it is considered to be the main

regulator of the HIF-α transcriptional factors (Fong & Takeda, 2008). PHD-2 targets proline 402 and 564 in HIF, and has a higher affinity to HIF-1α than HIF-2α in both normoxic and hypoxic conditions (Fong & Takeda, 2008). PHD-2 null homozygousity is lethal as it causes massive structural defects in the heart and placenta in mice (Takeda *et al.,* 2006). In addition, PHD-2 mutations were linked to erythrocytosis in humans (Ladroue *et al.,* 2012). PHD-2 expression may play a role in detecting aggressiveness and survival in many types of cancer; including breast cancer (Bordoli *et al.,* 2011; Fox *et al.,* 2011; Peurala *et al.,* 2012), pancreatic cancer (Su *et al.,* 2012), squamous cell carcinoma of head and neck (Jokilehto *et al.,* 2006), prostate cancer (Boddy *et al.,* 2005), and glioma (Henze *et al.,* 2010). Nuclear localization of PHD-2 is associated with tumour aggressiveness and with radiation response (Jokilehto *et al.,* 2006; Luukkaa *et al.,* 2009), but in breast cancer it is associated with increased survival (Peurala *et al.,* 2012). As a part of the PHD-2 role in hypoxia and HIF signalling, recent work has revealed the relationship between PHD-2 and adipose tissue metabolism (adipogenesis and fatty acid synthesis). In mice, the partial loss of PHD-2 gene function leads to less adipose tissue, smaller adipocytes and improvements in glucose tolerance and insulin sensitivity (Rahtu-Korpela *et al.,* 2014).

1.4.1.3. PHD-3 (EGLN-3)

Prolyl hydroxylase domain-3 is distributed equally between the cytoplasmic and nuclear compartments. PHD-3 consists of 239 amino acids with a molecular weight of 27.3 kDa (Fong & Takeda, 2008). It is highly expressed in the heart, placenta and liver, and moderately expressed in the brain and kidneys (Karuppagounder & Ratan, 2012). PHD-3 mRNA and protein expression are strongly induced by hypoxia, hypoxia mimetic agents or by growth factor deprivation in sympathetic neurons (Karuppagounder & Ratan, 2012). PHD-3 targets proline 564 in HIF, and has an equal affinity to HIF-1α and HIF-2α in normoxia, while in the hypoxic condition it possesses a higher affinity to the HIF-2 than HIF-1 isoform (Fong & Takeda, 2008). In addition to the hydroxylation function, PHD-3

hydroxylation-independent functions by targeted proteins represent a variety of signalling pathways such as PK-M2 protein which plays a central role in metabolic reprogramming as it functions as a switch between glycolysis and oxidative phosphorylation (Wang *et al.,* 2014) by regulating the assembly of PK-M2 and acting as a co-activator in PK-M2-derived HIF-1 target transcription (Luo *et al.,* 2011; Sun *et al.,* 2011). PHD-3 also targets NF-κB signalling in carcinogenesis and also in hypoxia (Koong *et al.,* 1994; Michiels *et al.,* 2002; Karin & Greten, 2005). PHD-3 binds the signalling pathway that mediates apoptosis and cell death (Bcl-2 and hPRP19) (Lee *et al.,* 2005; Peurala *et al.,* 2012).

1.4.1.4. PHD-4

Recently discovered to regulate HIF by hydroxylation of proline in the (LXX-LAP) sequence at two separated sites in the α-subunit (Karuppagounderand & Ratan, 2012). PHD-4 is in the endoplasmic reticulum and is up regulated by hypoxia. It is related to procollagen hydroxylase and it has three subtypes which show 42-59% of structural sequence similarity to each other and contains three iron binding residues, where the lysine that binds 2-oxoglutarate is replaced by arginine (Koivunen *et al.,* 2007).

1.4.1.5. Factor inhibits HIF

Factor inhibits HIF is an Asparagine hydroxylase, and is distributed evenly between the nucleus and cytoplasm. FIH consists of 348 amino acids with a molecular weight of 40.6 kDa, with the highest expression in breast tissue, testis, ovaries and kidneys. FIH mRNA and protein does not change in hypoxia. FIH activity is reduced by hypoxia and targets asparagine 803 and 851 for HIF-1α and HIF-2α, respectively (Fong & Takeda, 2008). FIH consists of jellyroll-like β-barrels formed from 8 β-strand and iron binding sites that contain 2-histidine (Laitala *et al.,* 2012). NFκB and Notch systems both contain ankyrin repeat domain (ARD) proteins to compete with HIF-α for FIH-dependent hydroxylation and actually forms better substrates than HIF-α *in vitro* (Loenarz & Schofield, 2008). Deletion of FIH influences metabolism and insulin sensitivity, elevating metabolic rate and improving glucose and lipid homeostasis (Zhang *et al.,* 2010).

1.4.2. PHD modulators as hypoxia mimetic agents

Prolyl hydroxylase domains are considered to be the cellular oxygen sensor, as they have a high affinity to oxygen with a Km-value range from 230 to 250 μM in comparison to other hydroxylase enzymes e.g. Collagen hydroxylase (Cioffi *et al.,* 2003; Hirsila *et al.,* 2003). In order to retain their maximum activity, PHDs need oxygen molecules, as one oxygen atom will couple to proline to form hydroxyl-proline and another oxygen atom is used for de-carboxylation of 2-oxoglutarate (2-OG) to succinate. In addition to this reaction, the PHDs require non-haem-Fe^{+2} for catalytic activity, which binds to the His-X-Asp/Glu-Xn-His motif to coordinate enzymatic activity (Gerald *et al.,* 2004). Moreover, the PHD needs ascorbic acid for returning the Fe^{+2} to its active form (Gerald *et al.,* 2004). PHDs activity is inhibited by hypoxia, nitric oxide, ROS, 2-OG analogues, and cobalt chloride (Maxwell & Salnikow, 2004).

Prolyl hydroxylase can be inhibited through multiple methods in normoxic conditions by disrupting the balance of Fe^{2+} using an iron chelator such as deferoxamine (DFO) or via competitive inhibition, with for example, cobalt chloride. These agents possess a lack of specificity and the risk of off-target effects are very high (Warnecke *et al.,* 2003; Bernhardt *et al.,* 2007). Another method for modulating PHDs activity is through the use of 2-oxoglutarate analogues such as L-Mimosine (L-Mim), dimethyloxalyl-glycine (DMOG), 3,4-dihydroxybenzoate (3,4-DHB), and N-[[1,2-dihydro-4-hydroxy-2-oxo-1-(phenylmethyl)-3-quinolinyl] carbonyl]-glycine (IOX2). However, these agents have drawbacks because they may inhibit other 2-oxoglutarate oxygenases, as 2-oxoglutarate dependent histone demethylases, which could cause an undesirable effect on the epigenetics of the cells. A new member 2-oxoglutarate inhibitor, IOX2, is more potent than DMOG, with relative IC_{50} values of 0.022 μM and 5 μM respectively (Chowdhury *et al.,* 2013). IOX2 inhibits both PHD-2 and FIH with about 5000 times more selectivity for PHD-2 than histone demethylases (Chowdhury *et al.,* 2013).

1.4.3. Clinical application of PHD inhibitors

Prolyl hydroxylase domain inhibitors are used to increase HIF signalling, thus it can be used in the treatment of many pathological conditions (Heyman *et al.,* 2011), for example, anaemia (Hsieh *et al.,* 2007), ischaemic diseases (Ockaili *et al.,* 2005; Fan *et al.,* 2015), wound healing (Fan *et al.,* 2015), stem cell preconditioning and other conditions (Hsieh *et al.,* 2007).

1.4.3.1. Anaemia

The main therapeutic implication of hypoxia mimetic agents (HMAs) is to treat anaemia by enhancing EPO secretion via up-regulation of HIF-1α. In addition, activation of various downstream genes that may have beneficial effects. Several review papers thoroughly cover the recent advances in the development of PHD inhibitors targeting anaemia (Hsieh *et al.,* 2007; Muchnik & Kaplan, 2011). The superiority of HMAs over iron repletion and administration EPO analogues, which are used to treat anaemia, are due to the high cost of EPO analogues their associated resistance, and side effects.

1.4.3.2. Ischemic Disease

When ischemic injury occurs, damage to the tissue associated with both initially limits oxygen supply and reperfusion leading to rapid restoration of oxygen (Hausenloy *et al.,* 2013) as the rapid re-oxygenation of injured tissues is usually associated with a profound inflammatory response. HIF plays an important role in the treatment of ischemic disease and this can have summarised in three main functions. First, when injured tissue is pre-exposed to non-lethal ischemia, in a process known as preconditioning, the injured tissue region will significantly reduce. HIF stabilisation is important for this effect (Eckle *et al.,* 2008). Secondly, the interaction between HIF and the circadian rhythm protein period 2 (PER2) is critical for the regulation of the metabolic pathway during ischemia, by adjusting the glycolytic enzyme production of the ischemic region, especially in the heart (Eckle *et al.,* 2014). Lastly, HIF stabilisation in remote ischemic preconditioning will lead to

enhancement in plasma interleukin-10 transcription, thereby reducing the size of the myocardial infarct (Cai *et al.,* 2013). Protecting neurons and repairing the brain after stroke was another potential function of HMAs (Karuppagounder & Ratan, 2012). Recent works from different research centres revealed that direct inhibition of PHDs by small molecule inhibitors rather than HIF stability plays a role in neuroprotection (Baranova *et al.,* 2007; Nagel *et al.,* 2011).

1.4.3.3. Inflammatory Disease

Inflammatory hypoxia is a characteristic of inflamed tissues, inflamed regions usually have a high metabolism accompanied with low levels of oxygen and glucose (Fraisl *et al.,* 2009; Bartels *et al.,* 2013; Eltzschig *et al.,* 2014). HIF-1 can be stabilized by both a low oxygen supply under hypoxia and pro-inflammatory molecules in the inflamed region and hypoxia can be considered as an inflammatory stimulus by enhancing pro-inflammatory cytokines (Schwartz *et al.,* 2011). HIF signalling pathways are involved in many human inflammatory diseases such as inflammatory bowel disease, Crohn's disease, acute lung injury, and infectious diseases (Fraisl *et al.,* 2009; Schwartz *et al.,* 2011). Stabilized HIF-1α signal activated anti-inflammation responses via induction of adenosine A2A receptor and netrin-1, inhibit excessive inflammation and reduces cellular apoptosis thus participating in tissue repair (Schwartz *et al.,* 2011).

1.4.3.4. Tissue Injury

The use of HMAs to stabilize HIF-1α can be used effectively in the treatment of wounds and other tissue injuries; this is due to fact that HIF signalling is involved in the regulation of various processes including inflammation, angiogenesis, and vasculogenesis (Kalucka *et al.,* 2013; Kant *et al.,* 2013; Zhang *et al.,* 2013). Ruthenborg *et al.,* (2014) provided more detailed information about the therapeutic potentials of HMAs in the treatment of pathogenic wound repair (e.g., diabetic wounds).

1.4.3.5. Asthma

Hypoxia is recognized during the asthma associated allergic inflammatory reaction. Cells respond to low oxygen by activation of the HIF pathway, which extend proinflammatory reactions and aggravation of the disease condition by constitutively express inflammasome proteins and are a potent source of the pro-inflammatory cytokines pro-IL1α and pro-IL1β (Huerta-Yepez *et al.,* 2011). Bronchial biopsies from patients with asthma show increased HIF pathway activity leading to the activation of genes, such as vascular VEGF that plays a role in airway remodelling and increased collagen synthesis and fibrosis (Ahmad *et al.,* 2012). Many works revealed that nonspecific HIF-1 inhibition leads to a reduction in the allergic inflammation and lung remodelling in animal models (Huerta-Yepez *et al.,* 2011). In addition, PHD-2 inhibitors such as ethyl 3,4-dihydroxybenzoic acid, an oxoglutarate analogue, increase airway responsiveness, cell infiltration, mucus production, and collagen deposition in the basal membrane of the epithelium in a mouse model of asthma (Ahmad *et al.,* 2012). This result shows the protective role of PHD-2 in the development of asthma (Huerta-Yepez *et al.,* 2008).

1.4.3.6. Obesity

The oxygen level reduction associated with obesity leads to increased adipose tissue expansion due to multiple factors such as inadequate vascular response, local inflammation, fibrosis, and metabolic dysfunction, all these effect results in a bad prognosis of condition (Crewe *et al.,* 2017). The changes in PHD-2 activity in obesity have a detrimental effect. In support, Matsuura *et al.,* (2013) revealed that PHD-2 deletion from adipocytes resulted in reduced weight gain, glucose intolerance, fat mass and lower macrophage infiltration that are associated with a high-fat diet model. In contrast Michailidou *et al.,* (2015) showed that PHD-2 knockout murine model displayed an increased adipose mass. However, despite the difference in adipose mass results, this group also observed a normal glucose tolerance in these mice, with reduced levels of circulating fatty acids and no increase in macrophage levels in white adipose tissue

(Michailidou *et al.,* 2015). The available body of data on the role of PHD-2 in obesity is, however, scarce and further work needs to be pursued to underlie the mechanisms responsible for this outcome.

1.5. Mitochondria, origin, stracture and functions

The mitochondrion is a cytoplasmic organelle embedded in a reticular network in the cell cytoplasm. This double-membrane structured organelle contains the machinery that is needed for the mitochondria to produce adenosine triphosphate (ATP), and to fulfil their roles in apoptosis, calcium homeostasis and the formation of iron sulphur clusters along with many other functions. Mitochondria contain their own DNA encoding a number of vital proteins for mitochondria function, but the vast majority of mitochondrial proteins are nuclear encoded (Anderson *et al.,* 1981). As mitochondria encode their own proteins this also means that they are susceptible to diseases that are caused by mutations in mitochondrial DNA (mtDNA) which not only affect mitochondria but also cellular function (Park and Larsson, 2011). Recently mtDNA has found use as tool for diagnosis of many disease conditions e.g. mt-ND1 gene encodes the ND1 protein, a subunit of NADH dehydrogenase, used in diagnosis of mitochondrial disorders including Leigh's syndrome (Thorburn and Rahman, 1993). There are two theories hypothesis mitochondria origin “endosymbiotic theory” was proposed by Margulis (1971) and hydrogen theory (Martin & Muller, 1998).

Mitochondria are elongated rod-shaped structures with a double membrane. Mitochondria have diameter of ~2.5 μm in length ~0.5 μm, with a highly folded inner membrane, called cristae, all enveloped by an outer membrane (Palade, 1952) as depicted in Figure (1.6) with Transmission electron microscopy (TEM).

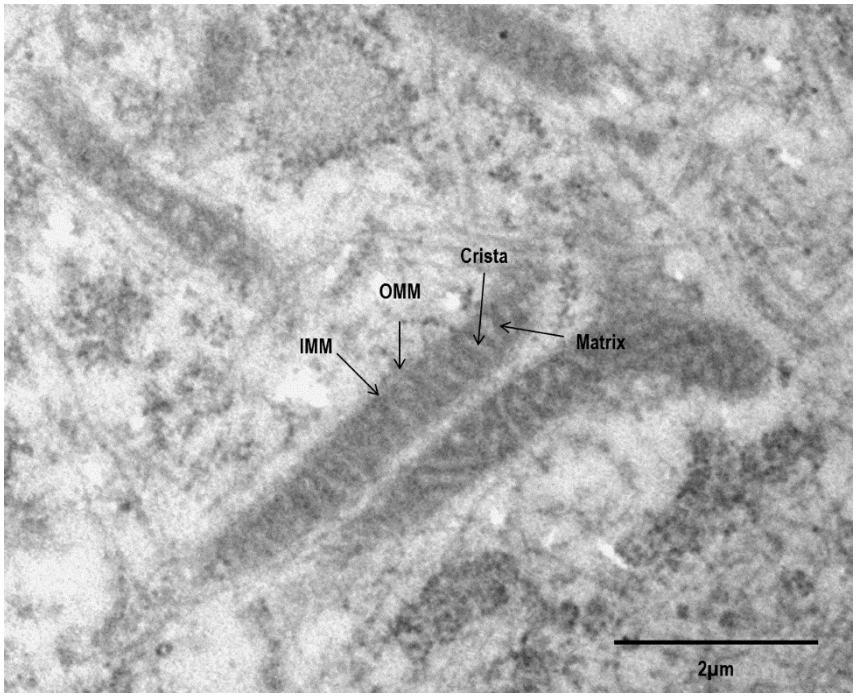

Figure 1.6. Mitochondria morphology and structure

Mitochondrion ultrastructure (TEM image) mitochondrion has double membranes outer and inner mitochondrial membrane (OMM and IMM) with internal matrix, each of which contains highly specialized proteins. The outer membrane contains many channels serve as sieve consist of protein porin. the inner membrane, which is highly folded membrane with large infoldings called cristae. IMM utilizes a group of transport proteins that will allow transport those materials essentials to the matrix only.

The outer mitochondrial membrane (OMM) contains high densities of mitochondrial voltage dependent anion channels (VDAC) which facilitate the passage of 10 kDa size molecules to the inter-membrane space (Shoshan-Barmatz *et al.,* 2014). The cardiolipin rich inner mitochondrial membrane (IMM) separates the inter-membrane space from the mitochondrial matrix and contains many transport proteins that act as a scaffold for the respiratory complexes where oxidative phosphorylation (OXPHOS) occurs, and provides an ideal environment that is essential for ATP formation (Paradies *et al.,* 2014). The highly folded IMM, provides an effectively large surface area for maximum respiratory complex protein integration to produce ATP via OXPHOS (Paradies *et al.,* 2014).

Many of the enzymatic processes take place in the mitochondrial matrix such as those required for oxidative metabolism such as the TCA cycle and β-oxidation of fatty acids. The matrix also contains mtDNA and is the site of replication, transcription and translation of this genome (Hawlitschek *et al.,* 1988; Pfanner *et al.,* 1989; Pfaff & Klingenberg, 1968; Liu & Chen, 2013).

Mitochondrial biogenesis is tightly regulated according to the energy requirements of the cell in order to provide an adequate amount of ATP. The first mechanism to respond to an increasing ATP demand is the increase of mitochondrial mass by activation of AMP activated protein kinase (AMPK) (Dominy & Puigserver, 2013), and Sirtuin 1 (SIRT1) (NAD^+ sensor). This trigger activation of peroxisome proliferator activated receptor γ coactivator-1α (PGC-1α) which is the main regulator of mitochondrial biogenesis. It initiates the transcription of nuclear encoded mitochondrial proteins such as nuclear respiratory factors 1 and 2 (NRF1 and NRF2), oestrogen related receptor α (ERRα), forkhead box class-o (Foxo-1), and peroxisome proliferator activated receptors (PPARs) (Puigserver & Spiegelman, 2003) where expression of these proteins leads to the eventual increase in mitochondrial mass (Dillon *et al.,* 2012). The second mechanism is activated by low temperatures in brown adipose tissues by activation of β_3 adrenergic receptor via the sympathetic nervous system as a measure of non-shivering thermogenesis involving proton uncoupling protein UCP-1 (Puigserver *et al.,* 1998).

Cell health is directly related to the mitochondria as intact cells have intact mitochondrial biogenesis and bioenergetic functions (Liesa & Shiriha, 2013). Mitochondria are a highly dynamic organelle which displays constant movement and changes in shape and size by fusion and fission processes, which are guided by a number of dynamin-like GTPases (Bürmann *et al.,* 2012). The processes of fusion and fission ensure correct membrane (inner and outer) fusion and distribution of mitochondrial contents like mtDNA, proteins and soluble factors (Scott & Youle, 2010). Fusion and fission processes play vital role in many cellular functions such as mitosis, energy sensing, ATP turnover, calcium

homeostasis, autophagy and apoptosis (Hyde *et al.,* 2010; Tait & Green, 2012). In addition, fusion and fission processes are the main regulator of the morphology of mitochondria. The balance between the two processes will determined if the mitochondria have correct-shape or are fragmented or elongated. The importance of these mitochondrial morphology changes is clear in many pathological conditions related to neurodegeneration (Markham *et al.,* 2014). Moreover, the fusion process take part in regulating mitochondrial respiration (Roy *et al.,* 2015).

Mitochondrial functions can have summarized by:

1.Oxidative Phosphorylation

2. Generation of reactive oxygen species

3. Calcium Handling

4. Iron-sulphur cluster biogenesis

Mitochondria encode 37 genes, 13 of which contribute protein subunits towards the OXPHOS complexes and 22 tRNAs and 2 rRNAs which enable OXPHOS subunit expression (Taanman, 1999). There are ≤10 copies of the 16,569 bp circular mtDNA genome per mitochondrion located within the mitochondrial matrix. Nuclear genome encodes the remaining 77 proteins required for OXPHOS which are translated within the cytoplasm and passed to the mitochondria. The mitochondrial genome does not contain introns (Anderson *et al.,* 1981). mtDNA copy number in each cell varies from 100,000 copies of mtDNA in female germline oocytes (Shoubridge & Wai, 2007) to ~250 mtDNA molecules in adult stem cells related to their small size and high nuclear cytoplasmic ratio (Coller *et al.,* 2001). mtDNA content inside the cell is related to energy expenditure. High energy demanding cells such as muscle and nerve require more mtDNA than other types (Shoubridge & Wai, 2007). Brown *et al.,* (2011) have suggested that single genomes are packaged together in complexes called nucleoids that contain protein machinery essential for the replication and transcription of mtDNA.

From above, the number of mitochondria can be roughly estimated from the amount of mtDNA noting that each mitochondrion has multiple copies of mtDNA (Phillips *et al.,* 2014). Southern blot analysis is traditional method for mtDNA quantification (Tang *et al.,* 2012), but nowadays, quantitative polymerase chain reaction (qPCR) techniques are more commonly used as they provide a relative number of mitochondrial genomes per cell by comparing mtDNA copy number to that of nuclear DNA (Phillips *et al.,* 2014). NADH dehydrogenase subunit I (ND-1) can be used along with specific nuclear-encoded housekeeping genes for normalization purposes (Phillips *et al.,* 2014).

1.5.1. Effect of reduced oxygen level and HMAs on mitochondria

1.5.1.1. Effects of hypoxia on mitochondrial structure and dynamics

Mitochondria are highly dynamic organelles; mitochondrial morphology is regulated by fission / fusion machineries which is modulated in response to changes in oxygen availability. Under hypoxia, faster glucose consumption occurs in an attempt to retain ATP production using less efficient anaerobic glycolysis (Lum *et al.,* 2007). Under hypoxic conditions, shortage of supplementation of substrates like acetyl-CoA and O_2 to mitochondria inducing major structural, functional, and dynamical changes. The structural and dynamical changes are characterized by impairment of fusion process that leads to mitochondrial depolarization, loss of mtDNA that may associated with altered respiration rates, and uneven distribution of the mitochondria within cells (Jezek *et al.,* 2009). Under continuous hypoxia neurons cells reduce mitochondrial size and change mitochondrial morphology and this may be related to changes in nitric oxide synthase activity (Guo *et al.,* 2008). HIF stabilization under hypoxia or by HMAs play a role in changing mitochondrial morphology and function through affecting cellular signals which are transduced within the cell in order to affect mitochondrial morphology and function (Chen *et al.,* 2005).

1.5.1.2. Effects of hypoxia on the respiratory chain complexes

Hypoxia and HMAs through stabilizing HIF play vital role in changing OXPHOS machinery such as stabilizing HIF induce of pyruvate dehydrogenase kinase, which inhibits pyruvate dehydrogenase activity leading to shift pyruvate away from TCA thus reduced respiration due to limitation of substrate and inducing expression of LDH-A that shift pyruvate a way from TCA toL-lactate (Kim *et al.,* 2006). HIF also changes subunit composition of cytochrome c oxidase subunit 4 isoform via increased COX4-1 destruction and increase COX4-2 expression (Brunori *et al.,* 2004). Moreover, HIF-1 mediates expression of BNIP3 which is a pro-apoptotic BH3-only protein associated with mitochondrial dysfunction acting as a potent inducer of autophagy (Hamacher-Brady *et al.,* 2007). In addition, hypoxia elevates NO levels via increased activity of nitric oxide synthases and NO will compete with cytochrome c oxidase for O_2 thus reducing respiratory chain activity (Galkin et al., 2007).

1.5.1.3. Effects of hypoxia on ROS production by Complex I &III

ROS form from the leak of 1-2% of electrons that pass through the mitochondrial respiratory chain under air oxygen culture conditions where complex I and to lesser extent complex III are considered the main sites for ROS formation (Poyton *et al.,* 2009). Under hypoxia or after HMAs, controversy has arisen around whether ROS formation increases or decreases, and this may be related to fact that HIF participates in ROS regulation while ROS itself plays a role in HIF expression and activity (Kotake-Nara & Saida, 2007; Owusu-Ansah *et al.,* 2008; Zeng *et al.,* 2011). The mtDNA encoded complex III and other respiratory chain proteins are crucial in ROS formation (Poyton *et al.,* 2009).

1.5.1.4. Effects of hypoxia on ATP synthase

ATP synthase (or F_1:F_0 ATPase) is a reversible rotary motor enzyme which uses proton movement across the mitochondrial IMM to synthesis of ATP from ADP under normoxic physiological conditions. Under hypoxia mitochondrial action potential decreases below the physiological steady-state reversing ATPase activity and using the produced energy to

pump out the protons from the matrix to the intermembrane space in synchronization with the adenine nucleotide translocator which maintains the physiological membrane potential (Bosetti *et al.,* 2002). So, under hypoxic condition the drop in cytoplasmic high energy phosphates is mainly related to reversion of ATP synthase activity requiring a strictly regulated mechanism to stop ATP waste. This is achieved by H^+/Δψm dependent IF1, protein binding to the catalytic F1 site at low pH and low Δψm resulting in a rapid - reversible dropping of the enzyme activity. In addition, H^+/Δψm dependent IF1 is also related to elevation ROS formation and induce mitophagy which are correlated to many pathological conditions as myocardial infarction, Alzheimer's disease and inflammatory diseases (Baracca *et al.,* 2002).

1.5.1.5. Effects of hypoxia on mitochondrial genome

Mitochondria are the main energy producing, oxygen consuming organelle and it responsible of ROS formation (Poyton *et al.,* 2009). Mitochondria participate and respond to HIF stabilization in hypoxia or after HMAs treatment. Mitochondria respond by reprogramming of the energy production by shifting metabolism to the anaerobic pathway. Moreover, mitochondria undergo successive fission and fusion to repair damage mtDNA and this mechanism allows for separation of mitochondria with damaged DNA via fission, and have healthy material from healthy mitochondria via fusion and this process is regulated by group of proteins that include mitofusin 1 (Mfn1), mitofusin 2 (Mfn2), dynamin-related protein 1 (Drp1), human fission factor-1 (FIS1) and optic atrophy factor 1 (OPA1). In addition, hypoxia increase mtDNA copy number and this may be related to the ability of HIF induce mRNA levels of *PGC-1α, TFAM and SSBP* genes (Chuang *et al.,* 2012).

1.6. Apoptosis

Apoptosis (programmed cell death) is controlled by an extrinsic pathway mediated by cell receptors or an intrinsic pathway mediated by cell damage. Cytochrome c is an important factor in apoptosis as cytochrome c release from mitochondria enables the apoptosome formation along with Apoptotic protease activating factor 1 (Apaf-1) which activates pro-caspase-9, leading to apoptosis (Parrish *et al.,* 2013). Cytochrome c release is a tightly regulated process that requires the binding of pro-apoptotic Bc-l2 family proteins Bax and Bak to the outer mitochondrial membrane leading to increase permeability of the membrane (Shamas-Din *et al.,* 2013). Under physiological conditions, Bcl-2 homolgy-3 (BH3) family of proteins inhibit Bcl-2 proteins from triggering apoptosis via cytochrome c release (Willis *et al.,* 2007). Stabilization of HIF-α (by hypoxia or after HMAs treatment) is involved in the regulation of many members of Bcl-2 family both pro-apoptotic (BNIP3 and Noxa) and antiapoptotic (Bcl-2, Bax, Bad, Bid, Mcl-1 and Bcl-xL). Proapoptotic activity induced by HIF-1α includes downregulation of Bcl-2, induction of BNIP3, and BH3-only domain protein Noxa. In contrast, HIF-1α can also protect from apoptosis by elevating Bcl-2 and Mcl-1 levels, Bcl-xL induction, and decreasing pro-apoptotic Bid, Bax, and Bak levels (Santore *et al.,* 2002).

1.7. Cell cycle

The cell cycle is a highly regulated series of events involving cell growth and division into two new daughter cells, to do so the cell undergo a series of events that are both accurately timed and precisely regulated involving cell growth, DNA replication, and division to produces two identical cells. Cell cycle consist of four distinct stages; Gap phase 1 (G1), DNA replication phase (S), and Gap phase 2 (G2), and mitotic division (M). under stressful growth conditions cells can exit G1 into G0 where they become quiescent and do not progress to G1 phase, remaining metabolically active and maintaining the

ability for subsequent re-entry into the cell cycle. Each stage regulated by highly ordered processes pushing cells from one phase to the next (Antico Arciuch *et al.,* 2012).

The cell cycle is connected to what called metabolic cycle; as during cell division cells switch between an oxidative phase; which involve the biosynthesis of many cellular components (G1 phase) utilising energy derived from mitochondria, followed by a reductive phase; with DNA-replication and biosynthesis of mitochondria (S/G2/M phases) where energy is sourced from non-respiratory energy production methods (Martínez-Diez et al., 2006). If there is insufficient energy to complete the cycle, the cells become trapped at the G1 (restriction point) of the cell cycle. Metabolic stress triggers G1 arrest and it control by AMP-activated protein kinase (AMPK) activity. AMPK is considered as a metabolic sensor of energy demand in higher eukaryotic cells (Cantó & Auwerx, 2010). Activated AMPK promotes the phosphorylation of p53 on Ser15 (Wu *et al.,* 2014), this step prevents p53 degradation leading to the accumulation of p53 which induces the expression of p21 gene. p21 act as cyclin-dependent kinase inhibitor, that induce cell-cycle arrest at either of G1 or G2 (Finn *et al.,* 2016). Owusu-Ansah *et al.,* (2008) revealed that mutations in genes encoding complex IV and complex I components will activate the G1/S checkpoint via decreased ATP production and a rise of AMP levels resulting in activation of AMPK or by increases in ROS formation resulting in activation of c-Jun N-terminal kinases (JNK) and Foxo. In mammalian cells cyclin D1 phosphorylates and inactivates retinoblastoma protein (pRB) indicating entry of cells into the S phase of the cycle, inhibiting mitochondrial function (Sakamaki *et al.,* 2006) and repressing the activity of nuclear respiratory factor-1 (NRF1) (Wang *et al.,* 2006). The studies of mechanisms that control mitochondrial biogenesis during the cell cycle have revealed that there is synchronized increase in mitochondrial mass and membrane potential throughout the progression from G1 to mitosis and after cell division these parameters will return back to normal (Wang *et al.,* 2006). Moreover, mtDNA contents increased from S to G2 phase

with a harmonized increase of NRF1 levels (Wang *et al.,* 2006). The relation between mitochondrial function control and NRF-1 was revealed by a Scapula *et al.,* (2012). Other study showed that defects in NRF1 associated with a defect in the maintenance of the mitochondrial membrane potential and very low mtDNA contents (Morrish & Hockenbery, 2014).

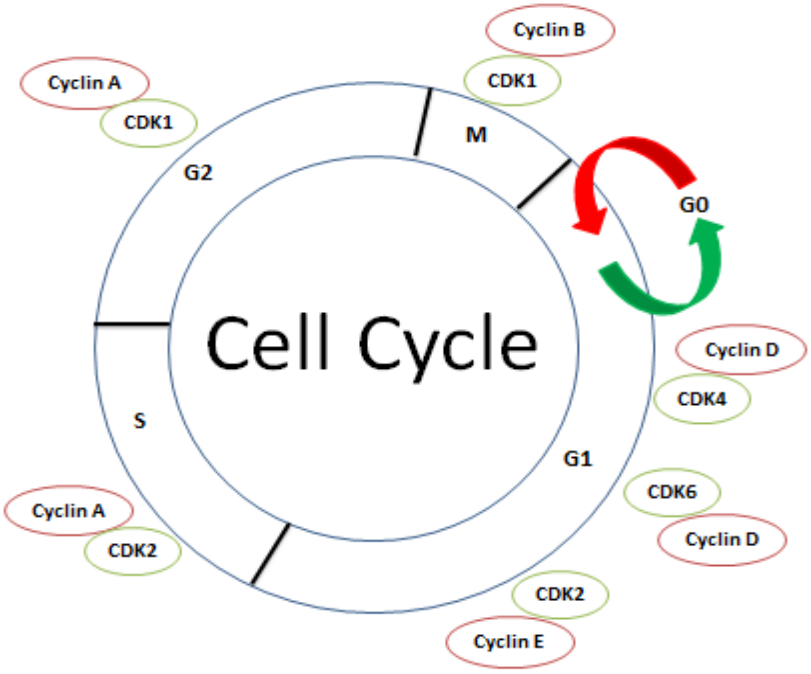

Figure 1.7. The cell cycle is divided into a number of stages.

The eukaryotic cell cycle is divided into a number of stages. Two gap phases (G1 and G2) allow cell growth in preparation for DNA duplication and chromosome segregation during interphase. DNA duplication is triggered after G1-phase and finished by the end of the S/G2 border lastly, M-phase. The green circles represent cyclin-dependent kinase (CDK), the red circles represent cyclin. The green arrow represent cell go to G0 and the red arrow represent the cell back to G1.

Peroxisome proliferator-activated receptor-gamma co-activator (PGC) is a member of a family of transcription co-activators that plays a central role in the regulation of cellular energy metabolism. PGC-1α and PGC-1β induce Mfn-2 expression via transcriptional mechanisms. PGC-1β induces morphological changes in mitochondria during the cell cycle (Zorzano & Claret, 2015). High energy demands lead to induction of PGC-1α that in turn will induce and stimulate many functions like mitochondrial biogenesis, Mfn-2

expression, and mitochondrial function modulation (Zorzano & Claret, 2015). Mitochondria follow a highly concerted behaviour when passing through the different stages of the cell cycle (Hyde *et al.,* 2010). Mitochondria at G0 are found in filamentous and fragmented forms. In the mitotic phase, fragmented mitochondria are positioned opposite telomeres of daughter cells in M phase which ensure concerted movement and dispersion between daughter cells. Mitochondria form an extended tubular network and tubular elements that undergo fission and fusion at G1/S (Gupte, 2015). This mitochondrial network at G1/S serves many cellular functions such as the production of increased mitochondrial ATP to compensate for the reduction in ATP production due to glycolysis produced ATP during G1/S, playing a vital role to ensure that a homogenized distribution of mitochondrial DNA in the continuous matrix is maintained, and that cells are protected from apoptosis at this crucial cell cycle stage (Mitra *et al.,* 2009). Inhibition of Drp1 induces mitochondrial hyper fusion which leads to increased cyclin-E levels initiating cell replication at G1/S phase (Mitra *et al.,* 2009).

Oxygen is one of the most demanded nutrients required by the cells in the cell cycle and lack or reduction in its concentration can lead to cell cycle arrest at G1 phase with reduction in S phase. It is postulated that hypoxia induce protein phosphatase 1 (PP1) activity a specific CDKs phosphatase that related to the reduction in CDK activity associated with an accumulation of hypo-phosphorylated-pRb (Krtolica *et al.,* 1998).

Hypoxia associated reduction in CDK activity is related to increases in p21 and p27 levels (CDK inhibitor). The exact role of HIF-1α in induction of p27 is still an area of debate, but the role of p27 is critical in the cell cycle arrest under hypoxic condition. HIF1α induction disrupts c-Myc-Max complex formation leading to decreased c-Myc transcription which induces p21 expression causing cell cycle arrest. In contrast, induction of HIF2α can facilitate c-Myc and Max complex formation with increased c-Myc transcription which in turn increases cyclin D2 expression and reduces p21 leading to activate cell proliferation (Krtolica *et al.,* 1998).

In addition to above HIFs play a role in regulation of transcription of several microRNAs particular miR210 which play role in regulates E2F3, a transcription factor causing severe downregulation in protein levels leading to cell cycle progression arrest (Medina *et al.,* 2008). HIF1α have the ability to block DNA replication under hypoxic condition by activation of ATR and its downstream target checkpoint kinase 1 (Chk1) leading to trapped cell at G1 phase (Hammond *et al.,* 2003). Minichromosome maintenance (MCM) proteins are main the components of the DNA helicase, which mediate DNA replication, an essential process prior to cell division. HIF-1a to the complex decreased phosphorylation and activation of the MCM complex by the kinase Cdc7. As a result, HIF-1a inhibited firing of replication origins, decreased DNA replication, and induced cell cycle arrest (Hubbi *et al.,* 2011).

1.8. Cells models

1.8.1. PC12 cell

In the early 70s, PC12 was described as cells derived from pheochromocytoma of rat adrenal medulla and have an embryonic origin from the neural crest with a mixture of neuroblastic and eosinophilic cells (Greene and Tischler, 1976). These cells are round; small (6-14μm diameter) can be cultured in serum-containing medium with a doubling time ranging from 2-3 days. They can survive after 30 passages in culture; no significant chromosomal changes were found (Brynczka et al, 2007). PC12 is used as a tool to overcome problems that associated with neuronal cell culturing and harvesting as it does not need growth factors and considered to be the best model for nerve cell differentiation (Fujita K et al, 1989). Importantly, PC12 are widely used to study hypoxia, receptor pharmacology and nerve cell differentiation. They are like the neoplastic adrenal chromaffin cells, after treatment with NGF they possess a neuronal phenotype (Greene & Tischler, 1976). The ease culture of PC12 provide large amount of information about cell proliferation and differentiation. Treating PC12 cells with nerve growth factor or

dexamethasone shift cell out of the cell cycle and induce terminally differentiate This makes PC12 cells very useful model for neuronal differentiation and neurosecretion. NGF treatment for 10–14 days cause aggregation of vesicles in the ends of the neurites. PC12 used in hypoxia research, as duration of hypoxia induces dramatic change in exocytosis. prion protein fragments and vesicle release in Parkinson's disease.

1.8.2. BM-MSCs

Friedenstein et al was the first to demonstrate that bone marrow contains two populations of cells: hematopoietic stem cells (HSCs) and a rare population of plastic-adherent stromal cells, which were referred to mesenchymal stromal cells (MSCs) (Williams and Hare et al, 2011). In the early 21st century, many studies demonstrated that human MSCs have the ability to transdifferentiate into endoderm-derived cells and cardiomyocytes (Toma et al, 2002). These cells have many important characteristics such as multipotency, migration, long term transduction stability and no immunogenicity thus it provides an interesting research tool which can be used in investigations of organ and tissue development and different pathological processes that occur during human development and drug discovery and development (Lee et al, 2004; Song et al, 2006).

Clinically, MSCs is used in kidney regeneration (Hopkins et al, 2009), blood precursor transplantation (Billet et al, 2008), cardiac repair (Nesselmann et al, 2008); wound healing (Fu et al, 2006) and treatment of arthritis (Chen and Tuan, 2008). The HIF pathway affects MSCs in many ways, such as modifying energy metabolism, iron metabolism, intracellular pH, vasomotor activity, migration, motility and modification of the extracellular matrix. However HIF can also induce apoptosis (cell death mechanisms via increased mitochondrial membrane permeability), increase ROS and RNS, and increase intracellular acidity that leads to significant increase in caspases activities (Csete; 2005).

1.9. Aim

The importance of multipotent stem cells applications in regenerative medicine raises the need to define a strategy to produce metabolically flixiablecells cells that can adapite to further insults and increase their number that represent the main problem facing multipotent stem cells such as MSCs applications. HMAs and engineered control oxygen technique used to produce the *in vitro* cell expanded-metabolic flexibile of multipotent stem cells. This work aims to define the impact of HMAs on multipotent stem cells. This study aims to compare the cell behavior changes in multipotent cells (both neural PC12 and hBM-MSCs) after incubation under different oxygen culture condition using control oxygen engineering and after drug-induced hypoxia using different types and concentrations of HMAs and check if control oxygen engineering produce additional effect on cell behavior after treats both types of cells with HMAs. In both cell types; our hypothesis of this study is, that there would be a distinct change in cell proliferation (cell count, MTT, cell cycle and apoptosis), cell differentiation, HIF expression and Mitochondrial dynamic (burden, action potential and mitochondrial genome copy number) under pharmacological induce hypoxia as well as oxygen engineering.

Keele University

Chapter 2 : Materials & Methods

2.1. Materials

Table 2.1. List of materials, catalogue number and supplier

Chemical name	Catalogue number	Supplier
(3-(4,5-dimethylthiazol-2yl)-2,5-diphenyl tetrazolium bromide	M2128	Sigma-Aldrich
3-isobutyl-1-methylxanthine	I7018	Sigma-Aldrich
4′,6-Diamidino-2-phenylindole	D9542	Sigma-Aldrich
Agarose	BP1356-500	Fisher Scientific
Alcian blue	A3157	Sigma-Aldrich
Alizarin red S	A5533	Sigma-Aldrich
Annexin V Binding Buffer	130-092-820	Miltenyi Biotec
Annexin V-FITC	130-092-052	Miltenyi Biotec
Ascorbic acid phosphate	A8960	Sigma-Aldrich
β-glycerophosphate	G9422	Sigma-Aldrich
Bovine serum albumin	BP9703-100	Fisher Scientific
Collagen IV from human placenta	C5533	Sigma-Aldrich
Cryopreserved human bone marrow mononuclear cells	2M-125C	Lonza
Cobalt Chloride	C8661	Sigma-Aldrich

DAPI	D9542	Sigma-Aldrich
Dexamethasone	D2915	Sigma-Aldrich
Deferoxamine mesylate	D9533	Sigma-Aldrich
Diglycidyl-ether of Polypropylene-glycol	R1072	Agar Scientific
Direct Load Wide Range DNA Marker	D7058	Sigma-Aldrich
Dimethyl Sulfoxide	D2650	Sigma-Aldrich
Dimethyloxalylglycine	D3695	Sigma-Aldrich
Dimethylaminoethanol	AGR1067	Agar Scientific
DNeasy Blood & Tissue Kit	69504	Qiagen
Donkey anti-mouse IgG-FITC antibody	SC-2099	Santa Cruz biotechnology
DyLight® 488 goat anti-mouse IgG (H+L)	ab96879	Abcam
Dulbecco's Modified Eagle Medium	BE12-707F	Lonza
Ethanol (absolute)	E0650/17	Fisher Scientific
ERL 4221	AGR1047R	Agar Scientific
Fetal bovine serum, South America origin	DE14-801F	Biosera
Fibronectin	F0895	Sigma-Aldrich
Flow cytometry staining buffer	FC001	R&D system biotechne

Fresh human bone marrow aspirate	ABM001-1	ALLCELLS
Gel Loading Buffer (0.05% bromophenol blue, 40% sucrose, 0.1 M EDTA, 0.5% SDS)	G2526	Sigma-Aldrich
Glycine	50046	SIGMA-ALDRICH
Horse serum	H 1270	Sigma-Aldrich
GAP-43 Antibody	NB300-143	Novus Biologicals
Glutaraldehyde solution 25%	G5882	Sigma-Aldrich
IOX_2	SML-0652	Sigma-Aldrich
Indomethacin	I7378	Sigma-Aldrich
Insulin	I9278	Sigma-Aldrich
Insulin, Transferrin, Selenium (ITS)	I3146	Sigma-Aldrich
Industrial methylated spirits (IMS)	I99050	Genta Medical
Isopropanol	P/7500/17	Fisher Scientific
L-Glutamine	BE17-605E	Lonza
L-Proline	P5607	Sigma-Aldrich
Methanol	M/3900/17	Fisher Scientific
Cryopreserved human bone marrow mononuclear cells (MNCs)	2M-125B	Lonza
Magnesium sulphate	M-5921	Sigma-Aldrich

Nerve Growth Factor 7S (NGF 7S, murine, natural)	13290-010	Thermo-fisher
Non-essential amino acids	BE13-114E	Lonza
Nonenyl Succinic Anhydride	AGR1054	Agar Scientific
Magnesium chloride	M-8266	Sigma-Aldrich
Oil Red O	O-0625	Sigma-Aldrich
Osmium Tetroxide	AGR1015	Agar Scientific
RNase, DNase-free	11119915001	Sigma-Aldrich
Paraformaldehyde	P-0840-53	Fisher Scientific
Penicillin, streptomycin, amphotericin B	BE17-745E	Lonza
Phosphate buffered saline	BE17-516F	Lonza
Phycoerythrin-conjugated CD105 antibody	130-098-845	Miltenyi Biotec
Phycoerythrin-conjugated CD14 antibody	130-098-167	Miltenyi Biotec
Phycoerythrin-conjugated CD19antibody	130-098-168	Miltenyi Biotec
Phycoerythrin-conjugated CD34 antibody	130-098-140	Miltenyi Biotec
Phycoerythrin-conjugated CD45 antibody	130-098-141	Miltenyi Biotec
Phycoerythrin-conjugated CD73 antibody	130-097-932	Miltenyi Biotec
Phycoerythrin-conjugated CD90 antibody	130-098-906	Miltenyi Biotec

Phycoerythrin-conjugated HLA-DR antibody	130-098-177	Miltenyi Biotec
Phycoerythrin-conjugated IgG1 antibody	130-098-849	Miltenyi Biotec
Potassium chloride	P9333	Sigma-Aldrich
Potassium phosphate	PHR 1330	Sigma-Aldrich
Propidium iodide	81845	Sigma-Aldrich
Quantifast SYBR green RT-PCR kit	204141	Qiagen
Synapsin I Antibody	PPS062	R&D Systems
Sodium bicarbonate	S-7277	Sigma-Aldrich
TAE Buffer	B49	Thermo-fisher
Taq PCR Master Mix Kit	201443	Qiagen
Transforming growth factor β3	100-36E	Peprotech
Tris HCl	T3253	Sigma
Tris Base	93352	Sigma
Triton X-100	9002-93-1	Sigma-Aldrich
Trypan blue	T8154	Sigma-Aldrich
Trypsin	15090	Life Technologies
Tween 20	66368	Analar

Ultrapure distilled water DNAse RNAse free	10977-035	Gibco

2.2. General cell culture and experiments

2.2.1. PC12

2.2.1.1. PC12 thawing and culture

PC12 cells were obtained commercially from (Sigma Aldrich-88022401-1VL). PC12 culture medium comprised DMEM (Sigma-Aldrich, Cat. No. D5796), 5% horse serum (Sigma-H1270), 5% foetal bovine serum (FBS), and 1% Penicillin-Streptomycin (BE17-745E). To establish culture a cryopreserved vial of PC12 cells were rapidly thawed in a 37^{o}C water bath for 2 minutes, decanted into 15 ml of fresh media, then cells spun down for 3 minutes at 300 x g, the supernatant removed, and the cell pellet resuspended in 7.5 ml media which was decanted into a T25 flask and the flask placed into a humidified 37^{o}C incubator with a 5% CO_2.

2.2.1.2. Cryopreservation of PC12

For cryopreservation PC12 cells were first counted, centrifuged at 300 x g for 3 minutes, supernatant removed, and the cell pellet resuspended at 1x10^{6} cells/ml freezing solution. The freezing solution was composed of 10% (v/v) DMSO, 70% DMEM and 20% FBS. The cell/freezing solution was then decanted into a 1.5 ml cryovial before being placed in a Mr Frosty TM (Nalgene®), a vessel filled with isopropanol, for controlled cooling to – 80oC overnight, before transferring into liquid nitrogen storage. The following day the cryovial was transferred into liquid nitrogen for long term storage.

2.2.1.3. PC12 media changes and passaging

Media was changed every 48 hrs by first performing centrifugation of cells and media at 300 x g for 3 minutes followed by removal of 1/3 supernatant and replacement with fresh culture medium. For passage cell pellets were resuspended in fresh media, counted, and seeded at a density of $4x10^4$ cell/ ml into either a standard 21% oxygen incubator, a 2% oxygen incubator, or a 2% oxygen workstation (see Section 2.2.1.5).

2.2.1.4. PC12 cell counting

The PC12 cell suspension was centrifuged for 3 minutes at 300 x g, reconstituted with 1ml of fresh media, 10 µl of cell suspension removed, mixed with 10 µl of trypan blue and counted with the Countess® Automated Cell Counting Platform system (Figure 2.1). This system provides an automated cell count and viability measurement using trypan blue staining combined with advanced image analysis. Following cell suspension mixing with trypan blue cells were loaded onto the chamber slide. Prior to use the Countess required optimisation for each cell type with reference to sensitivity, minimal size, maximal size and circularity parameters. The optimisation process was started by first choosing the cell count mode on the setting screen (Figure 2.2.A) followed by selection of the parameters button (Figure 2.2.B). With the parameters screen open the above parameters can be adjusted, the protocol named, and saved. The protocol can then be readily recalled and applied (Figure 2.2.C). Loaded slides were then inserted into the machine and the cell count button pressed on the touch screen.

Figure 2.1. Countess® Automated Cell Counting Platform system

Countess Cell counter Invitrogen (MP10227) is equipped with a camera (2.3X objective and 3.1 mega pixel) for image acquisition and Countess™ Software to for subsequent analysis. (A). Countess Cell counter chamber slide is a plastic disposable that holds the sample in two separate chambers for replication. The counting process occurs in the central location of the counting chamber. The entire volume of cells counted is 0.4 µl, the same as counting four (1 mm × 1 mm) squares in a standard haemocytometer (B) (Invitrogen Catalogue number C10227).

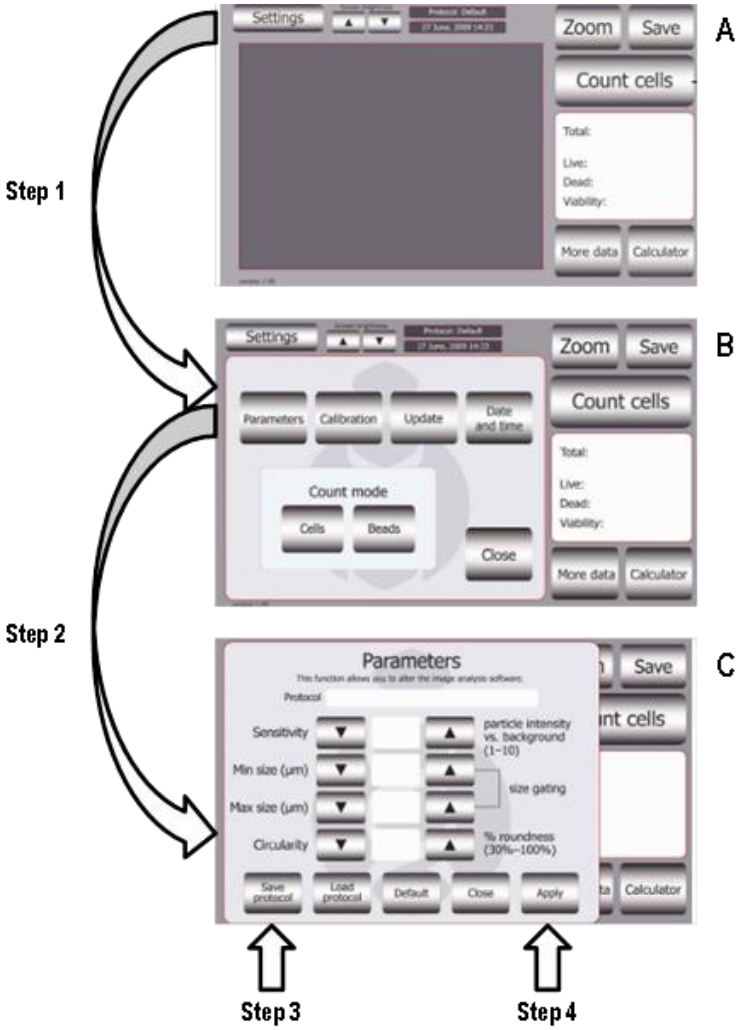

Figure 2.2. Optimisation of Countess® Automated Cell Counting Platform system

After switching on the home screen appears (A), the setting button is selected opening the setting screen (B), the parameters button is then selected (C), which contains the sensitivity, minimal size, maximal size and circularity options. Once determined the save button records the protocol for further use (Invitrogen Catalogue number C10227).

As outlined above automatic image acquisition was used to generate cell count and viability data. Cell number/ml, Live and dead cell number/ml, and Viability (% live/dead) data is generated (Figure 2.3).

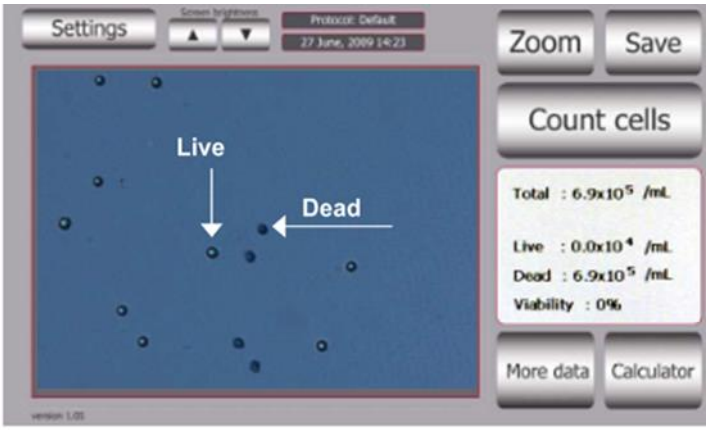

Figure 2.3. Countess Cell counter result screen

After optimisation of machine and chamber slide loading the Count cell button is pressed and the results screen generated showing the total number of the cells / ml, live and dead cells/ml, and viability (%). Picture edited from Invitrogen (Catalogue number C10227).

To standardise a PC12 cell suspension was centrifuged for 3 minutes at 300 x g, reconstituted with 1 ml of fresh media and 20 µl of cell suspension removed and mixed with 20 µl of trypan blue. 10 µl of the cell/trypan blue mixture was counted using a Neubauer haemocytometer by placing 10 µl of cell-trypan blue suspension under the coverslip of the haemocytometer via capillary action. Cells were then counted under a light microscope (x 10 lenses) (Figure 2.4). A mean cell count was calculated by counting cell numbers in the 4 x 4 corner regions to indicate cell numbers in each 0.1 µl of suspension, divided by 4 to generate an average, cell number multiple by 10^4 followed by the dilution factor for trypan blue to identify cells/ml. The remaining 10 µl of cell/trypan blue solution was counted using the Countess® Automated Cell Counting Platform software. The Countess was standardisation via comparison to the standard haemocytometer counting technique.

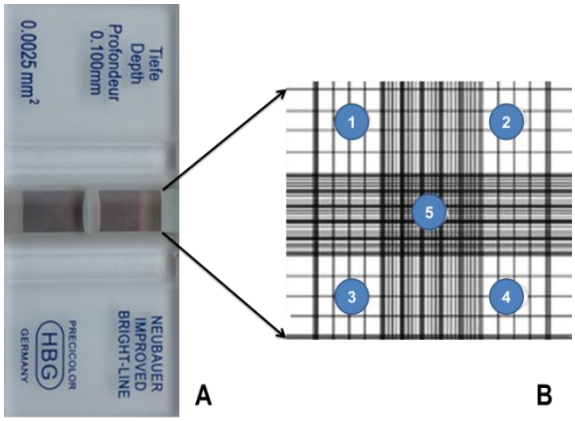

Figure 2.4. Neubauer haemocytometer

Neubauer haemocytometer is an enclosed chamber with two ports for sample introduction. The chamber contains precisely spaced lines in a grid pattern. There are two counting chambers per slide for replicates (A). Diagram count chamber of haemocytometer indicating the set of 16 squares that should be used for counting (B).

Cell counts obtained with the haemocytometer revealed no significant differences to those obtained with the Countess at any time point over a 96 hrs growth period. Haemocytometer-derived cell counts increased from 4 x 10^4/ml at 0 hrs to 6.7 x 10^4/ml at 24 hrs, and 9.5 x 10^4/ml, 18.6 x 10^4/ml, and 20 x 10^4/ml at 48 hrs, 72 hrs, and 96 hrs, respectively. Similarly, Countess-derived cell counts increased from 4 x 10^4/ml at 0 hrs to 6.9 x 10^4/ml at 24 hrs, and 11 x 10^4/ml, 18 x 10^4/ml, and 20.6 x 10^4/ml at 48 hrs, 72 hrs, and 96 hrs, respectively. Rates of increase and final cell numbers were broadly similar (Figure 2.5).

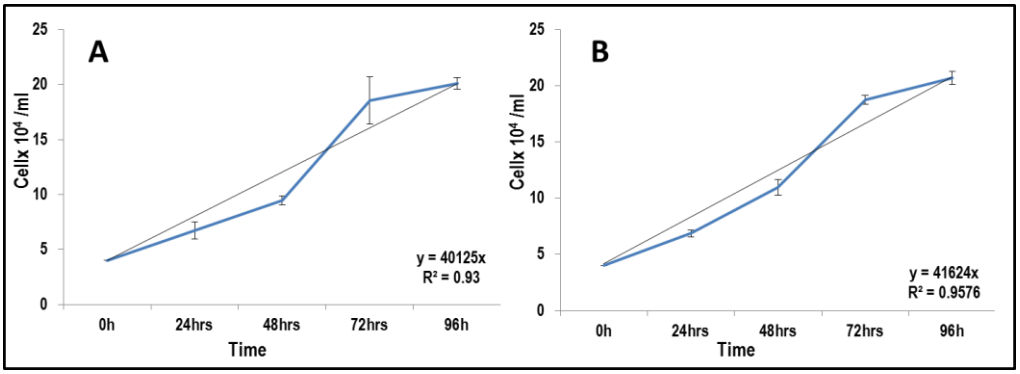

Figure 2.5. Standardisation of Countess® Automated Cell Counter to the standard haemocytometer counting technique

PC12 cells were seeded in T25 flasks at a density of 4x10^4 and cells counted every 24 hrs using both cell counting techniques. (A) Cell count using haemocytometer. (B) Cell count using Countess® Automated Cell Counter. x-axis represents time (hrs), y-axis represents cell x10^4 / ml. n=3, error bars indicate ± standard deviation.

2.2.1.5. Alternate oxygen level culture conditions

Alternate oxygen conditions were supplied by seeding cells into a standard cell culture incubator (Panasonic MCO-18AC-EP) which represents air oxygen, for intermittent hypoxia (2% O_2) a tri-gas incubator was used (Panasonic MCO-19M-PE) and the oxygen change as result of the incubator door opening (not more 5 min./ open). This condition aimed to mimic hypoxia/reoxygenation found after ischaemia *in vivo*. finally, a continuous normoxic environment (2% O_2) was created via a hermetic workstation with controllable oxygen levels (SCI-TIVE, Baker Ruskinn) (Figure 2.6).

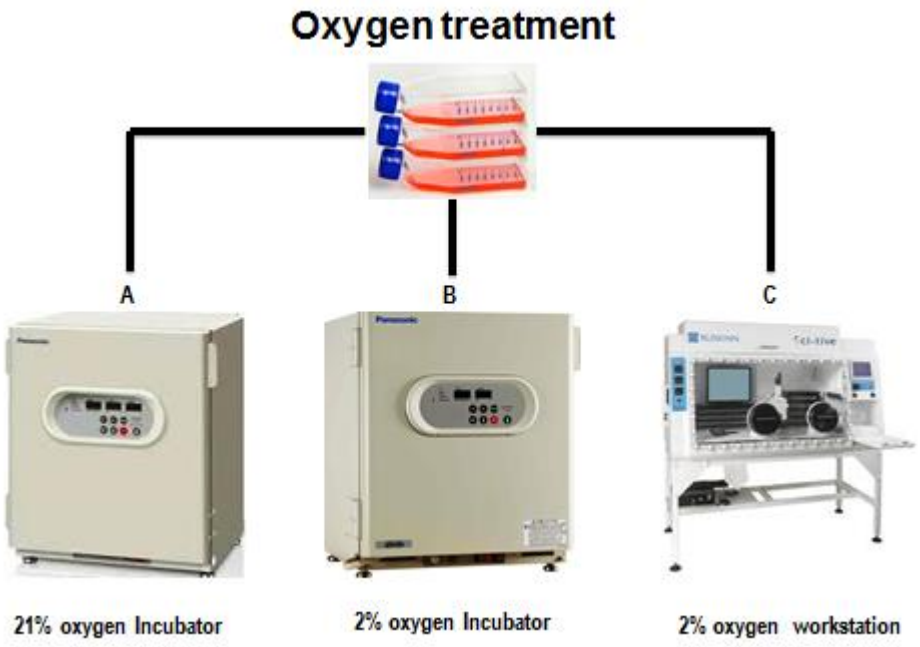

Figure 2.6. Oxygen level control methods

Different oxygen levels and control was achieved using different type of incubators. Air oxygen(A), intermittent hypoxia (2% O_2) (B) and a continuous normoxic environment (C).

2.2.1.6. PC12 metabolic activity

To determine metabolic activity the MTT (3-(4,5-dimethylthiazol-2yl)-2,5diphenyltetrazolium bromide) assay was performed. PC12 cells were first mixed by pipetting, and then centrifuged for 3 minutes at 300 x g, and cells re-suspended in 1 ml of fresh medium before being counted and diluted to allow a seeding density of 6 x10^3 cells / 150 µl in a 96 well plate in fresh medium. PC12 cells were then incubated at each oxygen level for 24, 48, 72 and 96 hrs. Following incubation media was replaced with fresh containing 10 µl of MTT solution (5mg /ml) and incubated at 37 ^{o}C for 3 hrs in the incubator. After incubation 50 µl of 1:1 DMSO: Isopropanol solution was added to each well followed by incubation for a further 45 minutes. Following on from the second incubation the contents of the well were mixed well by pipetting up and down before being placed into Synergy HT Multi-Detection Microplate Reader (BioTek Instruments) and read

at 570 nm (Figure 2.7). MTT controls included media only, media and cells, solubilising buffer.

2.2.1.7. PC12 cell cycle

To measure the cell cycle PC12 cells were seeded at a density of $4x10^4$ cell/ml, flasks positioned vertically, and incubated for 24, 48, 72 and 96 hrs. Following incubation, cells were centrifuged for 3 minutes at 300 x g at 4°C. The supernatant was aspirated from the pellet of cells and 2ml of ice cold 70% ethanol added slowly to the sample with vortexing. Samples were either used immediately or stored at - 20°C till needed. Before use cells were spun down for 5 minutes at 500 x g, ethanol aspirated from the cells and then washed with 1ml PBS, vortexed gently and then washed and centrifuged again for 5 minutes at 500 x g at 4°C. This was repeated twice. Following centrifugation cells were re-suspended in 200 µl solution of 50 µg/ml propidium iodide (PI) with 50µl of ribonuclease solution (100 µg/ml in distilled water) solution, incubated in the dark for 30-45 minutes before having fluorescence measured via a Cytomics FC500 flow cytometer (Beckman Coulter). The machine was started, software opened, cell sample placed in 10 ml flow tube after filtration with a muslin cloth. Voltages for fluorescence channels were set using an unstained sample and forward scatter (FS) and side scatter (SS) adjusted to clearly delineate the cell population. Dead cells, clumps and debris were excluded by gating. Doublets were then excluded through a gating in a dot plot of FL3 versus Log forward scatter, so that only the gated population was visible in the histogram. 10,000 events were acquired on flow cytometer. Data was analysed with FCS Express 5 (De Novo Software). DNA histograms were then generated for each sample and data presented as a percentage of cell in each phase (Figure 2.7).

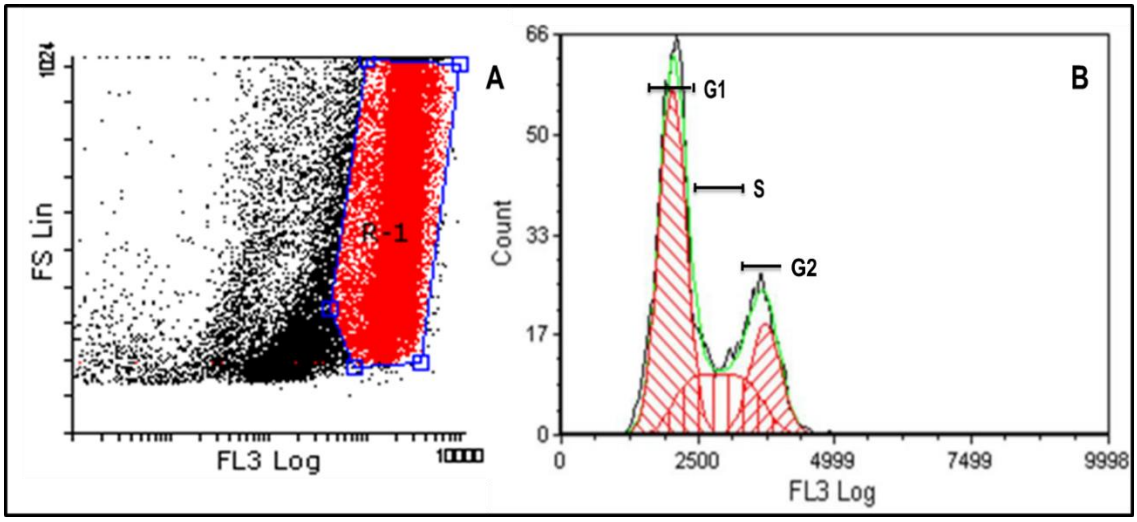

Figure 2.7. Cell cycle analysis for the PC12 cell line

(A) Representative flow cytometry analysis of the cell-cycle displaying the initial dot plot of FS versus FL3 where red dots represent gate cells. (B) Histogram represents cells at different cell cycle phases; G1, S and G2.

2.2.1.8. PC12 apoptosis

PC12 cells were seeded at a density of $4x10^4$ cell/ml, flasks positioned vertically, and cells incubated for 24, 48, 72 and 96 hrs (Figure 2.6). Following incubation cells were collected, centrifuged for 3 minutes at 300 x g, supernatant removed, and the cell pellet washed with PBS, before being centrifuged for a further 3 minutes at 300 x g. Cells were then re-suspended in Annexin-V binding buffer (10 mM HEPES, 140 mM NaCl, 2.5 mM $CaCl_2$), cells centrifuged again for 3 minutes at 300 x g, the supernatant removed and 10 µl of 1 µg/ml Annexin-V added before a 15 minutes incubation at room temperature in the dark. After incubation cells were washed with 500 µl of Annexin-V binding buffer, cells centrifuged at 300 x g for 3 minutes, supernatant removed, and another 500 µl of annexin-V binding buffer added before mixing with 10 µg/ml propidium iodide. Subsequently, the Cytomics FC500 flow cytometer (Beckman Coulter) machine was started, software opened, and the cell sample placed into a 10 ml flow tube following filtration with muslin cloth. Voltages for fluorescence channels were set using an unstained sample where FS and SS were adjusted to clearly delineate the cell population. A dot plot of FL3 (for PI)

versus FL1 (for Annexin-V) was then drawn (Figure 2.8). At least 20,000 events were collected per sample. Data was analysed with Flowing (Turku Centre for Biotechnology). Data is presented as a percentage of live, early apoptosis, late apoptosis, and necrotising cells. Negative controls were unstained cells, positive control cells were obtained by incubating cells at 55°C for 10 minutes.

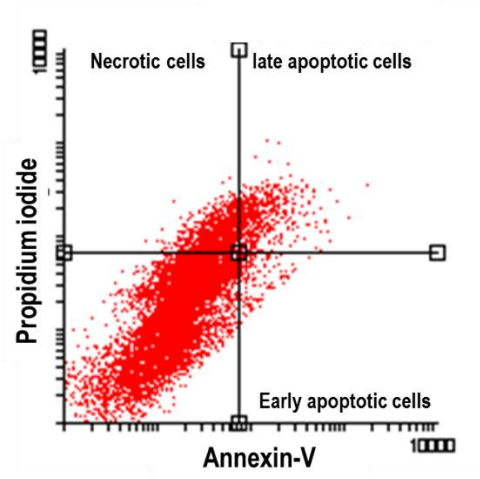

Figure 2.8. Annexin-V scatter plot

A representative scatter plot of PC12 cells stained with Annexin-V and PI measured with the Cytomics FC500 flow cytometer (Beckman Coulter). Data analysis performed with Flowing software (Turku Centre for Biotechnology).

2.2.1.9. Neurite outgrowth differentiation

PC12 cells were plated at a seeding density of 10^4 cells/ml into 24-well plates coated with collagen type IV. Coating was achieved by mixing lyophilised collagen type IV with 5 ml PBS until dissolved. 200 µl of the collagen solution was then placed in each well and allowed to sit for 1 hr at room temperature; wells were then washed three times with PBS. For the first 24 hrs adherent cells were grown in DMEM after which media was replaced with DMEM containing 5% FBS and 1% horse serum and incubated for a further 24 hrs. Fresh media supplemented with 100 ng/ml NGF7S was then added and over the next 7-10 days media changed every 48 hrs. Images were recorded using the Nikon Eclipse Ti microscope via a D5-Fil camera on NIS Elements software (Nikon).

2.2.1.10. Immunohistochemistry staining of PC12 differentiated using Synapsin-1 and GAP-43

Cells were washed with PBS, fixed with cold 4% paraformaldehyde for 25 minutes, and permeabilised with 0.1% PBS-Tween for 20 minutes before incubation in 1% bovine serum albumin blocking solution (Sigma, UK). Following incubation cells were again washed with PBS and fixed cells exposed to either 100 µl of synapsin1 primary antibody (R&D system) (1:2000) dilution or 100 µl of GAP-43 primary antibody (Novus Bio) (1:1000 dilution). Cells were then incubated in the dark for 3 hrs at room temperature. Following incubation cells were first washed with PBS and then incubated with 100 µl secondary antibody (donkey anti-mouse IgG-FITC and donkey anti-rabbit IgG-FITC for Synapsin-1 and GAP-43 respectively) (1:200 dilution) overnight in the dark before being washed with PBS. Cells were then stained with DAPI (50 ug/ml in PBS) for 5 minutes, DAPI removed, and cells washed with PBS 3 X 3 minutes each. The plate was then covered with aluminium foil until ready for imaging. Images were recorded on a Nikon Eclipse Ti inverted fluorescence microscope using a D5-Fil camera (Nikon) and NIS Elements software manufacturer (Nikon).

2.2.1.11. Mitochondrial burden and Action potential

PC12 cells were seeded into T25 flasks at density of $4x10^4$ cells/ml for 24, 48, 72 and 96 hrs. For experimental use cells were first mixed well by pipetting up and down before being transferred into a 15 ml tube and centrifuged for 3 minutes at 300 x g. After centrifugation media was aspirated off and replaced by fresh media supplemented by different concentrations of either MitoTracker® Green FM (Thermo Fisher) (5, 10, 50, 100, 200, 400 and 800 nM) or MitoTracker® Red FM (Thermo Fisher) (2.5, 5, 10, 25, 50, 100 and 200 nM) and cells incubated for 20 minutes. After incubation cells were washed with PBS and analysed on the Cytomics FC500 flow cytometer (Beckman Coulter). A minimum of 10,000 events were collected per sample. Data was analysed with Flowing software

(Turku Centre for Biotechnology). Analysis showed that 100 nM of MitoTracker® Green FM (Thermo Fisher) (mitochondrial burden) and 25 nM of MitoTracker® Red FM (Thermo Fisher) (mitochondrial membrane action potential), represented the values where a labelling plateau was encountered. (Figure 2.9).

The next step was ensuring that compensation could be performed where dual MitoTracker sample labelling was applied to avoid bleeding across channels. This was performed by ensuring that the median of the negative population was equal to the median of the positive population in the spill over channels. Voltage channels were first set for fluorescence channels using an unstained sample and FS/SS adjusted to clearly delineate the cell population clearly, gating was then applied to exclude dead cells, clumps and debris. Compensation was started from the red fluorochrome step-wise down to the green fluorochrome while checking the compensation in all channels.

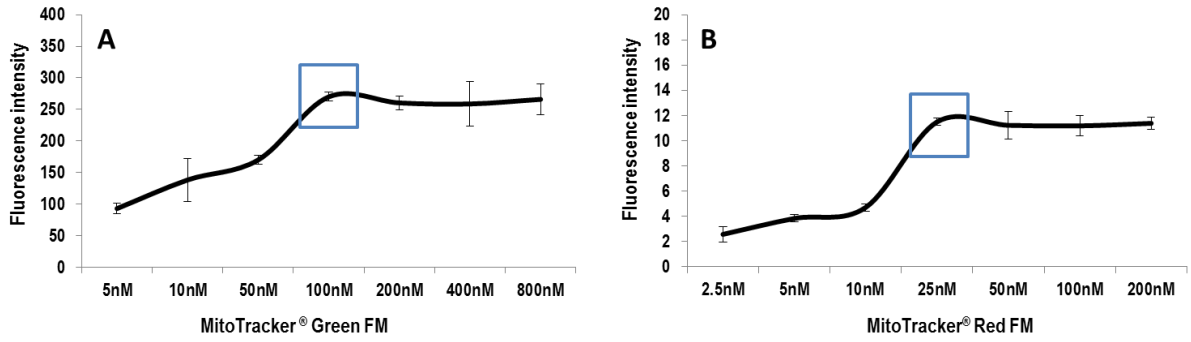

Figure 2.9. Standardisation of MitoTracker® Green FM and MitoTracker® Red FM concentrations

PC12 cells were used to determine the optimal concentration of both MitoTrackers. (A) Fluorescence intensity after treating cells with different concentrations of MitoTracker® Green FM (B) Fluorescence intensity after treating cells with different concentrations of MitoTracker® Red FM. The blue box represents the values where a labelling plateau was encountered. X-axis represent MitoTracker concentration (nM). Y-axis represents fluorescence intensity. Data represented as mean± SD.

2.2.1.12. Reactive oxygen species and nitroreductase activity measurement

Cells were seeded at $4x10^4$ cells /ml and incubated for 24, 48, 72 and 96 hrs for experimental use. For positive control purposes, the ROS inducer Pyocyanin (250 µM) and hypoxia mimetic (DFO) (200 µM) were introduced to cells followed by incubation under normal tissue culture conditions (37ºC, 5% CO_2). Pyocyanin and DFO were incubated for 30 minutes and 3.5 hrs, respectively. Unstained cells were used as negative controls. Cells were then resuspended (5x 10^5 cells) in 200 µL of ROS-ID® Hypoxia/Oxidative Stress Detection mixture comprising 6 µl of oxidative stress reagent (5 mM), 10 µl of nitroreductase detection agent (1 mM) in 10ml of 1x PBS for 30 minutes at 37^{o}C. After incubation, cells were washed with PBS and stored in the dark prior to analysis via Cytomics FC500 flow cytometer (Beckman Coulter). At least 10,000 events were collected per sample. Data was analysed using Flowing software (Turku Centre for Biotechnology).

2.2.1.13. Hypoxia inducible factor-1α and -2α subunit expression analysis

PC12 cells were seeded at $4x10^4$ cells /ml for and incubated for 24, 48, 72 and 96 hrs. Following incubation, the cells were fixed with 80% ice cold methanol for 5 minutes centrifuged for 3 minutes at 300 x g, and the methanol removed. Followed by permeabilisation with 0.1% PBS/Tween for 20 minutes cells were again centrifuged for 3 minutes at 300 x g, the permeabilisation solution removed and samples incubated in blocking solution consisting of 10% bovine serum albumin (Sigma, UK), 0.3 M glycine (Sigma, UK) supplemented with primary monoclonal antibodies for HIF-1α or HIF-2α (Abcam, USA) at concentration of 2 µg/$1x10^6$ cells and incubated for 30 minutes at 22ºC. The primary antibody-blocking solution was then removed via centrifugation at 300 x g for 3 minutes. The cells were then washed with PBS, centrifuged for 3 minutes at 300 x g, and then incubated with 500 µl of secondary antibody DyLight® 488 goat anti-mouse IgG (H+L) (Abcam, USA) (1/500 dilution) for 30 min at 22ºC. The isotype control antibody was

mouse IgG1. FC500 flow cytometer (Beckman Coulter) was used to analyse the samples. At least 10,000 events were collected per sample (Figure 2.10). Data was analysed using Flowing software (Turku Centre for Biotechnology).

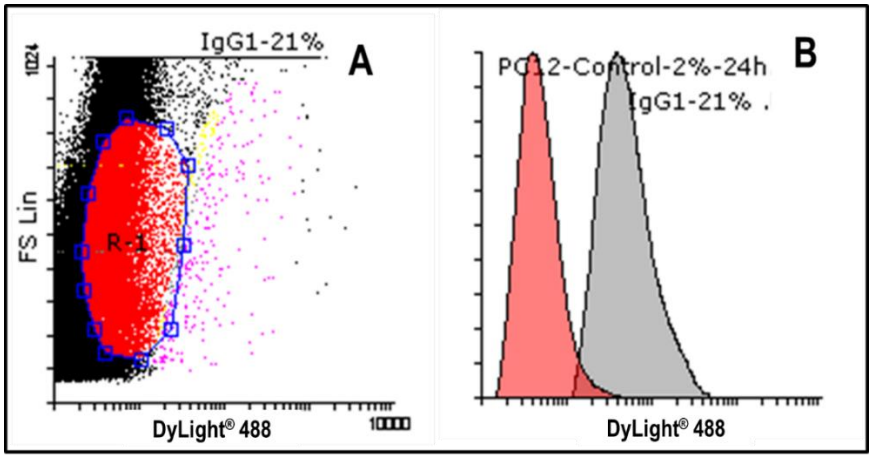

Figure 2.10. DyLight® 488 gating

Flow cytometer dot plot and histogram representing PC12 cells incubated with IgG1 control and primary monoclonal antibodies for HIF-1α or HIF-2α and secondary antibody DyLight® 488. (A) Dot plot of FS versus Log FL1. The red dots in R-1 gate represent the selected population. (B) Histogram represents FL1 where red indicates the fluorescence intensity of IgG1 (negative control) and grey represent cells positively stained with DyLight® 488. Data obtained from FC500 flow cytometer (Beckman Coulter) was used to analyse the samples. At least 10,000 events were collected per sample. Data was analysed using Flowing software (Turku Centre for Biotechnology).

2.2.2. hMSCs

2.2.2.1. hMSC isolation and culture from fresh bone marrow and cryopreserved mononuclear cells.

Human bone marrow cells were isolated from commercially sourced bone marrow (Caltag- Medsystems Ltd) following a modification of the plastic adherence technique described by D'Ippolito *et al.,* (2006) and refined by Kay *et al.,* (2015). Whole human bone marrow aspirate collected from the bilateral iliac crests of healthy donors was mixed with approximately 100 U of heparin/ml bone marrow aspirate and shipped. As soon as the bone marrow aspirate was received (usually between 48-72 hrs after aspiration) it was

seeded into flasks previously treated with 10 ng/ml fibronectin for 1hr at room temperature prior to being washed twice with complete media. Marrow was seeded at a density of $1x10^5$ mononuclear cells (MNC) /cm^2 based on the total cell number stated by the company (MNC equal 25-33% of total cell count). After calculating the required volume of bone marrow aspirate, the volume was completed to the desired volume with complete media composed of DMEM 4.5 g/L glucose with 5%(v/v) FBS, 2 mM L-glutamine (L-Glut), 1%(v/v) non-essential amino acids (NEAA) and 1%(v/v) penicillin, streptomycin and amphotericin B (100 U/ml penicillin, 100 µg/ml streptomycin, 0.25 µg/ml amphotericin B). After one week of culture 50% of media was gently removed and replaced with fresh antibiotic free media and after a further week 100% media change into antibiotic-free medium was performed, removing the majority of the remaining non-adherent leukocytes and erythrocytes. Following isolation, the media changes were carried out twice weekly with fresh media.

Commercially sourced MNC vials from Lonza Company were obtained from density separated cryopreserved, human bone marrow MNCs and stored in liquid nitrogen until required. Cell vials were rapidly thawed at 37°C in a water bath, contents transferred to a centrifuge tube of complete media (as for hMSC isolation from bone marrow) and centrifuged for 5 minutes at 250 x g. The supernatant was then aspirated, and cells re-suspended in complete media, counted and plated at $1x10^5$ MNCs /cm^2 and treated as for human bone marrow aspirate.

2.2.2.2. Cell Splitting and passaging

hMSCs were passaged by washing cells with PBS followed by the addition of 1-2.5 ml of 10% trypsin-EDTA (depend on flask size) and incubation in a 37^{o}C incubator until cells adopted a rounded-up morphology and were detached easily from the bottom of the flask by either gentle agitation or by a sharp knock to the side of the flask. Once detached the volume a five-fold excess of fresh media was added to inactivate trypsin and cells were centrifuged at 250 x g for 5 minutes. After centrifugation, the supernatant was aspirated,

and cells reconstituted with 1 ml fresh medium, 20 µl removed for counting and cells reseeded at the required density in fresh medium. hMSC were counted following enzymatic detachment from the flask surface with the Countess (see Section 2.2.1.4).

2.2.2.3. Cryopreservation

Cells were detached using trypsin-EDTA, centrifuged for 5 minutes at 250 x g, supernatant removed, and cells re-suspended in 1 ml of fresh media, 20 µl removed for cell count, centrifuged again for 5 minutes at 250 x g, supernatant again removed and cells re-suspended with freezing solution ($1x10^6$ cell/ml) and transferred into the cryovial. The freezing solution composed of 90% FBS and 10% (v/v) DMSO. The labelled cryovials were placed in a Mr Frosty ™ (Nalgene®) for controlled cooling to – 80°C overnight, before transferring into liquid nitrogen storage.

2.2.2.4. hMSCs metabolic activity

hMSCs were cultured in 24-well plates at a density of 6 $x10^3$ cell/well and incubated for 14 days 37°C in each oxygen condition with and witout HMAs treatment. After 14 days, cells were detached and the content of the well transferred into a sterile 1.5 ml sterile tube, centrifuged for 5 minutes at 250 x g, supernatant removed, and cells resuspended with 150 µl fresh media contain 10 µl of MTT solution (5mg /ml), transferred into to a 96 well plate and incubated for 3 hrs in a 37°C incubator. After incubation, MTT precipitate was solubilised using 50 µl of DMSO: isopropanol 1:1 mixture and samples incubated for a further 45 minutes at 37°C. After the last incubation period, the contents of the wells were mixed well by pipetting up and down before placing into the Synergy HT Multi-Detection Microplate Reader (BioTek Instruments) and read at 570 nm.

2.2.2.5. Colony forming unit firoblast assay

The number of colony was obtained by plating marrow into T25 flasks which previously treated with 10 ng/ml fibronectin for 1hr at room temperature prior to being washed twice with complete media. Aspirate was seeded at a density of $1x10^5$ mononuclear cells (MNC)

/cm^2 based on the total cell number stated by the company (MNC equal 25-33% of total cell count). Cells then leave to grow in standard MSCs culture media (section 2.2.2.2) for one week, then 50% of media was gently removed and replaced with fresh antibiotic free media and after a further week 100% media change into antibiotic-free medium was performed, removing the majority of the remaining non-adherent leukocytes and erythrocytes. Following isolation, cells washed with PBS, then 10 mL of a 0.5% crystal violet solution (Sigma) with methanol was added for 30 minutes. The cells washed with PBS and leaved to dryed over night then Images were recorded on a Nikon Eclipse Ti inverted fluorescence microscope using a D5-Fil camera (Nikon) and NIS Elements software manufacturer (Nikon).

2.2.2.6. hMSCs Cell cycle

hMSCs were cultured for 14 days at each oxygen condition (Figure 2.6). Following incubation period, cells detached and centrifuged at 250 x g for 5 minutes at 4°C. The supernatant was aspirated, and cells washed with 1 ml of ice cold 70% ethanol. These samples were either used directly or stored at - 20°C. For use ethanol was first aspirated after 5 minutes centrifugation at 300 x g at 4°C. A 200 µl solution of 50 µg/ml propidium iodide with 50 µl of ribonuclease solution (100 µg/ml in distilled water) was added and samples incubated in the dark for 30-45 minutes after which fluorescence measured via Cytomics FC500 flow cytometer (Beckman Coulter) as described in section 2.2.1.6. Data is presented as a percentage of cells in each phase.

2.2.2.6. hMSCs apoptosis

hMSCs were seeded and left to grow for 14 days at each oxygen condition. Cells were harvested and centrifuged for 5 minutes at 250 x g, PBS removed, and cell pellet re-suspended in 500 µl Annexin-V binding buffer, cells centrifuged for 5 minutes at 250 x g, supernatant removed and 10 µl of 1 µg/ml Annexin-V added and incubated for 15 minutes at room temperature in the dark. Cells were then washed with 500 ml of Annexin-V binding buffer and cells centrifuged at 250 x g for 5 minutes, supernatant removed, 500 µl

of Annexin-V binding buffer added, mixed with 10 µg/ml propidium iodide and measured with the Cytomics FC500 flow cytometer (Beckman Coulter) as described in section 2.2.1.8.

2.2.2.7. MSCs tri-lineage differentiation and characterisation

To determine differentiation potential, hMSCs were seeded at 2.5 x10^4/cm^2 in standard proliferation media overnight to allow attachment after which media was changed to differentiation media. Cells were then cultured in the appropriate differentiation media for 21 days with media changes every 3 days.

2.2.2.7.1. Chondrogenic differentiation

Monolayer chondrogenic differentiation was induced using media which consisted of low FBS 1% (v/v) DMEM supplemented with 1% (v/v) ITS, 1% (v/v) sodium pyruvate, 100 nM dexamethasone, 50 µM ascorbic acid phosphate, 40 µg/ml L-proline (Sigma-Aldrich) and 10 ng/ml TGF-β3. For staining cells were fixed with 95% methanol for 10 minutes, washed with PBS and stained with Alcian blue, as described in section 2.2.2.7.4.

2.2.2.7.2. Osteogenic differentiation

Osteogenic differentiation was induced using media supplemented with 50 µM ascorbic acid phosphate, 10 mM β-glycerophosphate and 100 nM dexamethasone for 21 days before monolayers were fixed with 95% methanol for 10 minutes, washed with PBS and stained with Alizarin Red S as per section 2.2.2.7.5.

2.2.2.7.3. Adipogenic differentiation

Adipogenesis was induced using media containing 500 nM dexamethasone, 500 µM 3-isobutyl-1-methylxanthine, 10 µg/ml insulin and 100µM indomethacin. Cells were fixed with 4% (w/v) paraformaldehyde in PBS for approximately 20 minutes washed with PBS and stained with Oil Red O for intracellular lipid droplets as described in section 2.2.2.7.6.

2.2.2.7.4. Alcian blue monolayer staining

Alcian blue 1% (w/v) was used to detect sulphated glycosaminoglycans on fixed monolayers. Alcian blue was prepared in 0.1 M HCl and passed through filter paper. To stain monolayers, fixed cells were washed with PBS before being covered with the Alcian blue stain overnight. The next day, the stain was removed and washed gently under running tap water until clear. Then stained monolayers were imaged.

2.2.2.7.5. Alizarin red S monolayer staining

Alizarin red S was used to detect mineralised calcium nodules in fixed monolayers. Alizarin red S of 2% (w/v) solution was prepared in distilled water (dH_2O) and filtered by filter paper. To stain monolayers, the fixed cells were washed with PBS before being covered with alizarin red S solution for 10 minutes. Then stain was removed, and monolayers washed gently under running tap water until clear. Wells were left to dry before imaging.

2.2.2.7.6. Oil Red O monolayer staining

Oil Red O stain was used to detect intracellular lipid droplets in the fixed monolayers. A saturated solution of Oil Red O was prepared as a stock solution using 300 mg of Oil Red O in 100 ml of 99% (v/v) isopropanol, this ensured maximum saturation of the solution and it was left at least 12 h before use. The working solution was prepared by mixing 40% of stock solution with 60% dH_2O (v/v) and filtered using a 0.22 µm syringe filter. The cell monolayer was washed with 350 µL of 60% isopropanol and then covered with the filtered Oil Red O working solution for 5 minutes after which the stain was removed, and the well rapidly washed once with PBS before imaging.

2.2.2.7.7. Immunostaining of BM-hMSCs tri-lineage differentiation after incubation at three oxygen culture conditions after treatment with HMAs

For detection of adipocytes differentiation goat anti-mouse FABP4 Antigen. Goat anti-human Aggrecan antigen used to detect chondrocytes differentiation, and a mouse anti-human Osteocalcin was used to detect osteocytes differentiation for confirm the differentiation status. The chondrocyctes and osteocytes were stained using the Northern LightsTM 557-conjugated Donkey anti-goat (Catalog #NL001; red) while adipocytes were stained with Anti-Mouse (Catalog #NL007; red) IgG secondary antibodies, and the nuclei were counterstained with DAPI (blue).

2.2.2.8. Characterisation of MSCs (Flow cytometry)

hMSCs were grown for 14 days at each oxygen conditions, cells washed with PBS and detached using 10% trypsin- EDTA at 37^{o}C incubator until cells were rounded up and detached easily. Media was added, and the cell suspension centrifuged for 5 minutes at 250 x g, counted, and re-suspended in flow cytometry buffer (0.5% (w/v) BSA and 2 mM EDTA in PBS) and aliquoted in 1.5 ml micro-centrifuge tubes at 1 x 10^5 cells/ tube, centrifuged again at 250 g for 5 minutes and the supernatant discarded. Phycoerythrin (PE) conjugated antibodies (CD14, CD19, CD34, CD45, CD73, CD90 and CD105, HLA-DR, IgG1 and IgG2a isotype controls) were diluted in 1:11 with flow cytometry buffer to a total volume of 1 ml and cell pellets re-suspended in the appropriate antibody solution and incubated in the dark for 15 minutes at 4 °C. Buffer was then added to stained cells to a total volume of 1 ml and cells centrifuged at 250 g for 5 minutes, supernatant s discarded and the cells re-suspended in 300 µL of flow cytometry buffer. At least 5000 events were acquired on a Cytomics FC500 flow cytometer (Beckman Coulter). Cell samples were placed into a 10 ml flow tube after filtration with muslin cloth. Voltages were set for fluorescence channels using an unstained sample and FS/SS adjusted to make clearly delineate the cell population. An PE versus Log FS dot plot was then gated to exclude dead cells, clumps and debris. Data were analysed using Flowing software (Turku Centre

for Biotechnology). Gates were used to exclude 99% of the appropriate isotype control events and determined the percentage positive events.

2.2.2.9. Mitochondrial burden and Action potential

hMSCs seeded 15 x 10^4 cell / flask were seeded and incubated for 14 days at the three oxygen conditions. After 14 days media was removed, and mitochondria labelled with a mixture of 100 nM MitoTracker® Green FM (Thermo fisher) and 25 nM MitoTracker® Red FM (Thermo fisher) in fresh culture medium. Cells were then incubated for 20 minutes at 37°C covered with aluminium foil before fixing with 4% paraformaldehyde in PBS for 20 minutes at room temperature (RT). Fixed cells were washed with PBS, detached using cell scraper, and kept in the dark until analysis on the Cytomics FC500 flow cytometer (Beckman Coulter). Cell samples were placed into a 10 ml flow tube after filtration with muslin cloth. Voltages for fluorescence channels were adjusted using an unstained sample; FS and scatters determined for cell population visualisation. An FL1 or FL2 versus Log FS dot plot was drawn and data analysed using Flowing software (Turku Centre for Biotechnology). At least 10,000 events were collected per sample.

2.2.2.10. Reactive oxygen species and nitroreductase activity measurement

hMSCs were cultured and detached as described above. Cells were then resuspended in fresh media supplemented with 200 µL of ROS-ID® Hypoxia/Oxidative Stress Detection mixture (6 µl of oxidative stress reagent (5 mM), 10µl of nitroreductase detection agent (1mM) in 10ml PBS) for 30 minutes at 37°C. After incubation, cells were washed with PBS, detached and kept in the dark until ready for analysis on the Cytomics FC500 flow cytometer (Beckman Coulter). Cell samples were placed in a 10 ml flow tube after filtration with muslin cloth. Voltages for fluorescence channels adjusted using an unstained sample; FS and FS for cell population visualisation. An FL1 or FL3 versus Log FS dot plot was drawn and data analysed using Flowing software (Turku Centre for Biotechnology). At least 10,000 events were collected per sample.

2.2.2.11. Hypoxia inducible factor-1α and -2α subunit expression analysis

hMSCs were cultured for 14 days in the three oxygen conditions. Cells were washed with PBS, detached transferred to a 15 ml tube and centrifuged for 5 minutes at 250 x g. Supernatant was then removed and cells fixed with 80% ice cold methanol for 5 minutes, centrifuged again for 5 minutes at 250 x g, methanol removed, permeabilised with 0.1% PBS-Tween for 20 minutes, and permeabilisation solution removed after centrifugation for 5 minutes at 250 x g. Cells were incubated in blocking solution (10% bovine serum albumin (Sigma, UK), 0.3 M glycine (Sigma, UK)) supplemented with mouse monoclonal HIF-1α or HIF-2α (Abcam, USA) antibody (2 µg/1x10^6 cells) and incubated for 30 minutes at 22ºC. Then primary antibody solution was removed, cells washed with PBS, and then incubated with 500 µl of secondary antibody DyLight® 488 goat anti-mouse IgG (H+L) (Abcam, USA) (1:500 dilution in PBS) for 30 min at 22ºC in the dark. Isotype control antibody was mouse IgG1 used under the same conditions. Acquisition of 10,000 events was performed. Data was analysed using Flowing software.

2.3. Preparation of hypoxia mimetic agents

A $CoCl_2$ stock solution (100 mM) was prepared by mixing 238 mg of $CoCl_2$ with 10 ml of deionised water. Two working solutions (10 and 1 mM) were prepared by further dilution. DFO stock solution (100 mM) was prepared by mixing 65.6 mg of DFO with 10 ml of deionised water, two working solutions (10 and 1 mM) were prepared by further dilutions. DMOG stock solution (100 mM) was prepared by mixing 50 mg DMOG powder with 2.8 ml of deionised water. Further dilutions of DMOG were freshly made with DW to prepare a working solution (10 mM) where 1 ml of stock solution was mixed with 9 ml of DW. IOX_2 stock solution (10 mM) was prepared by mixing 0.35234 µg of IOX_2 in 100 µl of warm DMSO and diluted with DW to the working solution concentration directly before use. All

solutions were filtered through a 0.2 µm filter and stored at 2-8°C. Toxicity testing for all was performed via MTT and cell counts across a range of dilutions. MTT.

2.4. Mitochondrial genome copy number (qPCR)

2.4.1. Extraction and quantification of mitochondrial DNA

Total DNA was isolated using the DNeasy Mini kit (Qiagen, UK). 1x 10^6 cell/ sample (PC12 or hMSCs) were lysed with 10% Proteinase K in PBS, 200 µl of buffer-AL, thoroughly vortexed and incubated for 10 minutes at 56 ^{o}C in a water bath. Following on from incubation 200 µl of molecular grade ethanol was added, samples thoroughly mixed and the resulting solution transferred to a DNeasy Mini spin column which was then centrifuged for 1 minute at 3500 x g. After centrifugation, the flow through was discarded leaving total DNA bound to the column membrane. Then column membrane was then washed with 500 µl of AW1 washing buffer and the column centrifuged at 3500 x g for 1 minute. The flow through was again discarded and 500 µl of AW2 washing buffer was added. The column was again centrifuged at 1100 x g for 3 minutes. The flow through was discarded. The column was then placed in a 1.5 ml tube. DNase & RNase-free water (50 µl) was carefully added to the centre of the spin column membrane and allowed to soak for 2 minutes. The column was then centrifuged for 1 min at 56 x g and the eluted DNA transferred to ice. DNA concentration was quantified using a Nano drop 2000 (Thermo Scientific, UK) and stored at -80°C until required.

2.4.2. Semi-quantitative polymerase chain reaction (PCR)

DNA was diluted before use with nuclease-free distilled water to a final concentration of 100 ng/µl. One step PCR was performed with *Taq* PCR Master Mix (Qiagen, UK). Following manufacturer's instructions, a master mix was first prepared which comprised of

6.25 µl reaction mix, 1.25 µl of each relevant primer (10 µmol), and 3.25 µl free nuclease water, per sample. Then 1 µl of diluted DNA was aliquoted into a 0.2 ml PCR tube on ice. Master mix was then added to each sample to give a final reaction volume of 12 µl. A no template negative control was included for all experiments.

PCR primers were designed using rat gene and human gene sequences from NCBI map viewer and designed using Primer3 open-source PCR primer design software and obtained from Invitrogen Ltd. (Paisley, UK). Designed primers were evaluated in NCBI Primer-BLAST to check specificity before being purchased from Invitrogen. Primer sequences and product sizes are listed in Table 2.2.

Table 2.2. PCR Primer sequences and product sizes

Primers	Sequence		Product size
Rattus Act b	Sense	TTGCCCTAGACTTCGAGCAA	213
	R	AGACTTACAGTGTGGCCTCC	
Rattus Gapdh	F	ACATGCACAGGGTACTTCGA	163
	R	TTACCCCAGCCTTCTCCATG	
Rattus mt-ND1	F	AGGACCATTCGCCCTATTCT	183
	R	GGGTAGGATGCTCGGATTCA	
Homosapiens ACTB	F	AACAGACTCCCCATCCCAAG	202
	R	CCAGAGGCGTACAGGGATAG	
Homo sapiens GAPDH	F	CGGGTCTTTGCAGTCGTATG	168
	R	CTGTTTCTGGGGACTAGGGG	
Homo sapiens mt-ND1	F	ATTATCGCCCCAACCCTCTC	191
	R	GCTCGTAGGGCTCCGAATAG	

PCR tubes and sample strips were then briefly centrifuged before being transferred to a Senso Quest Lab cycler (Geneflow) thermal cycler. The thermal cycler was programmed as listed in Table 2.3.

Table 2.3. Thermocycler programme

STEP	Thermal cycler programme
1	One cycle of 94 °C for 3 minutes (reverse transcription step).
2	Three cycles of 94 °C for 1 minutes (denature hot start antibodies and DNA melting).
3	35 cycles.
4	94 °C for 1minute (DNA melting).
5	Annealing temperature as appropriate for primer pair for 1 minute.
6	72 °C for 1 minute (DNA extension).
7	One cycle of 72 ^{o}C for 10 minutes.
8	15 °C ∞

2.4.3. Agarose Gel Electrophoresis

Following on from PCR amplification samples were fractionated on 2% agarose gel (4 g of agarose powder was dissolved in 200 ml 1x tris-acetate-EDTA (TAE) buffer (40 mM Tris Acetate, 2 mM Na_2 EDTA). Agarose was boiled in a microwave oven until clear and the, agarose solution immediately poured into a casting frame and a gel comb added. Ethidium bromide (0.7 µg/ml) was added to the dissolved agarose solution and mixed by swirling before being poured. After 1hr at room temperature, the gel had set and was ready to use. The gel was placed into the gel tank (Bio-Rad DNA Sub cell) and 5 µl of each PCR sample mixed with 5 µl of gel loading buffer (Sigma, UK) and then pipetted into the correct well. For comparison of fragment size, direct load wide range DNA marker (Sigma, UK) was also run. All gels were run for one hour at 100 V and were viewed using an Ultraviolet Trans illuminator using Syngene gel documentation system (Cambridge, UK).

2.4.4. Quantitative polymerase chain reaction (qPCR)

Relative gene expression was assessed using the QuantiTect SYBR Green PCR kit (Qiagen, UK). Replicate reactions for each gene of interest and for housekeeping genes were performed for each sample. To compare the gene expression difference among our samples the ΔΔCt were calculated. ΔCt value was calculated for each sample as the difference between the Ct for the gene of interest and the house keeping gene. ΔΔCt was measured as the difference between ΔCt values of an experimental sample and the control sample, the fold-change in gene expression was measured as $2^{-(\Delta\Delta Ct)}$.

Samples were prepared by adjusting the concentration of DNA to 100 ng/ml in a final volume of 3.5 µl of in nuclease free water and this volume placed into each experimental well of a chilled 96 PCR plate (Sigma, UK) and kept on ice till use. A master mix of 6.5 µl SYBR green, 0.5 µl of each relevant primer and 4 µl of Ultrapure distilled water DNAse RNAse free was prepared. Immediately before the transfer to the PCR machine 1 µl/sample of enzyme was added to the master mix thoroughly mixed, an optical adhesive cover (Thermo fisher, UK) used to seal the plate and then transferred to a Stratagene Mx3005P real time thermal cycler (Agilent Technologies, UK) using MxPro-3005P qPCR Software (Agilent Technologies, UK) The thermal cycler was programmed as shown in (Figure 2.11).

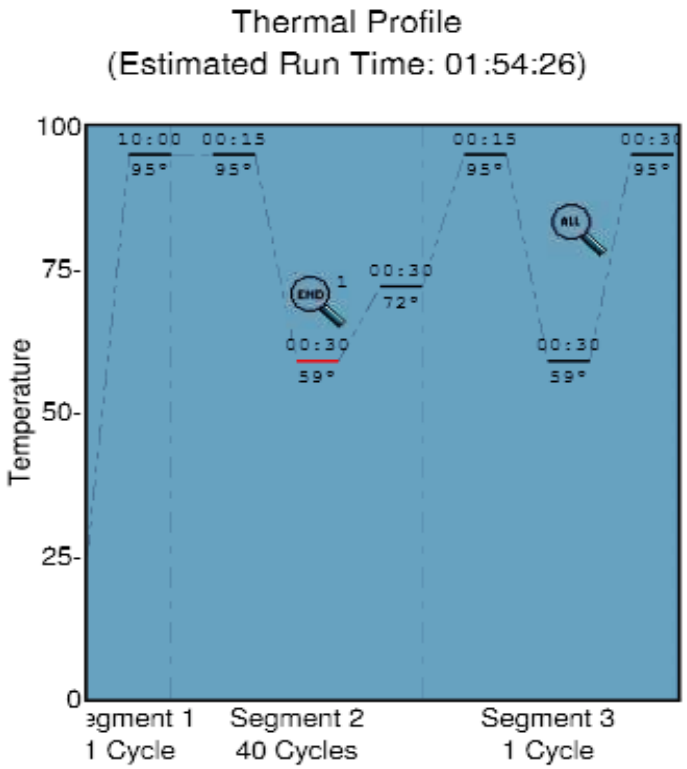

Figure 2.11. qPCR thermal cycle programme

Segment 1 corresponds to amplification of the product and segment 3 to the melt curve. Graph obtained from Stratagene Mx3005P real time thermal cycler (Agilent Technologies, UK) using MxPro-3005P qPCR Software (Agilent Technologies, UK)

2.5. Transmission Electron Microscope (TEM) study of MSCs ultrastructures

The cells were cultured under the three-oxygen condition for 14 days, washed with 2% (v/v) Glutaraldehyde in cacodylate buffer (pH 7.4) containing 2 mM $CaCl_2$ for half an hour at room temperature. Next cell samples were washed with 0.1 M cacodylate and then fixed in 1% (v/v) osmium tetroxide in 0.1 M cacodylate buffer for 1 hour before being washed in cacodylate buffer (pH 7.4) containing 2 mM $CaCl_2$. Cell samples were then dehydrated with different concentration of ethanol (70%, 80%, 90% and 100% respectively), put into epoxy resin (Alan Laboratories Ltd, Reading, UK), and implanted

into moulds. The resin was then polymerised at 60^{o}C for one day. Sectioning of polymerised resin was performed with a Reichert-Jung Ultra-cut E ultra-microtome (Leica Microsystems Nussloch GmbH Wetzlar, Germany).

The ultra-thin sections were stained in uranyl acetate made in ethanol (50% (v/v)), and then in Reynold's lead citrate. JEOL JEM-1230 transmission electron microscope (USA) was used for the visualisation of ultrathin sections. Images analysis using analysSIS® software (Olympus Soft Imaging Systems GMBH, Germany).

2.6. Statistical analysis

All data were expressed as mean ± SD, One-way ANOVA and post-hoc (Bonferroni) analysis were used to define changes in cell count and MTT activity after drug treatment at each time point. In addition, to examine the effect of concentration, time and the interaction between concentration and time on cell count. The mean difference is significant at the 95% level ($p < 0.05$).

Keele University

Chapter 3 : Effects of hypoxia mimetic agents on PC12

3.1. Introduction

PC12 cell is a pheochromocytoma cell line derived from *Rattus norvegicus*. It is a catecholamine-producing cell that synthesises, stores and releases dopamine and norepinephrine, similar to the chromaffin cells of the human adrenal medulla. PC12 has been extensively used as a neuronal model in neurochemical and neurobiological studies along with neuroblastoma SH-SY5Y cell line, ALS NSC-34 and NT2 cells (Greene & Tischler, 1976; Langlois & Duval, 1997; Madji Hounoum *et al.,* 2016; Xicoy *et al.,* 2017). PC12 cells differentiate in the presence of nerve growth factor (NGF) into neuronal cells that have properties of sympathetic neurons. Differentiated PC12 cells have axons and dendrites which are useful for neurite outgrowth assessment. PC12 cells grow rapidly *in vitro* and can be produced in large amounts, making them useful for studies where large quantities of cellular material may be required, for example protein-based assays. Of relevance to this thesis, PC12 cells have been used extensively to study oxygen-induced cellular changes due to their ease of culture (suspension), differentiation capacity, and appropriateness for stroke-related investigations. PC12 will proliferate or differentiate according to the mitogen stimulation that they receive. For example, epidermal growth factor (EGF) stimulates cells proliferation (Pennock & Wang, 2003), whereas nerve growth factor (NGF) tends to promote differentiation to sympathetic-like neurones (Aloe *et al.,* 2016). The longevity of the ERK stimulation is the main determinant for cellular fate where short ERK stimulation tends to promote continued cell division while more sustained ERK stimulation tends to encourage cellular differentiation (Kao *et al.,* 2001). Hypoxia is defined as an oxygen level less than that normally encountered by any given cell type (Semenza, 2010). Changes in oxygen levels, and specifically hypoxia, occur in many physiological and developmental processes, like in embryonic development. In addition, hypoxia can be considered to be both cause and effect for many pathological processes such as myocardial infarction and infection (Semenza, 2012). Changes in oxygen levels are typically reflected by changes in cellular events and processes. For example, hypoxia

has been shown to directly impact on various mitochondrial activities such as ATP production, ROS formation and enzyme activities. This is thought to be due to significant changes that occur at a gene expression level, in response to alterations in oxygenation (Solaini, 2010). Many studies suggest that cells respond to hypoxia through an evolutionary mechanism that is regulated, at least in part, by hypoxia-inducible factor (HIF-1α) (Majmundar *et al.,* 2010). HIF-1α appears to play a significant role in the regulation of many metabolic activities such as glucose haemostasis and lipid and amino acids metabolism. There is accumulating evidence, particularly in PC12 cells, that hypoxia and hypoxia-mimetic agents cause significant increases in the intracellular concentration of mitochondria-derived reactive oxygen species (ROS) (Crispo *et al.,* 2011; Lan *et al.,* 2011; Guo *et al.,* 2012). Hypoxia-mimetic agents exert their action by inhibiting prolyl-hydroxylase, an enzyme that regulates degradation of HIF-1α, which in turn regulates various transcription factors (Dengler *et al.,* 2014). The increased activity of HIF-1α has a positive effect on PC12 cell survival under hypoxic conditions. In this case, survival is thought to be facilitated by decreased inflammatory signalling, shifts in metabolism to glycolytic pathways, and activation of antioxidant mechanisms such as Nuclear factor E2-related factor 2 (Nrf2) (Kolamunne *et al.,* 2013; Zheng *et al.,* 2015). However, it is still unclear how hypoxia-mimetic agents affect mitochondrial function in PC12 cells. Indeed, few studies have investigated the effect of HMAs used concentrations on cell proliferation, metabolic activity, apoptosis, cell cycle ROS formation and nitroreductase activity in PC12 cells. The primary aim of this study is therefore to assess the *in vitro* effect of hypoxia-mimetic agents on PC12 cell viability under air oxygen culture conditions (21% O_2), intermittent 2% oxygen and continuous 2% culturing conditions (both at 2% O_2).

3.2. Methods

3.2.1. Materials

Molecular grade reagents and deionised water (Sigma, UK) were used. All chemicals used are listed in Chapter 2, Section 2.1.

3.2.2. Cell models

The PC12 cell line was cultured, maintained and passaged in suspension form as outlined in Chapter 2. Cells were maintained in a tissue culture incubator (as described in Chapter 2) using the following conditions: 37 °C, 5% CO_2 and 21% O_2 for air oxygen, and 37 °C, 5% CO_2 and 2% O_2 for intermittent hypoxia (IH) and continuous normoxia (CN) culture conditions.

3.3. Results

3.3.1. Effect of hypoxia mimetic agents on PC12 cell count and metabolic activity

Cell counts and metabolic activity (MTT) of PC12 cells were explored in the presence of HMAs. In this instance, cell count and MTT assay were being used as surrogate markers of cell viability. The aim of these experiments was to optimise HMA concentrations to a non-toxic dose for use in subsequent experiments. Cell count data is presented as number of cell x 10^4 and MTT data is presented as normalized to the corresponding experimental control. Cells were grown under air oxygen, intermittent hypoxia and continuous normoxic conditions in the presence or absence of hypoxia mimetic agents.

3.3.1.1. Determination of PC12 cell viability after treatment with different concentrations of $CoCl_2$ at different oxygen conditions.

Different oxygen conditions showed no significant effect on cell count over the 96 hrs. $CoCl_2$ induced no significant reductions in PC12 numbers at all concentrations tested in both AO and IH over 96 hrs. CN displayed increased sensitivity to $CoCl_2$ toxicity with significant reductions cell count was noted for concentrations ≥75 µM only. However, cells exposed to 50 µM $CoCl_2$ displayed the lowest reductions in cell counts across all oxygen conditions and time points. At this concentration (50 µM), cell count reductions were measured as 17%, 14%, 7% and 2% for air oxygen culture, 5%, 1%, 10% and 3% for IH culture, and 10%, followed by significant increase 21%, 37% and 40% for CN culture (at 24, 48, 72 and 96 hrs respectively) (Figure 3.1).

Different oxygen conditions showed no significant change on MTT activity over the 96 hrs. $CoCl_2$ induced significant reductions in MTT activity across all time-points and conditions tested except for 50 µM in CN (Figure 3.2). However, again similar to above cells exposed to 50 µM displayed the overall lowest levels of reductions in MTT activity of 8%, 9%, 8% and 14% for air oxygen, 13%, 15%, 25% and 29% for IH, and 3%, 4%, 5% and 5% for CN (at 24, 48, 72 and 96 hrs respectively) (Figure 3.2).

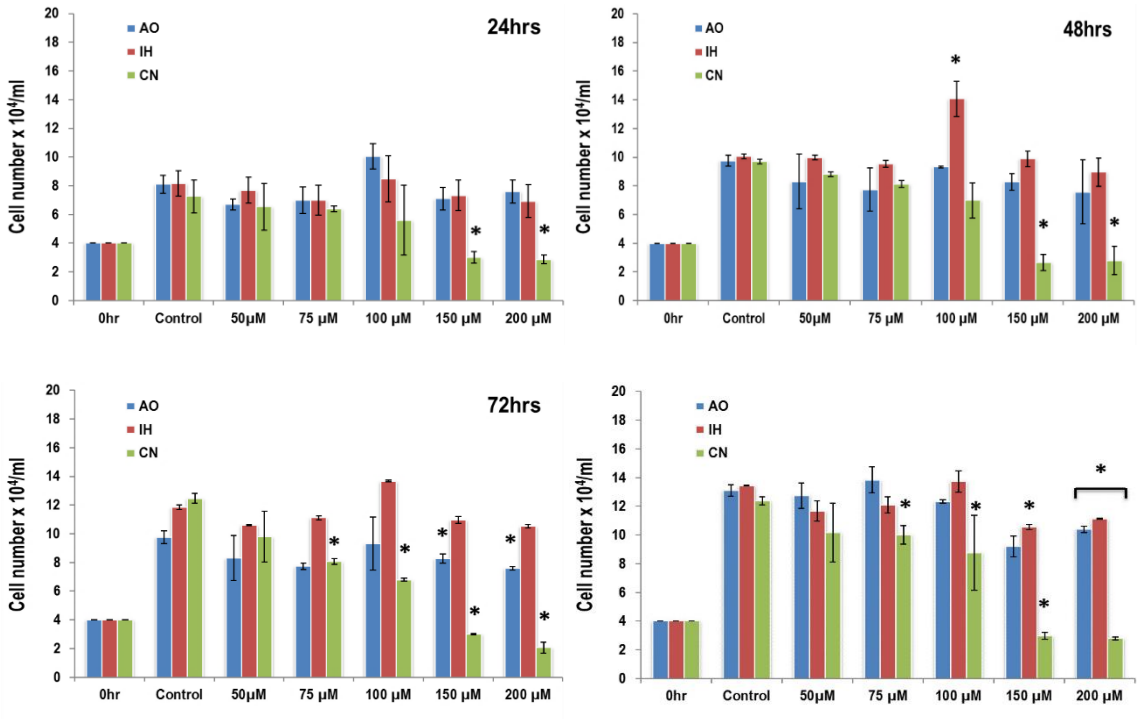

Figure 3.1. Effect of $CoCl_2$ on PC12 cell counts in different oxygen conditions

*Cell counts of PC12 cells at air oxygen (AO), intermittent hypoxia (IH), and continuous normoxia (CN) following exposure to different concentrations of $CoCl_2$ across a 96 hrs time-course. X-axis indicates different $CoCl_2$ concetration. Y-axis indicates cell number x10^4 / ml. Data are presented as mean ± standard deviation (SD). n=1 triplicate, * indicates significant change in comparison to control at each time point ($p<0.01$).*

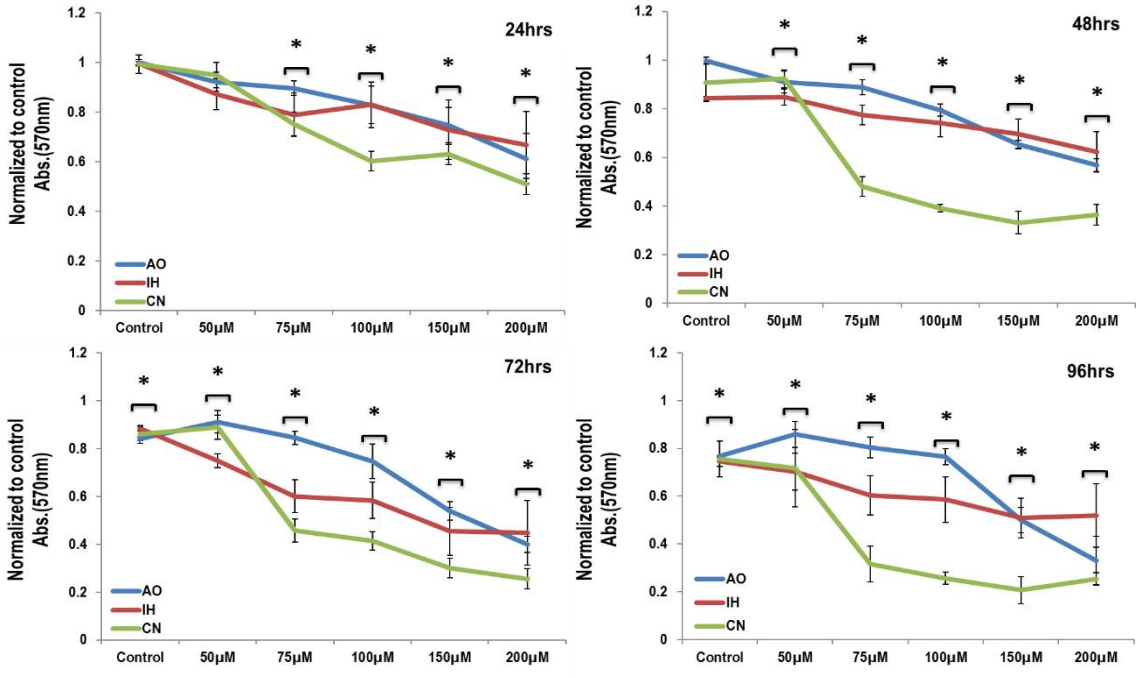

Figure 3.2. Effect of $CoCl_2$ on MTT activity of PC12 cultured in different oxygen conditions.

*MTT activity of PC12 cells at air oxygen (AO), intermittent hypoxia (IH), and continuous normoxia (CN) following exposure to different concentrations of $CoCl_2$ across a 96hrs time-course. X-axis indicates different $CoCl_2$ concetration. Y-axis indicates Abs. value normalized to Abs. of control at each time point. Data are normalized to untreated controls at each time point. n=1 triplicate, * indicates significant change in comparison to control at each time point ($p<0.01$).*

3.3.1.2. Determination of PC12 cell viability after treatment with different concentrations of DFO in different oxygen conditions

DFO induced significant reductions in PC12 numbers at all concentrations tested in both AO and CN over 96 hrs. IH displayed reduced sensitivity with significant reductions noted for concentrations ≥75 μM only (Figure 3.1). However, cells exposed to 50 μM DFO displayed the lowest reductions in cell counts across all oxygen conditions and time points. Cell count reductions were measured as 4%, 14%, 18% and 2% for AO culture, 3%, 6%, 3% and 14% for IH, and 23%, 17%, 37% and 26% for CN (at 24, 48, 72 and 96 hrs respectively) (Figure 3.3). Similarly, DFO significantly decreased metabolic activity, as measured by MTT assay, over the three oxygen conditions ($p<0.05$), at all time-points (24, 48, 72 and 96 hrs), and at all concentrations tested. However, similar again to above MTT activity displayed the least reductions at 50 μM with 5%, 14%, 21 and 17% for AO, 8%, 14%, 15% and 19% for IH, and 8%, 7%, 9% and 23% for CN (at 24, 48, 72 and 96 hrs respectively) (Figure 3.4).

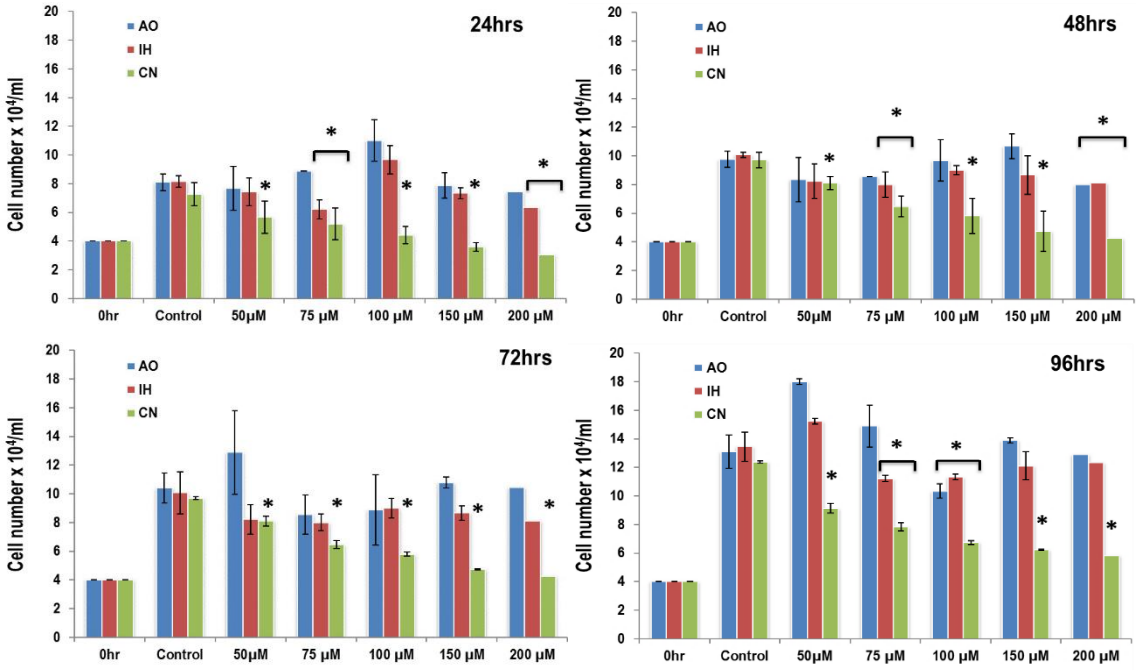

Figure 3.3. Effect of DFO effects on cell counts of PC12 cells cultured in different oxygen conditions

*Cell counts of PC12 cells at air oxygen (AO) (A), intermittent hypoxia (IH) (B), and continuous normoxia (CN) following exposure to different concentrations of DFO across a 96 hrs time-course. Y-axis indicates cell number x10^4/ ml. X-axis indicates different DFO concentrations. Data are presented as mean ± standard deviation (SD). n=1 triplicate, * indicate significant difference compared to control at beach time point (p<0.01).*

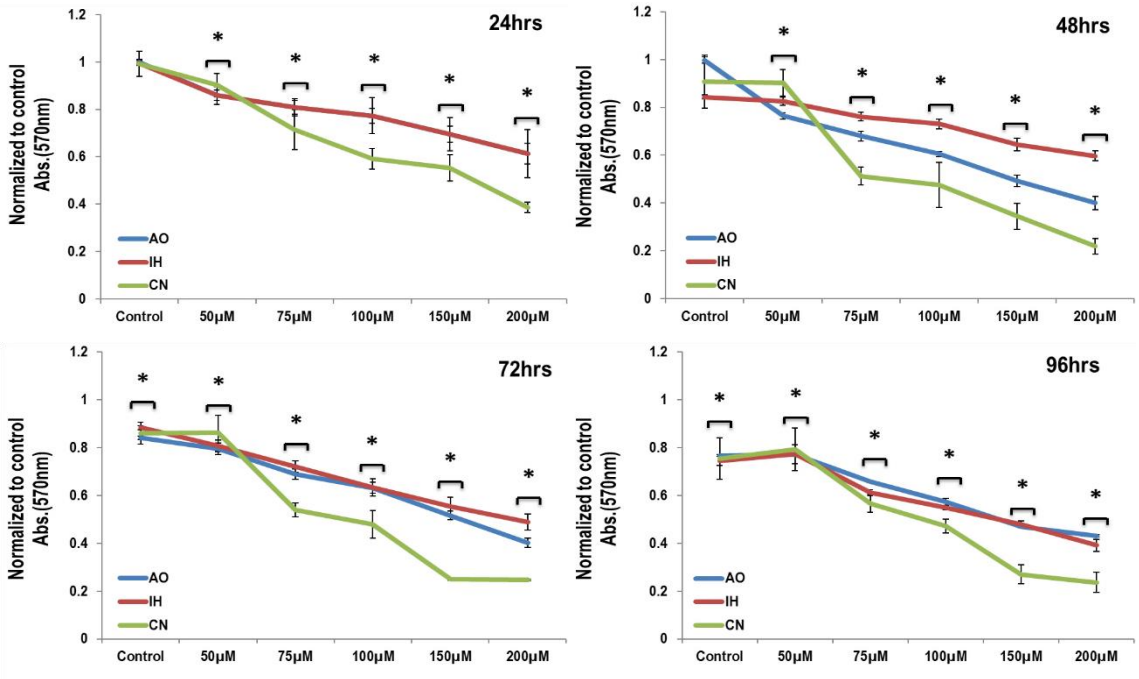

Figure 3.4. Effect of DFO on MTT activity of PC12 cells cultured in different oxygen conditions

*MTT activity of PC12 cells at air oxygen (AO), intermittent hypoxia (IH), and continuous normoxia (CN) following exposure to different concentrations of DFO across a 96 hrs time-course. Y-axis indicates Abs. value normalized to Abs. of control at each time point. X-axis indicates different DFO concentrations. Data are normalized to untreated controls at each time point. n=1 triplicate, * indicates significant change in comparison to control at each time point ($p<0.01$).*

3.3.1.3. Determination of PC12 cell viability after treatment with different concentrations of DMOG at different oxygen conditions

DMOG induced significant reductions in PC12 numbers at all concentrations tested in IH over 96 hrs (Figure 3.5). AO and CN displayed reduced sensitivity with significant reductions noted for concentrations ≥250 μM only (Figure 3.5). However, cells exposed to 100 μM DMOG displayed the lowest reductions in cell counts across all oxygen conditions and time points. Cell count reductions were measured as 10%, 23%, 14% and 29% for AO, 14%, 11%, 16.6% and 20% for IH, and 13%, 26%, 21% and 34% for CN for CN (at 24, 48, 72 and 96 hrs respectively) (Figure 3.5). DMOG significantly decreased metabolic activity, as measured by MTT assay, in AO and IH ($p<0.05$), at all time-points (24, 48, 72 and 96 hrs), and at all concentrations tested (Figure 3.6). The exception to this was CN at values ≤100 μM (Figure 3.6). Reductions in MTT at 100 μM were 4%, 13%, 30% and 17% for AO, 7%, 13%, 14% and 19% for IH, and 7%, 6%, 9% and 22% for CN (at 24, 48, 72 and 96 hrs respectively) (Figure 3.6).

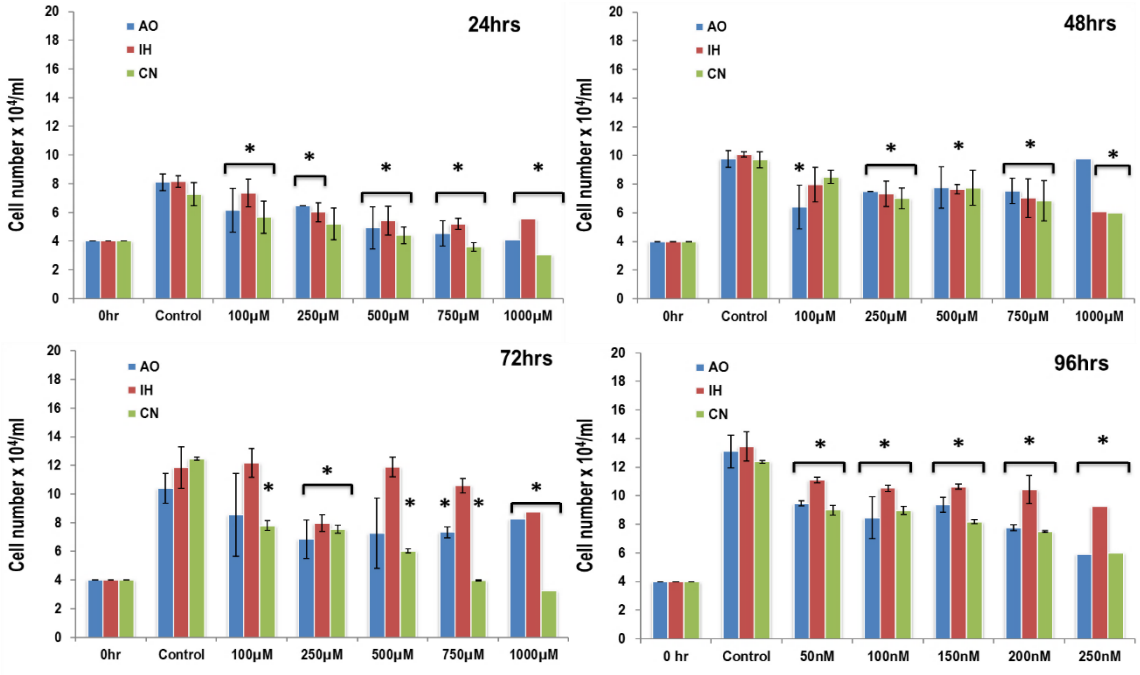

Figure 3.5. Effect of DMOG on PC12 numbers in different oxygen conditions

*Cell counts of PC12 cells at air oxygen (AO), intermittent hypoxia (IH), or continuous normoxia (CN) following exposure to different concentrations of DMOG across a 96 hrs time-course. Y-axis indicates cell number 10^4/ ml. X-axis indicates different DMOG concentrations. Data are presented as mean ± standard deviation (SD). n=1 triplicate, * indicates significant changes in comparison d to control at each time point (p<0.01).*

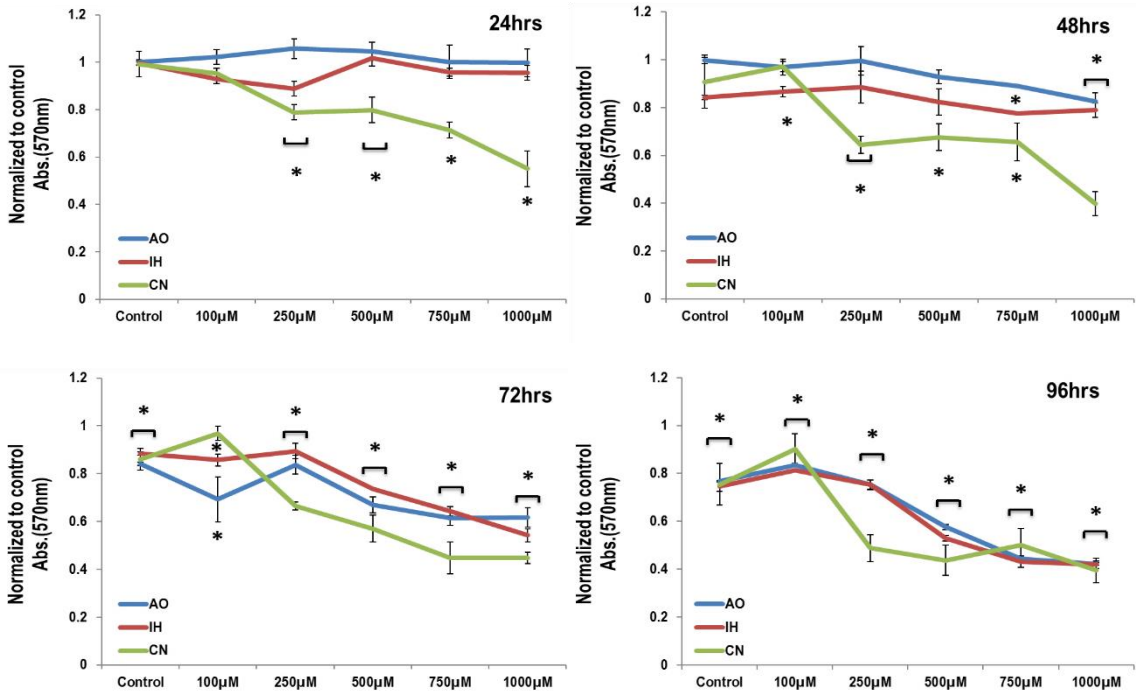

Figure 3.6. Effect of DMOG on MTT activity of PC12 cells cultured in different oxygen conditions

*MTT activity of PC12 cells at air oxygen (AO), intermittent hypoxia (IH), or continuous normoxia (CN) following exposure to different concentrations of DMOG across a 96 hrs time-course. Y-axis indicates Abs. value normalized to Abs. of control at each time point. X-axis indicates different DMOG concentrations. Data are normalized to untreated controls at each time point. n=1 triplicate, * indicates significant change in comparison to control at each time point (p<0.01).*

3.3.1.4. Determination of PC12 cell viability after treatment with different concentrations of IOX2 in different oxygen conditions

IOX2 induced significant reductions in PC12 numbers at all concentrations tested in both AO and IH over 96 hrs (Figure 3.7). CN displayed reduced sensitivity with significant reductions noted for concentrations ≥100nM only (Figure 3.7). However, cells exposed to 50 nM displayed the lowest reductions in cell counts across all oxygen conditions and time points. Cell count reductions were measured as 12%, 6%, 20% and 19% for AO, 3%, 11%, 20%and 17% for IH and 23%, 17%, 38% and 17% for CN (at 24, 48, 72 and 96 hrs respectively) (Figure 3.7). IOX2 significantly decreased metabolic activity, as measured by MTT assay, in all conditions ($p<0.05$), at all time-points (24, 48, 72 and 96 hrs), and at all concentrations tested (Figure 3.8). Reductions in MTT at 50 nM were 9%, 17%, 29 % and 17% for AO, 14%, 20%, 15% and 16 % for IH, and 5%, 6%, 10% and 13% for CN (at 24, 48, 72 and 96 hrs respectively) (Figure 3.8).

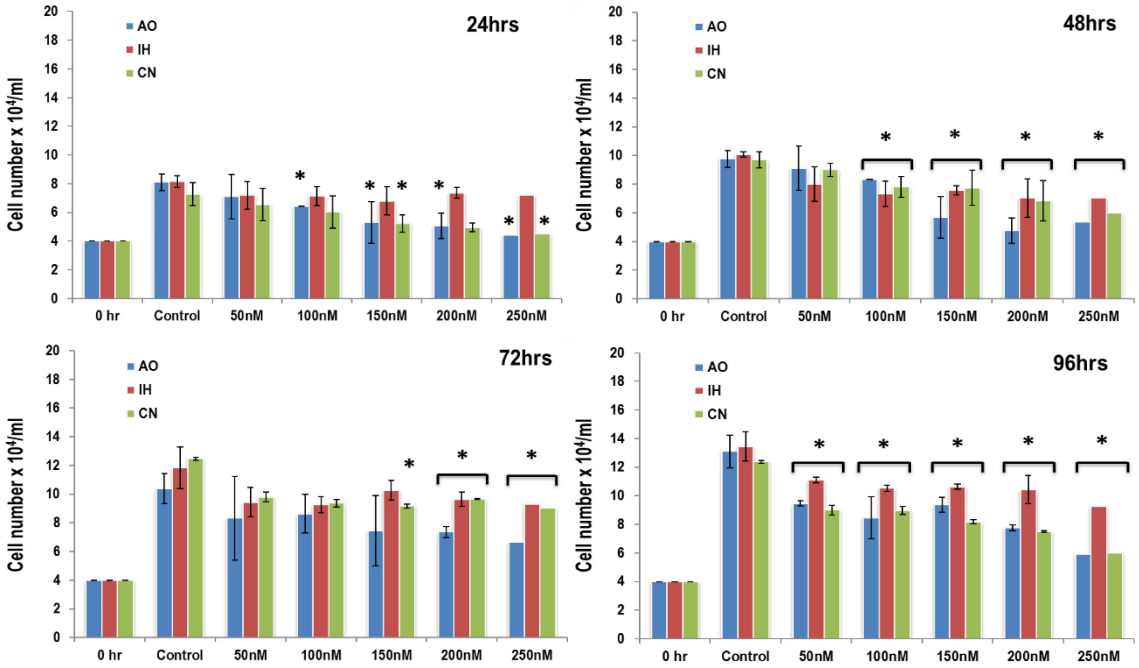

Figure 3.7. Effect of IOX2 effects on cell counts of PC12 cells cultured in different oxygen conditions

*Cell counts of PC12 cells at air oxygen (AO), intermittent hypoxia (IH), and continuous normoxia (CN) following exposure to different concentrations of IOX2 across a 96 hrs time-course. Y-axis indicates cell number x10^4. X-axis indicates different IOX2 concentrations. Data are presented as mean ± standard deviation (SD). n=1 triplicate, *indicates significant change in comparison d to control at each time point (p<0.01).*

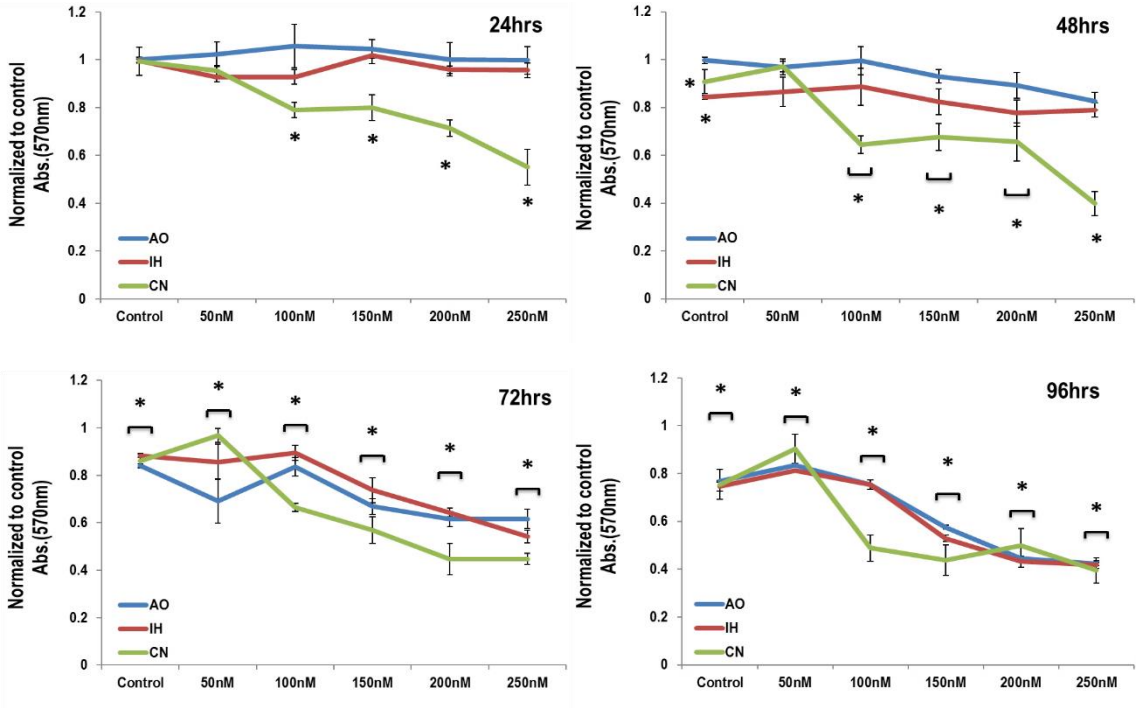

Figure 3.8. Effect of IOX2 on MTT activity of PC12 cells cultured in different oxygen conditions

*MTT activity of PC12 cells in air oxygen (AO), intermittent hypoxia (IH) (B), or continuous normoxia (CN) following exposure to different concentrations of IOX2 across a 96 hrs time-course. Y-axis indicates Abs. value normalized to Abs. of control at each time point. X-axis indicates different IOX2 concentrations. Data are normalized to untreated controls at each time point. n=1 triplicate, * indicates significant change in comparison to control at each time point (p<0.01).*

The reduction in cell count and MTT activity after ≥75 μM $CoCl_2$ and ≥75 μM (iron dependent HMAs) may related to ability to competing or chelating iron from binding site PHD enzyme (respectively) leading to induce hypoxia response by reduce HIF1-α degradation which affecting cell cycle and apoptosis (Zeng *et al.,* 2011). In addition, these agents may be affecting cytoplasmic enzymes as nitroreductases and mitochondrial enzymes as NAD(P)H dehydrogenase activity that lead to increase sensitivity of PC12 to $CoCl_2$ and DFO toxicity and ROS formation.

This reduction in cell count and MTT after ≥100 μM DMOG and ≥100 nM IOX2 may related to the fact that DMOG and IOX2 inhibit PHD enzyme by act as a substrate leading to indice hypoxia response and this may be affecting cell cycle and cell survival. These

agents have significant effect on mitochondrial metabolism and function by changing intracellular acidification, rapidly inhibits mitochondrial respiration which even precedes activation of HIF pathways (Zhdanov *et al.,* 2015). The difference in cell count and MTT activity between the two agents may be related to the lack of selectivity for PHD and FIH in DMOG.

Following on from definition of the HMA dose that minimally affected PC12 cell viability (50 µM for $CoCl_2$ and DFO, 100 µM for DMOG and 50 nM for IOX2) we sought to confirm that these agent at used doses still have ability to induce of HIF-1α and HIF-2α.

3.3.2. Effect of hypoxia mimetic agents on HIF expression

Hypoxia inducible factors (HIFs) are proteins that serve as heterodimeric transcription factors responsible for regulation of oxygen homeostasis. They are stabilised under hypoxia due to a lack of activity of enzymes from the prolyl-hydroxylase family. PHDs when active hydroxylate HIFs at specific residues directing them for subsequent ubiquitination and degradation (Semenza, 2007). HIFs stability is therefore regulated mainly by post-translational prolyl hydroxylation catalysed by the HIF prolyl hydroxylase domain proteins (PHDs) (Fan *et al.,* 2014). There are three known HIF-α isoforms (HIF-1α, HIF-2α, and HIF-3α). HIF-1α is ubiquitously expressed; HIF-2α expression is specific to endothelia, parenchyma, and interstitial cells, and finally HIF-3α of which less is known. Studies described the effects of hypoxia and HMA on HIF-1α and HIF-2α expression, in which HMAs were applied at high concentrations associated with reduced cell viability and short-term exposures (Rodríguez-Jiménez *et al.,* 2008; Cartee *et al.,* 2012; Giansanti *et al.,* 2013). We sought to determine whether HIF-1α and HIF-2α expression was induced in either AO, IH, or CN cultured PC12 cells and whether the HMA doses we had identified induced HIF-1α expression to levels comparable with AO, IH, or CN culture.

Using FACS analysis of immuno-labelled suspension cultured PC12 we established that AO cultured cells displayed a consistent baseline expression of 33.85± 8.77%. PC12 stocks used to initiate all experiments were measured to establish control levels and are represented as the X-axis intersection with the Y-axis (Figure 3.9).

In this work, we find that IH cultured cells displayed an immediate upregulation of HIF-1α after 24 hrs to 64% which was down regulated to 55% by 48 hrs and maintained thereafter at 49% at 72 hrs and 55% at 96 hrs. In contrast to IH, CN displayed a consistently low expression profile over the entire time course (29% at 24 hrs, 35% at 48 hrs, 35% at 72 hrs, and 33% at 96 hrs). Taken together this demonstrated that IH and CN culture induced distinct HIF-1α stabilisation profiles (Figure 3.9).

Having established the baseline HIF-1α profiles for each oxygen condition we next sought to determine the role of the HMA at the previously identified minimal concentrations over 96 hrs of culture. In AO culture, significant upregulation was noted with all HMAs, after 24 hrs, to levels comparable to those noted for IH; $CoCl_2$ 65%, DFO 62%, DMOG 61%, and IOX2 77% (Figure 3.9.A). HIF-1α levels were substantially reduced for all HMAs by 48 hrs ($CoCl_2$ 50%, DFO 46%, DMOG 48% and IOX2 52%) to levels still consistent with IH. At 72 hrs $CoCl_2$ levels had reduced to baseline 35% whereas the remaining HMAs continued to display consistency with IH (DFO 53.5%, DMOG 48.8%, IOX2 56.8%). At 96 hrs, HIF-1α had dropped to a consistent elevated above baseline level with all HMAs tested. The overall profile of HMAs in AO was that they bore a close resemblance to IH cultured cells but not CN. IH cultured PC12 cells were also supplemented with HMAs to establish if an additive or negative feedback loop could be identified. HIF-1α expression levels in HMA supplemented media were comparable to IH throughout the 96 hrs period indicating an absence of an additive or negative effect (Figure 3.9.B). CN cultured cells displayed a distinct HIF-1α profile where marginal upregulation was noted after 48 hrs (43.45%), but low levels of expression at all other time-points, with levels comparable to AO (Figure 3.9.C). The presence of HMAs again resulted in distinct responses where $CoCl_2$

supplementation marginally upregulated HIF-1α at 24 hrs to 40%, not at 48 hrs, and was comparable at all other points. DFO and IOX2 supplementation resulted in HIF-1α levels consistent with CN throughout whereas DMOG supplemented PC12 displayed comparable levels at all time-points apart from 96 hrs where some up regulation was noted. To sum up at used concentrations HMAs (except DMOG and IOX2 at 96 hrs) have no additive effect on HIF-1α expression over both IH and CN culture condition.

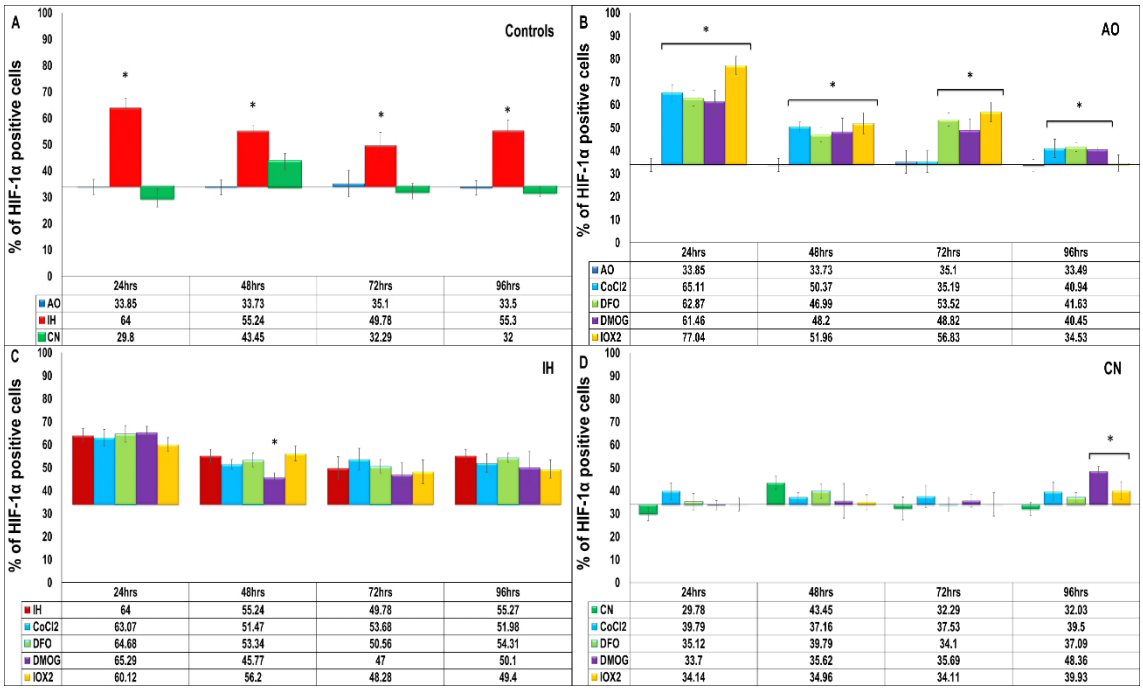

	24hrs	48hrs	72hrs	96hrs
AO	33.85	33.73	35.1	33.5
IH	64	55.24	49.78	55.3
CN	29.8	43.45	32.29	32

	24hrs	48hrs	72hrs	96hrs
AO	33.85	33.73	35.1	33.49
CoCl2	65.11	50.37	35.19	40.94
DFO	62.87	46.99	53.52	41.63
DMOG	61.46	48.2	48.82	40.45
IOX2	77.04	51.96	56.83	34.53

	24hrs	48hrs	72hrs	96hrs
IH	64	55.24	49.78	55.27
CoCl2	63.07	51.47	53.68	51.98
DFO	64.68	53.34	50.56	54.31
DMOG	65.29	45.77	47	50.1
IOX2	60.12	56.2	48.28	49.4

	24hrs	48hrs	72hrs	96hrs
CN	29.78	43.45	32.29	32.03
CoCl2	39.79	37.16	37.53	39.5
DFO	35.12	39.79	34.1	37.09
DMOG	33.7	35.62	35.69	48.36
IOX2	34.14	34.96	34.11	39.93

Figure 3.9. Effect of hypoxia mimetic agents on HIF-1α expression in different oxygen conditions

*The percentage of anti-HIF-1α (ab16066) labelled cells is shown. PC12 were exposed to (50 µM $CoCl_2$, 50 µM DFO, 100 µM DMOG and 50 nM IOX2) for 24 hrs, 48 hrs, 72 hrs and 96 hrs in AO, IH and CN. Data are presented as mean of % of HIF-1α positive ± standard deviation (SD). n=1 triplicate, * indicates significant difference in comparison to the % of HIF-1α positive cells at each time point.*

HIF-1α expression over the 96 hrs showed reduction in magnitude with time and this finding reflect that the cells develope adaptation to oxygen levels and this correct for both IH and after treatment with HMAs and this may relate to activation of negative feedback

genes that regulate HIF-1α expression by increase HIF-3α4 expression which weaken the HIF-1α / DNA binding (Drevytska *et al.,* 2012).

HIF-2α displayed an expression profile distinct to that seen with HIF-1α. The experimental seeding population displayed a baseline expression of 60% which is indicated by the intersection of the x-axis with the y-axis (Figure 3.10). AO cultured cells were as expected consistent with baseline at 24 hrs (61.36%) but levels decreased to 53.33 at 48 hrs, 50.35% at 72 hrs and 48.57% at 96 hrs; CN cultured cells were consistent with baseline through to 72 hrs with a sharp down-regulation to 48% noted thereafter while IH cultured cells displayed some up regulation at 24 hrs to 75% followed by down regulation to levels comparable with AO and CN at 96 hrs (Figure 3.10). In AO, $CoCl_2$ induced an initial up regulation at 24 hrs to levels comparable with IH, followed by downregulation to levels comparable with baseline at 72 hrs and slight upregulation above baseline at 96 hrs. DFO induced slight upregulation at 24 and 48 hrs, down regulation below baseline at 72 hrs, followed by upregulation to levels comparable with $CoCl_2$ at 96 hrs. AO cultured DMOG supplemented cells displayed an upregulation at 24 hrs comparable to $CoCl_2$ which had dropped by 48 hrs to a position of marginal upregulation and was maintained at that levels through to 96 hrs. IOX2 displayed a similar upregulation profile to $CoCl_2$ and DMOG at 24 hrs followed by downregulation to baseline levels through to 72 hrs and marked upregulation at 96 hrs. The overall profile of HMA driven HIF-2α regulation over 96 hrs was distinct from AO, IH, and CN cultured cells. Supplementation of IH cultured PC12 with HMAs again resulted in a shared response profile with IH for $CoCl_2$, DFO, and DMOG at 24 hrs (Figure 3.10.B). For $CoCl_2$ this was reduced to baseline levels by 48 hrs and thereafter. DFO maintained upregulation at 48 hrs, was markedly decreased at 72 hrs, followed by upregulation at 96 hrs. HIF-2α levels were reduced in DMOG at 48 hrs and were below baseline at 72 hrs and thereafter. IOX2 induced baseline levels of HIF-2α expression throughout the 96 hrs timeline. CN cultured cells displayed a constant HIF-2α

profile over 72 hrs comparable to baseline expression followed by down regulation after 96 hrs. The presence of HMAs again resulted in distinct responses where $CoCl_2$ supplementation up regulated HIF-2α at 24 hrs 77%, at 48 hrs and 72 hrs HIF-2α profile is comparable to CN with higher expression observed after 96 hrs. DFO and DMOG supplementation resulted in HIF-2α levels constantly higher than CN throughout whereas DFO supplemented PC12 displayed higher level at 96 hrs where some up regulation was noted. IOX2 induced baseline levels of HIF-2α expression throughout the 72 hrs with higher expression level was observed after 96 hrs.

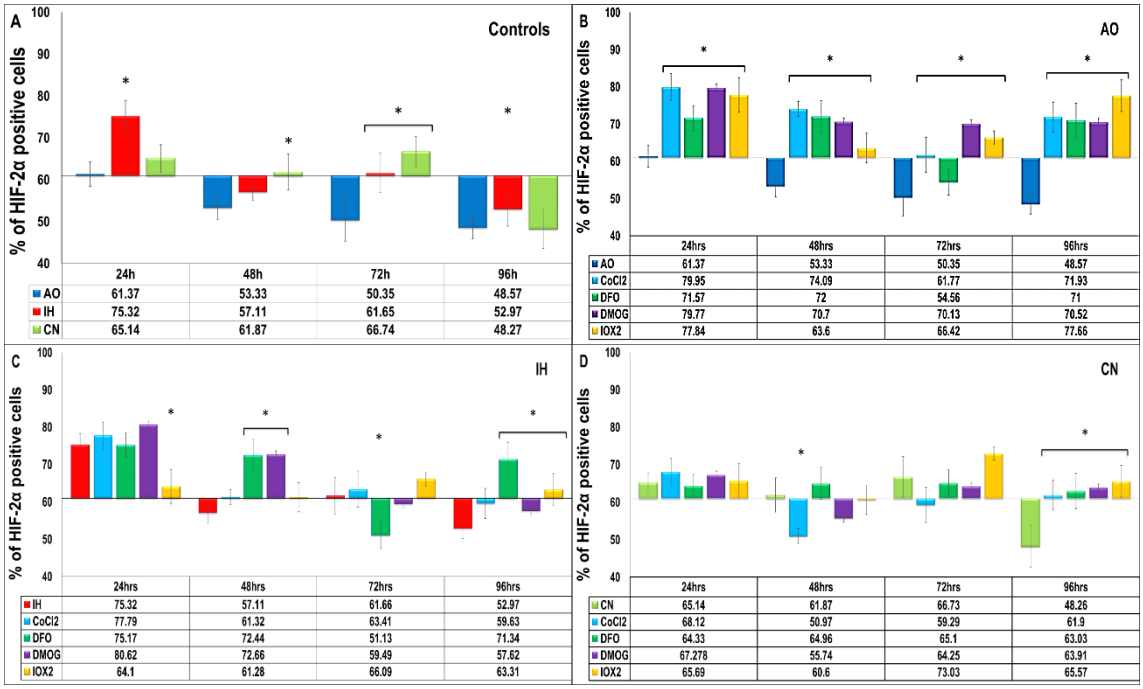

Figure 3.10. Effect of hypoxia mimetic agents on HIF-2α expression in oxygen conditions

*The percentage of anti-HIF-2α (ab8365). PC12 cells were exposed to (50 μM $CoCl_2$, 50 μM DFO, 100 μM DMOG and 50 nM IOX2) for 24 hrs, 48 hrs, 72 hrs and 96 hrs in AO (A), IH (B) and CN (C). Data are presented as % of HIF-1α positive ± standard deviation (SD). n=1 triplicate, * indicates significant difference in comparison to the % of HIF-2α positive cells at each time point.*

Again HIF-2α expression showed reduction to the level less than baseline expression with time and this finding reflect that HIF-2α no longer orchestrates adaptive responses may related to the switch in HIF-1/HIF-2 signaling over 96hrs under hypoxia that involve in cell

survival in energy crisis by regulating balance between energy saving and reduction in PC12 proliferation on one hand and active cell growth and tumor expansion, on the other hand (Zhdanov *et al.,* 2013).

3.3.3. Effect of hypoxia mimetic agents on PC12 cell differentiation capacity.

A core feature of PC12 is their neural differentiation capacity following exposure to the correct conditions. These are achieved by encouraging adhesion of the suspension culture cells via provision of a Collagen IV coated substrate. Differentiation is then spontaneous at low levels but can be enhanced via provision of NGF. We sought to determine if AO, IH, and CN would induce comparable levels of differentiation, quantify the enhancement induced by NGF, and determine if HMAs would mirror IH and/or CN responses. Differentiation was quantified by counting cells with neurite extensions (See Section 2.2.1.9).

To confirm neurogenic differentiation, we next performed immunofluorescence for both GAP-43 and Synapsin-1; neurogenic differentiation markers (Rossoll & Bassell, 2009). SH-SY5Y is a human derived cell line isolated from neuroblastoma biopsy from bone marrow used as an *in vitro* model of neuronal function and differentiation. These cells possess an adrenergic phenotype, express neurogenic markers GAP-43 and Synapsin-1 (Zhang *et al.,* 2008), and SH-SY5Y was included as a control.

There were no significant effects for different oxygen culture condition on PC12 cells neurite development capacity without induction by NGF (Figure 3.11 and 12). In addition, all oxygen condotions elevated GAP-43 while synapsin-1 elevated only under IH culture condition in comparison to base line expression of SH-SY5Y (Figure 3.13 and 14 respectively).

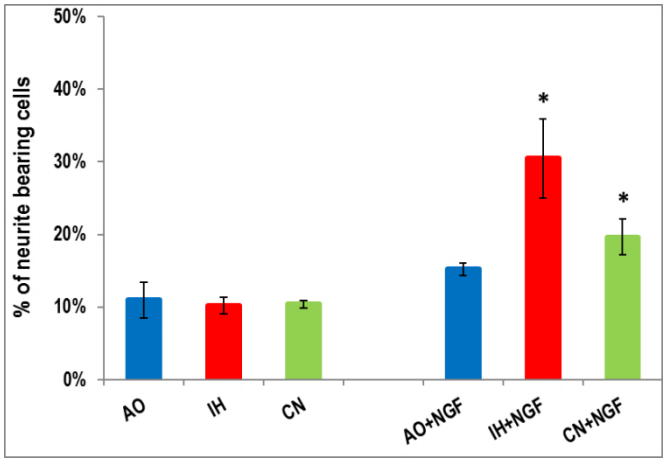

Figure 3.11. Neuronal differentiation is enhanced by NGF in an oxygen-independent manner

*PC12 cell were cultured in collagen IV pre-coated 24-well plate with and without NGF stimulation for 7-10 days at three different oxygen culture conditions. Histogram shows the percentage of neurite bearing PC12. X-axis indicates the oxygen and NGF treatment. Y-axis indicates the percentage of neurite bearing cells. Error bars indicates standard deviation. * indicates significant difference in comparison to control (without and with NGF treatment respectively) p< 0.01.*

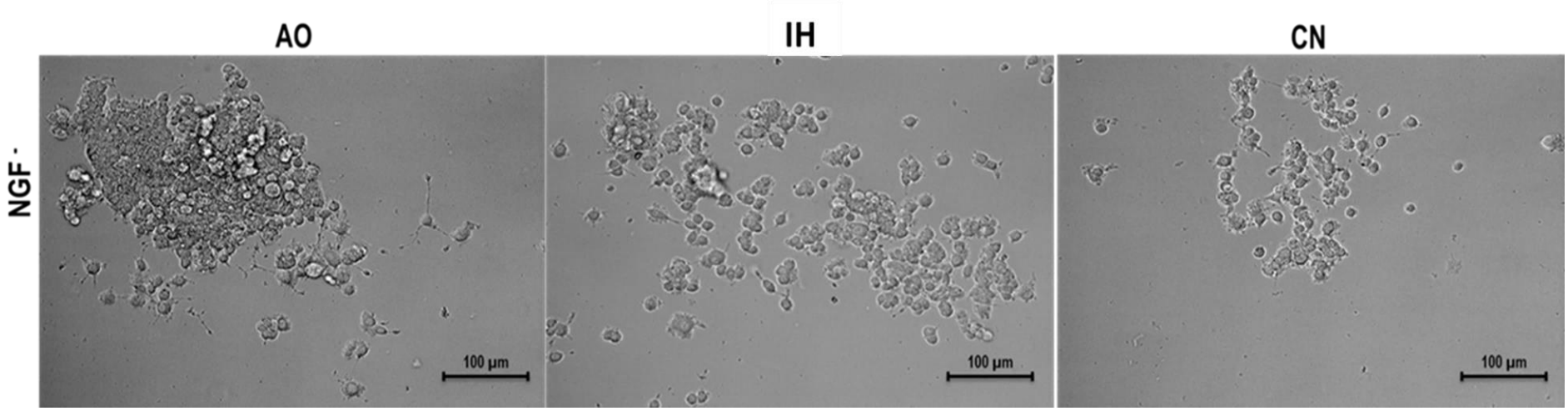

Figure 3.12. Neurite outgrowths of PC12

PC12 were plated at a seeding density of 10^4 cells/ml into 24-well plates coated with collagen type IV and incubated for 7-10 days at AO +/- NGF, PC12 incubated at IH +/- NGF, PC12 incubated at DMOG +/- NGF, Scale bar equal 100 µm.

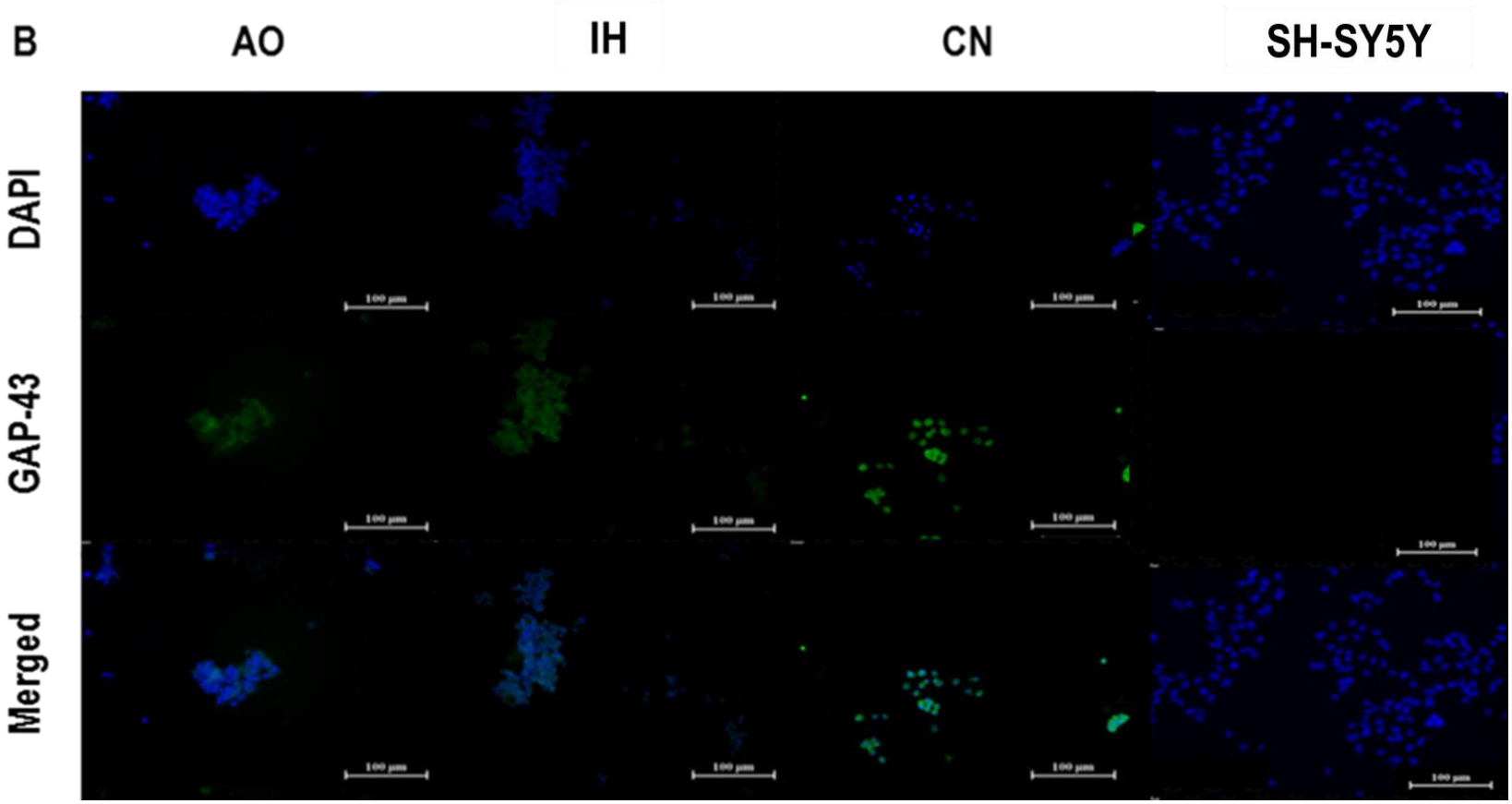

Figure 3.13. Effect of different oxygen culture conditions on GAP-43 expression

PC12 cultured under different oxygen conditions with and without addition of NGF.The cell labelled with anti-GAP-43 primary antibody and then incubated with anti-rabbit IgG-FITC secondary antibody. GAP-43 expression in PC12 without NGF treatment (Blue indicates DAPI, Green indicates GAP-43). expression in PC12 without NGF treatment (Blue indicates DAPI, Green indicates GAP-43). SH-SY5Y used as positive control. Scale bar indicates 100 µm.

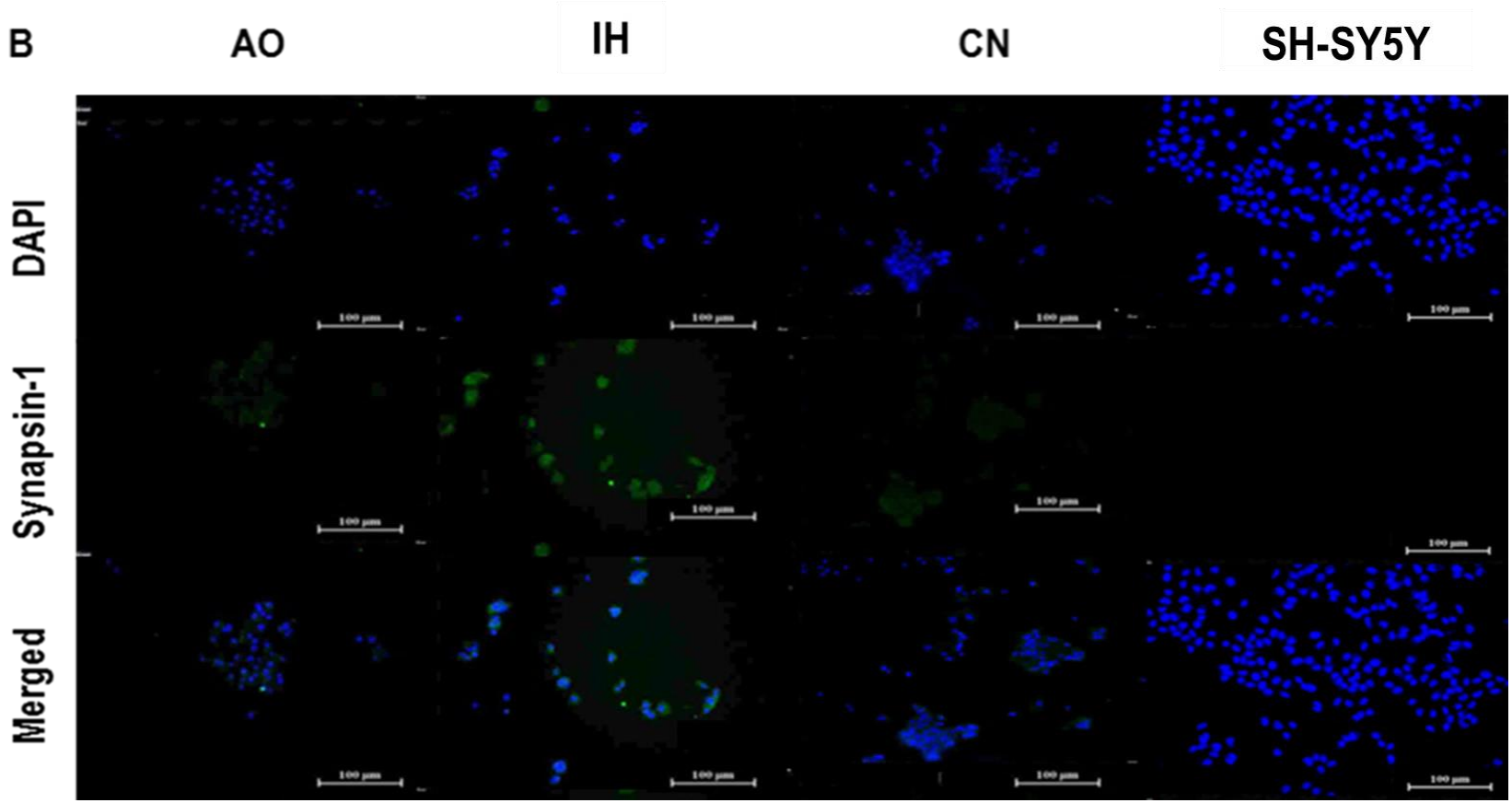

Figure 3.14. Effect of different oxygen culture conditions on Synapsin-1 expression

PC12 cultured under different oxygen conditions with and without addition of NGF. The cell labelled with anti-synapsin-1 primary antibody and then incubated with anti-mouse IgG-FITC secondary antibody. Synapsin-1 expression in PC12 without NGF treatment (Blue indicates DAPI, Green indicates Synapsin-1). (Blue indicates DAPI, Green indicates Synapsin-1). SH-SY5Y used as positive control. Scale bar indicates 100 µm.

After NGF induction, significantly increased neurite outgrowth of PC12 cell was observed after incubation in IH and CN in comparison to NGF induced cells (Figures 3.11 and 3.15). In addition, all oxygen condotions elevated GAP-43and synapsin-1 elevated only under IH culture condition in comparison to base line expression of SH-SY5Y (Figures 3.16 and 3.17 respectively).

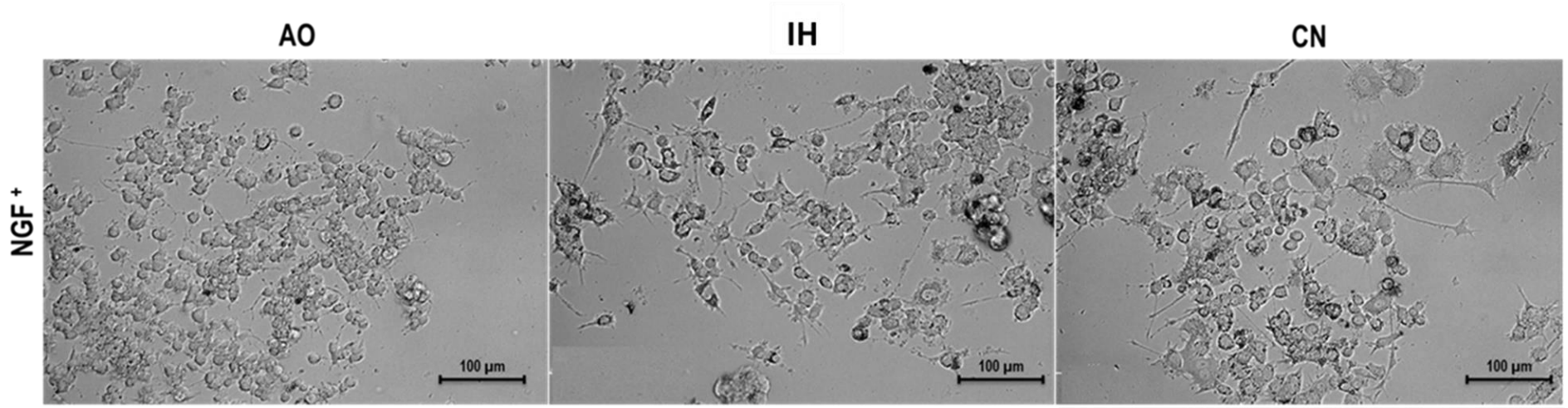

Figure 3.15. Neurite outgrowths of PC12

PC12 were plated at a seeding density of 10^4 cells/ml into 24-well plates coated with collagen type IV and incubated for 7-10 days at AO + NGF, PC12 incubated at IH + NGF, PC12 incubated at DMOG +- NGF, Scale bar equal µm 100.

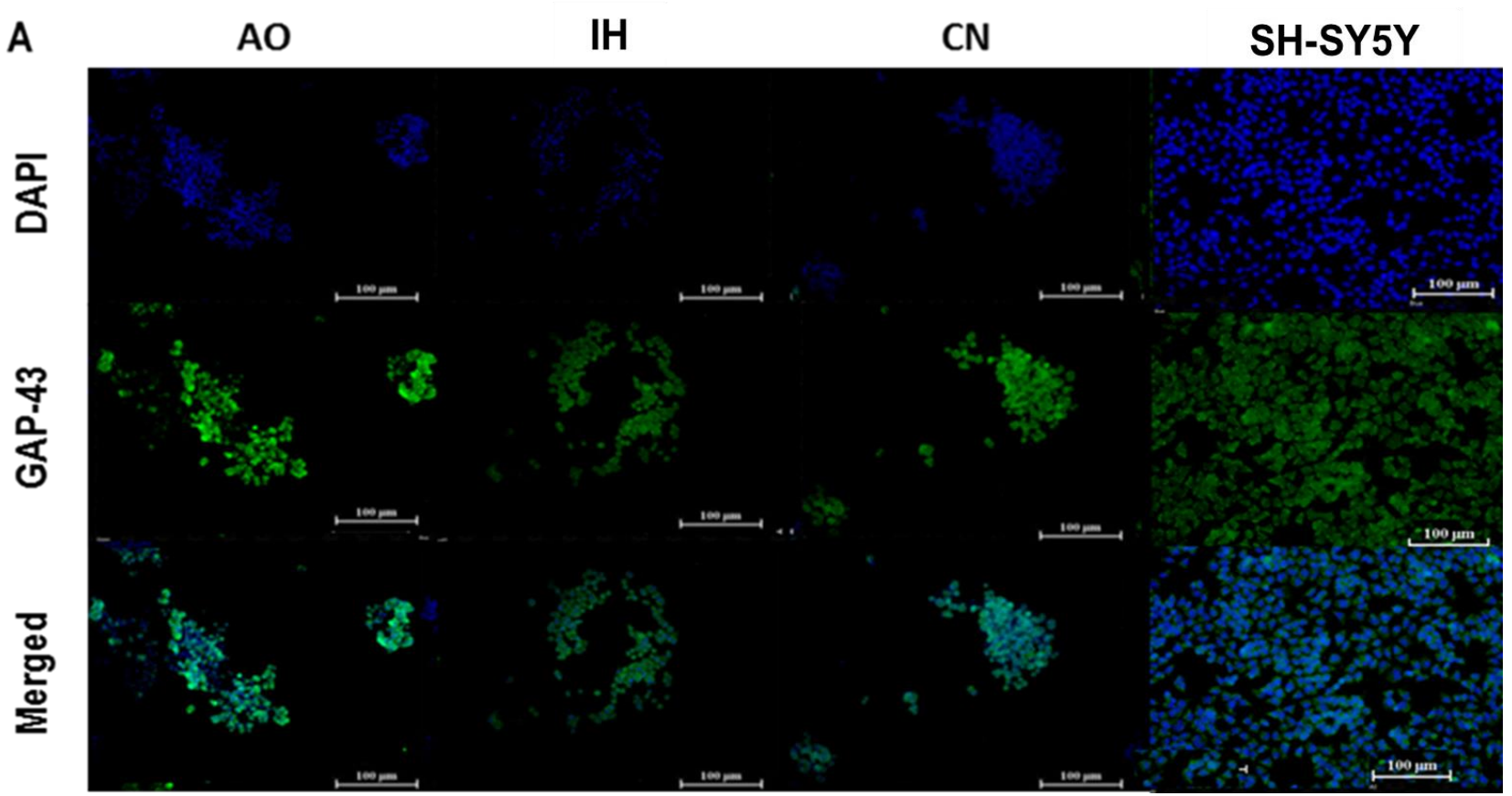

Figure 3.16. Effect of different oxygen culture conditions on GAP-43 expression

PC12 cultured under different oxygen conditions with and without addition of NGF.The cell labelled with anti-GAP-43 primary antibody and then incubated with anti-rabbit IgG-FITC secondary antibody. GAP-43 expression in PC12 with NGF treatment (Blue indicates DAPI, Green indicates GAP-43. SH-SY5Y used as positive control. Scale bar indicates 100 µm.

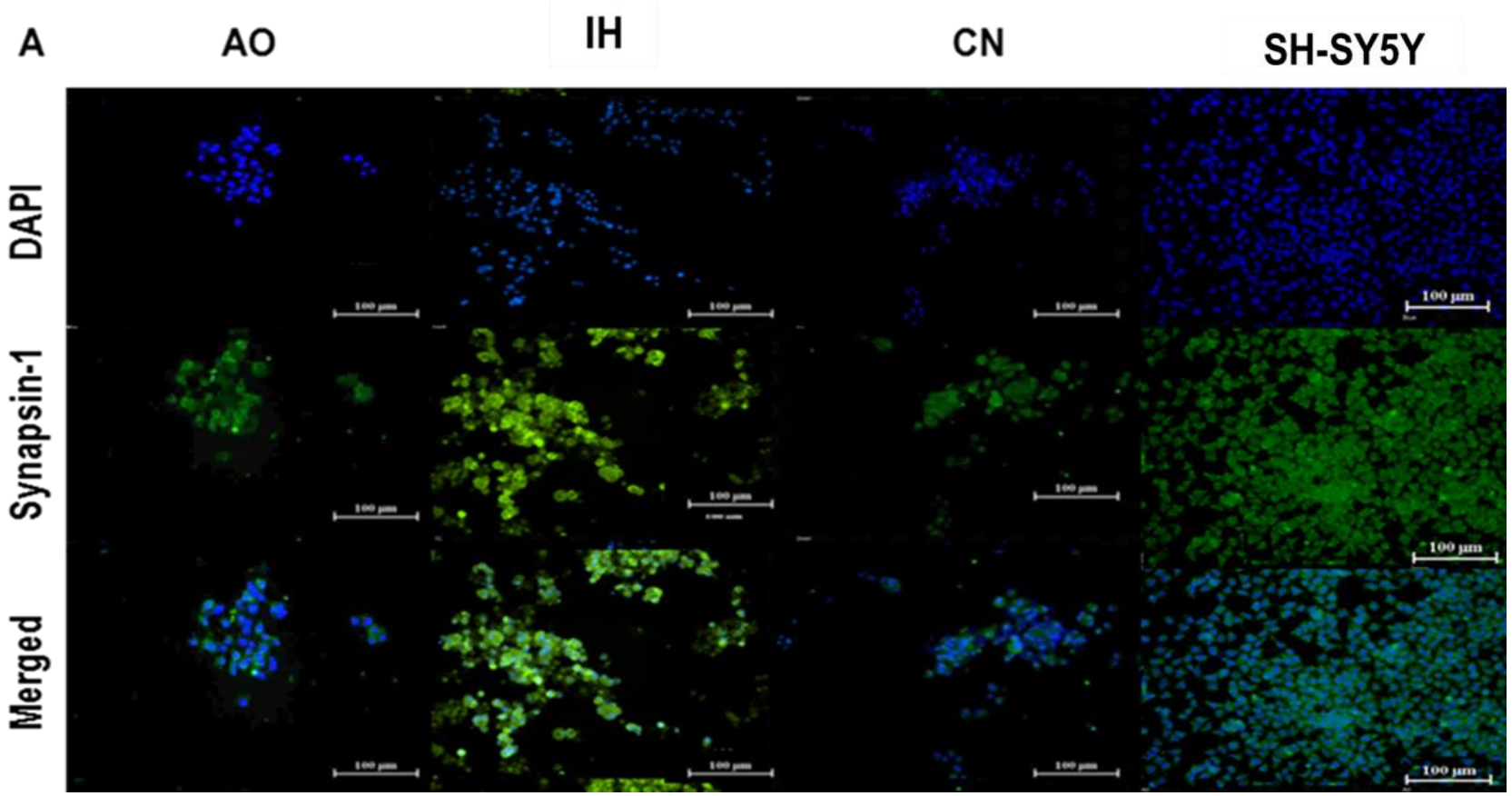

Figure 3.17.Effect of different oxygen culture conditions on Synapsin-1 expression

PC12 cultured under different oxygen conditions with and without addition of NGF. The cell labelled with anti-synapsin-1 primary antibody and then incubated with anti-mouse IgG-FITC secondary antibody. (A) Synapsin-1 expression in PC12 with NGF treatment (Blue indicates DAPI, Green indicates Synapsin-1). SH-SY5Y used as positive control. Scale bar indicates 100 µm.

Only DMOG culture under AO significantly increase percentage of neurite bearing cells (8%) in comparison to control AO ($p<0.05$) (Figure 3.18A and 19). HMAs alone showed no remarkable effect on GAP-34 and synapsin-1 expression in comparison to AO (Figure 3. 20 and 3.21).

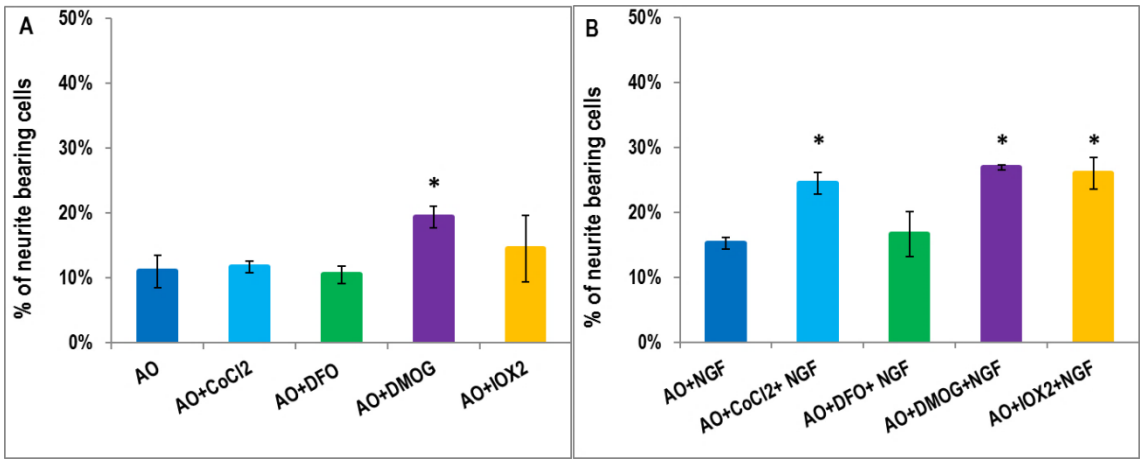

Figure 3.18. HMAs display distinct impacts on neuronal differentiation without NGF response

*PC12 cell were cultured in collagen IV pre-coated 24-well plate with and without NGF stimulation for 7-10 days after treatment with hypoxia mimetic agents at air oxygen (AO). Histogram shows the percentage of neurite bearing PC12 after treatment with HMAs alone (A) and after combination of NGF+ HMAs (B). X-axis indicates the oxygen and HMAs. Y-axis indicates the percentage of neurite bearing cells. Error bars indicates standard deviation. * indicates significant difference in comparison to control (p< 0.01).*

After NGF supplementation at AO, $CoCl_2$, DMOG and IOX2 significantly increase percentage of neurite bearing cells (9, 11 and 10%) in comparison to control AO+NGF ($p<0.05$) (Figure 3.18.B and 19). At AO, iron dependent HMAs (CoCl2 and DFO) remarkably reduced GAP43, 2 oxoglutrate HMAs showed no significant effect on GAP43 expression (Figure 3.20). HMAs (except $CoCl_2$) caused obvious elevation in synapsin-1 expression (Figure 3.21).

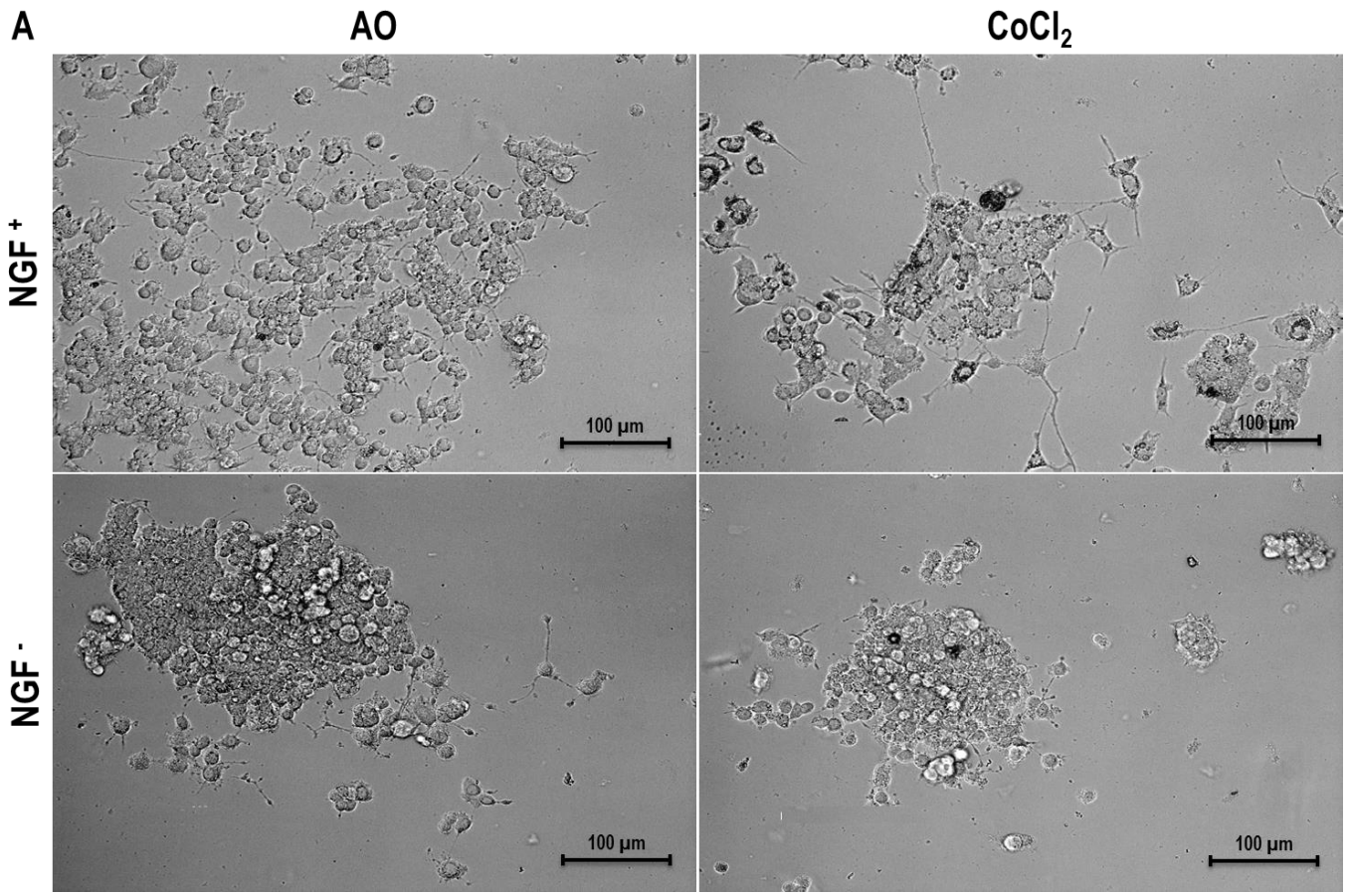
A
AO
CoCl2
NGF +
NGF -
100 µm
100 µm
100 µm
100 µm

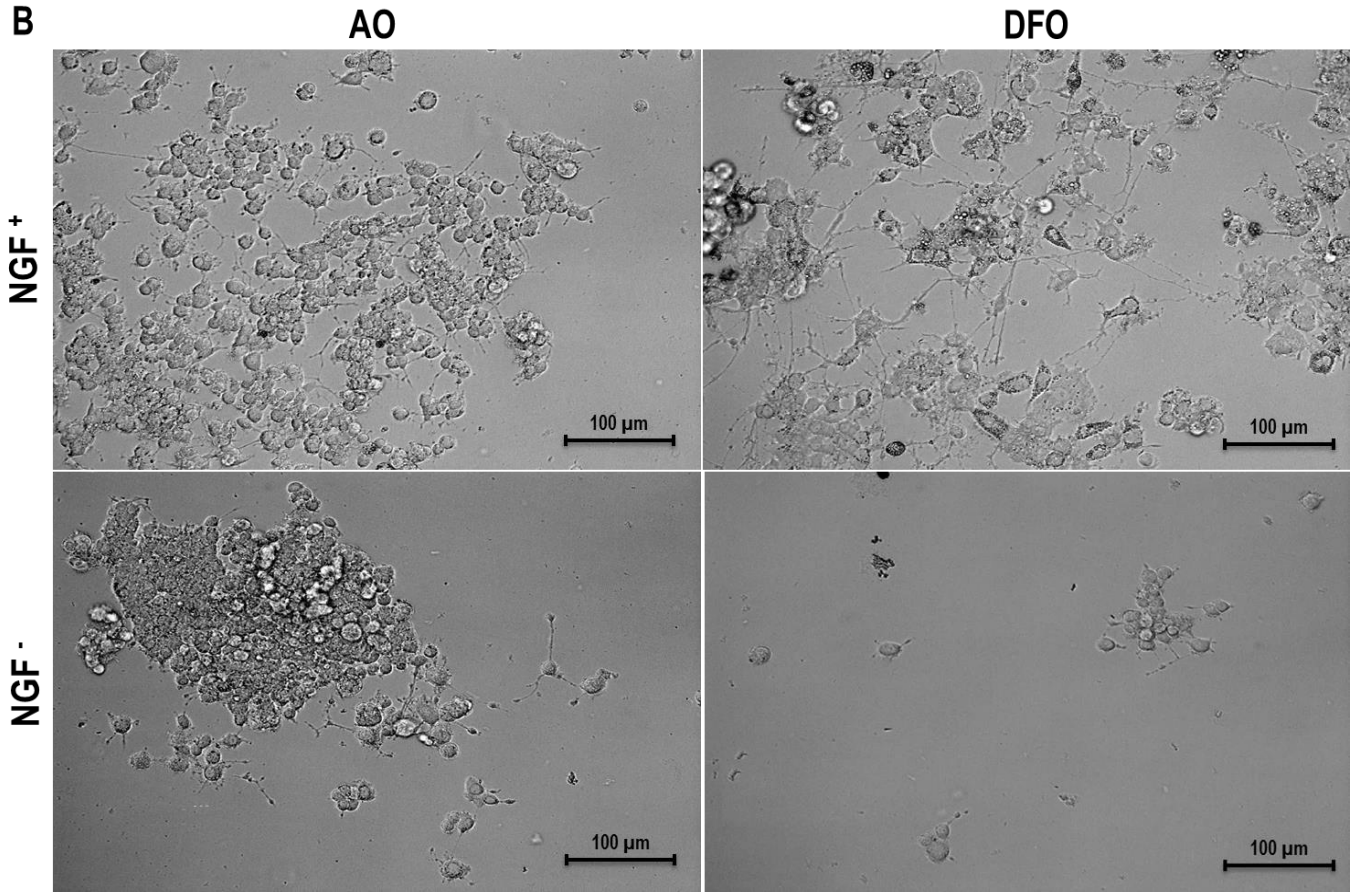
B
AO
DFO
NGF +
NGF -
100 µm
100 µm
100 µm
100 µm

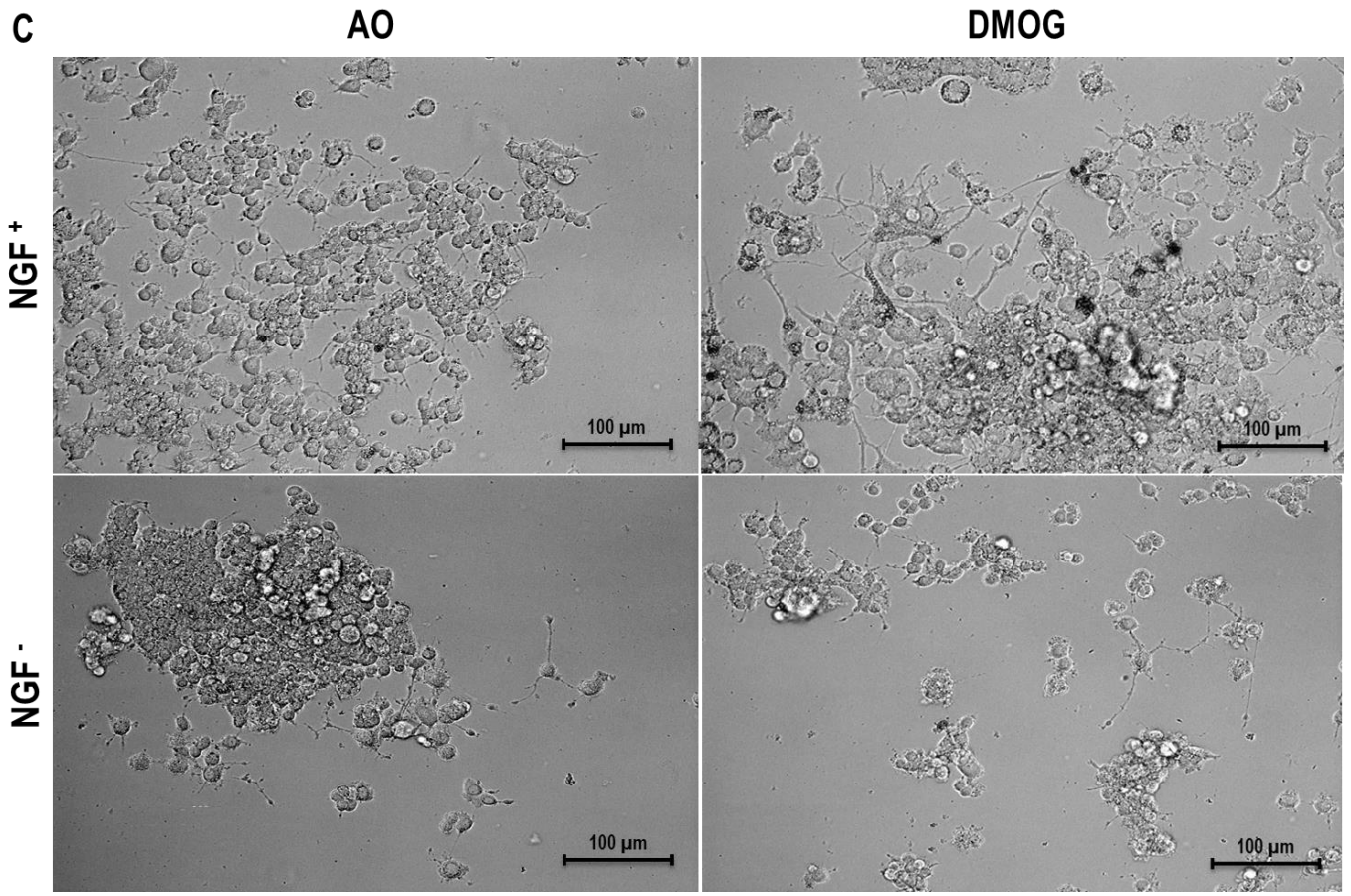
C
AO
DMOG
NGF +
NGF -
100 µm
100 µm
100 µm
100 µm

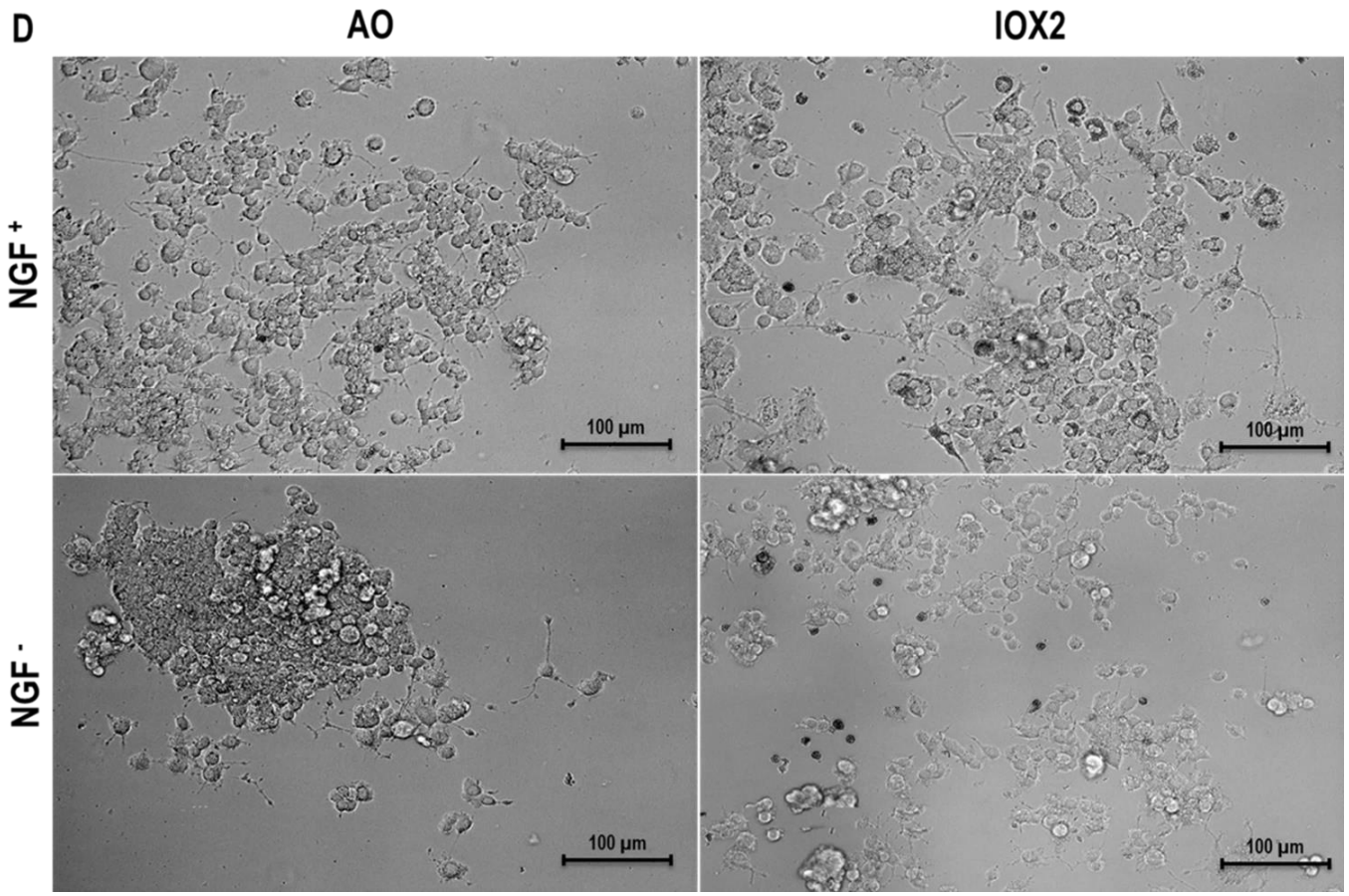

Figure 3.19. Neurite outgrowths of PC12 at AO

PC12 were plated at a seeding density of 10^4 cells/ml into 24-well plates coated with collagen type IV and incubated for 7-10 days (A) PC12 supplemented with $CoCl_2$ +/- NGF, (B). PC12 supplemented with DFO +/- NGF, (C). PC12 supplemented with DMOG +/- NGF, (D). PC12 supplemented with IOX2 +/- NGF. Scale bar equal 100 µm.

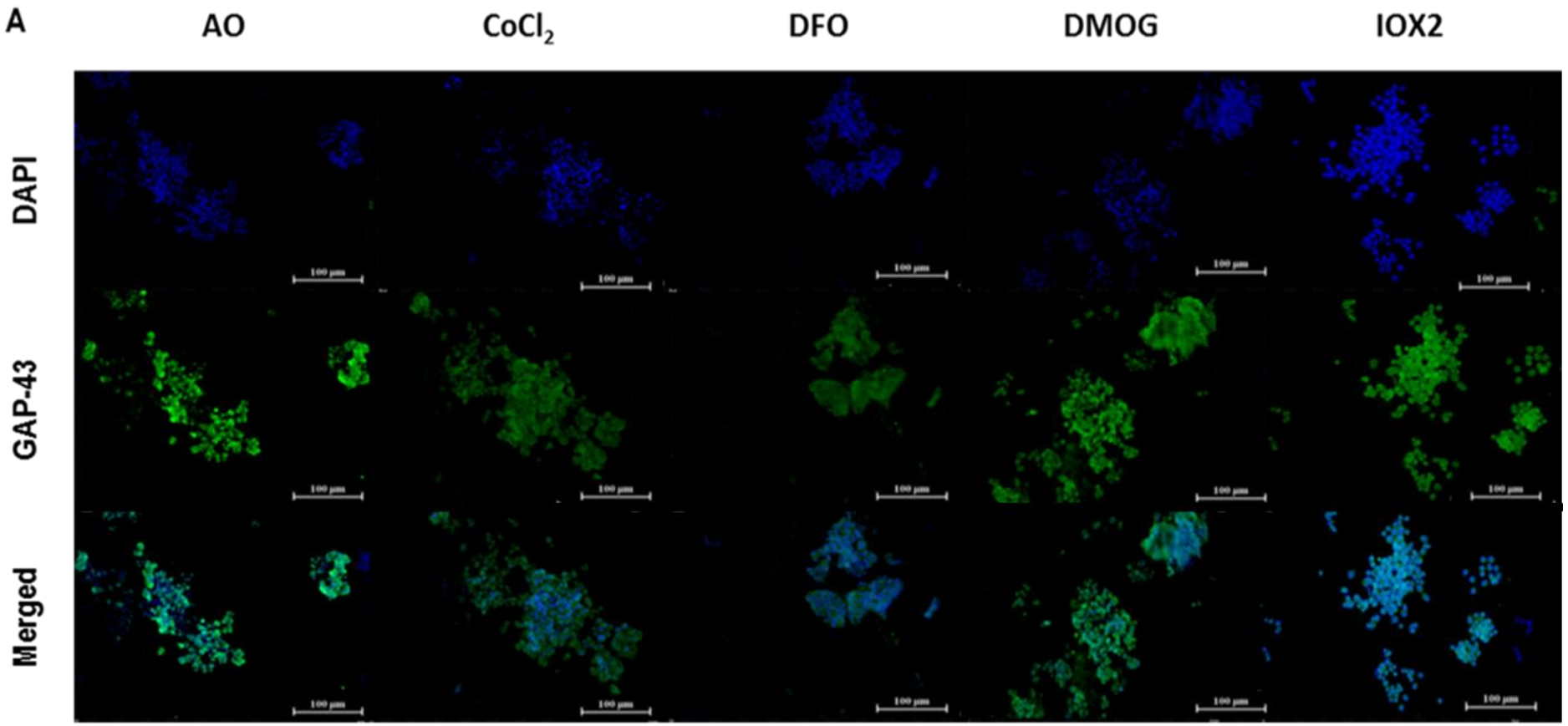
A
AO
CoCl2
DFO
DMOG
IOX2
DAPI
GAP-43
Merged

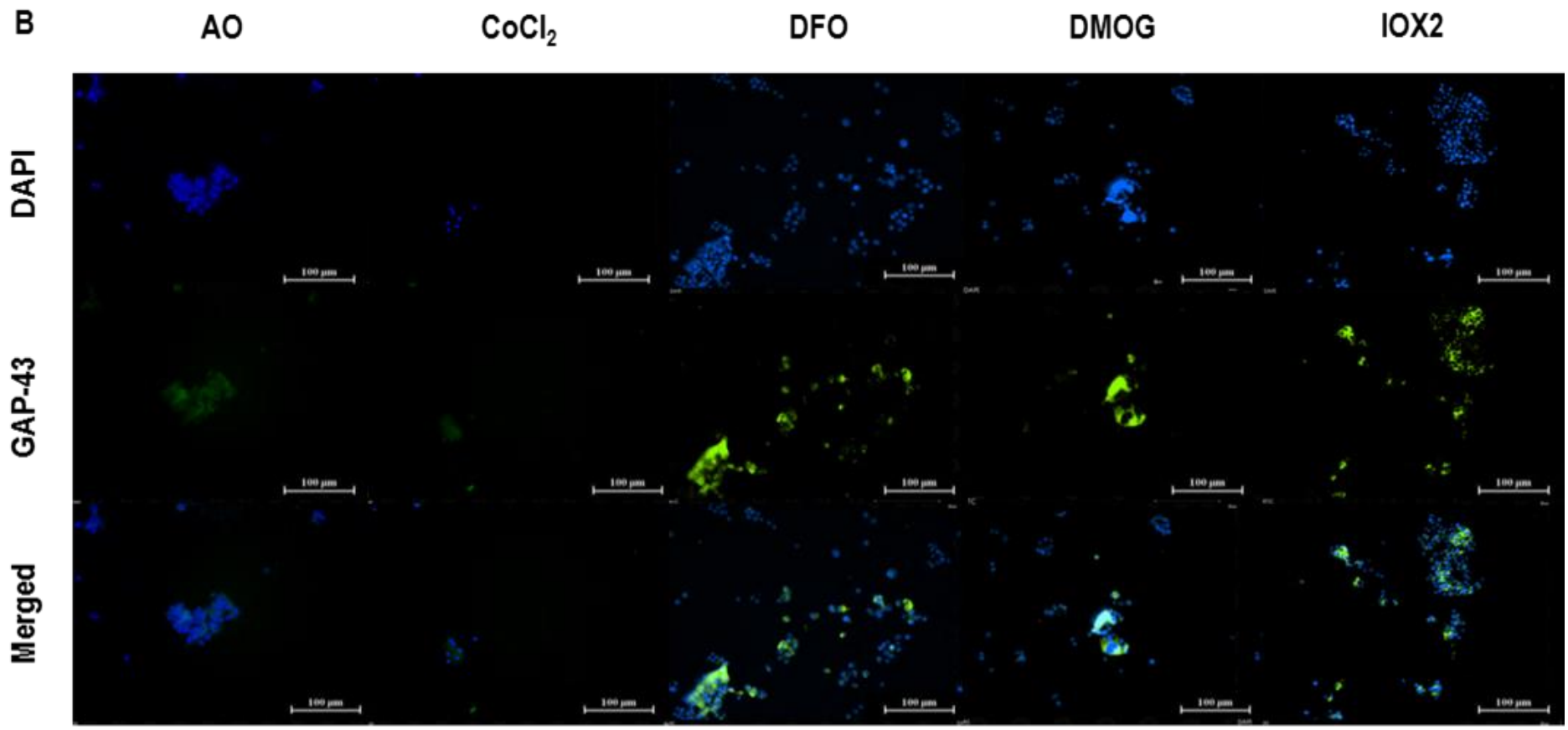

Figure 3.20. Effect of HMAs on GAP-43 expression in PC12 at AO

PC12 cultured under air oxygen condition with and without addition of NGF.The cell labelled with anti-GAP-43 primary antibody and then incubated with anti-rabbit IgG-FITC secondary antibody. (A) GAP-43 expression in PC12 with NGF treatment (Blue indicates DAPI, Green indicates GAP-43). (B) GAP-43 expression in PC12 without NGF treatment (Blue indicates DAPI, Green indicates GAP-43). Scale bar indicates 100 µm

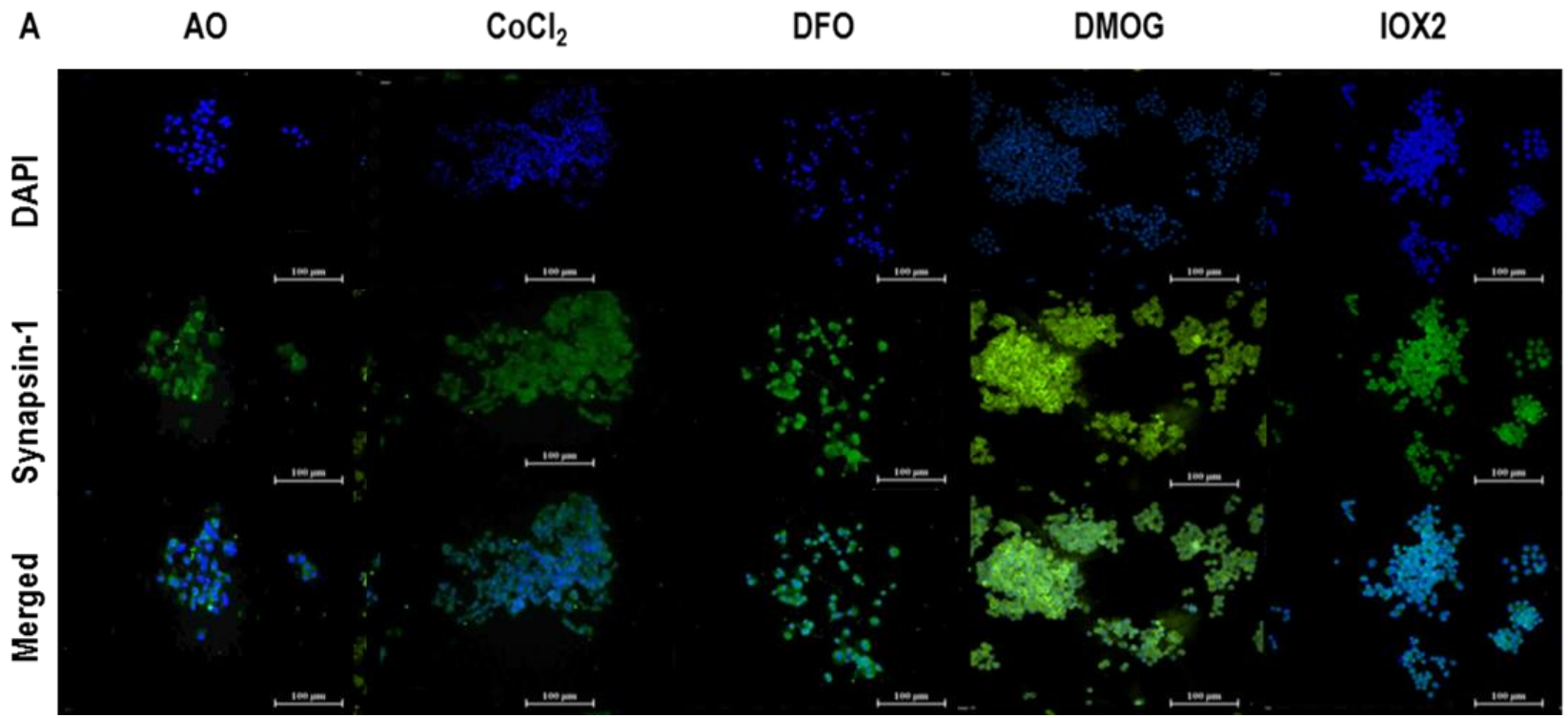
A
AO
$CoCl_2$
DFO
DMOG
IOX2
DAPI
Synapsin-1
Merged

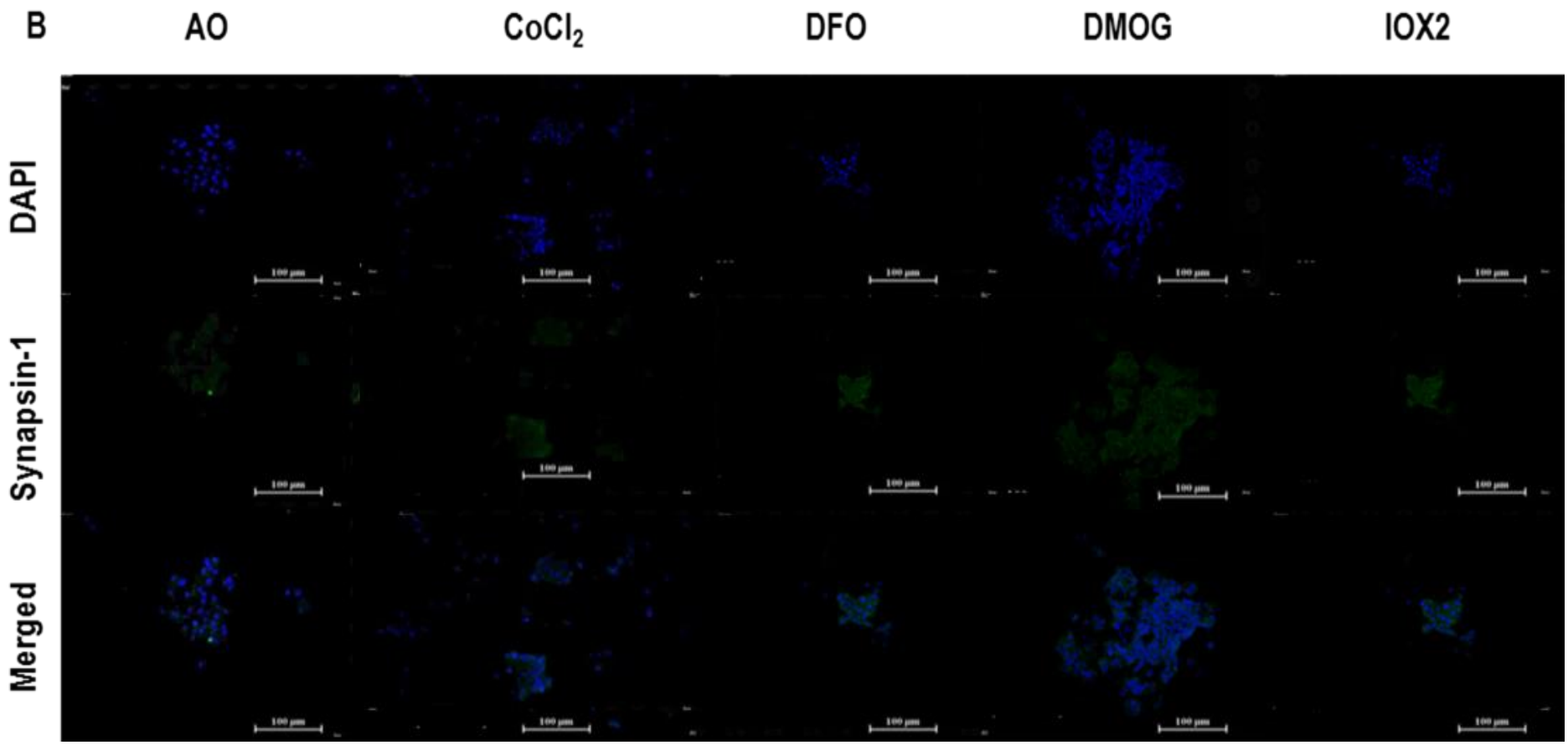

Figure 3.21. Effect of HMAs on Synapsin-1 expression in PC12 in AO

PC12 cultured under air oxygen condition with and without addition of NGF the cell labelled with anti-synapsin-1 primary antibody and then incubated with anti-mouse IgG-FITC secondary antibody. (A) Synapsin-1 expression in PC12 with NGF treatment (Blue indicates DAPI, Green indicates GAP-43). (B) Synapsin-1 expression in PC12 without NGF treatment (Blue indicates DAPI, Green indicates Synapsin-1). Scale bar indicates 100 µm.

neurite outgrowth at IH, significant effect elevated after supplementation with DFO and IOX2 while $CoCl_2$ and DMOG have no effect of neurite outgrowth (Figure 3.22A and 23). DFO, DMOG and IOX2 remarkably increase in GAP-43 (Figure 3. 24). No change in synapsin-1 expression was noticed after HMAs supplementation (Figure 3.25).

IH and NGF exposure stimulated a 3X increase in PC12 cell differentiation (Figure 3.22B and 23). while IH + NGF only $CoCl_2$ and IOX2 caused significant reduction in neurite formation capacity in comparison to IH + NGF treated cells (Figure 3.19.B). GAP-43 expression reduced after $CoCl_2$ and DMOG with no obvious effect for DFO and IOX2 (Figure 3.23). Synapsin-1 showed no obvious change after treatment with all HMAs (Figure 3.24 and 25).

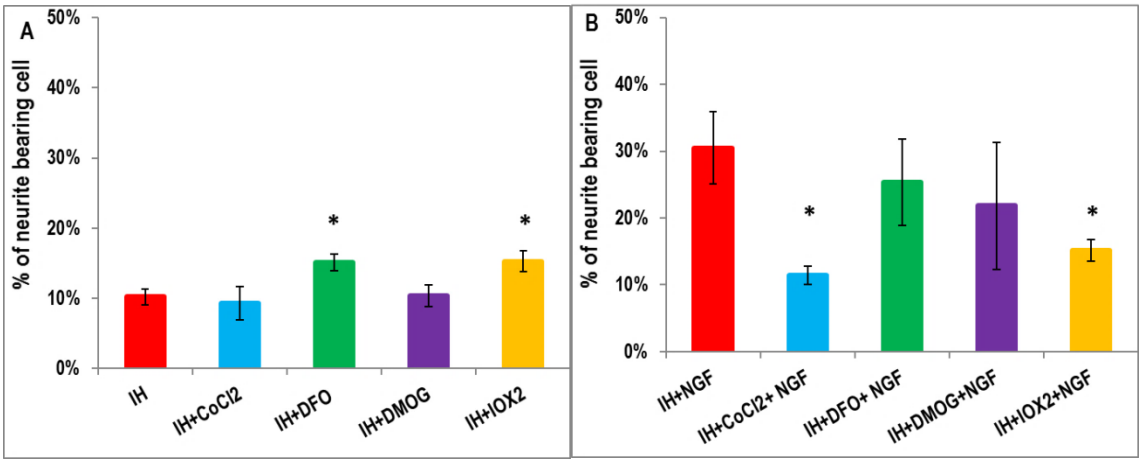

Figure 3.22. PC12 neurite outgrowth quantification in IH

*PC12 cell were cultured in collagen IV pre-coated 24-well plate with and without NGF stimulation for 7-10 days after treatment with hypoxia mimetic agents at intermittent hypoxia oxygen (IH). Histogram shows the percentage of neurite bearing PC12 cell after treatment with HMAs alone (A) and after combination of NGF+ HMAs (B). X-axis indicates the oxygen and HMAs. Y-axis indicates the percentage of neurite bearing cells. Error bars indicates standard deviation. * indicates significant difference (p< 0.01).*

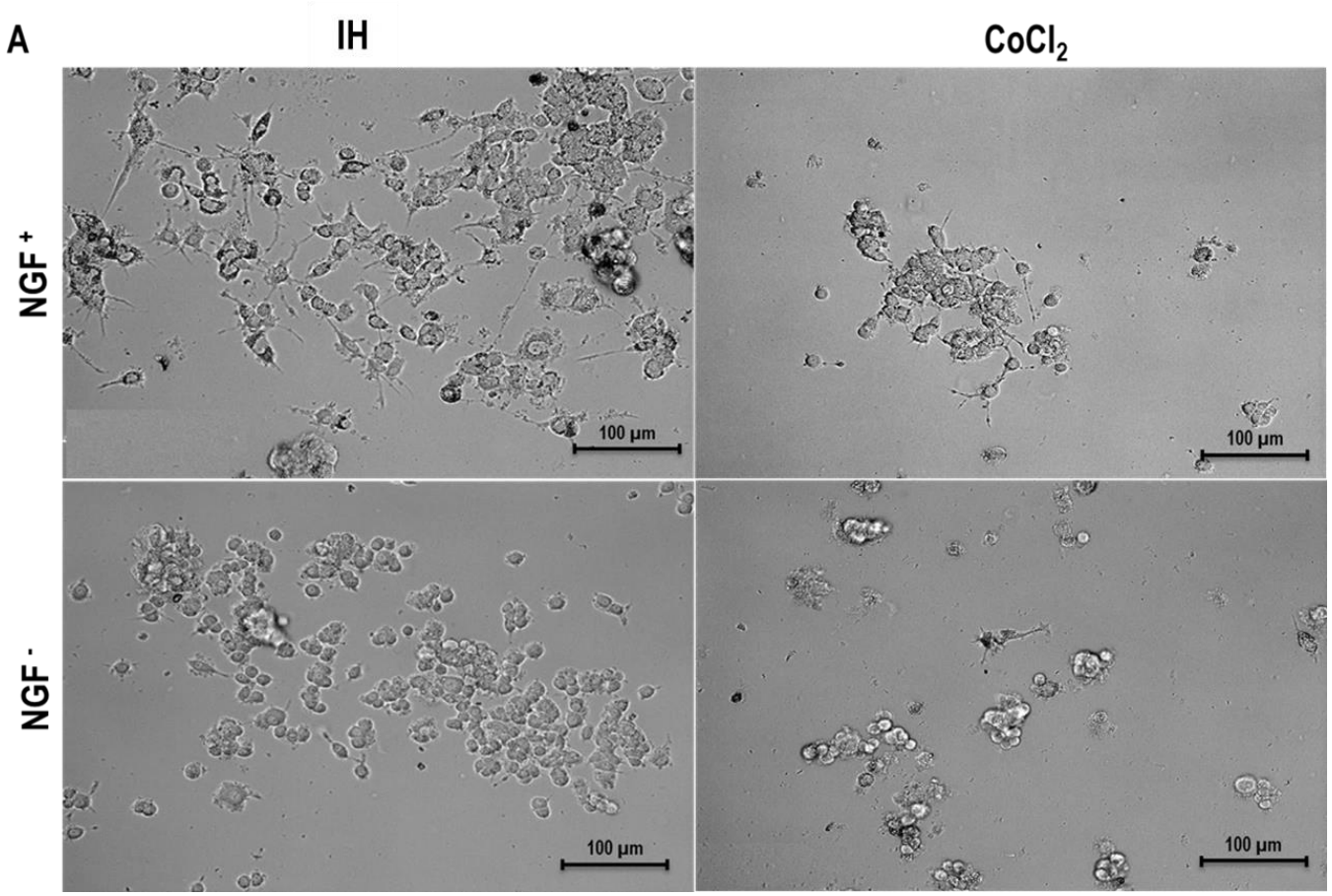
A
IH
$CoCl_2$
NGF +
NGF -
100 µm
100 µm
100 µm
100 µm

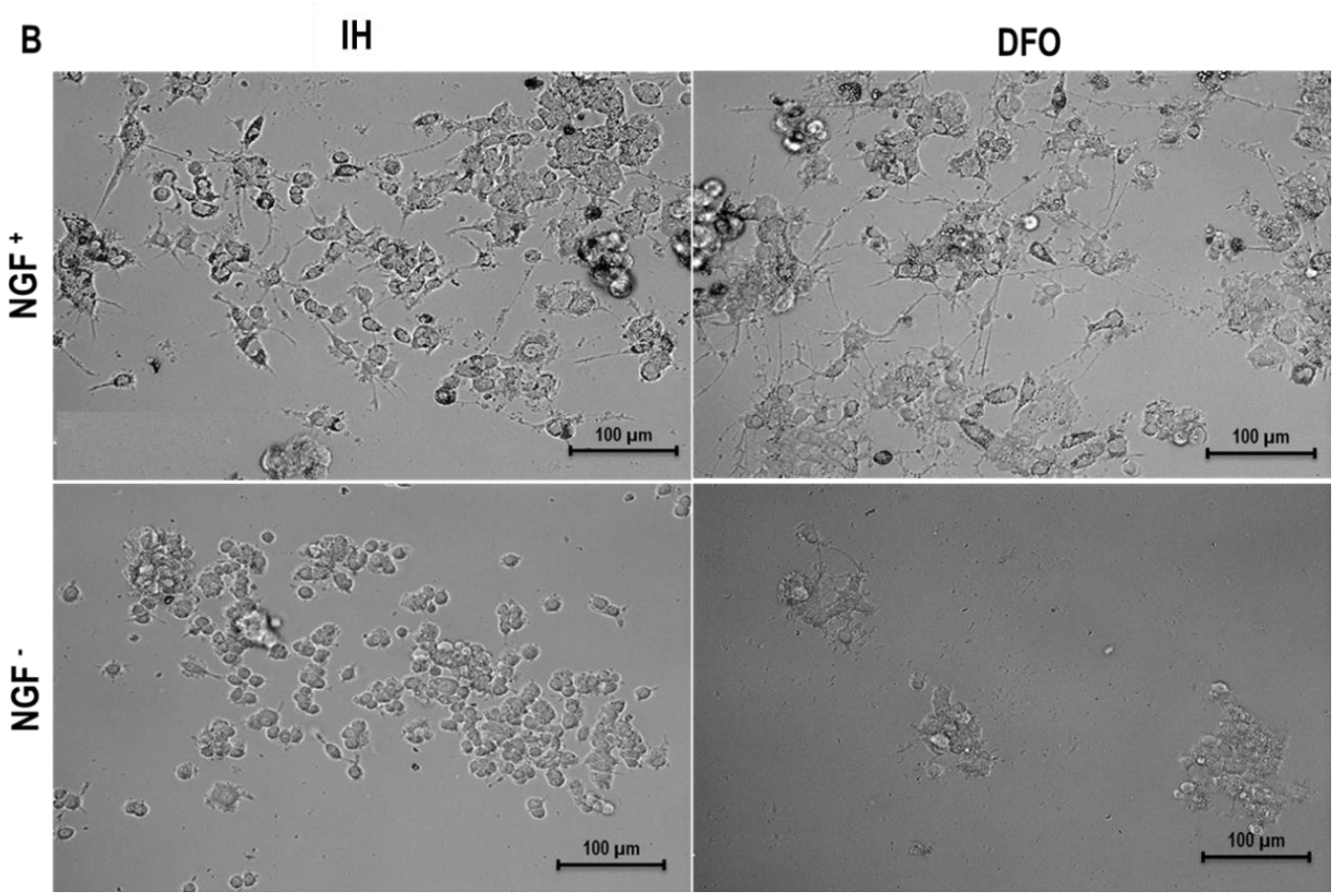
B
IH
DFO
NGF +
NGF -
100 µm
100 µm
100 µm
100 µm

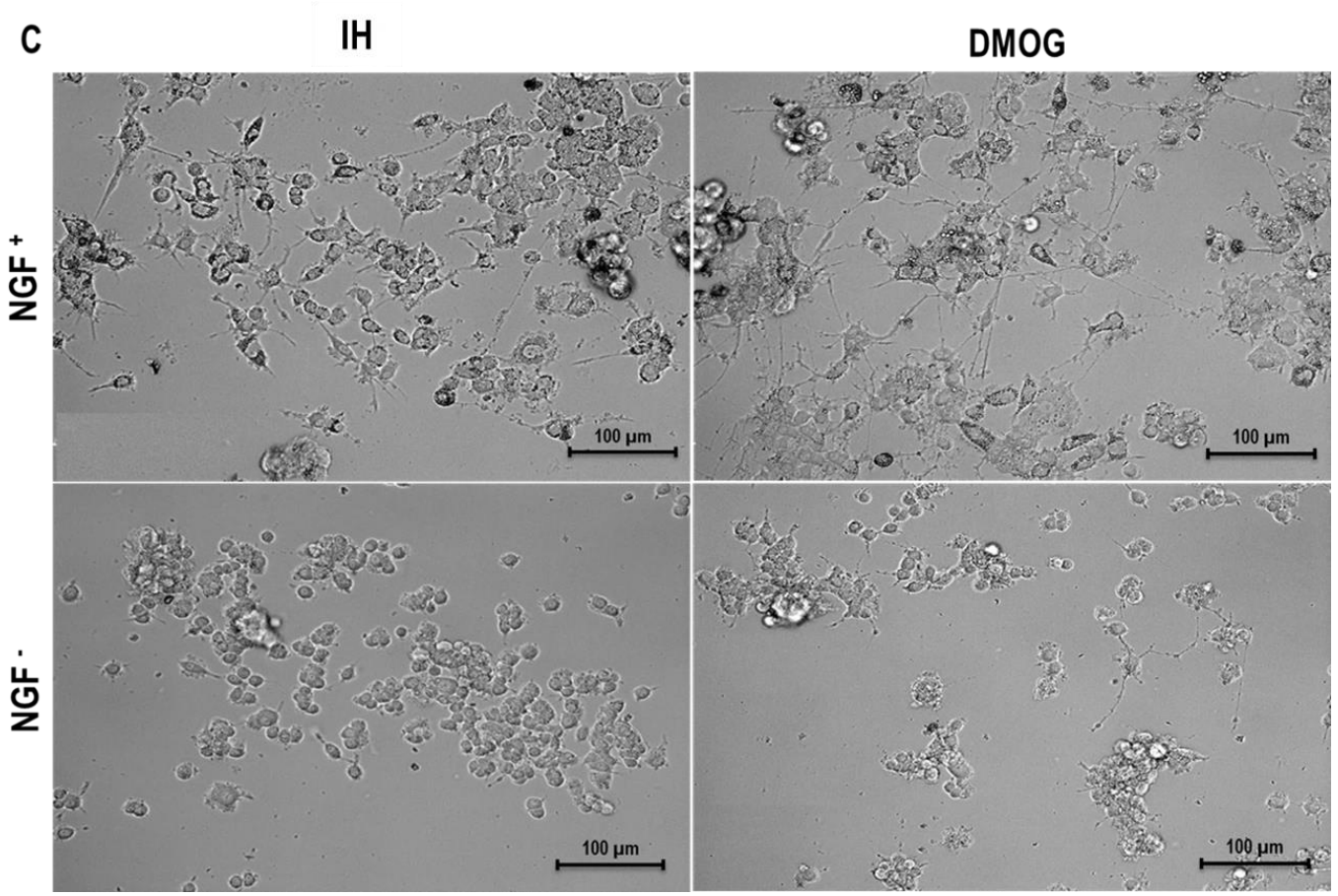
C
IH
DMOG
NGF +
NGF -
100 µm
100 µm
100 µm
100 µm

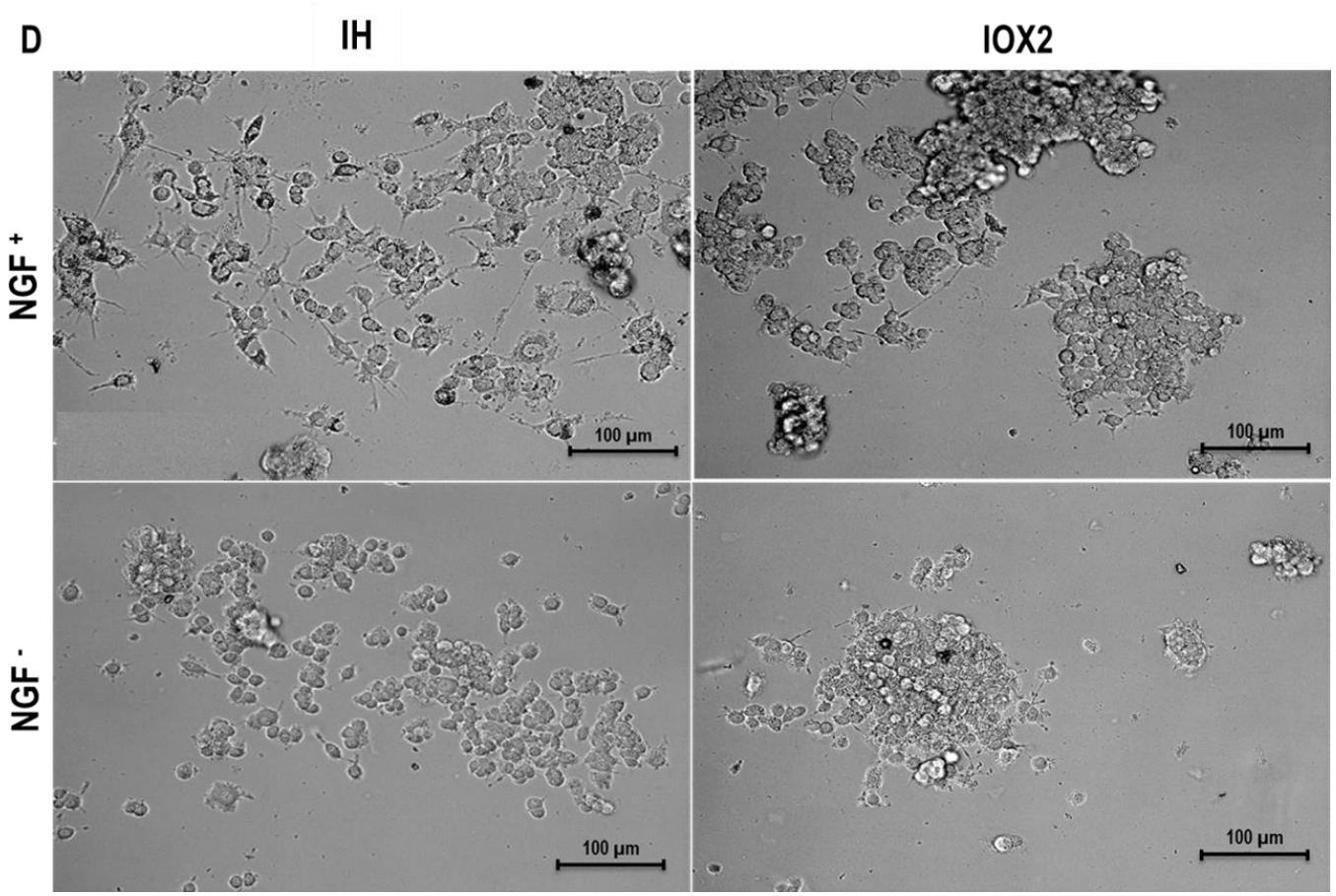

Figure 3.23. Neurite outgrowths of PC12 at IH

PC12 were plated at a seeding density of 10^4 cells/ml into 24-well plates coated with collagen type IV and incubated for 7-10 days. (A) PC12 supplemented with $CoCl_2$ +/- NGF, (B). PC12 supplemented with DFO +/- NGF, (C). PC12 supplemented with DMOG +/- NGF, (D). PC12 supplemented with IOX2 +/- NGF. Scale bar equal 100 µm.

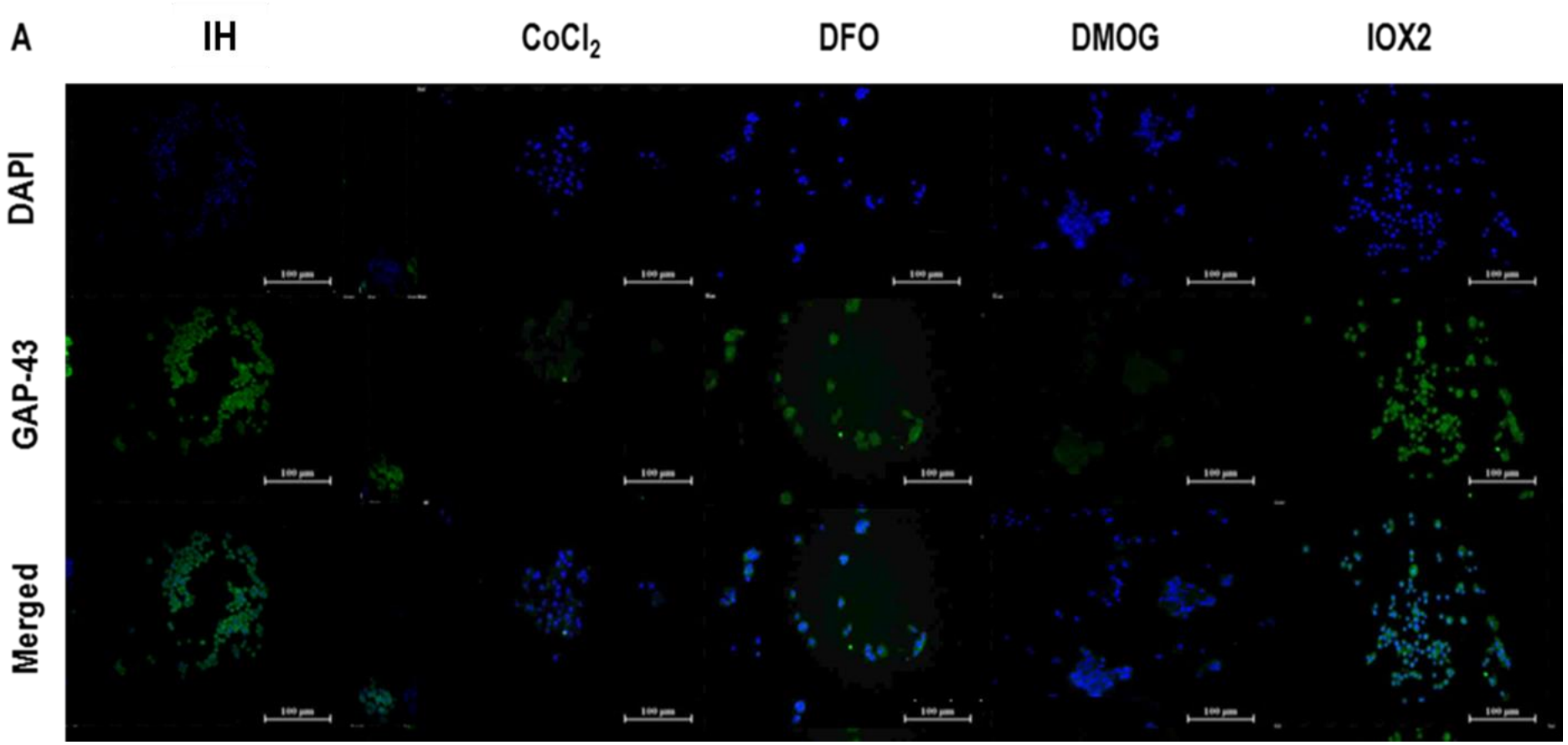
A
IH
CoCl2
DFO
DMOG
IOX2
DAPI
GAP-43
Merged

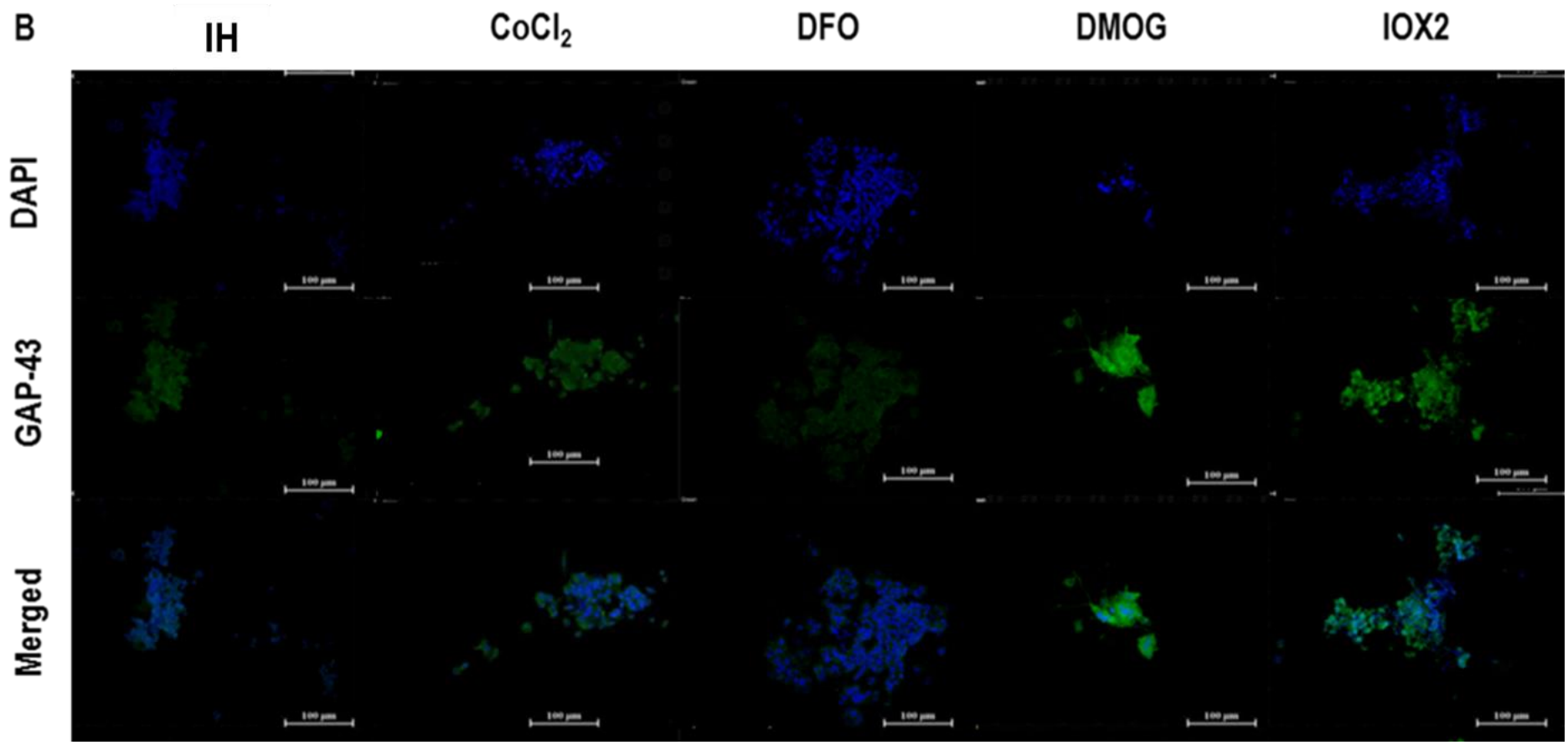

Figure 3.24. Effect of HMAs on GAP-43 expression in PC12 at IH

PC12 cultured under intermittent hypoxia condition with and without addition of NGF. The cell labelled with anti-GAP-43 primary antibody and then incubated with anti-rabbit IgG-FITC secondary antibody. (A) GAP-43 expression in HMA supplemented PC12 with NGF. Blue indicates DAPI nuclei, Green indicates GAP-43. (B). GAP-43 expression in HMA supplemented PC12 without NGF. Scale bar indicates 100 µm.

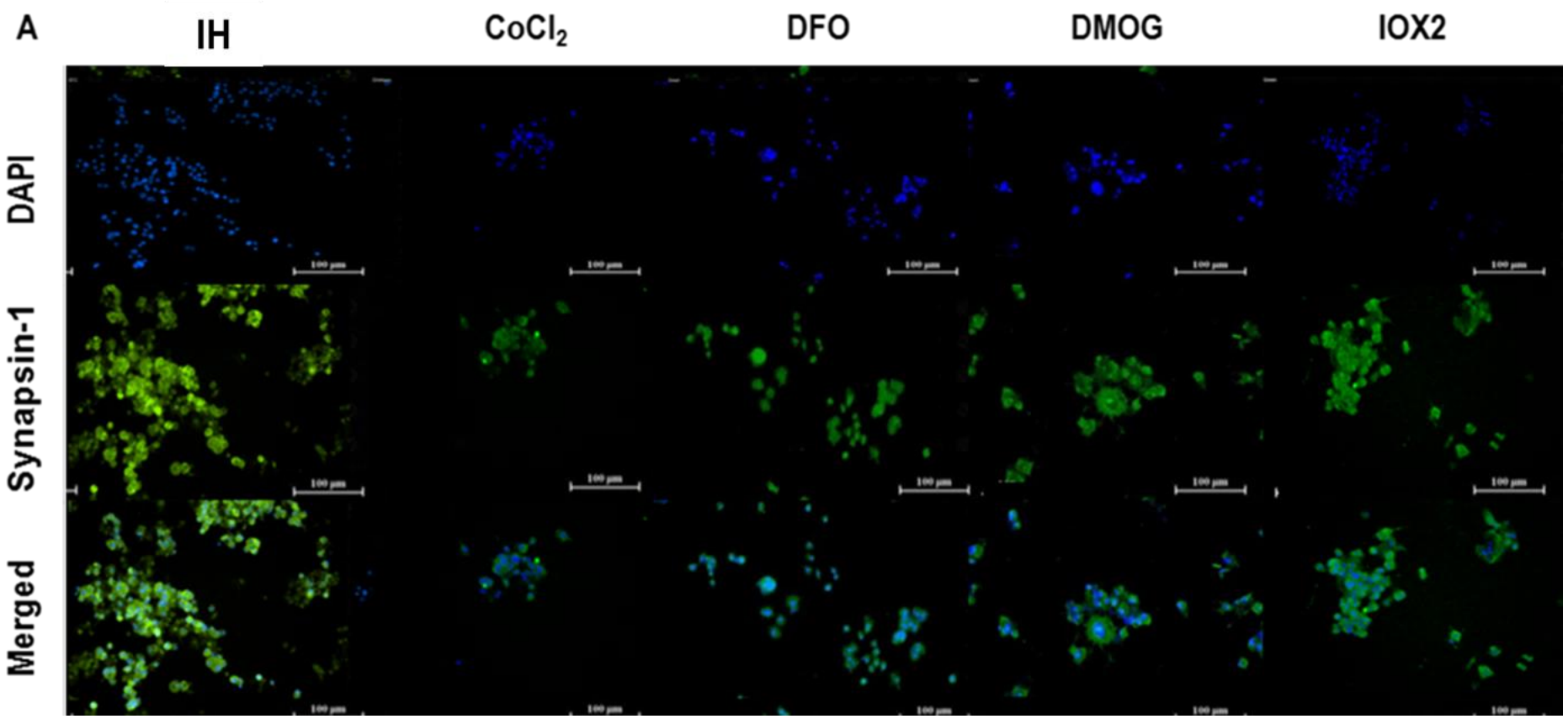
A
IH
$CoCl_2$
DFO
DMOG
IOX2
DAPI
Synapsin-1
Merged

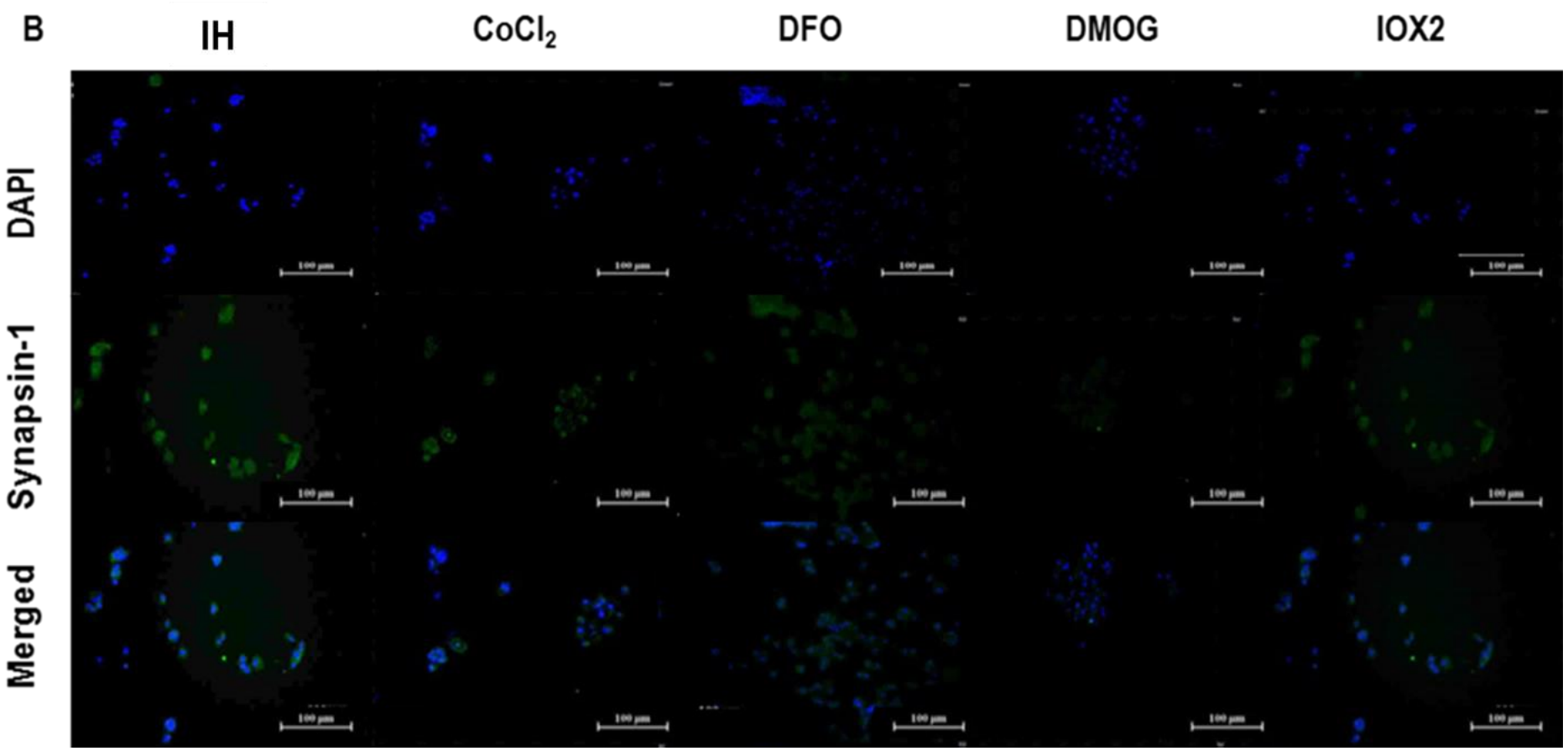

Figure 3.25. Effect of HMAs on Synapsin-1 expression in PC12 at IH

PC12 cultured under intermittent hypoxia condition with and without addition of NGF. The cell labelled with anti-synapsin-1 primary antibody and then incubated with anti-mouse IgG-FITC secondary antibody (A) Synapsin-1 expression in HMA supplemented PC12 with NGF (Blue indicates DAPI nuclei, Green indicates Synapsin-1). (B). Synapsin-1 expression in HMA supplemented PC12 without NGF. Scale bar indicates 100 µm.

CN + NGF exposure stimulated an 80% increase in PC12 cell differentiation in comparison to non NGF treated cells. DFO and IOX2 significantly elevated neurite outgrowth (Figure 3.26A and 27). All HMAs remarkably reduced GAP-43 expression while they have no effect on synapsin-1 (F igure 3.28 and 29).

CN + DFO significantly increase neurite formation in comparison to CN +NGF (Figure 3.26A and 27). CN + NGF + $CoCl_2$ and DMOG displayed a marked and significant reduction in differentiated cell number vs. CN+ NGF treated cells (Figure 3.26B). HMAs showed no obvious effect on GAP-43 and synapsin-1 expression while only DMOG can induce some elevation in syanpsin-1 (Figure 3.28 and 29).

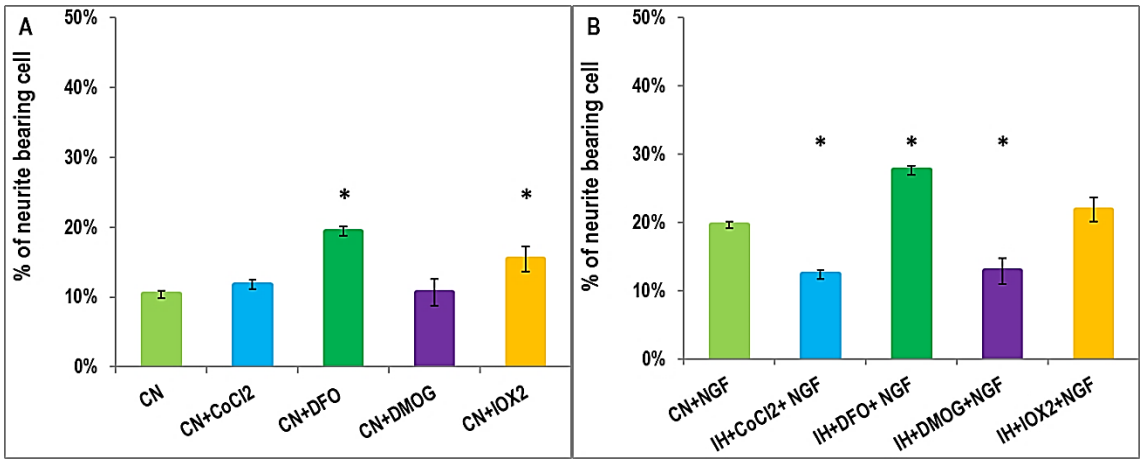

Figure 3.26. Neurite outgrowths of PC12 at CN

*PC12 cell were cultured in collagen IV pre-coated 24-well plate with and without NGF stimulation for 7-10 days after treatment with hypoxia mimetic agents at continuous normoxia (CN). Histogram shows the percentage of neurite bearing PC12 cell after treatment with HMAs alone (A) and after combination of NGF+ HMAs (B). X-axis indicates the oxygen and HMAs. Y-axis indicates the percentage of neurite bearing cells. Error bars indicates standard deviation. * indicates significant difference (p< 0.01).*

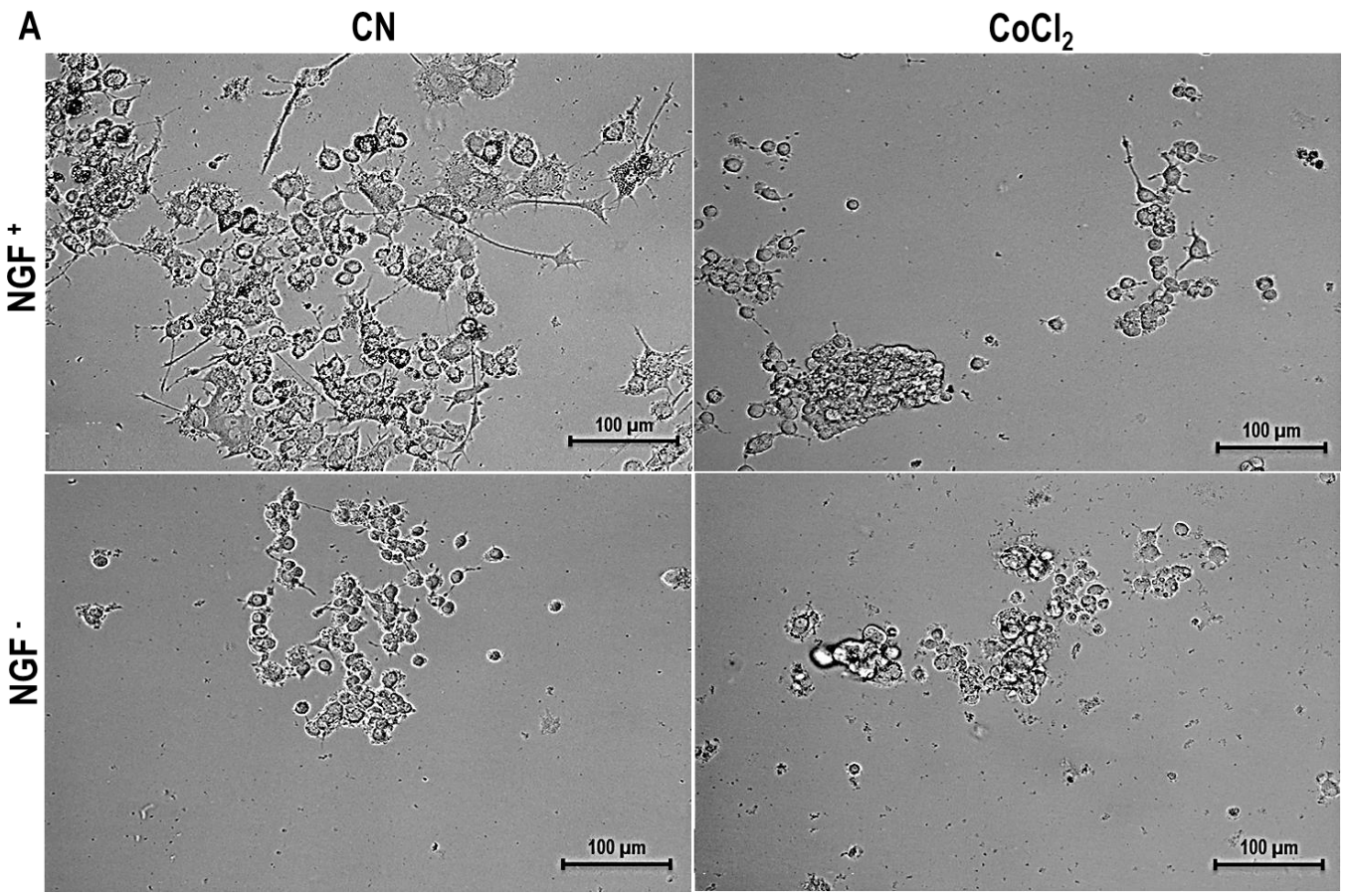
A
CN
CoCl2
NGF+
NGF-
100 µm
100 µm
100 µm
100 µm

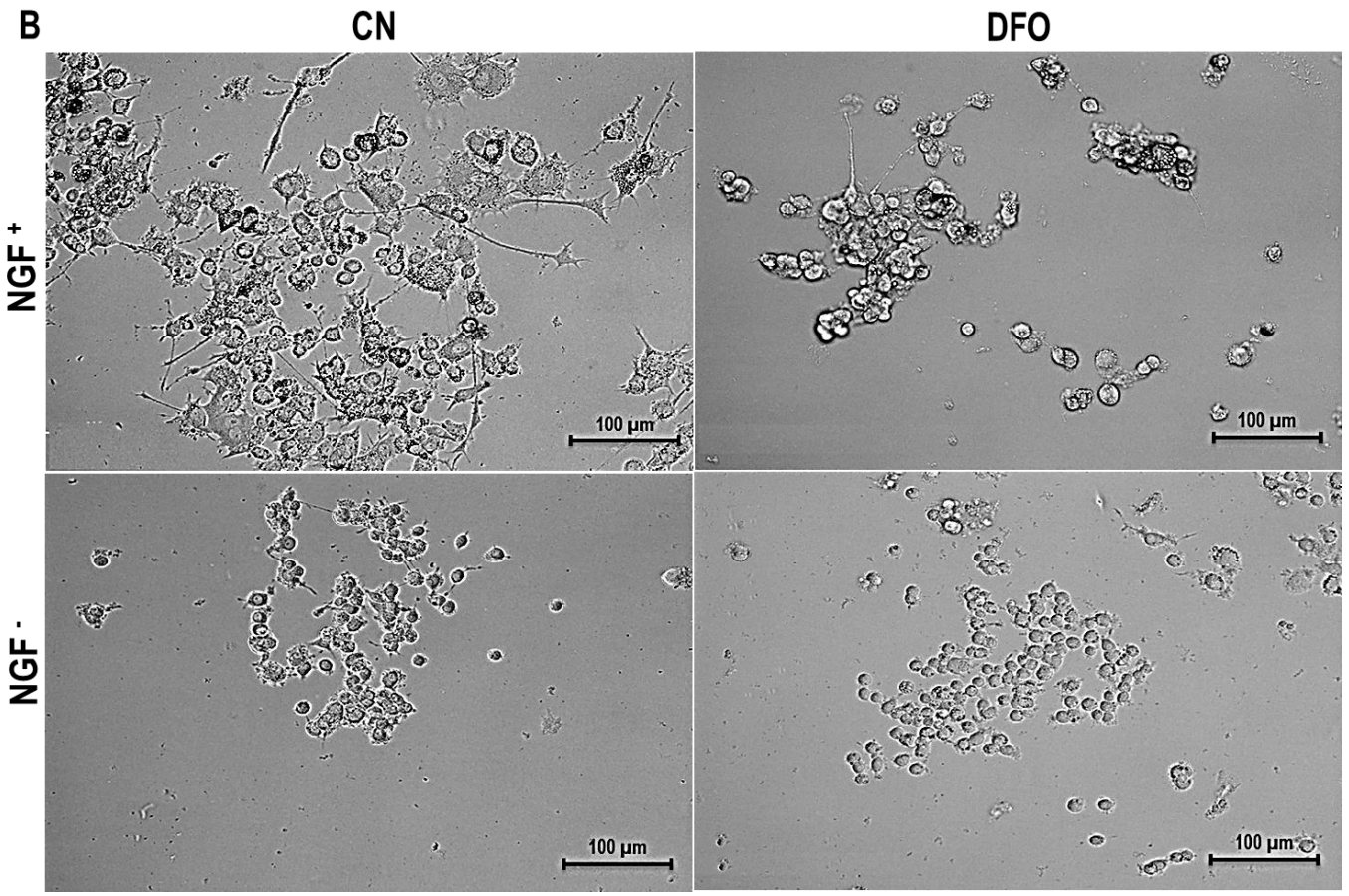
B
CN
DFO
NGF +
NGF -
100 µm
100 µm
100 µm
100 µm

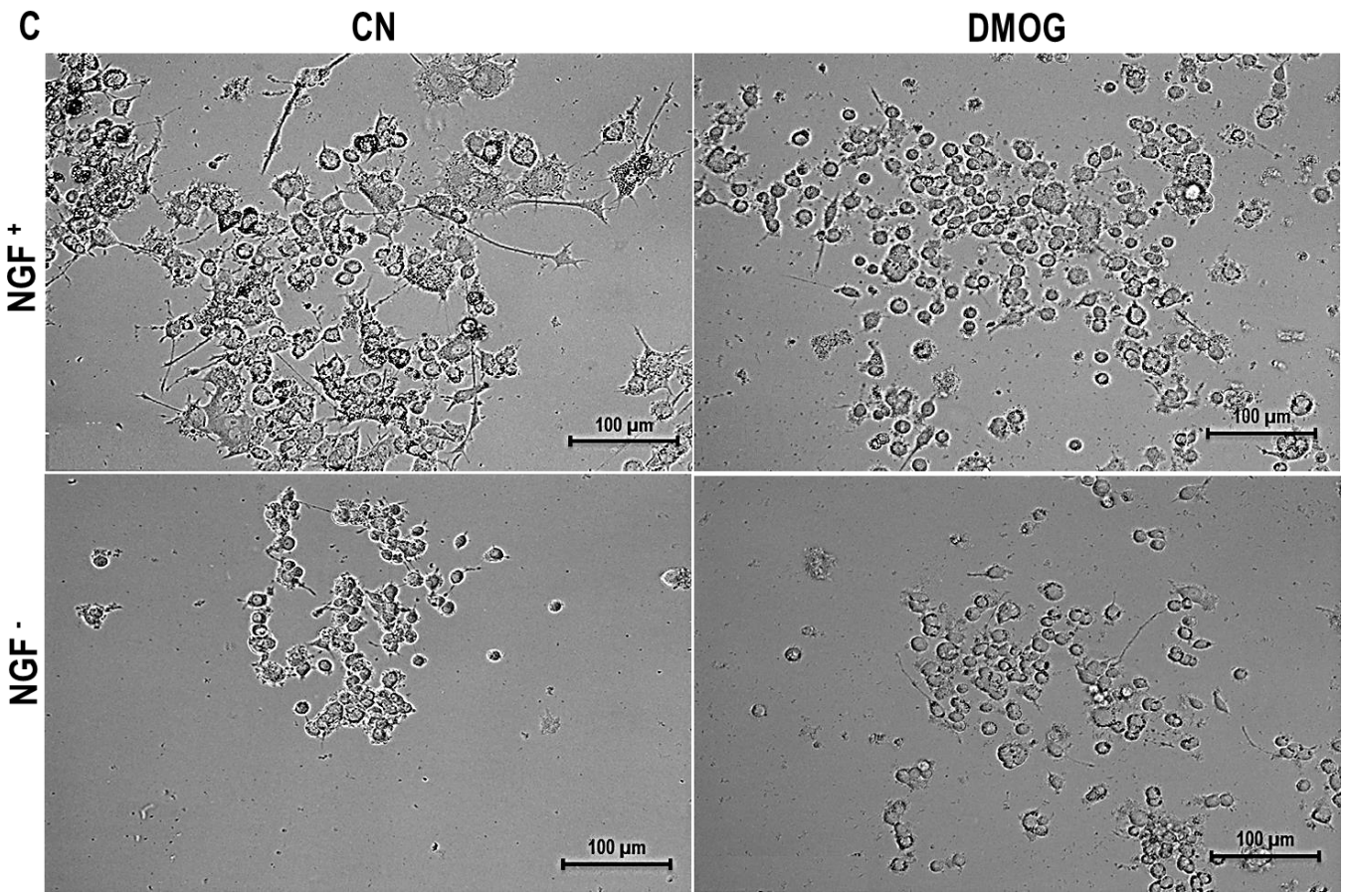
C
CN
DMOG
NGF+
NGF-
100 µm
100 µm
100 µm
100 µm

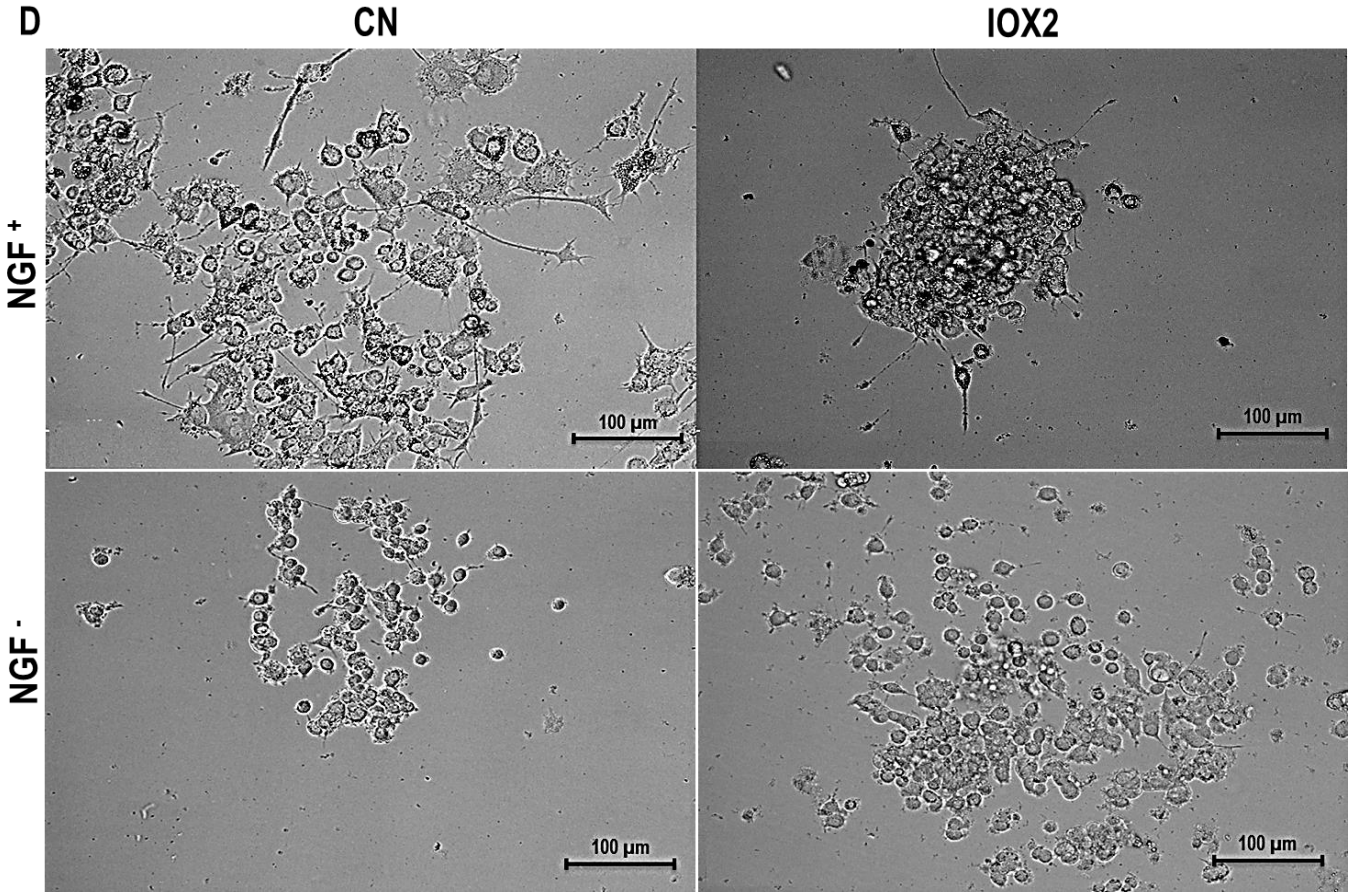

Figure 3.27. Neurite outgrowths of PC12 at CN

PC12 were plated at a seeding density of 10^4 cells/ml into 24-well plates coated with collagen type IV and incubated for 7-10 days. (A) PC12 supplemented with $CoCl_2$ +/- NGF, (B). PC12 supplemented with DFO +/- NGF, (C). PC12 supplemented with DMOG +/- NGF, (D). PC12 supplemented with IOX2 +/- NGF. Scale bar equal 100 µm.

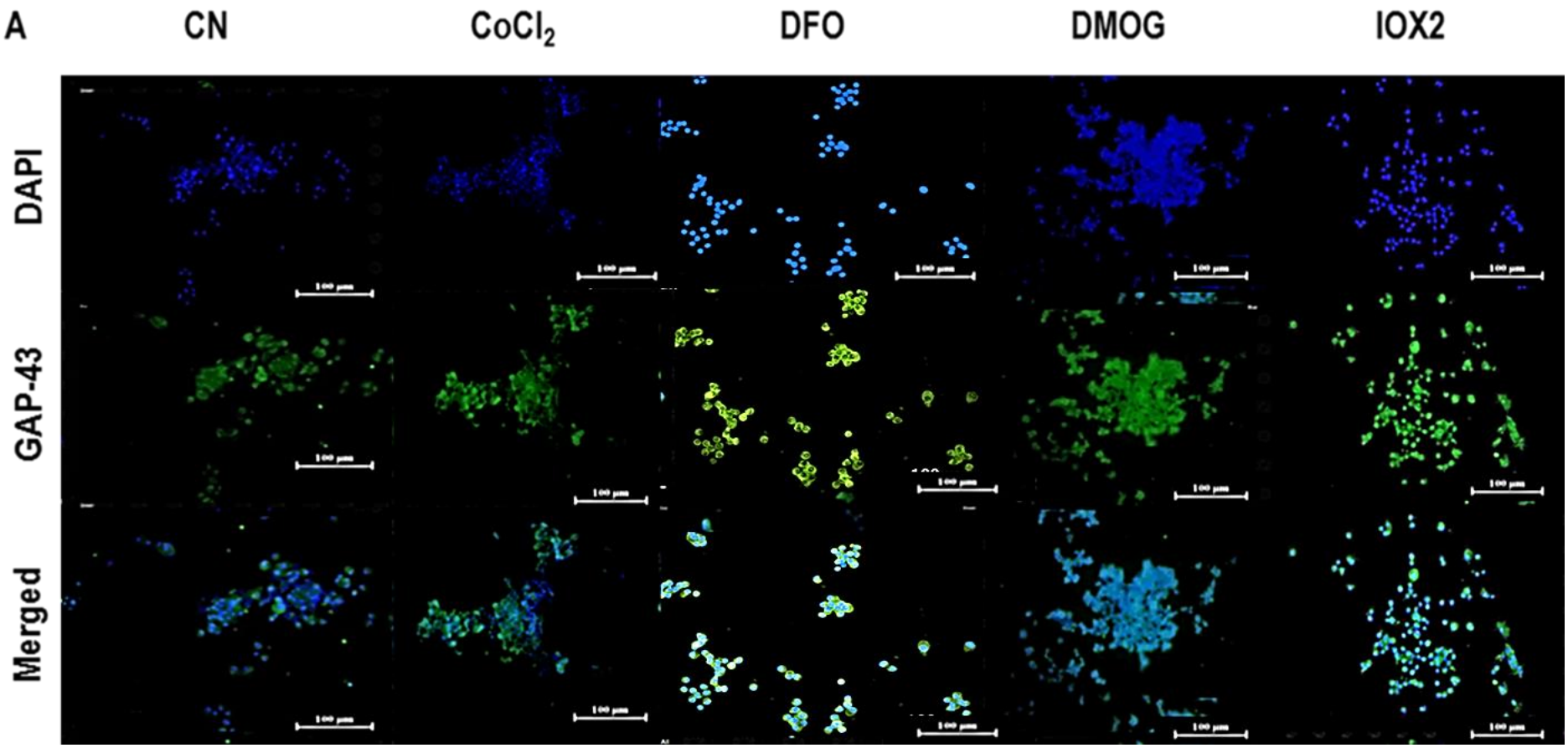
A
CN
$CoCl_2$
DFO
DMOG
IOX2
DAPI
GAP-43
Merged

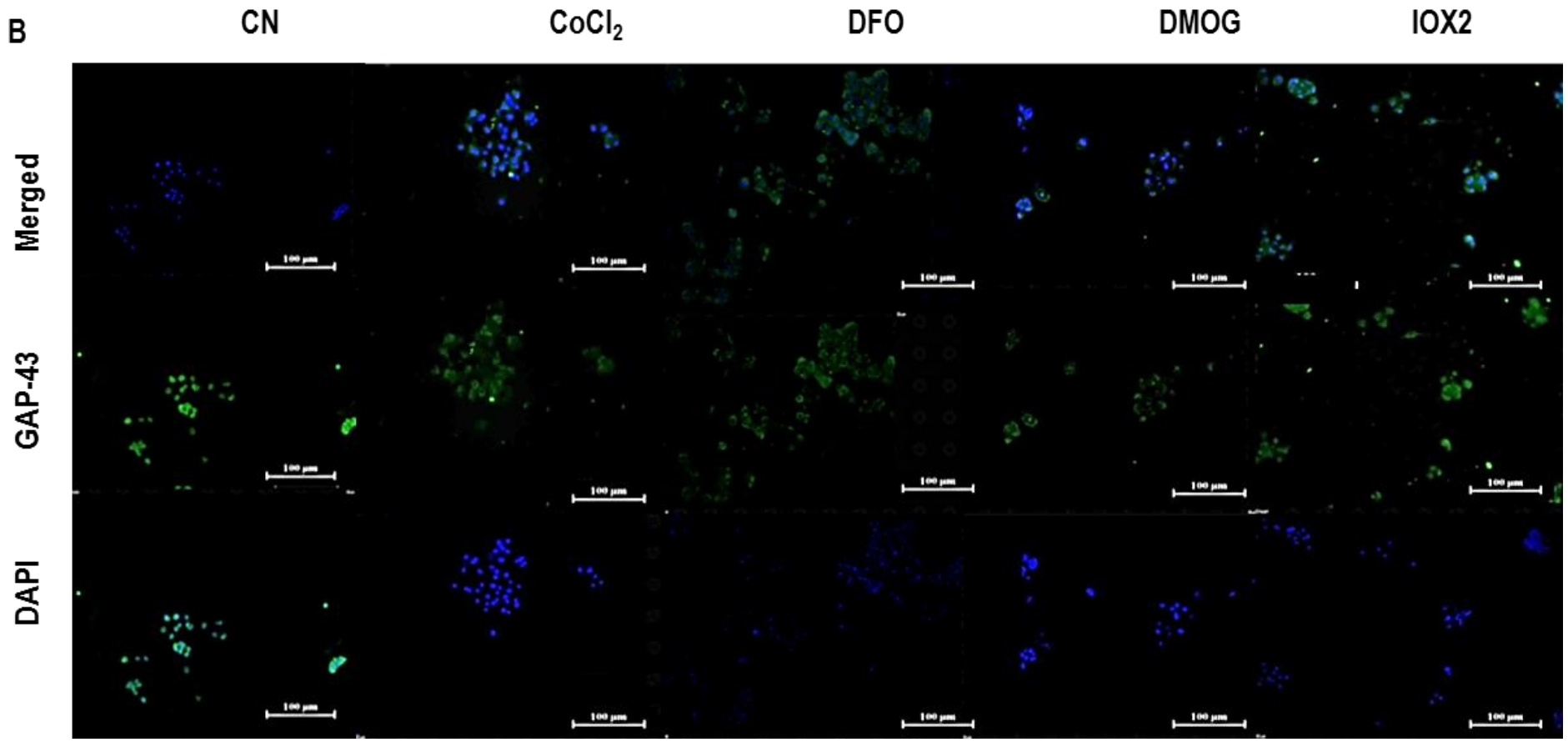

Figure 3.28. Effect of HMAs on GAP-43 expression in PC12 at CN

PC12 cultured under continuous normoxia condition with and without addition of NGF. The cell labelled with anti-GAP-43 primary antibody and then incubated with anti-rabbit IgG-FITC secondary antibody (A) GAP-43 expression in HMA supplemented PC12 with NGF. Blue indicates DAPI nuclei, Green indicates GAP-43. (B). GAP-43 expression in HMA supplemented PC12 without NGF. Scale bar indicates 100 µm.

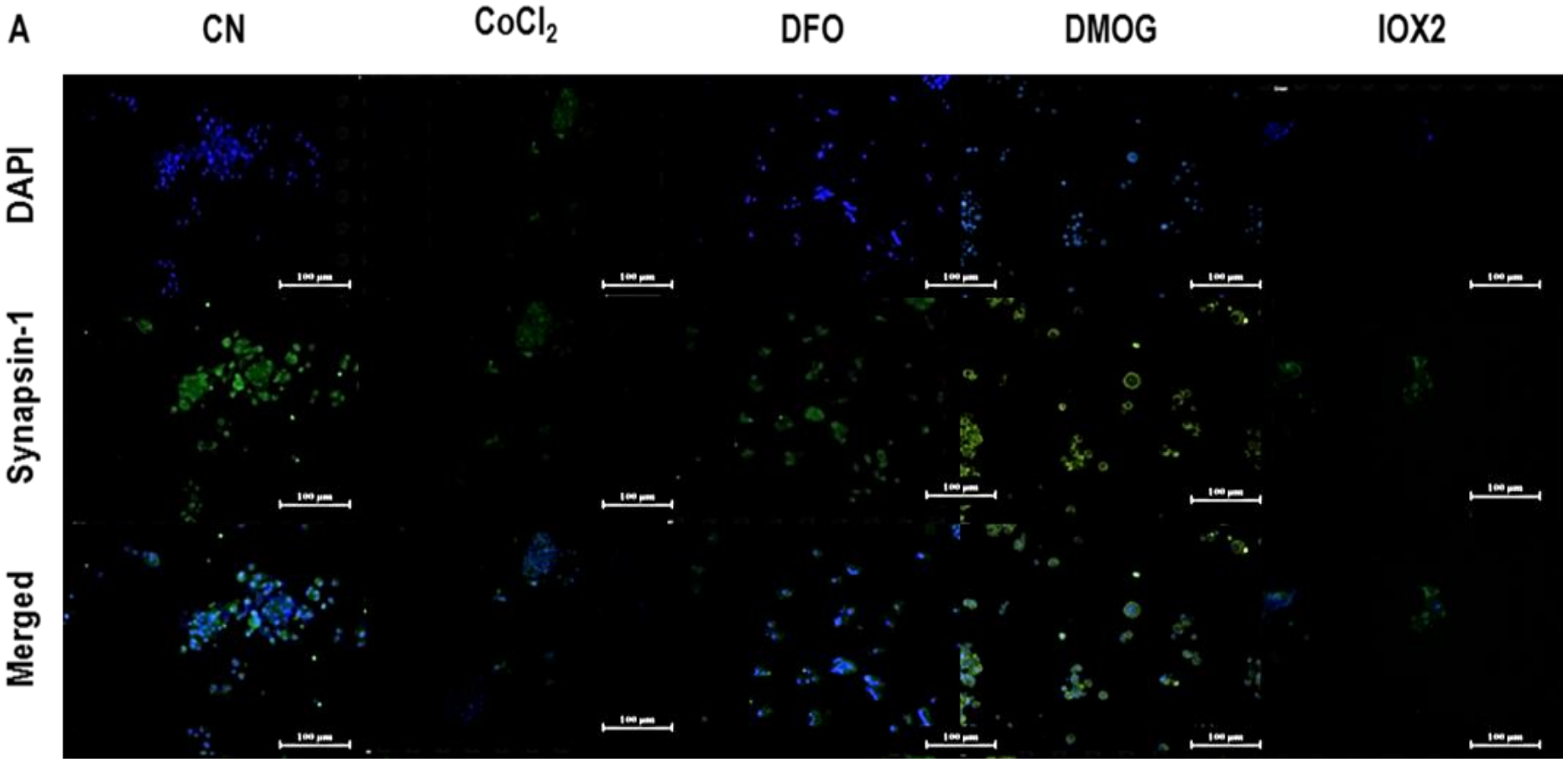
A
CN
$CoCl_2$
DFO
DMOG
IOX2
DAPI
Synapsin-1
Merged

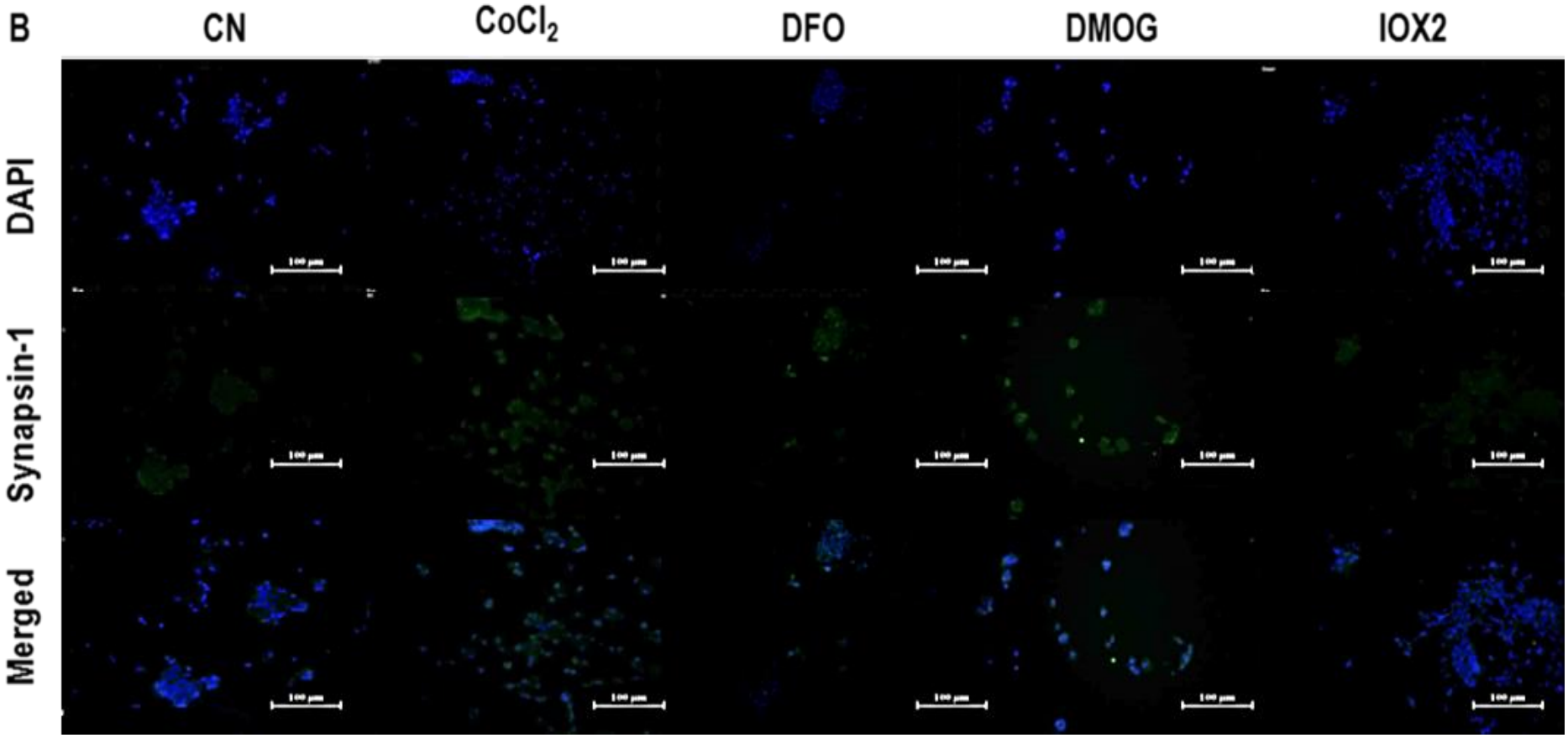

Figure 3.29. Effect of HMAs on Synapsin-1 expression in PC12 at CN

PC12 cultured under continuous normoxia condition with and without addition of NGF. The cell labelled with anti-synapsin-1 primary antibody and then incubated with anti-mouse IgG-FITC secondary antibody. (A) Synapsin-1 expression in HMA supplemented PC12 with NGF. Blue indicates DAPI nuclei, Green indicates Synapsin-1. (B) Synapsin-1 expression in HMA supplemented PC12 without NGF. Scale bar indicates 100 µm.

In vitro model is vtial in screening of huge number of chemicals thet have potential pharmacological use. PC12 cell is one of the most known model to study the developmental neurotoxicants, assessment of critical neurodevelopmental processes and neuronal differentiation. neurotrophic factor NGF induce signaling pathways that control differentiation, and effect of chemicals on neurite outgrowth. NGF treated PC12 cells cease to proliferate, extend multiple neurites, and possess sympathetic neurons properties. Differentiation and neurite outgrowth can be quantitative assessment using simple contrast microscopy in live cells, or by fluorscene imaging after immunocytochemistry staining.

The results of this work showed that there is no significant effect for different oxygen culture conditions on neurite outgrowth when cells un induced by NGF in contrast NGF induced cells showed significant elevation when incubated at IH (3 fold) and CN (80%) and this may be related to the fact that HIF-) Is a transcriptional activator of the tropomyosin receptor kinase A and B (Trk A and B) neurotrophin receptor gene thus have synergistic effect with NGF elevated (Martens *et al.,* 2007). our findings suggest that hypoxia induces neurite outgrowth in PC12 cells via a pathway different from that activated by NGF. Expose to IH at critical stages of development may contribute to aberrant neurite outgrowth and could be a factor in the pathogenesis of certain delayed developmental neurological disorders.

HMAs companied by a significant decrease in the expression of the neuronal specific axonal marker of differentiation, GAP-43, as determined by immunofluorescence and these results support the finding that HMAs uncoupled GAP-43 expression from neurite outgrowth and that hypoxia-induced neurite outgrowth is mediated by activation of adenosine A2A receptors coupled to adenylate cyclase (O'D riscoll and Gorman, 2005). HMAs under all oxygen culture conditions showed no obvious change in synapsin-1 expression.

3.3.4. Effect of hypoxia mimetic agents on PC12 cells apoptosis

During embryonic development, tissue maintenance and stress conditions like hypoxia and apoptosis occur as physiological processes. Apoptosis is characterised by certain morphologic changes which include changes in the plasma membrane, cytoplasm and nucleus condensation, and DNA cleavage. Changes in plasma membrane structure are amongst the earliest criteria. During apoptosis, phospholipid phosphatidylserine (PS) in the cell membrane is translocated to the outer side of the plasma membrane from the inner side, exposing PS to the external cellular environment. Annexin V is a 35-36 kDa Ca^{2+} dependent phospholipid-binding protein that has a high affinity for exposed PS. To retain affinity and sensitive, Annexin V conjugated to fluorochrome including Allophycocyanin (APC). Exposed PS in apoptotic cells bind APC Annexin V in combination with the membrane impermeable DNA dye propidium iodide (PI) used to differentiate between viable, apoptotic and secondary necrotic cells.

To establish if the reduction in cellular viability was due to programmed cell death (apoptosis), the Annexin V assay was performed as outlined in Chapter 2, Section 2.2.1.8.

PC12 cells incubated at AO, IH and CN culture shows that there was significant increase in early apoptosis and necrosis after incubation, while at IH only significantly increase late apoptosis with no significant effect was noticed at CN culture condition in comparison to AO culture condition.

Under AO culture, all HMAs induced early apoptosis in comparison to control AO at nearly at all time points ($p<0.01$). No significant effect was noticed in late apoptosis after treatment with HMAs over 96 hrs. After treatment with DMOG and IOX2 significant increase in necrotic cells percentage after first 48 hrs and 24 and 48 hrs respectively.

While after 96 hrs all HMAs significantly reduced necrotic cells percentage in comparison to control AO at each time points (Figure 3.30).

Under IH culture condition, $CoCl_2$ and DFO significantly increase early apoptosis at 24, 72 and 96 hrs with significant increase was noticed on early apoptosis after treatment with all DMOG after 96 and IOX2 at 24 hrs. No significant effect was noticed on late apoptosis (Figure 3.31).

The percentage of necrotic cells significantly reduced after treatment with DFO, DMOG and IOX2 after 96 hrs, while it increased after 24 and 48 hrs after necrosis in co DFO, DMOG ans IOX2 in comparison to control IH at each time point ($p<0.01$ (Figure 3.29). Finally, under CN culture HMAs significantly elevate early apoptosis and late apoptosis over the 96 hrs. Necrosis significantly elevated over 96 hrs (Figure 3.30). To sum up HMAs cause significant elevation in early apoptosis and necrosis in PC12 under all oxygen culture conditions (Figure 3.32).

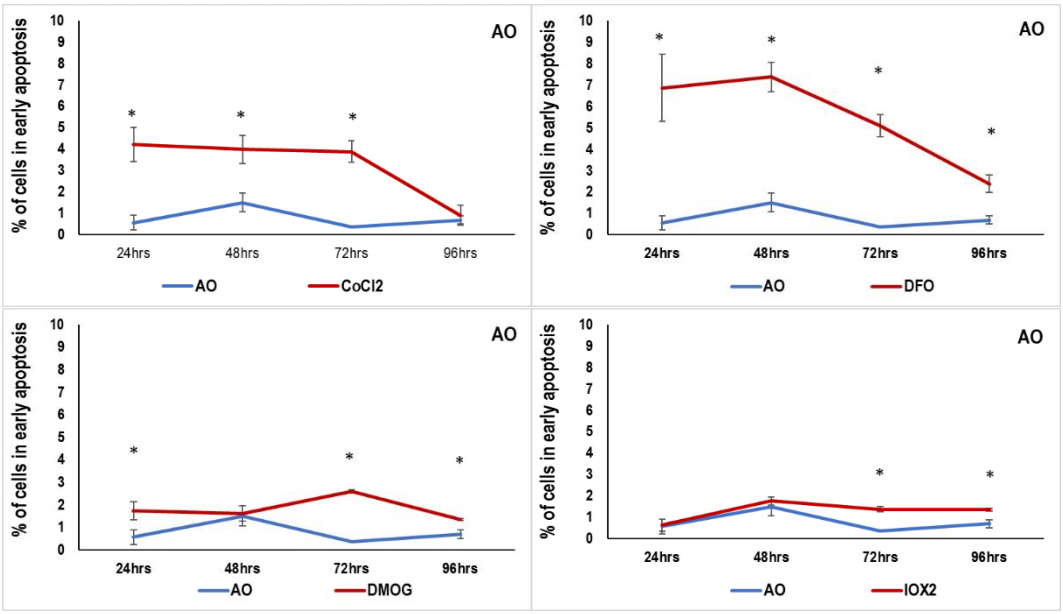
% of cells in early apoptosis
AO
24hrs
48hrs
72hrs
96hrs
AO
CoCl2
DFO
DMOG
IOX2

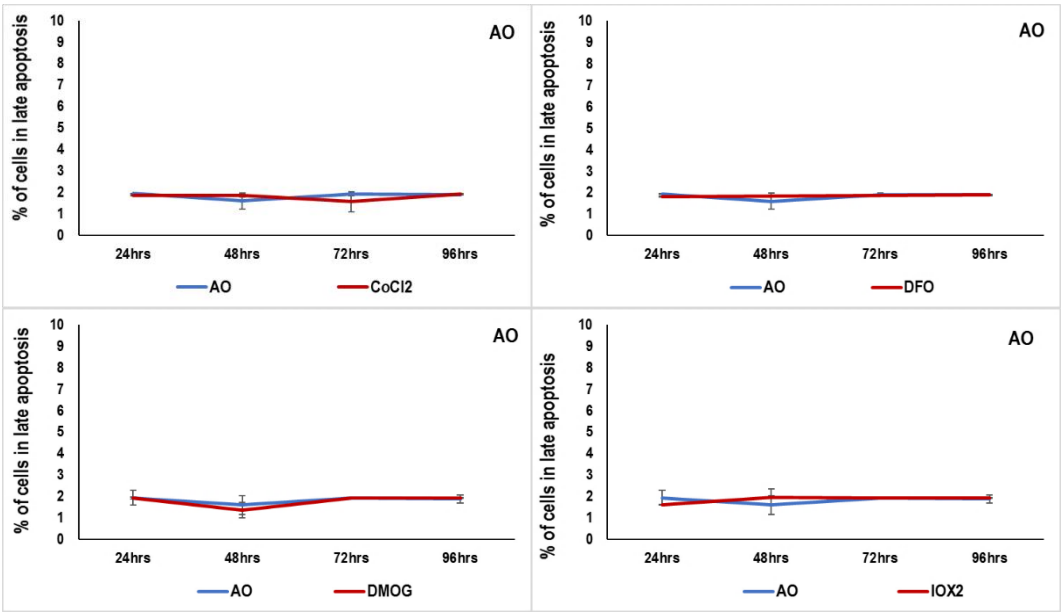
% of cells in late apoptosis
AO
24hrs
48hrs
72hrs
96hrs
AO
CoCl2
DFO
DMOG
IOX2

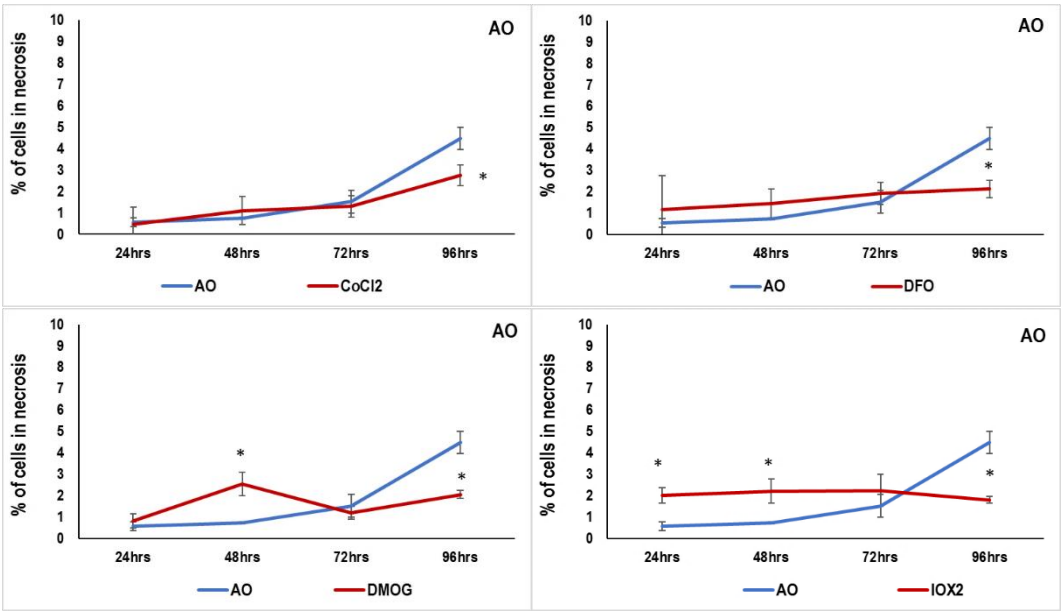

Figure 3.30. PC12 apoptosis/necrosis under air oxygen

*Following exposure to (50 µM $CoCl_2$, 50 µM DFO, 100 µM DMOG and 50 nM IOX2) for 24 hrs, 48 hrs, 72 hrs and 96 hrs, the percentage of early, late apoptotic and apoptotic PC12 at AO was plotted. Data are presented as mean ± standard deviation (SD). n=1 triplicate, * indicates significant difference in comparison to AO at each time point (p<0.01).*

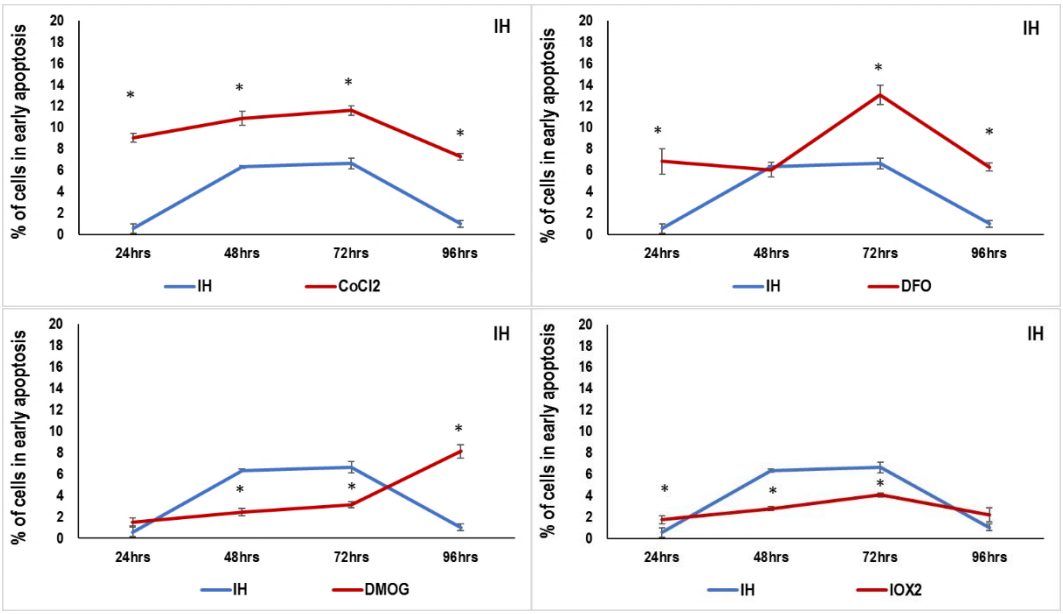
% of cells in early apoptosis
IH
24hrs
48hrs
72hrs
96hrs
IH
CoCl2
DFO
DMOG
IOX2

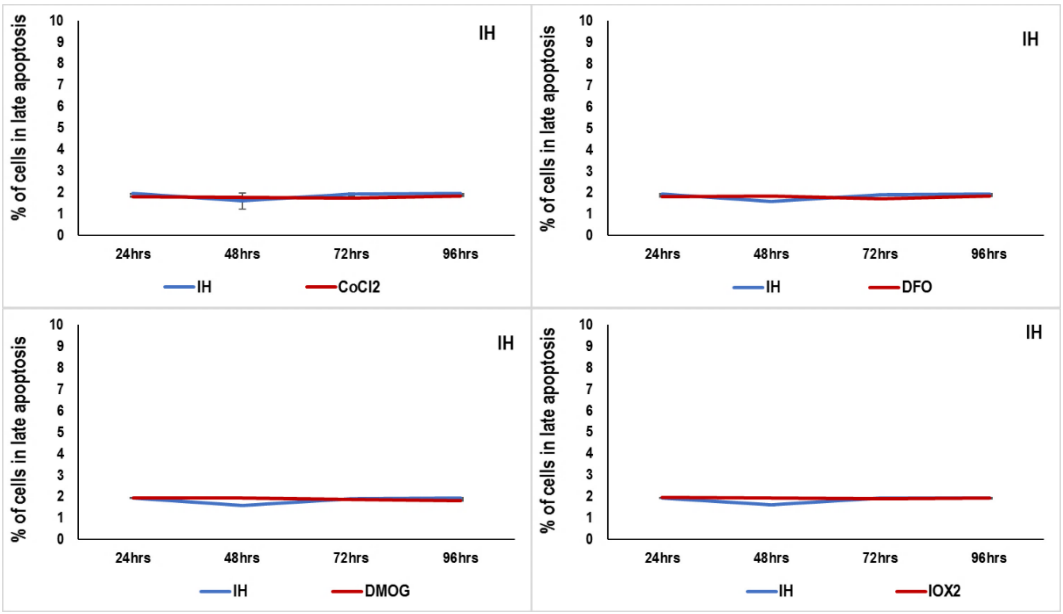
% of cells in late apoptosis
IH
24hrs
48hrs
72hrs
96hrs
IH
CoCl2
DFO
DMOG
IOX2

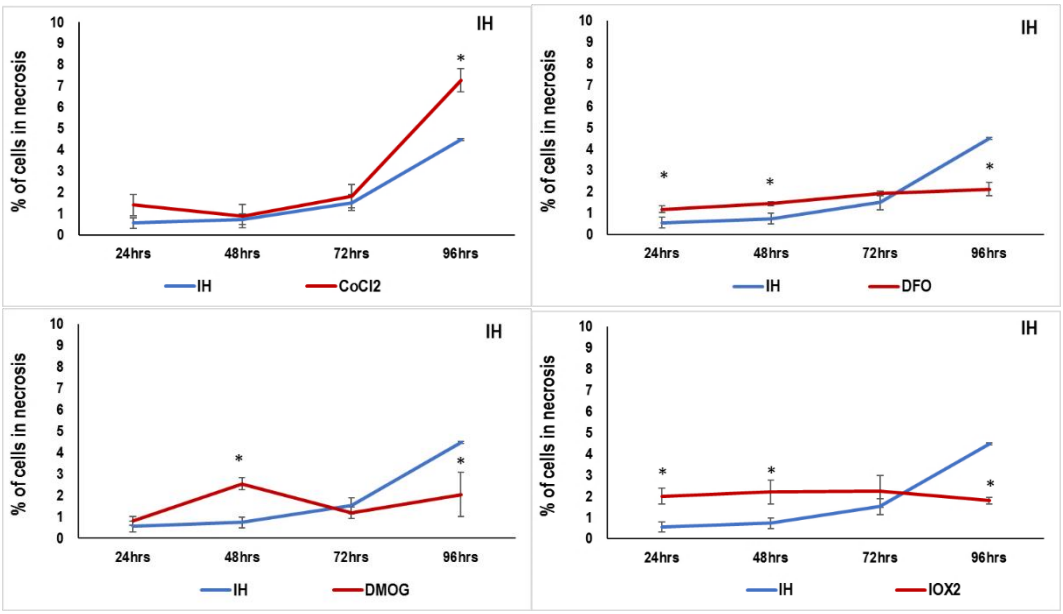

Figure 3.31. PC12 apoptosis/necrosis under intermittent hypoxia

*Following exposure to (50 µM $CoCl_2$, 50 µM DFO, 100 µM DMOG and 50 nM IOX2) for 24 hrs, 48 hrs, 72 hrs and 96 hrs, the percentage of early, late apoptotic and apoptotic PC12 at IH was plotted. Data are presented as mean ± standard deviation (SD). n=1 triplicate, * indicates significant difference in comparison to AO at each time point (p<0.01).*

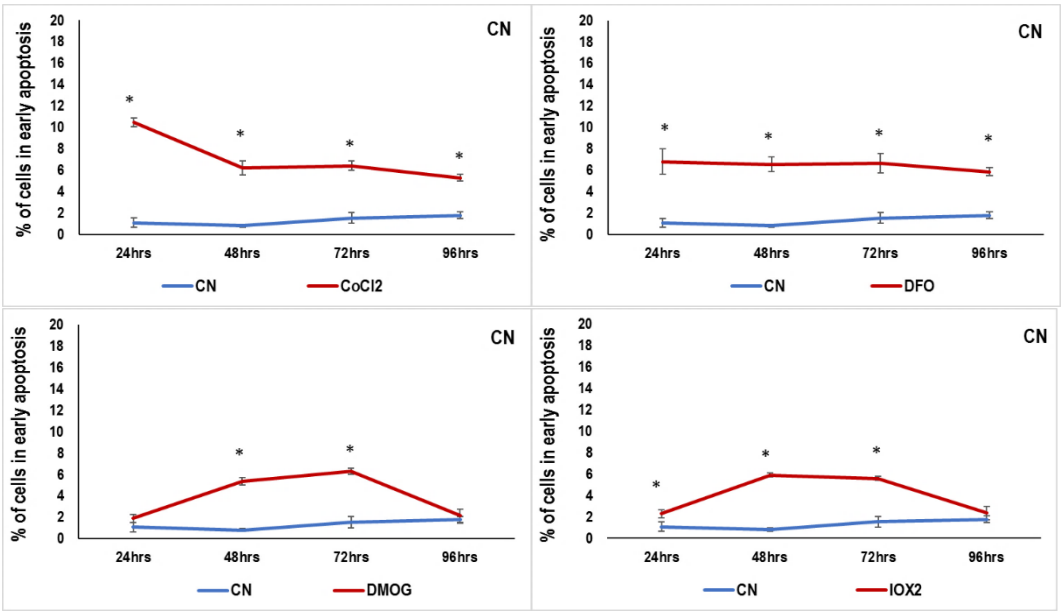
% of cells in early apoptosis
CN
24hrs
48hrs
72hrs
96hrs
CN
CoCl2
DFO
DMOG
IOX2

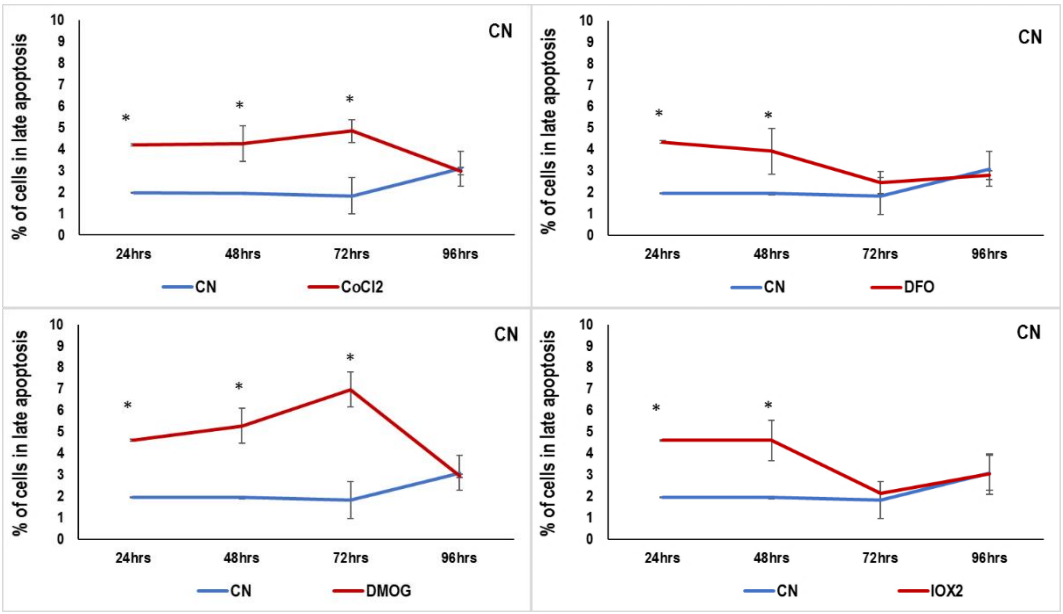
% of cells in late apoptosis
CN
24hrs
48hrs
72hrs
96hrs
CN
CoCl2
DFO
DMOG
IOX2

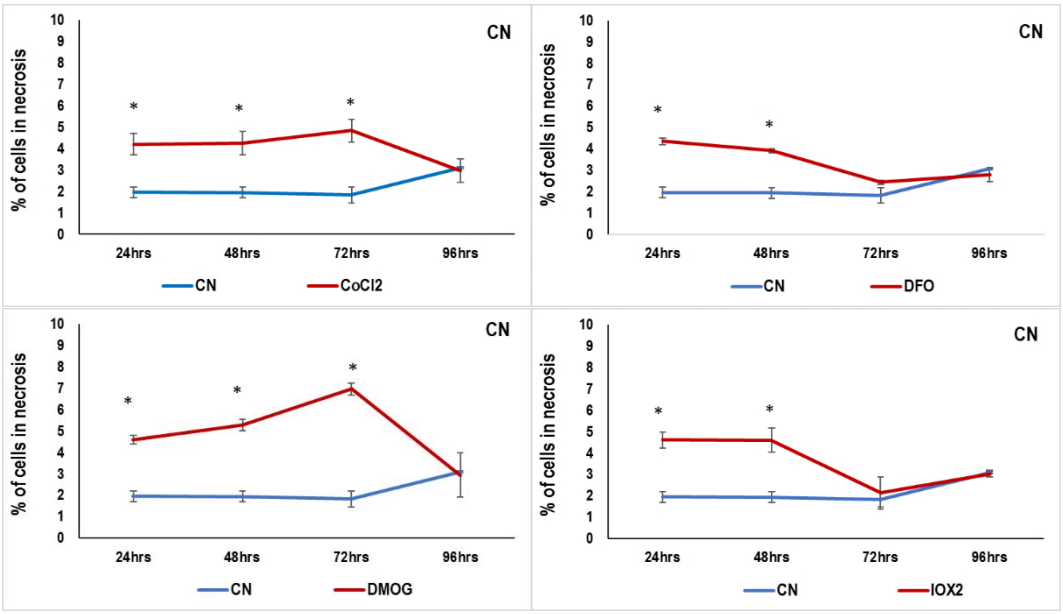

Figure 3.32. PC12 apoptosis/necrosis under continuous normoxia

*Following exposure to (50 µM $CoCl_2$, 50 µM DFO, 100 µM DMOG and 50 nM IOX2) for 24 hrs, 48 hrs, 72 hrs and 96 hrs, the percentage of early, late apoptotic and apoptotic PC12 at CN was plotted. Data are presented as mean ± standard deviation (SD). n=1 triplicate, * indicates significant difference in comparison to AO at each time point (p<0.01).*

Intermittent hypoxia significantly elevated early apoptosis by increased p53 and oxidative stress lead to activation of caspase-3. Chemical hypoxia may induce inflammatory reactions by increasing in NO production and IL-6 secretion from PC12 cells. NO is a one of the most toxic substance several proinflammatory factors. HMAs may upregulated the expression levels of NOS by activation of mitogen-activated protein kinase (MAPK) family, which is contain three main members: extracellular signal-regulated protein kinase 1/2 (ERK1/2), C-Jun-N-terminal kinase (JNK) and p38-MAPK. MAPK family plays a critical role in the regulation of growth and differentiation. HMAs +CN culture elevated all stages of cell death and this may have related to direct effect of oxygen changes on mitochondrial functions (Guo *et al.,* 2006; Iglesias *et al.,* 2013; Chen *et al.,* 2017).

3.3.5. Effect of hypoxia mimetic agents on PC12 cell cycle progression

The previous results showed that hypoxia mimetic agents affected cell growth and induced cell apoptosis. We next sought to determine if HMAs impacted on the cell cycle. Cell cycle is an energy demanding and very highly regulated process. Oxygen is an essential nutrient for the oxidative phosphorylation process considered as greatest net energy producing process, when compared with glycolysis. As such, for a cell to commit to cell division, it must overcome energy checkpoints (Moniz *et al.,* 2015). Therefore, it would make sense that the components of the oxygen-sensing system directly influence cell cycle progression. The four steps of cell cycle involve different phases: cell growth, replication of DNA, transfer of duplicated chromosomes to daughter cells and cell division. These phases are controlled by different proto-oncogenes and tumour suppressors which regulate DNA repair of genetic damage and prevent tumorigenesis (Figure1.7).

Propidium iodide (PI) is the most commonly used dye for DNA content and cell cycle analysis. The PI intercalates into the major groove of double-stranded DNA producing a highly fluorescent signal when excited at 488 nm with a broad emission centred around 600 nm. PI also binds to RNA, it is mandatory to treat the cells with RNase for optimal DNA resolution. The excitation of PI at 488 nm facilitates its use on the flow cytometers (Figure 3.33. A, B and C).

This work revealed that in control cells G0/G1 phase of cell cycle significantly increase ($p<0.01$) after IH and CN culture in comparison to AO, in contrast significant reduction in S phase under IH and CN conditions in comparison to AO ($p<0.001$). G2-M phase significantly decrease after 24 hrs at both IH and CN in comparison to AO ($p<0.01$) with no significant effect was noticed after 48 to 96 hrs.

Under AO culture condition only IOX2 causes significant increase in G0/G1 phase after 24 hrs and and 48 hrs in comparison to AO control ($p<0.05$) (Figure 3.34). HMAs reduced S phase at 24 and 48 hrs while after 72 and 96 hrs IOX2 in comparison to control AO

($p<0.01$) while DMOG significantly increase cell population at S phase after 72 and 96 hrs in comparison to control AO ($p<0.01$) (Figure 3.35). DMOG and IOX2 significantly decrease G2-M phase after 72 and 96 hrs in comparison to control AO ($p<0.01$) (Figure 3.36).

Under IH culture condition, $CoCl_2$, DMOG and IOX2 significantly reduced G1 phase after 24 hrs while IOX2 significantly elevated G0/G1 phase, but after DMOG and IOX2 reduced G0/G1 phase after 48 hrs with no significant effect was noticed after 72 hrs. After 96 hrs $CoCl_2$ reduced with significant increase with IOX2 (Figure 3.34). $CoCl_2$ significantly reduced S phase after 24 and 96 hrs in comparison to control IH ($p<0.01$) (Figure 3.35). G2-M phase significant increase after 24 and 96 hrs of $CoCl_2$ treatment in contrast IOX2 significantly reduced G2-M population after 24, 72 and 96 hrs in comparison to control IH ($p<0.01$) (Figure 3.36).

Under CN culture condition, G0/G1 phase population increase after 24 and 96 hrs of $CoCl_2$ treatment, after 48 hrs DFO, DMOG and IOX2 significantly reduced G0/G1 population in comparison to control CN ($p<0.01$) (Figure 3.34). where all HMAs significantly increase S phase population after 24 hrs it follow by significant reduction after 72 hrs in comparison to control CN ($p<0.01$). $CoCl_2$ and DMOG elevated S phase population after 48 hrs. DMOG and IOX2 continue to reduce S phase after 96 hrs with no significant effect for the other HMAs (Figure 3.35). Under all culture conditions, G2-M phase showed significant reduction HMAs after 96 hrs (Figure 3.36).

To sum up IH and CN trapped cell in G0/G1 phase and reduced S phase in contrast HMAs induce pattern different completely from that was seen under the IH and CN culture conditions.

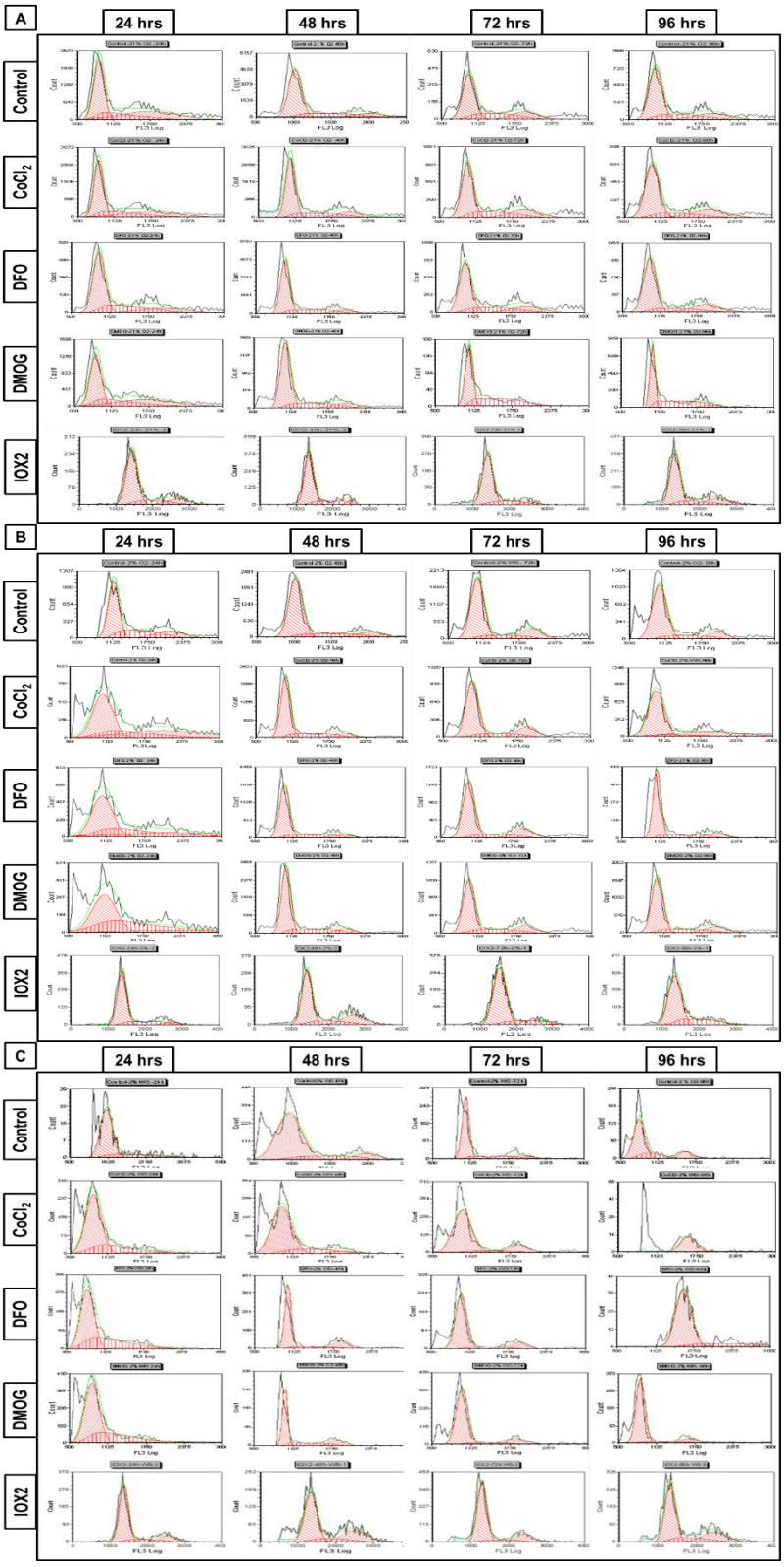

Figure 3.33. Cell cycle analysis

Representative DNA fluorescence histograms of PI stained cells and the peaks indicated G0/G1, S and G2-M as shown in Figure 2.7. PC12 cells cultured under air oxygen (A), intermittent hypoxia (B) and continuous normoxia (C) culture conditions follow by exposure to (50 µM $CoCl_2$, 50 µM

DFO, 100 µM DMOG and 50 nM IOX2) for 24 hrs, 48 hrs, 72 hrs and 96 hrs. The untreated PC12 cells were consider as control. PC12 then stained with PI and assessed by flow cytometry (FACS).

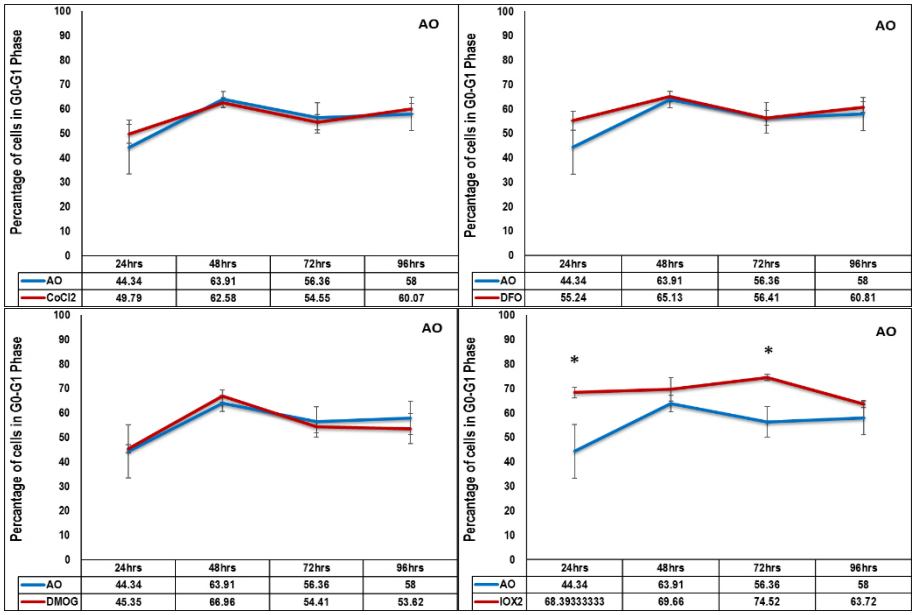

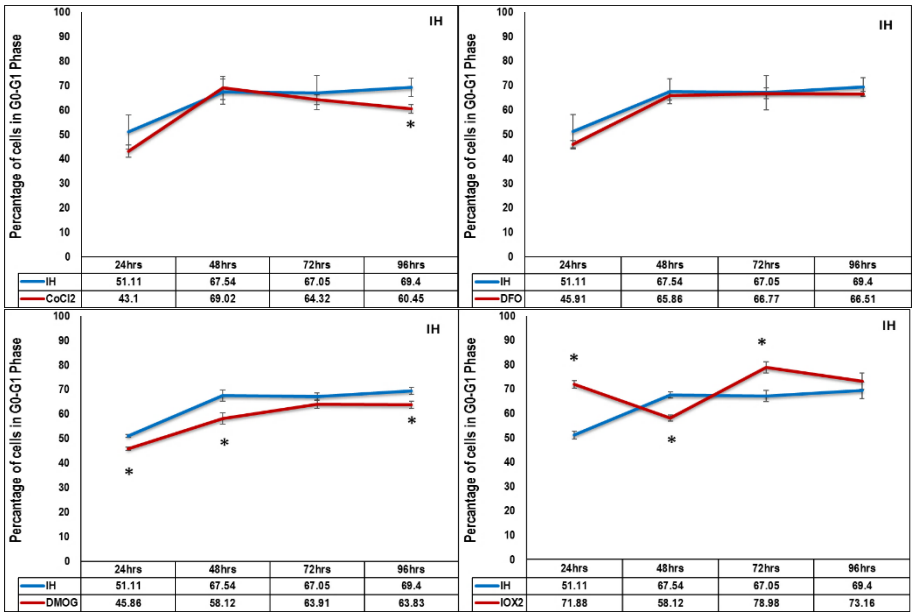

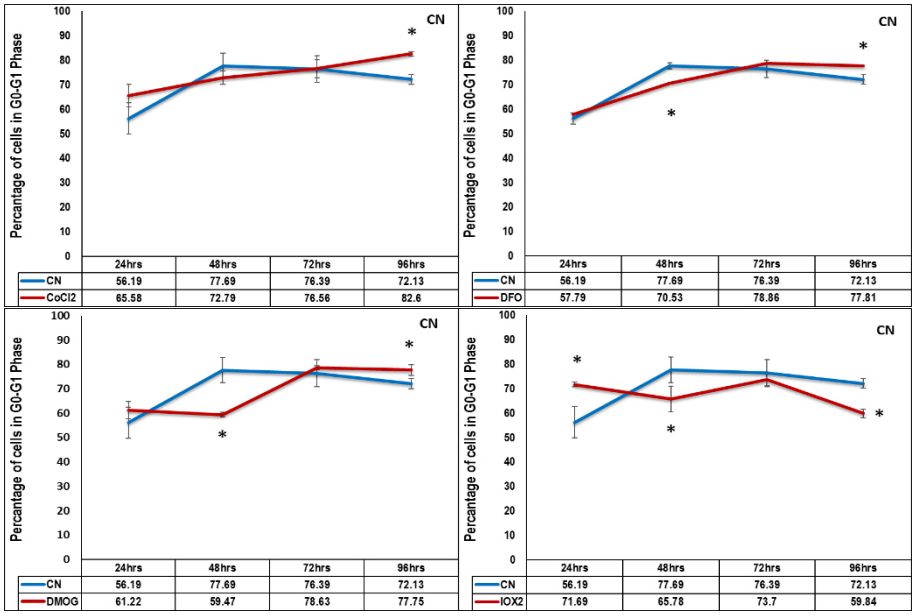

Figure 3.34. Effect of hypoxia mimetic agents on the G0/G1 phase cell cycle of PC12 cells cultured at three different culture conditions

*Following exposure to (50 µM $CoCl_2$, 50 µM DFO, 100 µM DMOG and 50 nM IOX2) for 24 hrs, 48 hrs, 72 hrs and 96 hrs under air oxygen (AO), intermittent hypoxia (IH) and continuous normoxia (CN) culture conditions the percentage of cells in each cycle phase were analysed using flow cytometer. X-axis represents different treatments respectively. Y-axis represents percentage of cells in G0/G1 phase. Data are presented as mean of percentage of cells in this phase ± standard deviation (SD). n=1 triplicate, * indicates significant difference in comparison to control at each time point and at each oxygen culture condition (p<0.01).*

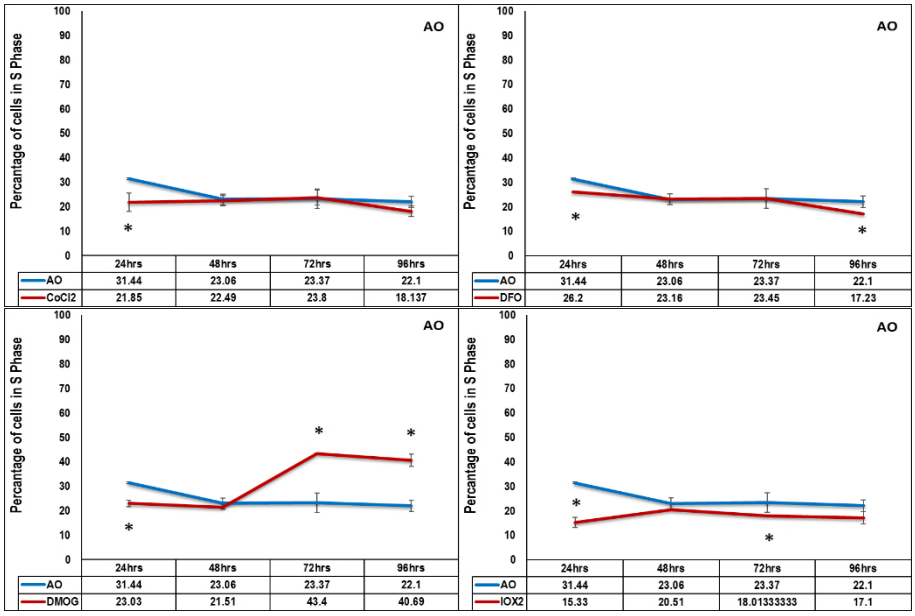
AO
Percantage of cells in S Phase
100
90
80
70
60
50
40
30
20
10
0
24hrs 48hrs 72hrs 96hrs
AO 31.44 23.06 23.37 22.1
CoCl2 21.85 22.49 23.8 18.137
AO
Percantage of cells in S Phase
24hrs 48hrs 72hrs 96hrs
AO 31.44 23.06 23.37 22.1
DFO 26.2 23.16 23.45 17.23
AO
Percantage of cells in S Phase
24hrs 48hrs 72hrs 96hrs
AO 31.44 23.06 23.37 22.1
DMOG 23.03 21.51 43.4 40.69
AO
Percantage of cells in S Phase
24hrs 48hrs 72hrs 96hrs
AO 31.44 23.06 23.37 22.1
IOX2 15.33 20.51 18.01333333 17.1

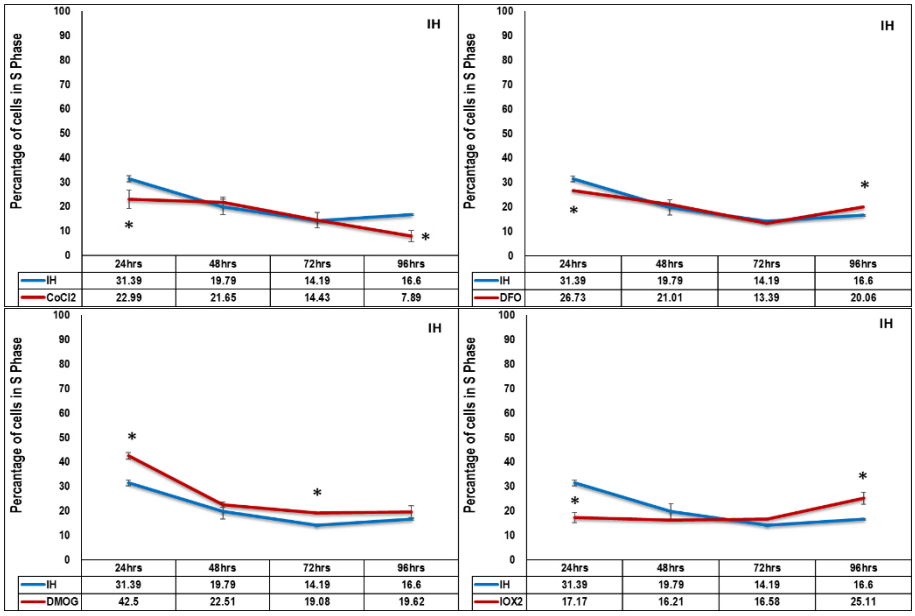
IH
Percantage of cells in S Phase
100
90
80
70
60
50
40
30
20
10
0
24hrs 48hrs 72hrs 96hrs
IH 31.39 19.79 14.19 16.6
CoCl2 22.99 21.65 14.43 7.89
IH
Percantage of cells in S Phase
24hrs 48hrs 72hrs 96hrs
IH 31.39 19.79 14.19 16.6
DFO 26.73 21.01 13.39 20.06
IH
Percantage of cells in S Phase
24hrs 48hrs 72hrs 96hrs
IH 31.39 19.79 14.19 16.6
DMOG 42.5 22.51 19.08 19.62
IH
Percantage of cells in S Phase
24hrs 48hrs 72hrs 96hrs
IH 31.39 19.79 14.19 16.6
IOX2 17.17 16.21 16.58 25.11

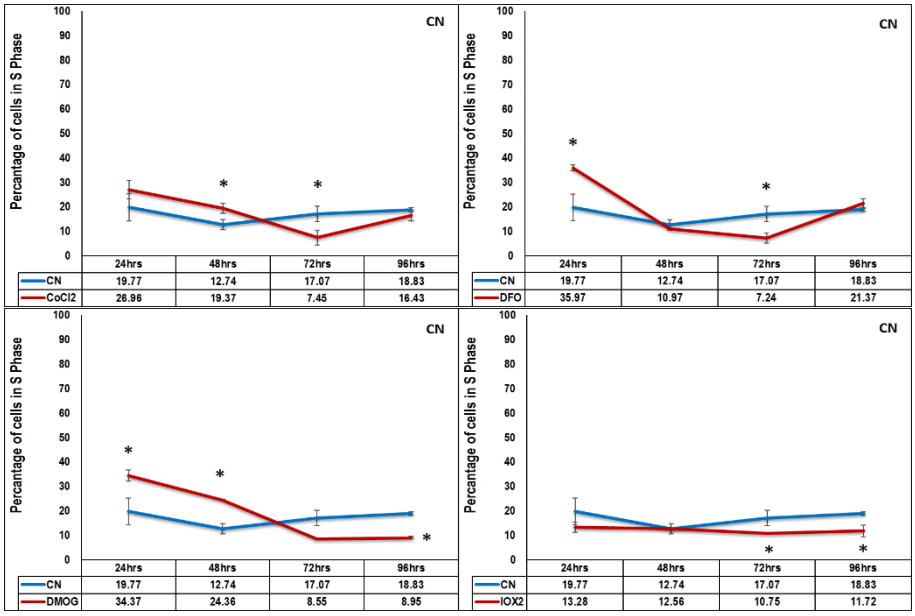

Figure 3.35. Effect of hypoxia mimetic agents on the S–phase cell cycle of PC12 cells cultured at three different culture conditions

*Following exposure to (50 µM $CoCl_2$, 50 µM DFO, 100 µM DMOG and 50 nM IOX2) for 24 hrs, 48 hrs, 72 hrs and 96 hrs under air oxygen (AO), intermittent hypoxia (IH) and continuous normoxia (CN) culture conditions the percentage of cells in S phase were analysed using flow cytometer. X-axis represents different treatments respectively. Y-axis represents percentage of cells in S phase. Data are presented as mean of percentage of cells in this phase ± standard deviation (SD). n=1 triplicate, * indicates significant difference in comparison to control at each time point and at each oxygen culture condition (p<0.01).*

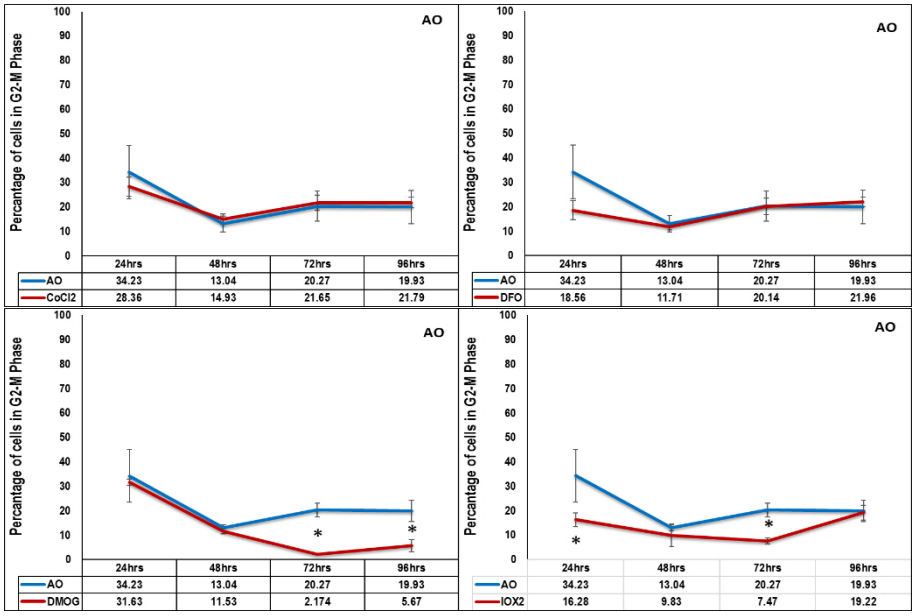
AO
Percantage of cells in G2-M Phase
100
90
80
70
60
50
40
30
20
10
0
24hrs 48hrs 72hrs 96hrs
AO 34.23 13.04 20.27 19.93
CoCl2 28.36 14.93 21.65 21.79
AO
Percantage of cells in G2-M Phase
24hrs 48hrs 72hrs 96hrs
AO 34.23 13.04 20.27 19.93
DFO 18.56 11.71 20.14 21.96
AO
Percantage of cells in G2-M Phase
*
*
24hrs 48hrs 72hrs 96hrs
AO 34.23 13.04 20.27 19.93
DMOG 31.63 11.53 2.174 5.67
AO
Percantage of cells in G2-M Phase
*
*
24hrs 48hrs 72hrs 96hrs
AO 34.23 13.04 20.27 19.93
IOX2 16.28 9.83 7.47 19.22

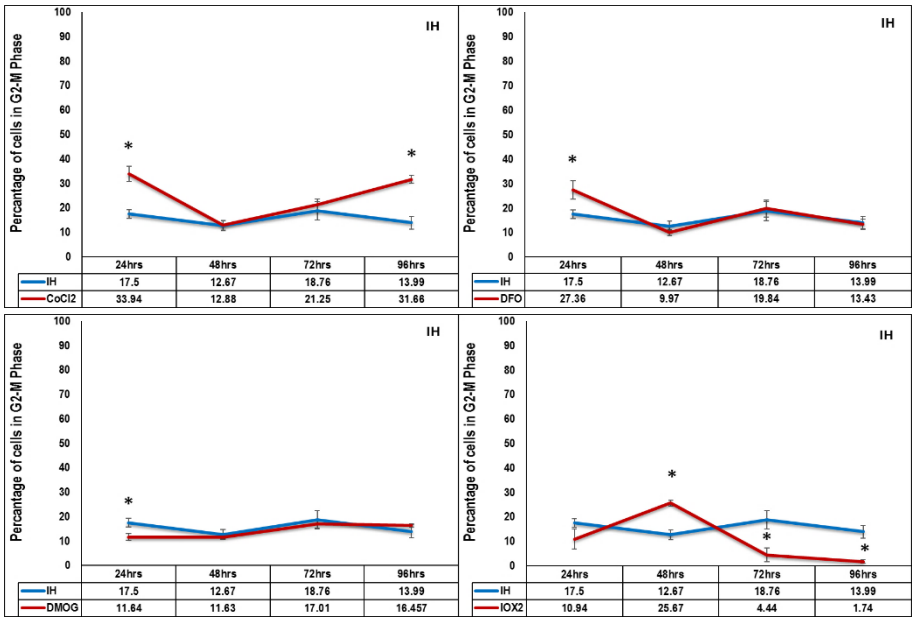
IH
Percantage of cells in G2-M Phase
100
90
80
70
60
50
40
30
20
10
0
*
*
24hrs 48hrs 72hrs 96hrs
IH 17.5 12.67 18.76 13.99
CoCl2 33.94 12.88 21.25 31.66
IH
Percantage of cells in G2-M Phase
*
24hrs 48hrs 72hrs 96hrs
IH 17.5 12.67 18.76 13.99
DFO 27.36 9.97 19.84 13.43
IH
Percantage of cells in G2-M Phase
*
24hrs 48hrs 72hrs 96hrs
IH 17.5 12.67 18.76 13.99
DMOG 11.64 11.63 17.01 16.457
IH
Percantage of cells in G2-M Phase
*
*
*
24hrs 48hrs 72hrs 96hrs
IH 17.5 12.67 18.76 13.99
IOX2 10.94 25.67 4.44 1.74

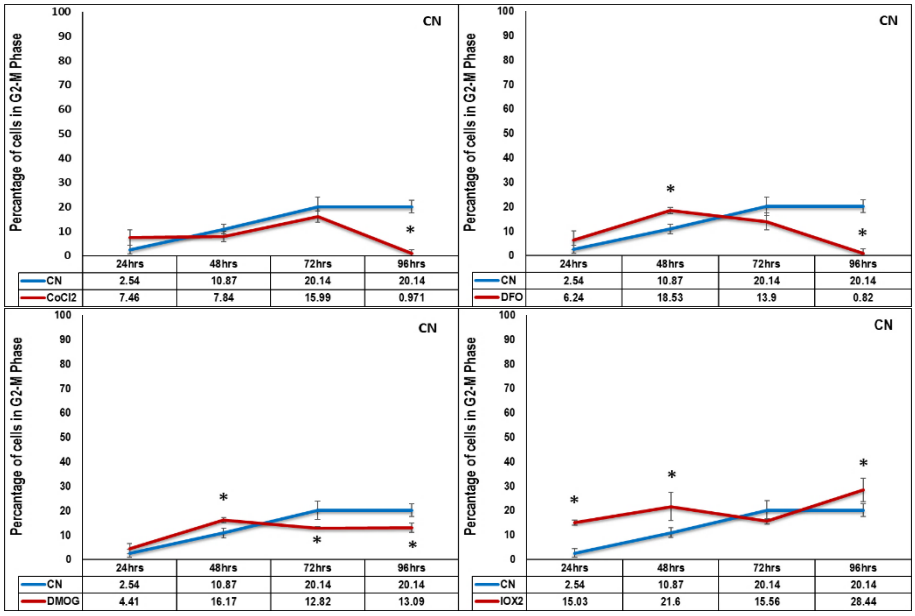

Figure 3.36. Effect of hypoxia mimetic agents on the G2-M phase cell cycle of PC12 cells cultured at three different culture conditions

*Following exposure to (50 µM $CoCl_2$, 50 µM DFO, 100 µM DMOG and 50 nM IOX2) for 24 hrs, 48 hrs, 72 hrs and 96 hrs under air oxygen (AO), intermittent hypoxia (IH) and continuous normoxia (CN) culture conditions the percentage of cells in G2-M phase were analysed using flow cytometer. X-axis represents different treatments respectively. Y-axis represents percentage of cells in S phase. Data are presented as mean of percentage of cells in this phase ± standard deviation (SD). n=1 triplicate, * indicates significant difference in comparison to control at each time point and at each oxygen culture condition (p<0.01).*

The cell cycle analysis revealed that PC12 treated with hypoxia and hypoxia mimetic agents were trapped in G0/G1 phase of cell cycle (Avramovich-Tirosh *et al.,* 2007; Chen *et al.,* 2014; Marin *et al.,* 2016).

This is the first report discuss the effect of IOX2 on cell cycle under three oxygen culture conditions. AO culture condition, IOX2 trapped cells in G0-G1 with no significant effect on S phase and reduce G2-M phase with variable changes was noticed with IH and CN. This effect may have related activation of HIF-1 that associated with arrest in G 1 or early S phase, the progression of cells through the cell cycle is regulated by a series of proteins known as the cyclins, and their associated partners enzymes cyclin-dependent kinases

(CDK) (Swanton, 2004). The major proteins associated with the G 1 /S boundary are the cyclin D family (D1, D2 and D3), their respective CDKs, CDK4 and CDK6, and cyclin E, with its respective CDK, CDK2 (Ekholm *et al,* 2000). The G 1 /S cyclin/CDKs function to control the phosphorylation of the retinoblastoma protein (pRb) (Bartek *et al.,* 1996).

3.3.6. Effect of hypoxia mimetic agents on ROS production and nitroreductase activity of PC12 cells

Various stimuli during normal physiological functions produce reactive oxygen (ROS) and reactive nitrogen species (RNS) species (Newsholme *et al.,* 2012; Bolisetty & Jaimes, 2013). ROS, include superoxide anion (O_2), hydroxyl radical ($^{\cdot}OH$) and hydrogen peroxide (H_2O_2). ROS play vital roles in physiological activities which including intracellular signalling, host defence and redox regulation (Finkel, 2011). Over-production of ROS can be triggered by endogenous and exogenous factors (Bhattacharyya *et al.,* 2014) in order to adapt the stressful changes, organisms developed a variety of mechanisms that prevent the formation of ROS or convert them to inactive derivatives these mechanisms include both enzymatic and non-enzymatic mechanisms. The enzymes involve superoxide dismutase, catalase and glutathione-related enzymes) and non-enzymatic mechanisms involve glutathione and vitamin E antioxidant systems (Rahman, 2007). Oxidative stress occurs when an imbalance occurs between oxidants and antioxidants in favour of the oxidants which leads to cellular damage responsible for degenerative conditions like those that occur in Alzheimer's, Parkinson's and atherosclerosis, among others (Rahal *et al.,* 2014).

There are controversial reports about ROS formation in different cell lines under CN culture conditions (Bogdanova *et al.,* 2016; Di Meo *et al.,* 2016). The experimental seeding population displayed a baseline ROS formation and all values normalized to this value and it which is indicated by the intersection of the x-axis with the y-axis and all

values normalized to this value. The results of this work showed that there were significant increases in ROS formation after 48 and 72 hrs of incubation under all oxygen culture conditions in comparison to ROS formation under AO culture condition ($p<0.01$) (Figure 3.36).

After 24 hrs under AO, $CoCl_2$, DFO, DMOG and IOX2 caused significant reduction in ROS formation (30%, 30%, 36%and 35% respectively) ($p<0.01$). After 48 hrs, HMAs possess no significant effect on ROS formation while at 72 hrs, $CoCl_2$, DMOG and IOX2 elevated ROS formation (11%, 9% and 14%) ($p<0.05$) followed by drop in ROS formation levels (30%, 59%, 47% and 34%) after 96 hrs in comparison to control at each time point ($p<0.01$) (Figure 3.37).

After 24 hrs under IH culture, $CoCl_2$ showed no significantly change in ROS formation. In contrast, DFO, DMOG and IOX2 significantly increase (18%, 16% and 28%) in comparison to control IH. $CoCl_2$ after 48 hrs significantly elevated (15%) in comparison to IH ($p<0.001$). while DFO, DMOG and IOX2 decrease (37%, 29% and 27%) in comparison to control IH ($p<0.01$). After 72 hrs, HMAs reduced ROS formation (50%, 65%, 75% and 73%) in comparison to IH ($p<0.01$). After 96 hrs under IH culture with $CoCl_2$, DFO, DMOG and IOX2 treatment reduced (122%, 143%, 128% and 129%) after ($p<0.001$) (Figure 3.38).

Finally, incubation of PC12 for 24 hrs at CN culture condition supplemented with HMAs elevated (13%, 10%, 18% and 92%) in comparison to CN ($p<0.01$). after 48 hrs, $CoCl_2$ and DMOG reduced ROS formation while DFO and IOX2 elevated ROS formation (28% and 70%) in comparison to control CN ($p<0.01$). After 72 hrs, $CoCl_2$ reduced (27%) ROS formation in contrast IOX2 elevated (106%) ROS formation in comparison to IH ($p<0.01$). $CoCl_2$, DFO and DMOG reduced ROS formation (69%, 83% and 77%) in comparison to control CN ($p<0.001$) (Figure 3.39).

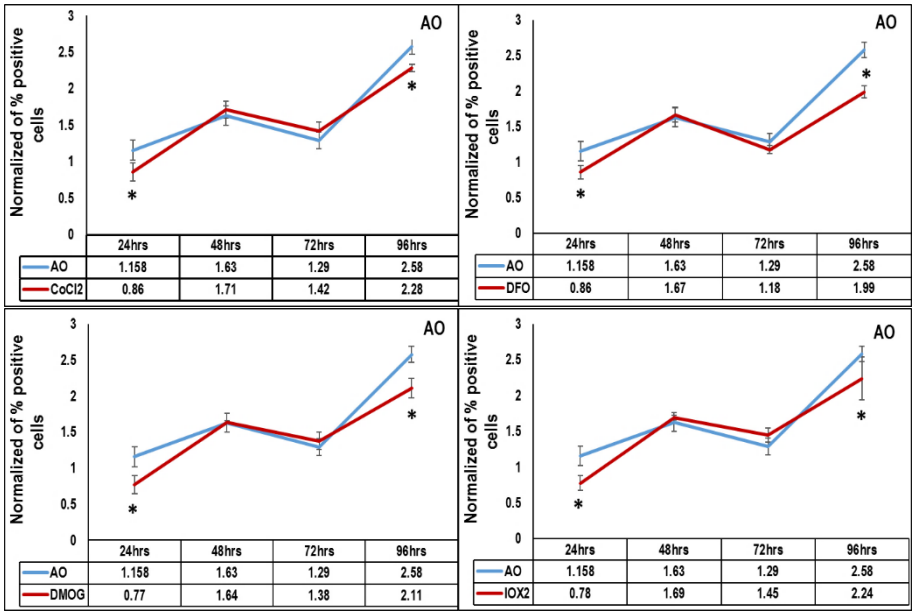

Figure 3.37. Effect of hypoxia mimetic agents on the ROS formation of PC12 cultured in AO culture condition

*Histogram of normalized fluorescence intensity of PC12 after stain with ROS-ID® Hypoxia/Oxidative stress detection reagent. PC12 cells exposure to (50 µM $CoCl_2$, 50 µM DFO, 100 µM DMOG and 50 nM IOX2) for 24 hrs, 48 hrs, 72 hrs and 96 hrs. Data are presented as mean of normalized value ± standard deviation (SD). n=1 triplicate, * indicates significant difference in comparison to control at each AO at each time point (p<0.01).*

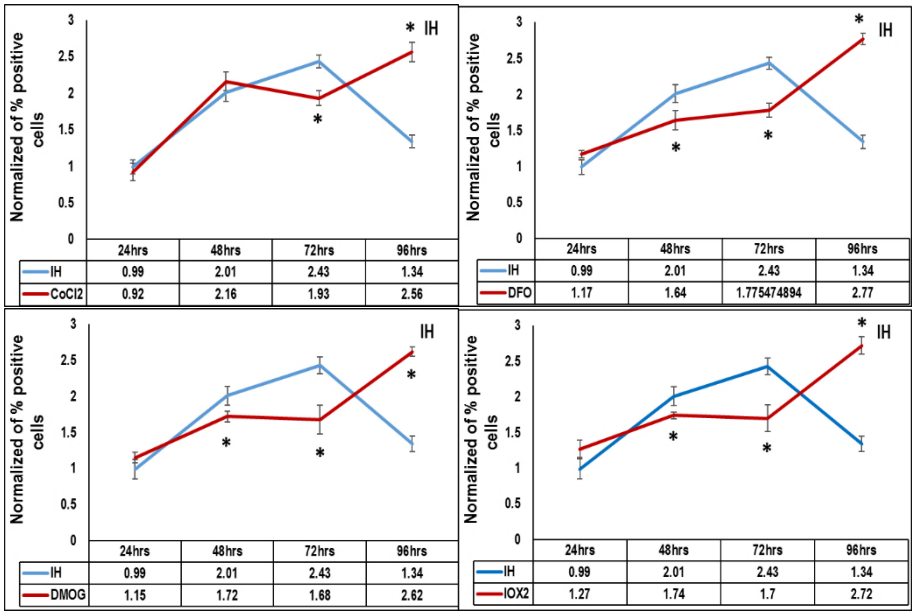

Figure 3.38. Effect of hypoxia mimetic agents on the ROS formation of PC12 cultured in the IH culture condition

*Histogram of normalized percentage of positive cells of PC12 after stain with ROS-ID® Hypoxia/Oxidative stress detection reagent. PC12 cells exposure to (50 µM $CoCl_2$, 50 µM DFO, 100 µM DMOG and 5 0nM IOX2) for 24 hrs, 48 hrs, 72 hrs and 96 hrs. Data are presented as mean of normalized value ± standard deviation (SD). n=1 triplicate, * indicates significant difference in comparison to control IH at each time point (p<0.01).*

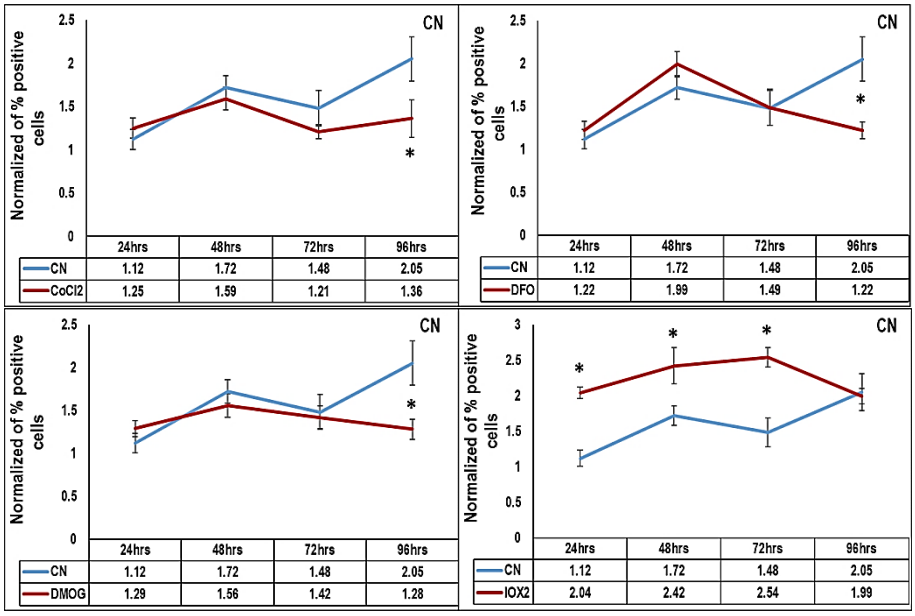

Figure 3.39. Effect of hypoxia mimetic agents on the ROS formation of PC12 cultured in CN culture condition

*Histogram of normalized percentage of positive cells of PC12 cells after stain with ROS-ID® Hypoxia/Oxidative stress detection reagent. PC12 cells exposure to (50µM $CoCl_2$, 50 µM DFO, 100 µM DMOG and 50 nM IOX2) for 24 hrs, 48 hrs, 72 hrs and 96 hrs. Data are presented as mean of normalized value ± standard deviation (SD). n=1 triplicate, * indicates significant difference in comparison to control CN at each time point (p<0.01).*

Nitroreductase activity (NTR) of PC12 cells incubated under AO, IH and CN showed that there was no significant for oxygen culture condition after 24 hrs in comparison to AO followed by elevation (35% and 101%) after 48 and 72 hrs incubation at IH culture condition in comparison to control AO ($p<0.01$), but after 96 hrs IH and CN reduced (110% and 44%) in comparison to control AO (Figure 3.40).

After 24 hrs incubation of PC12 with $CoCl_2$, DFO, DMOG and IOX2 at AO, significant reduction in NTR activity was noticed (26%, 27%, 35% and 34%) compare to 24hrs AO. After 48 hrs, the NTR activity showed no significant change. After 72 hrs, $CoCl_2$, DMOG and IOX2 elevated NTR activity (14%, 7% and 34%) in comparison to AO. In contrast, DFO reduced NTR activity (10%) in comparison to AO ($p<0.01$). HMAs reduced

nitroreductase activity after 96 hrs (21%, 53%, 42% and 41%) in comparison to AO ($p<0.01$).

HMAs possess no significant effect on NTR activity after 24 hrs, DFO, DMOG and IOX2 reduced nitroreductase activity (33%, 14% and 18%) after 48 hrs in comparison to IH ($p<0.01$). After 72 hrs reduced nitroreductase activity (45%, 58%, 67% and 56%) in comparison to control IH ($p<0.01$). HMAs elevated NTR activity after 96 hrs (108%, 127%, 113 and 110%) in comparison to control IH ($p<0.01$) (Figure 3.41).

Under CN culture condition, NTR activity showed no significant effect after 24 hrs. After 48 hrs, $CoCl_2$ reduced NTR activity (23%, 14% and 8%) in comparison to control CN ($p<0.05$). After 72 hrs, $CoCl_2$ significantly reduced nitroreductase activity vs. control CN ($p<0.01$). After 96 hrs, HMAs significantly decreased nitroreductase activity when compared to control CN at 96 hrs (64%, 77%, 65% and 19% respectively) ($p<0.01$) (Figure 3.42).

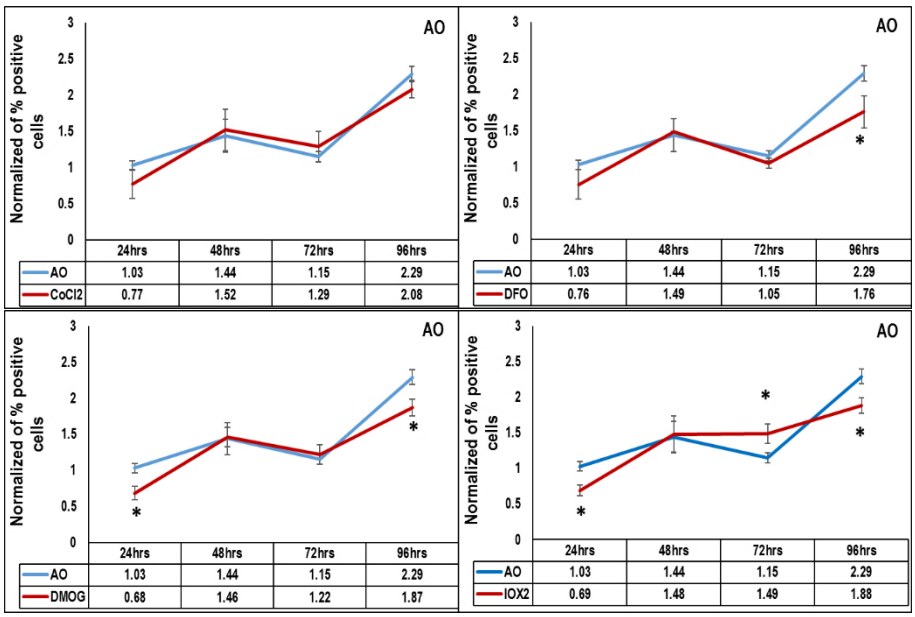

Figure 3.40. Effect of hypoxia mimetic agents on the nitroreductase activity of PC12 cells cultured in AO culture condition

Histogram of normalized fluorescence intensity of PC12 after stain with ROS-ID® Hypoxia/Oxidative stress detection reagent. PC12 exposure to (50 µM $CoCl_2$, 50 µM DFO, 100 µM DMOG and 50 nM IOX2) for 24 hrs, 48 hrs, 72 hrs and 96 hrs. Data are presented as mean of

*normalized value ± standard deviation (SD). n=1 triplicate, * indicates significant difference in comparison to control at each time point (p<0.01).*

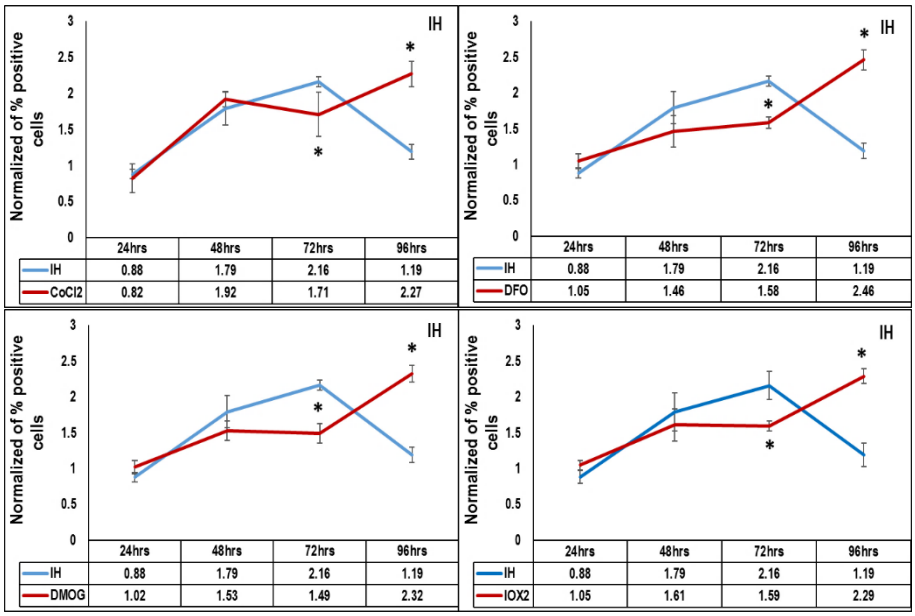

Figure 3.41. Effect of hypoxia mimetic agents on the nitroreductase activity of PC12 cultured in IH culture conditions

*Histogram of normalized percentage of positive cells of PC12 after stain with ROS-ID® Hypoxia/Oxidative stress detection reagent. PC12 cells exposure to (50 µM $CoCl_2$, 50 µM DFO, 100 µM DMOG and 50 nM IOX2) for 24 hrs, 48 hrs, 72 hrs and 96 hrs. Data are presented as mean of normalized value ± standard deviation (SD). n=1 triplicate, * indicates significant difference in comparison to control at each time point (p<0.05).*

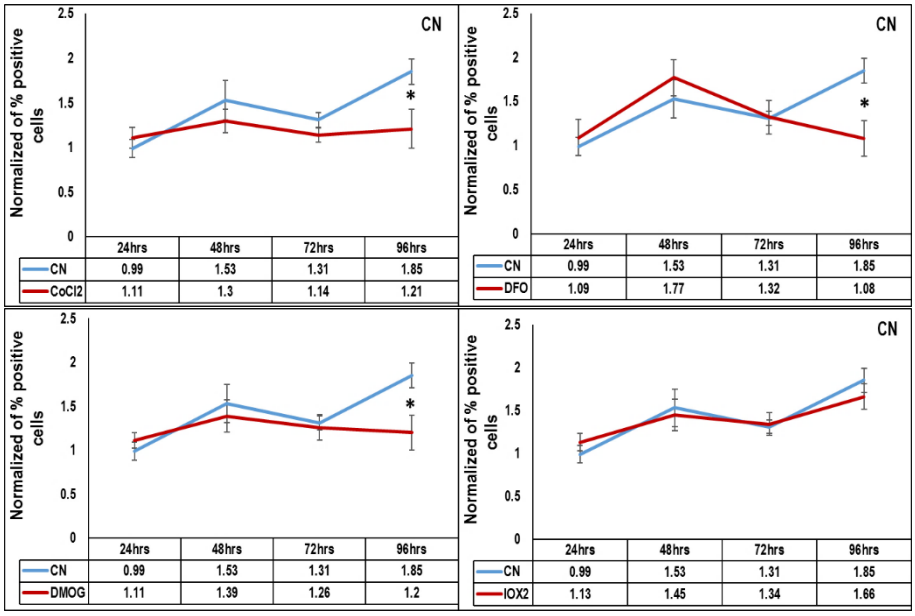

Figure 3.42. Effect of hypoxia mimetic agents on the nitroreductase activity of PC12 cultured in CN culture condition

*Histogram of percentage of positive cells of PC12 after stain with ROS-ID® Hypoxia/Oxidative stress detection reagent. PC12 cells exposure to (50 µM $CoCl_2$, 50 µM DFO, 100 µM DMOG and 50 nM IOX2) for 24 hrs, 48 hrs, 72 hrs and 96 hrs. Data are presented as mean of normalized value ± standard deviation (SD). n=1 triplicate, * indicates significant difference in comparison to control at each time point (p<0.01).*

HMAs significantly reduced ROS formation under both AO and CN and this may have related to activation of antioxidant enzymes by HIF-1 e.g. increased SOD-2 gene expression. In contrast, IH after 96 hrs significantly elevated ROS formation and this may relate to the mitochondrial changes that associated with IH and this agree with Chandel et al. (1998) who dscribed cell fail to increase ROS generation during hypoxia after treatment with HMAs at IH. NTR are a family of evolutionarily related enzymeshave ability to reduce nitrogen-containing compounds, including those containing the nitro functional group. NTR members utilise FMN as a cofactor. HMAs significantly reduced NTR activity under both AO and CN and this may have related to activation of antioxidant enzymes by HIF-1(Owusu-Ansah *et al.,* 2008).

3.4. Discussion

There are many reports that confirm the role of physiological normoxia and precondition with hypoxia mimetic agents in cell viability and differentiation of PC12 (Li *et al.,* 2015). However, most of these works considered 21% oxygen culture condition as normoxia and considered any oxygen concentration lower than 21% as hypoxia and compare the effect of hypoxia mimetic agent to that value. To understanding the effect of hypoxia mimetic agents on cell viability, apoptosis, cell cycle. It would be useful in comparison to the effect of hypoxia mimetic agents to controlled engineered hypoxic conditions which reflect the physiological oxygen concentration inside the body. PC12 cell viability, apoptosis, and cell cycle were measured and compared these changes to the changes in HIFs expression. In this study, we tested the response of PC12 cell lines to different hypoxia mimetic agents under air oxygen culture condition, intermittent hypoxia and continous normoxic culture conditions: (1) to establish cellular models of PC12 cell behaviour under different oxygen culture conditions, (2) to determine if hypoxia mimetic agents mimic physiological normoxia in PC12 cell. After dose scan, we selected the doses (50 µM, 50 µM, 100 µM and 50 nM of $CoCl_2$, DFO, DMOG and IOX2 respectively) that cause minimal change on cell count and MTT activity.

In this work, we found some variations between cell count and MTT activity of the cells that treated hypoxia mimetic agents under both CN and IH culture condition and this may have related to the inhibition of mitochondrial activity by HIF-1α stabilisation during changes in oxygen level which will affect the production of NAD(P)H, that play important role in MTT reagent reduction.

To define if chosen concentrations still act as hypoxia mimetic agents (induce HIFs), PC12 cells were treated with chosen concentrations and incubated in the three oxygen conditions and this is first report using such low concentrations of hypoxia mimetic agents (especially DMOG and IOX2) to induce HIF expression, higher concentrations usually

were used in many studied (Guo *et al.,* 2006; Genetos *et al.,* 2010; Zeng *et al.,* 2011). Our results showed that HIF-1α expression was significantly increase in way like intermittent hypoxia (Prabhakar & Semenza, 2007).

There are contradicting reports about the effect of hypoxia mimetic agent on PC12 differentiation (Kotake-Nara *et al.,* 2005; Genetos *et al.,* 2010; Chen *et al.,* 2014). The results of the effect of both hypoxia and hypoxia mimetic agents on PC12 cell shows that hypoxia mimetic agents have no additive effect on PC12 differentiation over NGF at air oxygen culture condition, however these agents inhibit the differentiation effect of NGF at both IH and CN culture conditions and this may relate to prolong ERK1/2 phosphorylation leading cell differentiation inhibition (Chen *et al.,* 2014).

The study of the role of hypoxia and hypoxia mimetic agents on cell death revealed that hypoxia mimetic agents significantly increase early apoptosis (Guo *et al.,* 2006; Iglesias *et al.,* 2013; Chen *et al.,* 2017), and this may have related to activation of caspase 3/7 direct by c-Jun NH_2 terminal kinase (JNK)/ stress activated protein kinase (SAPK) or indirectly by inhibition of anti-apoptotic protein Bax/ Bak or stabilisation of p53 by HIF-1α (Greijer & van der Wall, 2004; Sermeus & Michiels, 2011).

The cell cycle analysis revealed that PC12 treated with hypoxia and hypoxia mimetic agents were trapped in G0/G1 phase of cell cycle (Avramovich-Tirosh *et al.,* 2007; Chen *et al.,* 2014; Marin *et al.,* 2016) and this may have related to activation of protein phosphatase 2A (PP2A) and inhibition of extracellular signal-regulated kinase 1/2 (ERK1/2) phosphorylation contribute to inhibiting PC12 proliferation through G0/G1 phase arrest (Chen *et al.,* 2014).

The ROS formation and nitroreductases activity showed significant increase after 96 hrs of treatment with HMAs (Kotake-Nara & Saida, 2007; Owusu-Ansah *et al.,* 2008; Zeng *et al.,* 2011). ROS/ RNS formation represent the link between HIF expressions, apoptosis and cell cycle. PC12 provided us with a good functional model to assess of HMAs as tool

for mimic control oxygen culture. To progress with this finding further work is needed to look at a primary cell model that is more clinically suitable such as BM-hMSCs.

3.5 Conclusion

This study confirms the ability of individual hypoxia mimetic agents to induce HIF-1α expression which related to the significant increase apoptosis, and cycle arrest at G0/G1 phase that associated with an increase ROS formation in PC12 cell in all three oxygen conditions.

Chapter 4 : Effects of hypoxia mimetic agents on BM-hMSCs

4.1. Introduction

Friedenstein *et al.,* were the first to demonstrate that bone marrow contains two populations of cells; hematopoietic stem cells (HSCs) and a rare population of plastic-adherent stromal cells, which were referred to mesenchymal stromal cells (BM-hMSCs) (Williams & Hare, 2011). Human bone marrow-derived mesenchymal stem cells (BM-hMSCs) are in current use in many clinical trials globally (Wang *et al.,* 2016). These trials cover many pathological and injury conditions ranging from osteoarthritic lesions of the knee (Chen &Tuan, 2008) to neurological indications including ischemic stroke (Nesselmann *et al.,* 2008); kidney regeneration (Hopkins *et al.,* 2009), blood precursor transplantation (Billet *et al.,* 2008), and wound healing (Fu *et al.,* 2006). BM-hMSCs are canonically described as having a multipotent (osteoblast, chondrocyte, adipocyte) differentiation potential, a guideline immunophenotype (positive: CD105, CD73 and CD90, and negative: CD45, CD34, CD14, CD19 and HLA-DR), and as being a plastic adherent cell isolated from the bone marrow (Nery *et al.,* 2013; Yousefifard *et al.,* 2016). The architecture of bone marrow consists of a sinusoidal organisation of blood vessels that leads to low physiological oxygen levels (Simon & Keith, 2008). Recently it is well established that reduced oxygen culture conditions enhance isolation and expansion of hMSCs from bone marrow which is important to ensure good clinical outcome (Boregowda *et al.,* 2012; Haque *et al.,* 2013; Heywood & Lee, 2016).

There is accumulating studies that hypoxia and hypoxia mimetic agents can produce significant effects on BM-hMSCs at different physiological levels through induction of HIF pathway and this include: modifying energy metabolism (Chang & Hung, 2016; Hu *et al.,* 2016), iron metabolism (Ejtehadifar *et al.,* 2015), intracellular pH (Saraswati *et al.,* 2015), vasomotor activity (Shalaby *et al.,* 2016), migration (Choi *et al.,* 2016), motility, and modification of the extracellular matrix. However, HIF can also induce apoptosis (cell death mechanisms via increased mitochondrial membrane permeability), change ROS

and RNS formation, and increase intracellular acidity that leads to significant increase in caspases activities (Rodrigues *et al.,* 2012).

Little research has been performed thus far on the effect of hypoxia mimetic agents on cell viability, cell cycle, ROS states and nitroreductases activity in BM-hMSCs. The primary aim of this study was to assess the *in vitro* effect of hypoxia mimetic agents on BM-hMSCs viability under AO, IH and CN conditions.

4.2. Methods

4.2.1. Materials

Analytical grade reagents and deionised water (Sigma, UK) were used. All chemicals employed are listed in Chapter 2, Section 2.1.

4.2.2. Cell models

The BM-hMSCs cells were recovered from commercially obtained bone marrow aspirate as outlined in Chapter 2. Cell models were maintained at an atmosphere of 37°C and 5% CO_2 under AO, IH and CN culture conditions.

4.3. Results

4.3.1. Effect of hypoxia mimetic agents on BM-hMSCs count and metabolic activity

The toxicity of hypoxia mimetic agents increases as concentrations rise. The aim of these experiments was to optimise the concentrations at which cell viability was comparable to control for use in subsequent experiments. Cell count and metabolic activity of BM-hMSCs was explored via cell count and MTT assay. In this instance cell count and MTT assay

were being used as markers of cell viability. Cell count data is presented as cell number x 10^4 and MTT data is presented as normalized to the corresponding experimental control. Cells were grown under air oxygen, intermittent hypoxia and continuous normoxic conditions and in the presence or absence of hypoxia mimetic agents to determine if any effects of hypoxia mimetic agents on cell viability change with oxygen concentration changes.

4.3.1.1. Determination of BM-hMSCs viability after treatment with different concentrations of $CoCl_2$ at different oxygen conditions.

$CoCl_2$ concentrations ≥75 µM significantly decreased cell count and metabolic activity, as measured by MTT assay, over the three oxygen conditions ($p<0.01$). However, cells exposed to $CoCl_2$ 50 µM showed the lowest reduction in cell count across all oxygen conditions. At this concentration (50 µM), cell count reductions were measured as 20% for AO, 14% for IH and 45% for CN culture (Figure 4.1). Furthermore, MTT activity at this concentration was 40% for AO, 41% for IH, and 23% for CN (Figure 4.2).

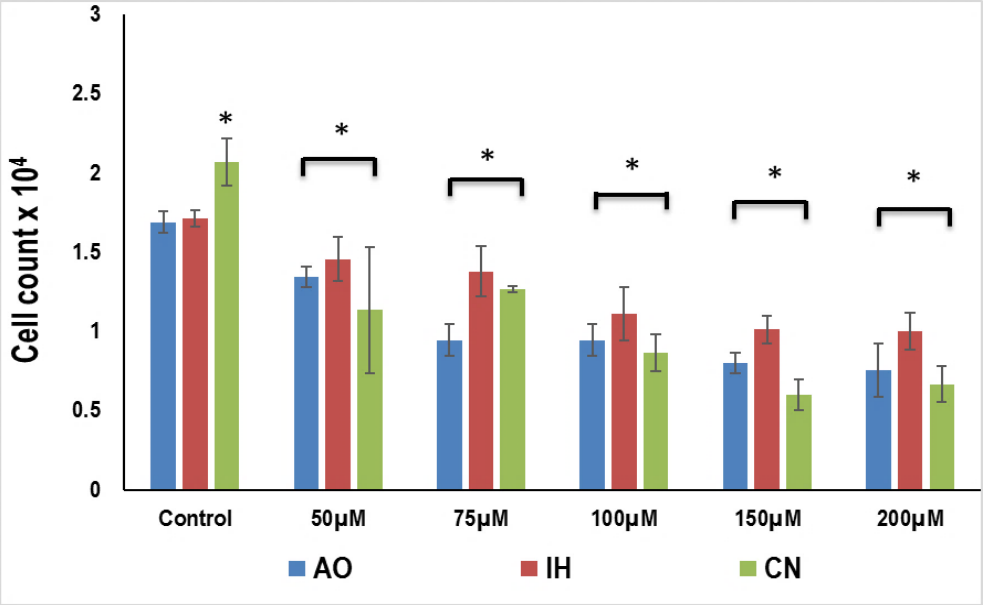

Figure 4.1. Effect of $CoCl_2$ on cell count of BM-hMSCs cultured in the different oxygen conditions

*Cell counts of BM-hMSCs at air oxygen (AO), intermittent hypoxia (IH), and continuous normoxia (CN) following exposure to different concentrations of $CoCl_2$ for 14 days. Y-axis indicates cell number $x10^4$. X-axis indicates different oxygen culture conditions. Data are presented as mean ± standard deviation (SD). n=1 triplicate, * indicates significant change in comparison to control in each condition (p<0.05).*

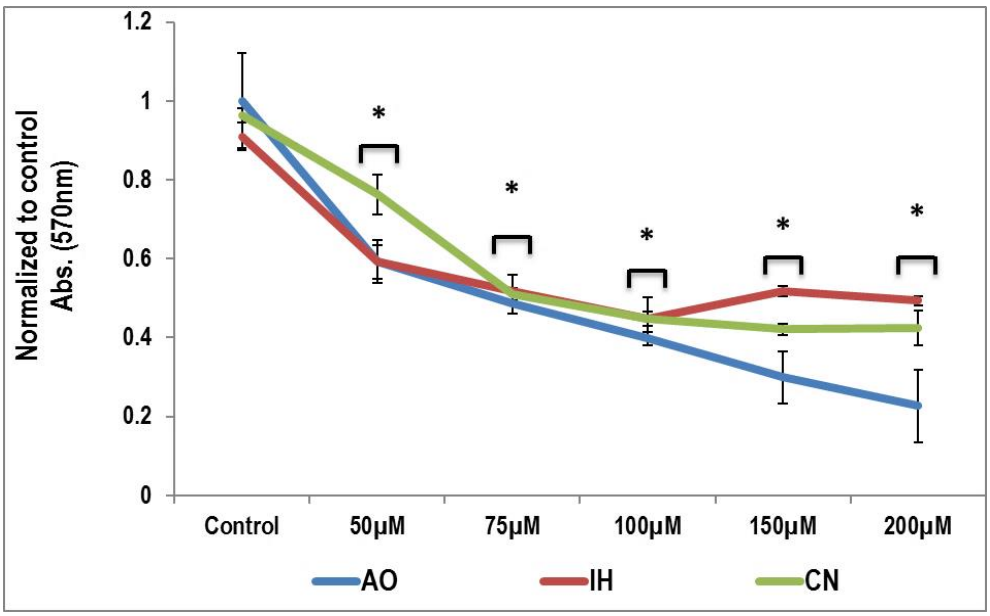

Figure 4.2. Effect of $CoCl_2$ on MTT activity of BM-hMSCs cultured in the different oxygen conditions

*MTT activity of BM-hMSCs at air oxygen (AO), intermittent hypoxia (IH), and continuous normoxia (CN) following exposure to different concentrations of $CoCl_2$ for 14 days. Y-axis indicates Abs. value normalized to Abs. of control at each time point. X-axis indicates different treatment conditions. Data are normalized to untreated controls at each oxygen culture condition. Data are presented as mean ± standard deviation (SD). n=1 triplicate, * indicates significant change in comparison to control at each condition (p<0.01).*

4.3.1.2. Determination of BM-hMSCs viability after treatment with different concentrations of DFO at different oxygen conditions.

DFO concentrations ≥75 µM substantially decreased cell count and metabolic activity, as measured by MTT assay, over the three oxygen conditions ($p<0.01$). However, cells exposed to DFO 50 µM showed the smallest reduction in cell count across all oxygen conditions. At this concentration (50 µM), cell count reductions were measured as 15% for AO culture, 13% for IH and 48% for CN (Figure 4.3). Furthermore, MTT activity at this concentration was 48% for AO culture, 44% for IH, and 35% for CN (Figure 4.4).

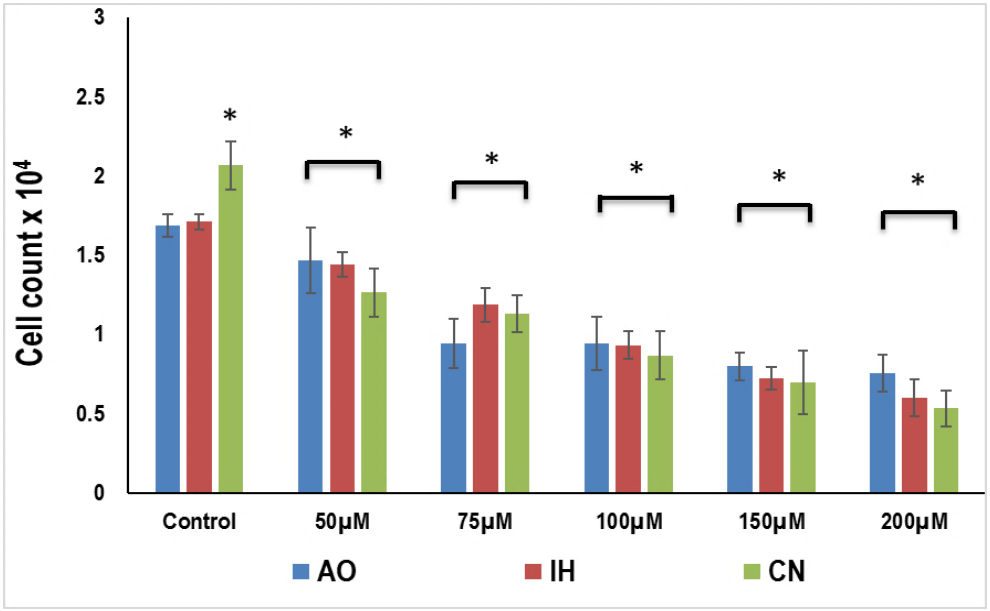

Figure 4.3. Effect of DFO on cell count of BM-hMSCs cultured in the different oxygen conditions

*Cell counts of BM-hMSCs at air oxygen (AO), intermittent hypoxia (IH), and continuous normoxia (CN) following exposure to different concentrations of DFO for 14 days. Y-axis indicates cell number x10^4. X-axis indicates different oxygen culture conditions. Data are presented as mean ± standard deviation (SD). n=1 triplicate, *indicates significant change in comparison to control in each condition ($p<0.05$).*

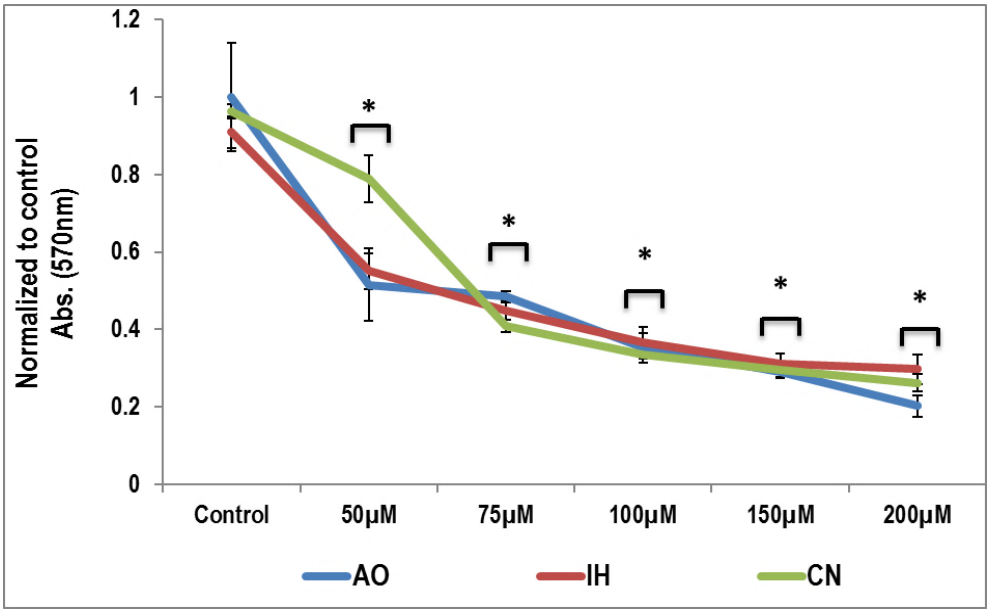

Figure 4.4. Effect of DFO on MTT activity of BM-hMSCs cultured in the different oxygen conditions

*MTT activity of BM-hMSCs at air oxygen (AO), intermittent hypoxia (IH) , and continuous normoxia (CN) following exposure to different concentrations of DFO for 14 days. Y-axis indicates Abs. value normalized to Abs. of control at each time point. X-axis indicates different treatment conditions. Data are normalized to untreated controls at each oxygen culture condition. Data are presented as mean ± standard deviation (SD). n=1 triplicate, * indicates significant change in comparison to control in each condition (p<0.01).*

4.3.1.3. Determination of BM-hMSCs viability after treatment with different concentrations of DMOG at different oxygen conditions.

DMOG concentrations ≥ 250 µM significantly decreased cell count and metabolic activity, as measured by MTT assay, over the three oxygen conditions ($p<0.01$). However, cells exposed to DMOG 100 µM showed the smallest reduction in cell count across all oxygen conditions. At this concentration (100 µM), cell count reductions were measured as 10% for AO culture, 4% for IH and 30% for CN (Figure 4.5). Furthermore, MTT activity at this concentration was 34% for AO culture, 30% for IH, and 30% for CN (Figure 4.6).

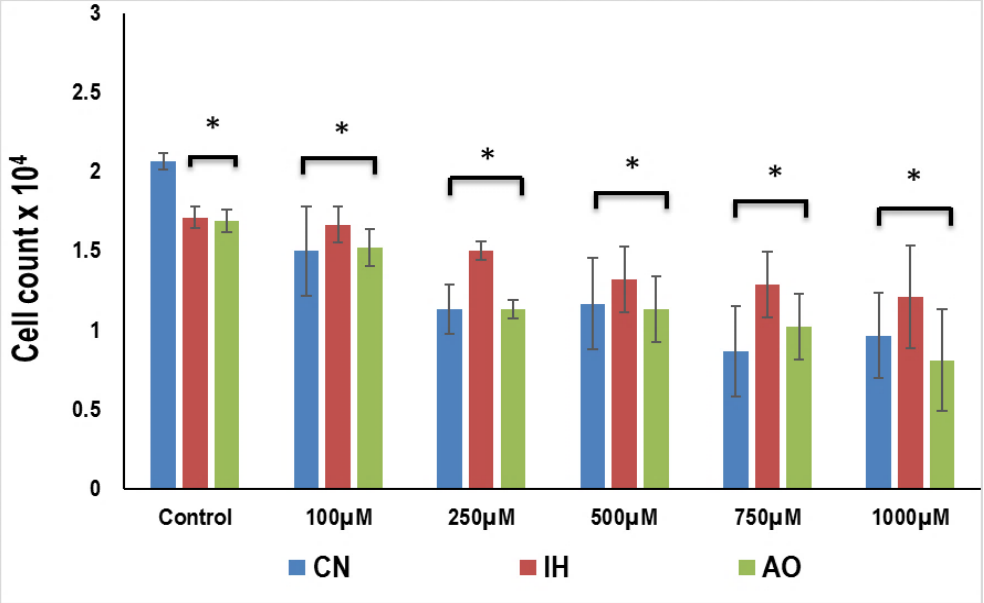

Figure 4.5. Effect of DMOG on cell count of BM-hMSCs cultured in the different oxygen conditions

*Cell counts of BM-hMSCs at air oxygen (AO), intermittent hypoxia (IH), and continuous normoxia (CN) following exposure to different concentrations of DMOG for 14 days. Y-axis indicates cell number x10^4. X-axis indicates different oxygen culture conditions. Data are presented as mean ± standard deviation (SD). n=1 triplicate, * indicates significant change in comparison to control in each condition ($p<0.05$).*

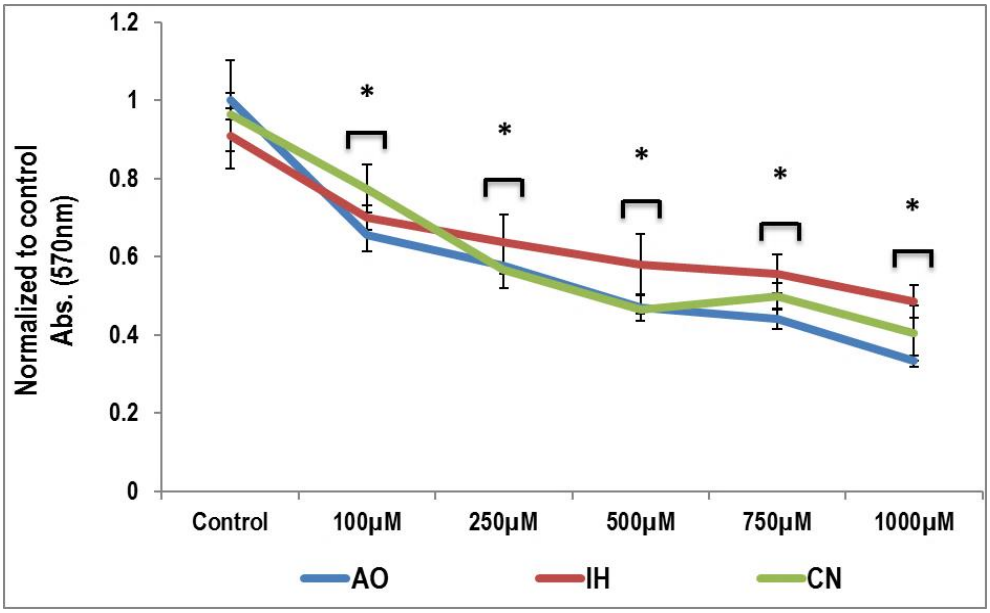

Figure 4.6. Effect of DMOG on MTT activity of BM-hMSCs cultured in the different oxygen conditions

*MTT activity of BM-hMSCs at air oxygen (AO), intermittent hypoxia (IH), and continuous normoxia (CN) following exposure to different concentrations of DMOG for 14 days. Y-axis indicates Abs. value normalized to Abs. of control at each time point. X-axis indicates different treatment conditions. Data are normalized to untreated controls at each oxygen culture condition. Data are presented as mean ± standard deviation (SD). n=1 triplicate, * indicates significant change in comparison to control in each condition (p<0.01).*

4.3.1.4. Determination of human BM-hMSCs viability after treatment with different concentrations of IOX2 at different oxygen conditions.

IOX2 concentrations ≥ 500 nM significantly decreased cell counts over the three oxygen conditions ($p<0.01$) while metabolic activity, as measured by MTT assay, was significantly decreased at all vales ≥ 50 nM. However, cells exposed to 50 µM IOX2 *58showed the smallest reduction in cell count across all oxygen conditions. At this concentration (50 µM), cell count reductions were measured as 3.9% for AO culture, 0.6% for IH and 1.3% for CN (Figure 4.7). Furthermore, MTT activity at this concentration was 30% for AO culture, 31% for IH, and 29% for CN (Figure 4.8).

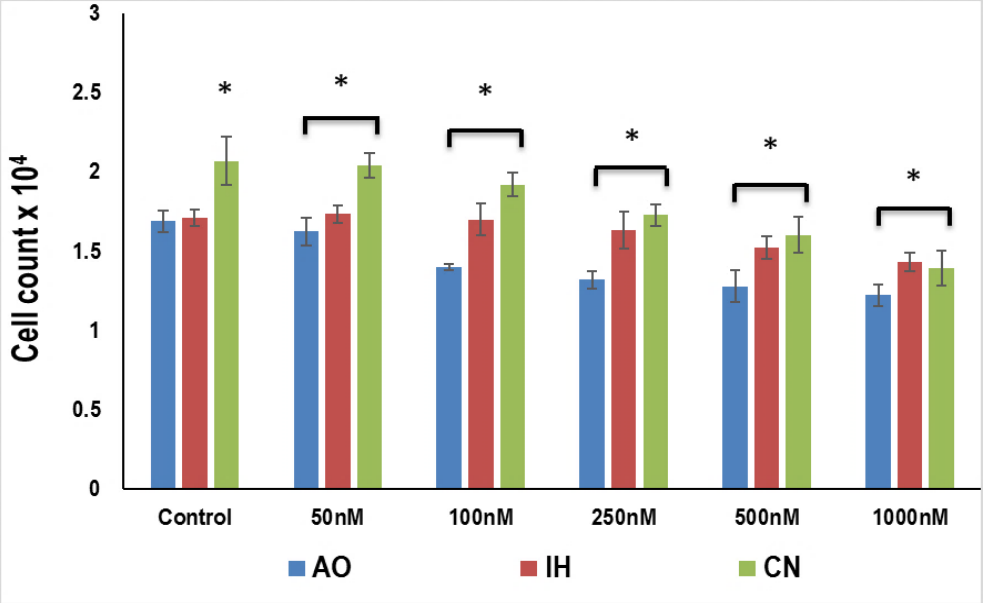

Figure 4.7. Effect of IOX2 on cell count of BM-hMSCs cultured in the different oxygen conditions

*Cell counts of BM-hMSCs at air oxygen (AO), intermittent hypoxia (IH), and continuous normoxia (CN) following exposure to different concentrations of IOX2 for 14 days. Y-axis indicates cell number x10^4. X-axis indicates different oxygen culture conditions. Data are presented as mean ± standard deviation (SD). n=1 triplicate, *indicates significant change in comparison to control in each condition ($p<0.05$).*

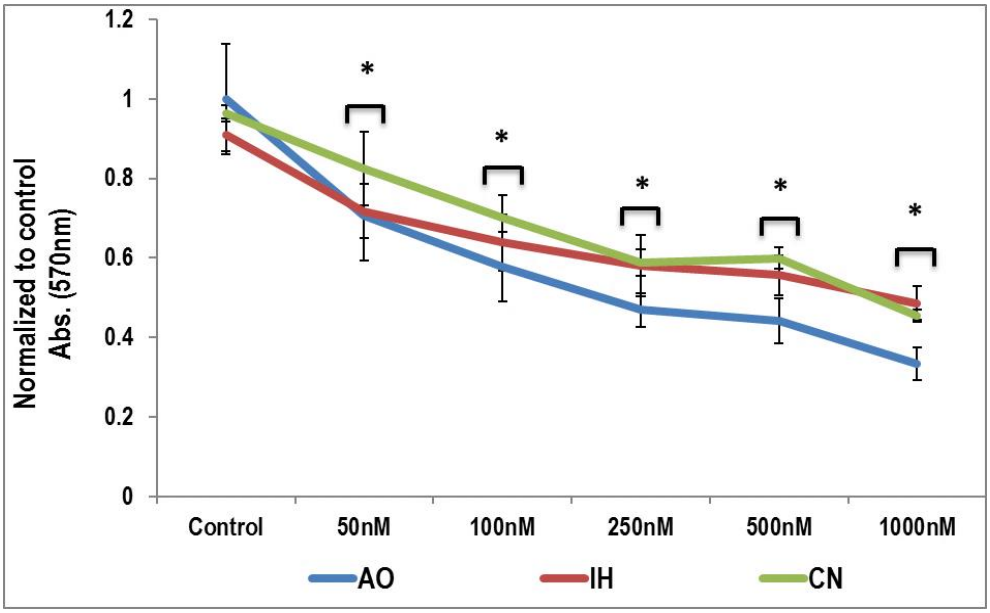

Figure 4.8. Effect of IOX2 on MTT activity of BM-hMSCs cultured in the different oxygen conditions

*MTT activity of BM-hMSCs at air oxygen (AO), intermittent hypoxia (IH), and continuous normoxia (CN) following exposure to different concentrations of IOX2 for 14 days. Y-axis indicates Abs. value normalized to Abs. of control at each time point. X-axis indicates different treatment conditions. Data are normalized to untreated controls at each oxygen culture condition. Data are presented as mean ± standard deviation (SD). n=1 triplicate, * indicates significant change in comparison to each condition (p<0.01).*

In this work, we found even with low HMAs doses that were used in this work, MSCs cell showed reduction in cell count and MTT activity and this may relate to changes cell cycle and apoptiosis pattern that induced by hypoxia (Ge *et al.,* 2016; Zeng *et al.,* 2011). MTT activity reduced by 30-40% with lowest concentration and this may relate to the effect of HMAs on mitochondrial function (Genetos *et al.,* 2010).

4.3.2. Effect of hypoxia and hypoxia mimetic agents on BM-hMSCs HIFs expression

HIFs expression plays vital role in BM-hMSCs biology. An evaluation of HIF-1α expression in AO cultured cells indicated that a consistent baseline expression of 31% of the cell population displayed positive expression. In all experimentation, the AO baseline expression level is indicated via the point of x-axis / y-axis intersection (Figure 4.9) HIF-1α expression was significantly up regulated in the IH culture condition (+29%) ($p<0.01$) with no significant change at CN. HMAs used in combination with AO culture resulted in significant upregulation for $CoCl_2$ (38% increase above baseline), DFO (31% increase above baseline), DMOG (19% increase above baseline), and IOX2 (29% increase above baseline) (Figure 4.9.A). HMAs combined with IH culture resulted in similar increases above AO baseline as seen with IH alone with a slight, though significant, ~+10% (of IH level) upregulation noted with all HMAs tested (Figure 4.9.B). In contrast to IH but similar to AO, CN culture supplemented with HMAs resulted in significant upregulation for $CoCl_2$ (30% increase above CN baseline), DFO (29 % increase above CN baseline), DMOG (28% increase above CN baseline) and IOX2 (30 % increase above CN baseline) (Figure 4.9.C). The overall profile of HIF-1α expression in HMA supplemented AO cultured BM-hMSCs was that they bore a close resemblance to IH cultured cells indicating that HMAs replicate an IH phenotype. It is also noteworthy that HMAs were not overtly additive to HIF-1α expression in IH cultured cells but that were highly so in CN cultured cells.

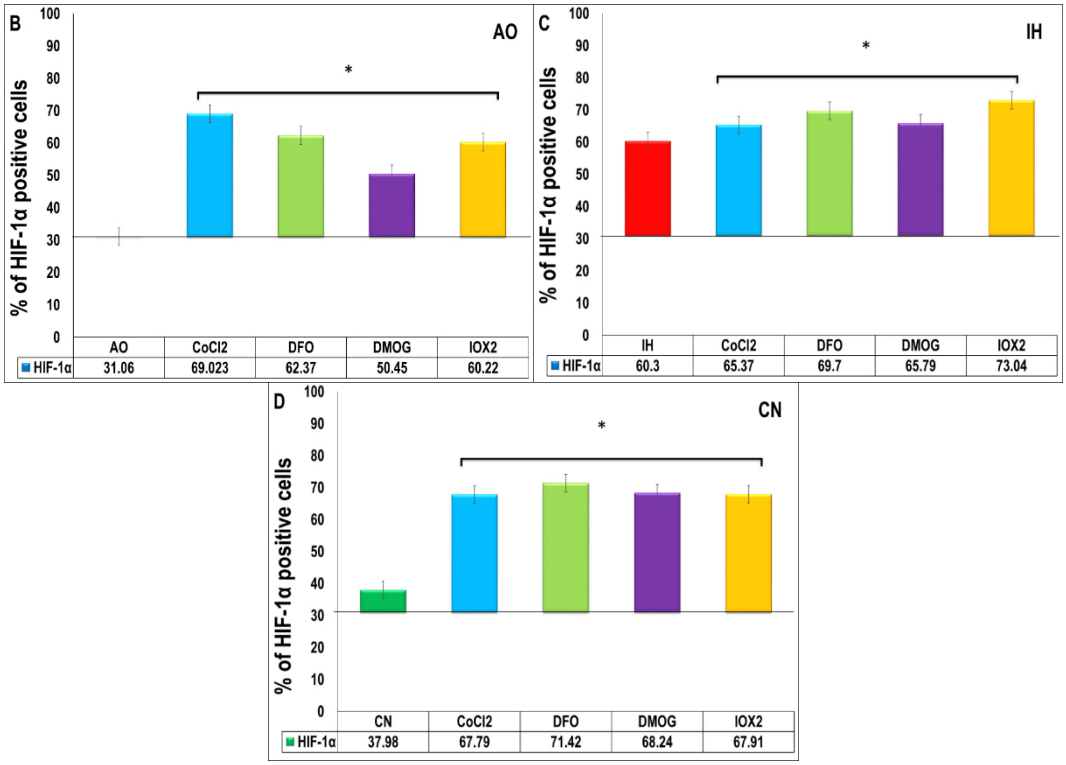

Figure 4.9. Effect of hypoxia mimetic agents on HIF-1α expression in BM-hMSCs cultured in the different oxygen conditions

*The percentage of anti-HIF-1α (ab16066) labelled cells is shown. BM-hMSCs cells were exposed to (50 µM $CoCl_2$, 50 µM DFO, 100 µM DMOG and 50 nM IOX2) for 14 days in AO, IH and CN. Data are presented as % of HIF-1α positive ± standard deviation (SD). n=1 triplicate, * indicates significant difference in comparison to the % of HIF-1α positive control cells at each culture condition (p<0.01).*

Similar to above, before beginning HIF-2α experimental analysis the baseline HIF-2α expression of AO cultured BM-hMSCs was determined as 74%, this is indicated as the intersection point of the x-axis/y-axis in all graphs (Figure 4.10). HMAs used in combination with AO culture resulted in significant upregulation of HIF-2α with $CoCl_2$ (10% increase above baseline), DFO (13% increase above baseline), DMOG (17% increase above baseline), and IOX2 (15% increase above baseline) (Figure 4.10.A). IH culture resulted in a significant upregulation of HIF-2α expression (+6%) above baseline ($p<0.05$). In contrast to AO, HMAs supplementation to BM-hMSCs at IH resulted in a varied

response, whereas $CoCl_2$ and DFO+IH resulted in no significant change while DMOG and IOX2 + IH resulted in significant downregulation versus IH baseline.

The varied response to HIF-2α expression was continued with CN cultured BM-hMSCs. Baseline CN displayed broad similarity to baseline AO while $CoCl_2$ supplemented CN resulted in significant HIF-2α upregulation (+21%), DFO and IOX2 supplementation in CN resulted in little change and DMOG resulted in a non-significant increase.

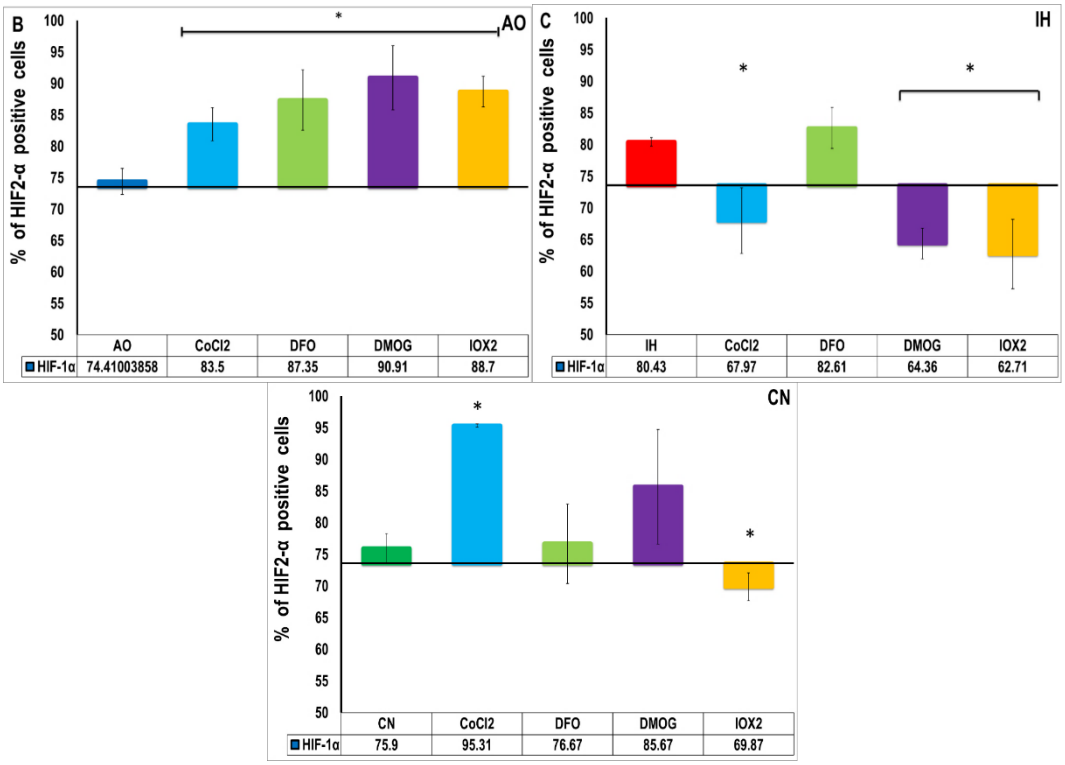

Figure 4.10. Effect of hypoxia mimetic agents on HIF-2α expression of BM-hMSCs cultured in the different oxygen conditions

*The percentage of anti-HIF-2α (ab8365) labelled cells is shown. BM-hMSCs cells were exposed to (50 μM $CoCl_2$, 50 μM DFO, 100 μM DMOG and 50 nM IOX2) for 14 days in AO, IH and CN. Data are presented as % of HIF-2α positive ± standard deviation (SD). n=1 triplicate, * indicates significant difference in comparison to the % of HIF-2α positive control cells at each culture condition (p<0.01).*

4.3.3. Effect of hypoxia mimetic agents on BM-hMSCs CFU-F isolation from bone marrow

We next sought to explore the effect of AO, IH, CN, and HMA's on colony-forming unit fibroblasts (CFU-Fs) isolation with reference to a previous study which indicated that MSC colony formation was not directly related to HIF changes (Tamama *et al.,* 2011).

We first explored the role of different oxygen culture conditions on CFU-F isolation from bone marrow aspirate under AO, IH and CN. The results showed that both IH culture and CN culture resulted in significant increases in the number of CFU-F isolated (+44 and +68 in IH and CN, respectively) ($p<0.01$) (Figure 4.11.A).

We next evaluated the role, if any of HMAs, in replicating the increases observed with IH and CN. All HMAs tested in AO resulted in a significant increase ($p<0.01$) in frequency of CFU-F isolation above control; $CoCl_2$ (+22), DFO (+8), DMOG (+18), and IOX2 (+30) (Figure 4.11.B). In contrast IH culture supplemented with HMAs resulted in significant decreases ($p<0.01$) in relation to control; $CoCl_2$ (-23), DFO (-62), DMOG (-45), and IOX2 (-24) (Figure 4.11.C). Finally, CN culture supplemented with HMAs was in agreement with IH but again distinct to AO with decreases vs. control noted as; $CoCl_2$ (-60), DFO (-74), DMOG (-37), and IOX2 (-48) ($p<0.01$) (Figure 4.11.D). Pearson correlation showed that only IOX2 was negatively related to AO (r^2 =0.6195, $p<0.0118$). Where under IH culture condition, $CoCl_2$ and DFO negatively correlated to IH control (r^2 =0.9643, $p<0.0001$, r^2 =0.7251, $p<0.0036$) in contrast IOX2 positively correlated (r^2 =0.7982, $p<0.0012$). Under CN culture $CoCl_2$ and DFO positively correlated to CN control (r^2 =0.9986, $p<0.0001$ and r^2 =0.9918, $p<0.0001$). In summary, the HMAs effect on CFU-F isolation was distinctive from that induced by merely changing oxygen level.

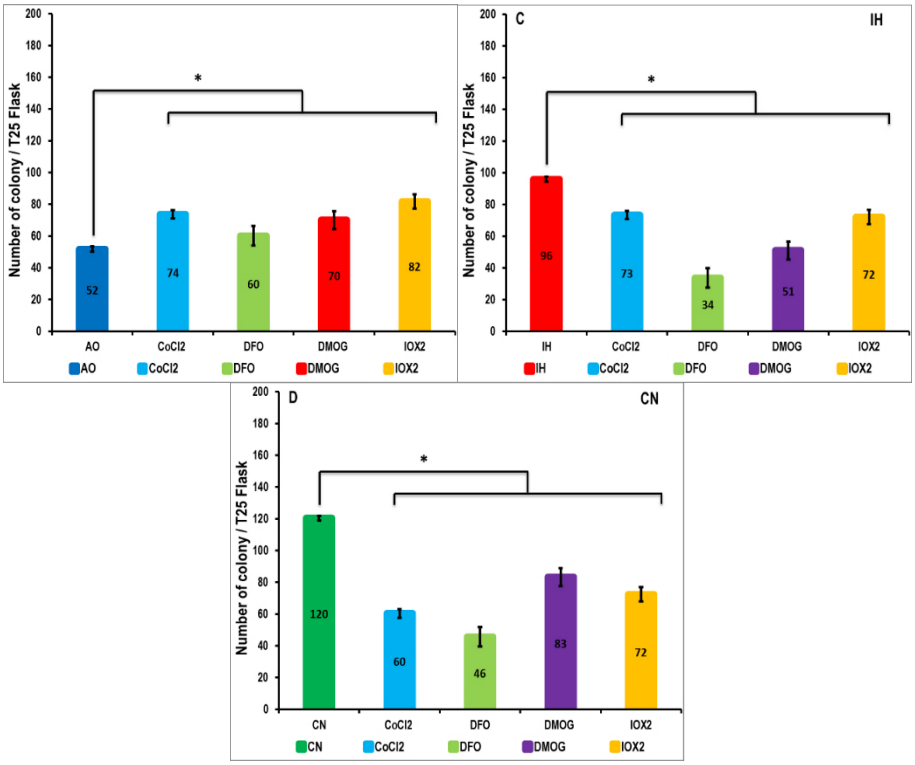

Figure 4.11. The influence of HMAs on BM-hMSCs CFU-F recovery from bone marrow aspirate

*MSCs CFU-F recovery from bone marrow aspirate in three different oxygen culture conditions with and without HMA treatment. (A) represents cells incubated under AO, IH and CN culture condition (controls). (B) represent cells after treatment with HMAs under AO culture condition. (C) represent cells after treatment with HMAs under IH culture condition. (D) represent cells after treatment with HMAs under CN culture condition. X-axis indicates different treatment with HMAs. Y-axis represents CFU-F / T25 flask. Data presented as mean and the error bar represent standard deviation. n=3, * indicates significant difference when compared to the control for each oxygen culture condition (p< 0.01).*

BM-MSCs represent an important candidate for regenerative applications because of their high proliferative capacity and the potential to differentiate into other cell types. HMAs were investigated as a preconditioning agent on clonogenic potential of primary MSCs cultured under different oxygen culture condition and the results shows that HMAs increase colony number in manner similar but with lower magnitude than that noticed under IH or CN and this may relate to regulation of Wnt/β-catenin signaling, which is critical for maintenance of stemness in MSCs. HMAs like IH by inducing HIF-1 which may

have upregulated transcripts glucose-6-phosphate isomerase/autocrine motility factor (*GPI*) and *MMP8*, and downregulated transcripts: *CDH1* (E-cadherin), *CTNNA1* (α-catenin), *APC*, *SMAD2*, and *SMAD3*, all of which are playing role in regulation of mesenchymal transition and canonical Wnt signaling through modulation β-catenin trafficking and signaling, either directly or through release or increase of cell adhesions (Zeng *et al.,* 2011; Boyette *et al.,* 2014).

4.3.4. Effect of hypoxia mimetic agents on BM-hMSCs tri-lineage differentiation potential and immunophenotype

The multi-lineage differentiation capacity of BM-hMSCs is a key reason for their use in regenerative medicine (Bernardo *et al.,* 2007). The study of BM-hMSCs tri-lineage differentiation capacity both under different oxygen levels and after treatment with HMAs was determined via histological staining and imaging of the differentiated cells (Figure 4.12). The ability of these cells to tri-lineage differentiation is a defining property of BM-hMSCs and it is essential to confirm this property in primary cells and observe any changes as a result of the different oxygen level and after treatment with HMAs.

Following culture in osteogenic differentiation media, strongly stained mineralised regions were noted for BM-hMSC grown in AO, IH, and CN indicating that the different oxygen culture conditions had no significant effect on osteogenic differentiation. Kay *et al.,* noted reduced levels in CN and this come with broad agreement with previous observations (Kay *et al.,* 2015). A global inhibition of osteogenesis was not observed in any culture condition combination though non-quantified but noteworthy reductions were noted for AO + HMAs, IH + DFO, CN + HMAs (Figures 4.12, 13 and 14). Adipogenesis was indicated by intracellular lipid droplet visualised with oil red O. Clear adipogenic differentiation was noted in AO and CN but appeared reduced in IH. HMAs did not observably reduce differentiation in AO, promoted differentiation in IH, and had no clear effect in CN (Figures

4.12, 13 and 14). Alcian blue staining for chondrogenesis displayed elevation after culture in CN even after treatment with HMAs in comparison to control AO. No significant effect of HMAs was seen at IH culture condition (except IOX2 at IH). Under CN culture condition HMAs had no significant effect on chondrogenesis (except DFO) (Figures 4.12, 13 and 14).

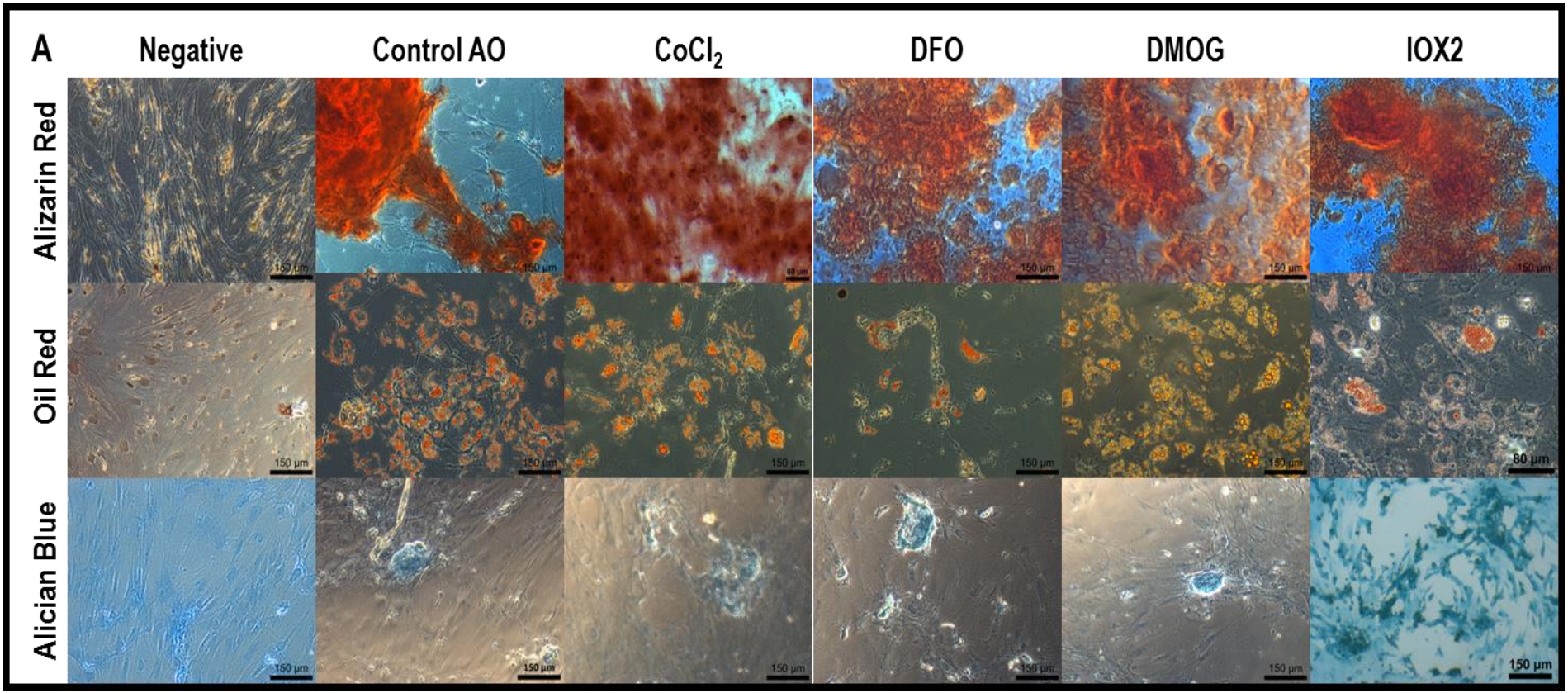
A
Negative
Control AO
$CoCl_2$
DFO
DMOG
IOX2
Alizarin Red
Oil Red
Alician Blue
150 µm
80 µm

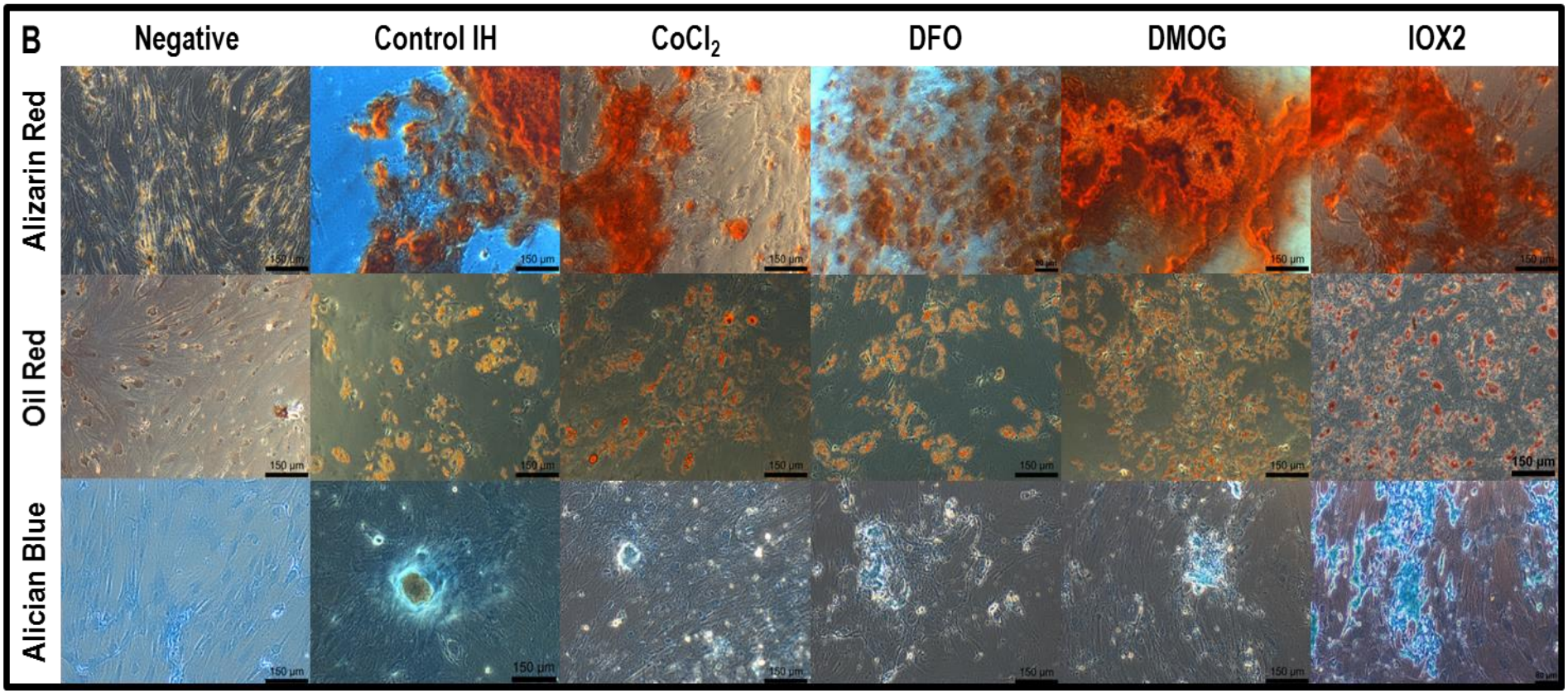
B
Negative
Control IH
CoCl2
DFO
DMOG
IOX2
Alizarin Red
Oil Red
Alician Blue
150 µm

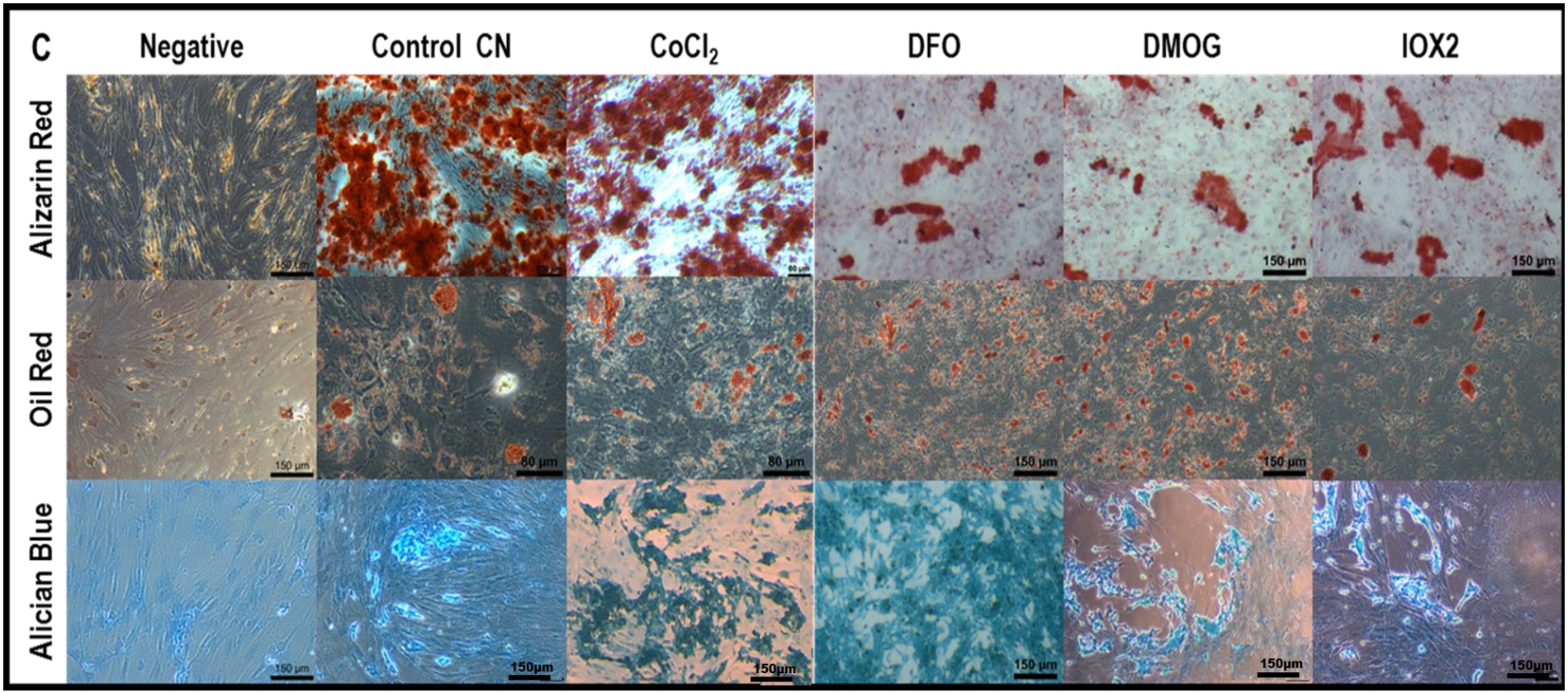

Figure 4.12. Tri-lineage differentiation of BM-hMSCs in three distinct oxygen culture conditions with and without HMAs treatment

BM-hMSCs were induced to differentiate toward osteogenic lineage and verified by alizarin red staining after induction (scale bar, 150 µm), adipogenic lineage and verified by Oil Red O (scale bar, 150 µm), and chondrogenic lineage verified by Alician blue staining (scale bar, 150 µm). (A) represents cell incubated in AO, (B) represents cells cultured under IH, and (C) represents cell incubated in CN. One representative of 3 independent experiments is shown.

To further explore the impact of oxygen culture condition and HMAs on differentiation we next employed an antibody-directed fluorescence approach looking at expression of osteocalcin (osteogenesis), FABP4 (adipogenesis), and aggrecan (cartilage). Osteocalcin expression appeared to be down-regulated in AO + HMAs, IH, and CN + DFO or IOX2 (Figure 4.13 A, B and C). FABP4 the marker of adipocyte differentiation showed no significant effect of HMAs under three culture conditions. Lastly, aggrecan showed no significant changes after HMAs except DFO under IH culture where it caused down regulation of aggrecan (Figure 4.13 A, B, and C).

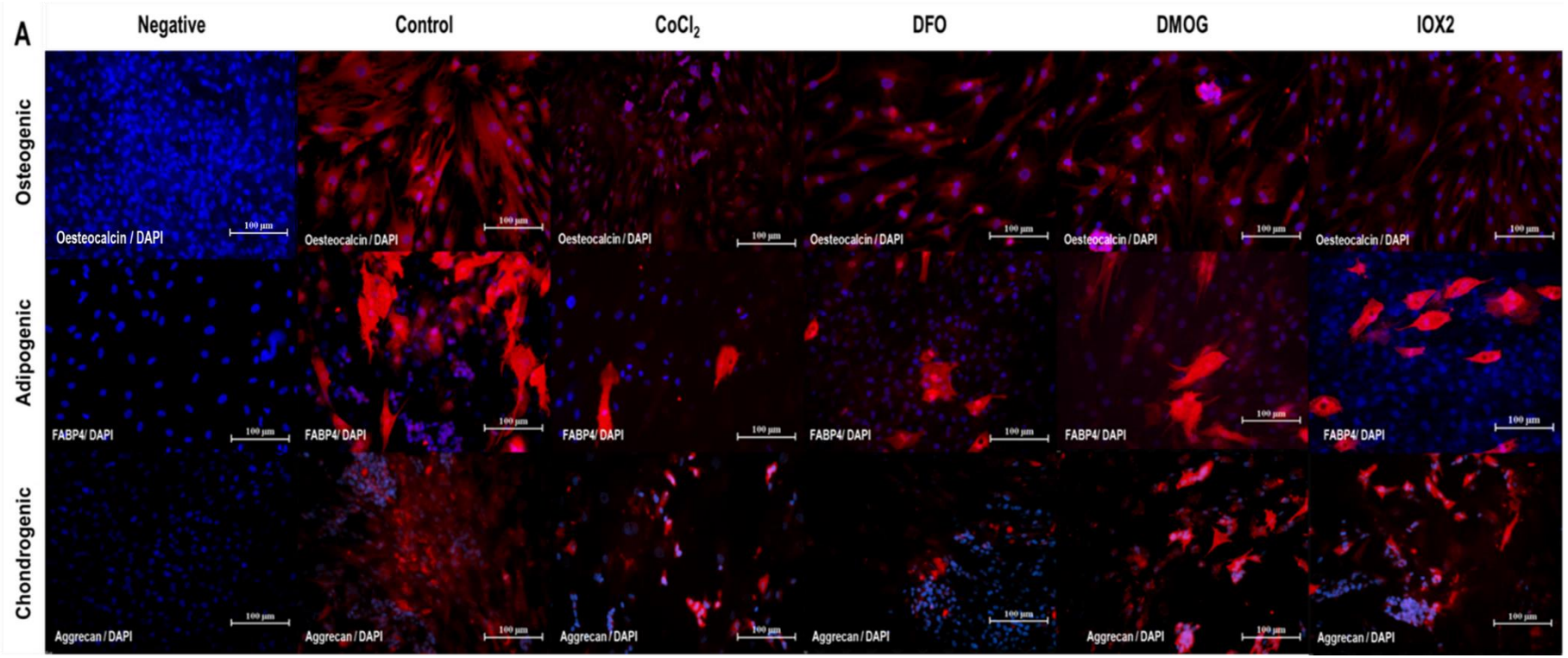
A
Negative
Control
CoCl2
DFO
DMOG
IOX2
Osteogenic
Adipogenic
Chondrogenic
Oesteocalcin / DAPI
FABP4/ DAPI
Aggrecan / DAPI
100 µm

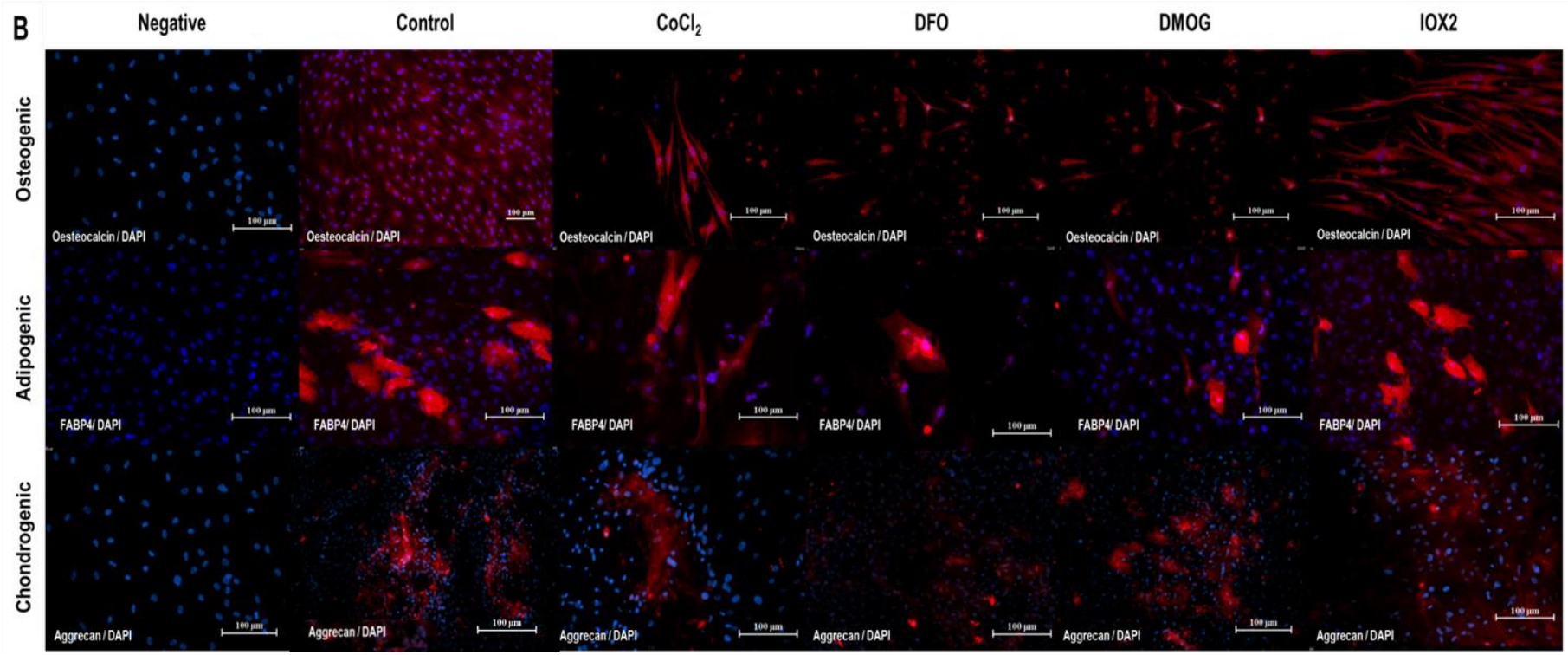
B
Negative
Control
$CoCl_2$
DFO
DMOG
IOX2
Osteogenic
Adipogenic
Chondrogenic
Oesteocalcin / DAPI
FABP4/ DAPI
Aggrecan / DAPI
100 µm

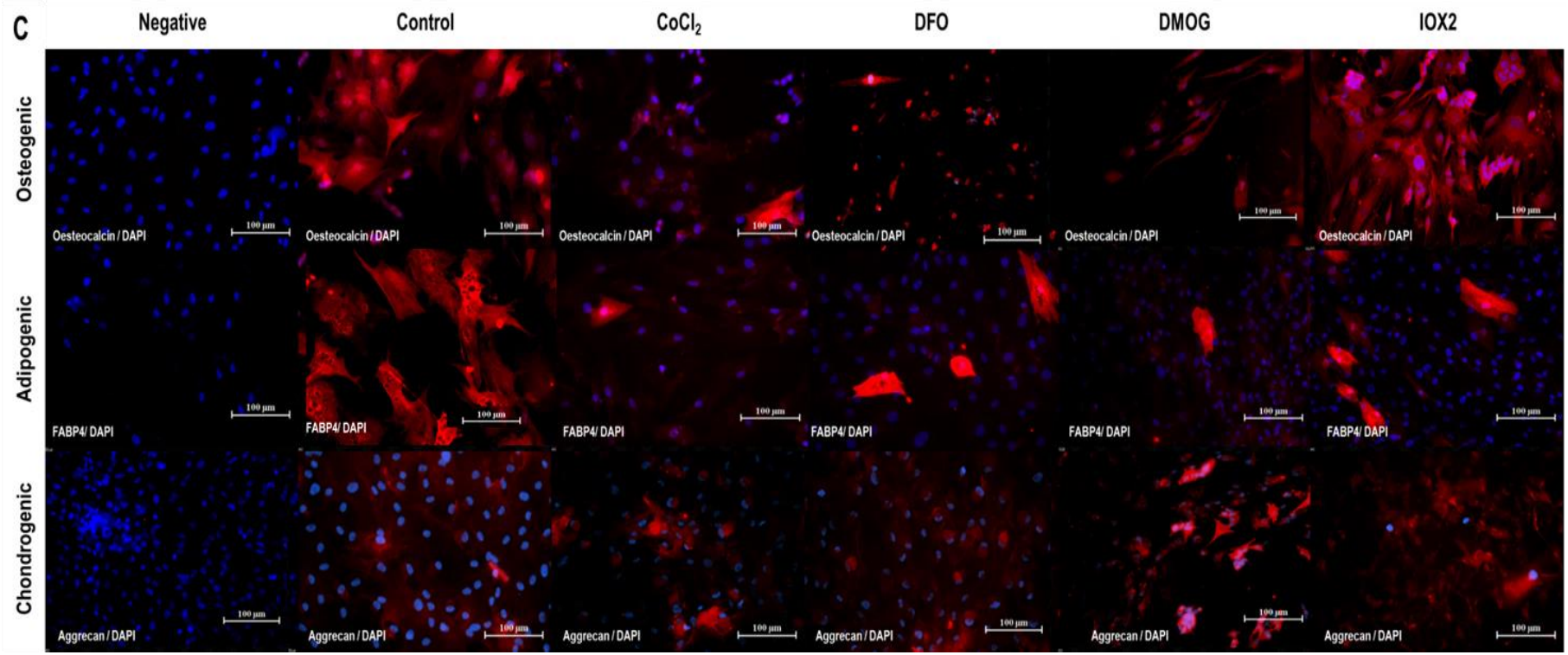

Figure 4.13. Differentiation specific protein expression in BM-hMSCs following tri-lineage differentiation in three oxygen culture conditions with HMA treatment

Human mesenchymal stem cells were cultured for 21 days in growth media supplemented with specific supplementation according to the Human Mesenchymal Stem Cell Functional Identification Kit (Catalogue # SC006). Figure (A) represents hMSCs cultured at AO culture condition with and without HMAs treatment. Figure (B) represents hMSCs cultured at IH culture condition with and without HMAs treatment. Figure (C) represents hMSCs cultured at CN culture condition with and without HMAs treatment. Red fluorescence represents either Osteocalcin, FABP4, or Aggrecan, as indicated. Blue stain represent nucleus stained with DAPI. Scale bar=100 µm. One representative of 3 independent experiments is shown.

After confirming the differentiation capacity of these cells, we next sought to define the effect of different oxygen culture conditions in combination with HMAs on the BM-hMSC immunophenotype. All cells were incubated with antibodies directed towards CD14, CD19, CD34, CD45, HLA-DR, CD73, CD90 and CD105 according to the widely identified marker panel for BM-hMSCs (Ramos *et al.,* 2016). Staining was compared relative to the recommended non-specific isotype control, either IgG1 or IgG2a depending on the antibody. Histograms of percentage of positively stained cell for all markers are shown in (Figure 4.14). The percentage of cells considered positively stained was determined by gating the stained population with a gate that excluded 99% of all isotype control events.

Both isotype controls stained equally across all oxygen conditions and after treatment with HMAs, also matching unstained cells demonstrating minimal non-specific fluorescence. CD19, CD34 and CD45, markers typically negative in BM-hMSCs, were all considered negative where ≤5% positively stained cells indicating non-haematopoietic lineages was observed.

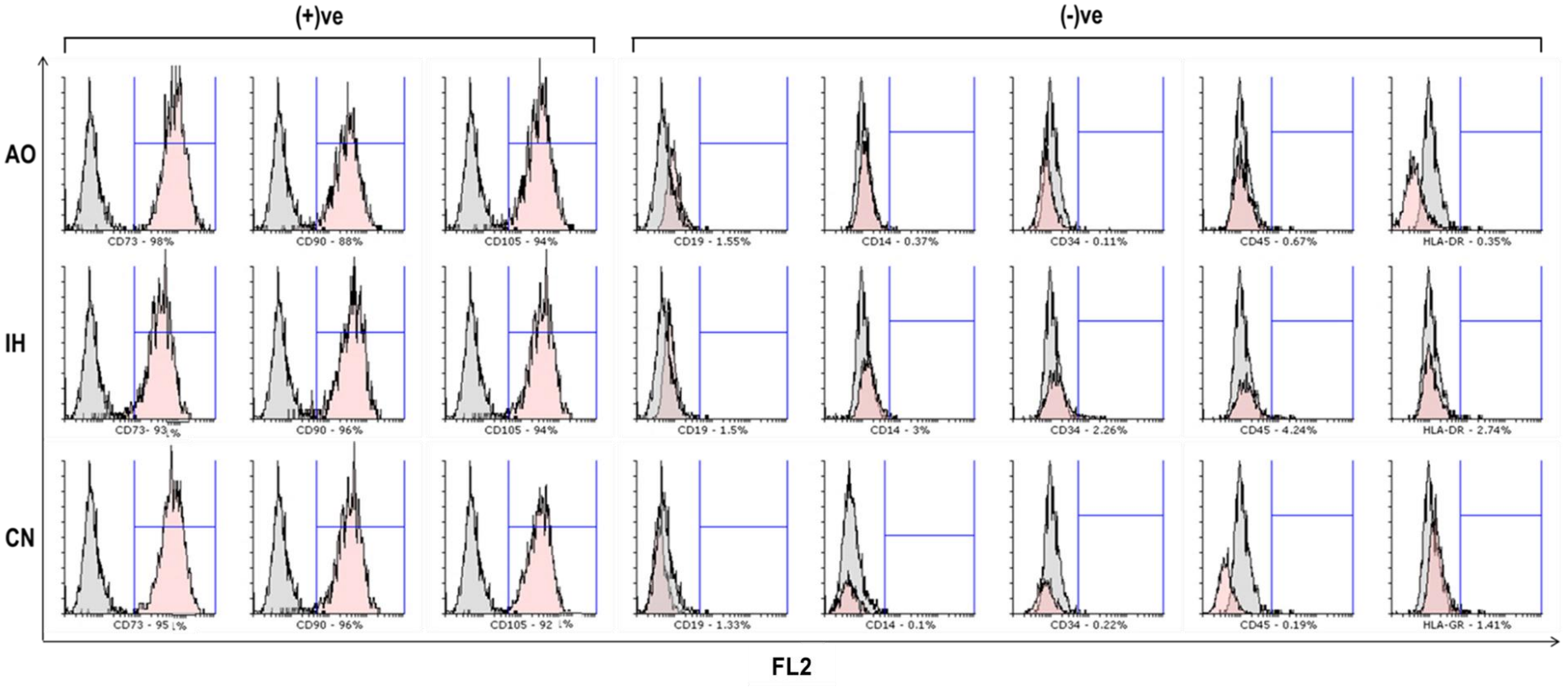

Figure 4.14. Immunophenotyping of cells from BM-hMSCs

Cells recovered in AO, IH and CN were assessed by flow cytometry against the panel of markers used to identify BM-hMSCs. Overlay histograms of each antibody was compared to the relevant isotype control at AO, IH and CN culture conditions. The grey area represents isotype control IgG expression and the pink area depicts marker expression. The results are representative of three independent experiments. Positive markers (CD73, CD90, and CD105) and negative markers (CD14, CD19, CD34, CD45 and HLA-DR) were applied.

Significant, though slight, increases in levels of CD14, CD34, CD45, HLA-DR and CD90 were noted in IH ($p<0.01$ vs. AO). Similar levels of increase in expression were noted for IH with HLA-DR and CD90 with accompanying decreases in CD14 and CD45 ($p<0.01$) (Figure 4.15.A).

AO supplementation with $CoCl_2$ resulted in significant increases for CD14, CD34, CD45, and HLA-DR when compared to AO control ($p<0.01$) (Figure 4.15.B). DFO exposure resulted in significant increases for CD14, and CD34, and significant reductions for CD73 and CD105 when compared to AO control ($p<0.01$) (Figure 4.15.B). DMOG exposure resulted in significant increases for CD14, CD34, CD45 and HLA-DR, and significant reductions for CD19 and CD90 (Figure 4.15.B) when compared to AO control ($p<0.01$). Similarly, to above IOX2 exposure resulted in significant increases for CD14, CD19, CD34, CD45 and HLA-DR, and significant reductions for CD90 when compared to AO control ($p<0.01$) (Figure 4.15.B).

We next sought to describe the impact of HMA supplementation on IH culture. $CoCl_2$ exposure resulted in significant increases for CD34, CD45 and HLA-DR, and significant reductions for CD19 and CD105 when compared to IH control ($p<0.01$) (Figure 4.15.C). DFO exposure resulted in significant decreases for CD34, CD45, HLA-DR and CD90 when compared to IH control ($p<0.01$) (Figure 4.15.C) while DMOG supplementation also resulted in CD34, HLA-DR, and CD90 downregulation along with CD14. IOX2 exposure resulted in significant increases for CD19 when and significant reductions for CD14, CD45, HLA-DR and CD90 compared to IH control ($p<0.01$) (Figure 4.15.C).

Finally, we determined if the CN cultured BM-hMSCs immunophenotype was sensitive to HMA supplementation. $CoCl_2$ exposure resulted in significant increases for CD14, CD34, and CD45 and significant reductions for both CD19 and CD105 when compared to CN control ($p<0.01$) (Figure 4.15.D). DFO exposure resulted in a broadly consistent pattern where significant decreases were noted for CD14, CD19, HLA-DR and CD90 and significant increases in CD45 when compared to CN control ($p<0.01$) (Figure 4.15.D).

DMOG exposure resulted in increases for CD19 and HLA-DR and a decreased CD14 when compared to CN control ($p<0.01$). IOX2 exposure, similar to above, also resulted in reductions in expression for CD14, CD19, CD34, HLA-DR and reductions for CD14 ($p<0.01$) (Figure 4.15.D).

To sum up, IH significantly elevated all hematopoietic markers especially CD14, CD34, CD45 and HLA-DR, in addition to the mononuclear cell origin suggesting high likelihood of being monocytes which then further different to macrophage and dendritic cells (Vasandan *et al.,* 2016). Under AO culture condition, HMAs induced expression of hematopoietic markers especially CD14, CD34, CD45 and HLA-DR and the changes mimic IH pattern but with lower magnitude in comparison to AO. In contrast under IH culture condition, CD14, CD45 and HLA-DR expression significantly reduces in comparison to IH after HMAs treatment. CN culture condition, HMAs more distinctive variable pattern of markers of MSCs in comparison to CN was noticed.

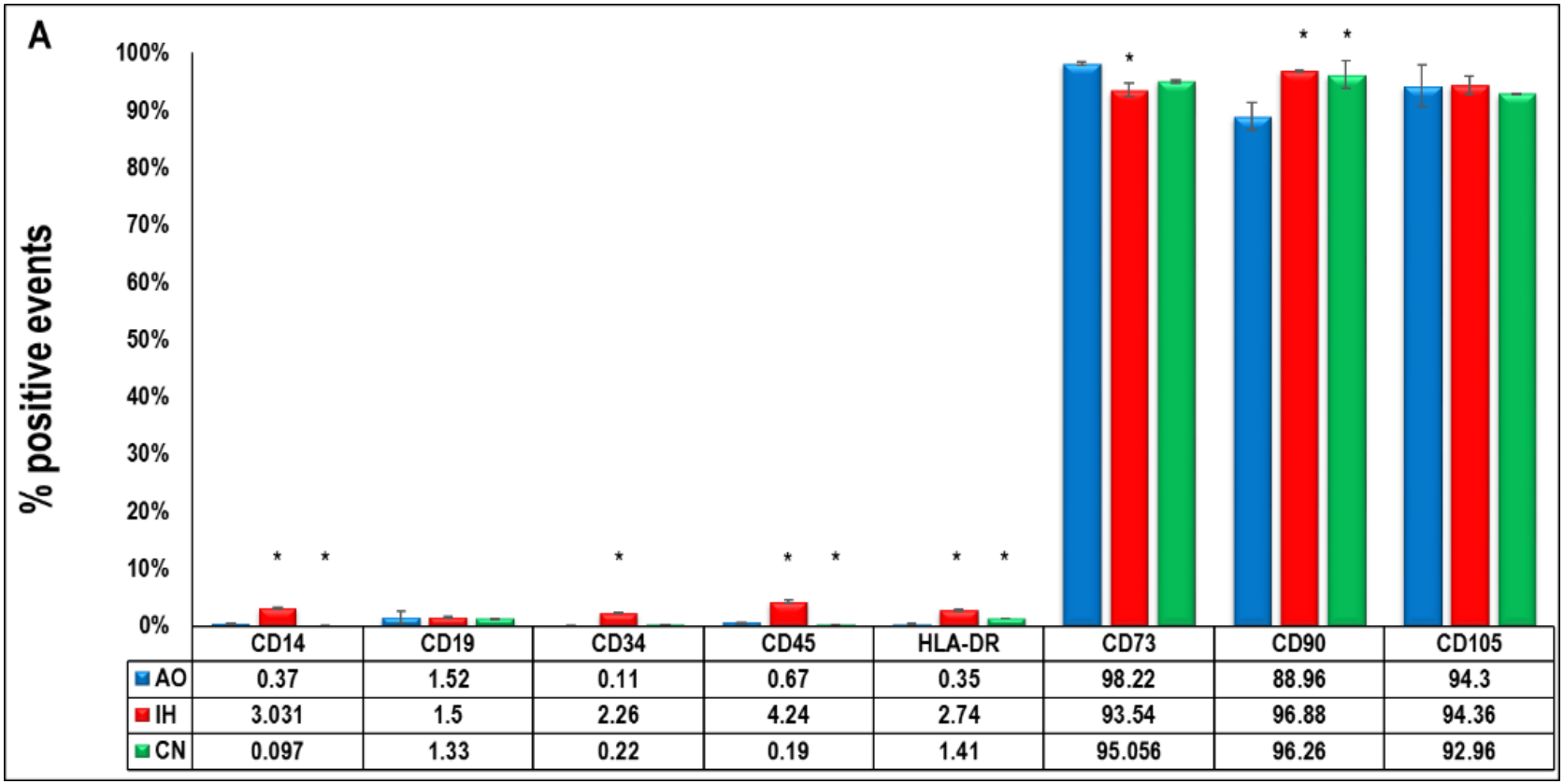

	CD14	CD19	CD34	CD45	HLA-DR	CD73	CD90	CD105
AO	0.37	1.52	0.11	0.67	0.35	98.22	88.96	94.3
IH	3.031	1.5	2.26	4.24	2.74	93.54	96.88	94.36
CN	0.097	1.33	0.22	0.19	1.41	95.056	96.26	92.96

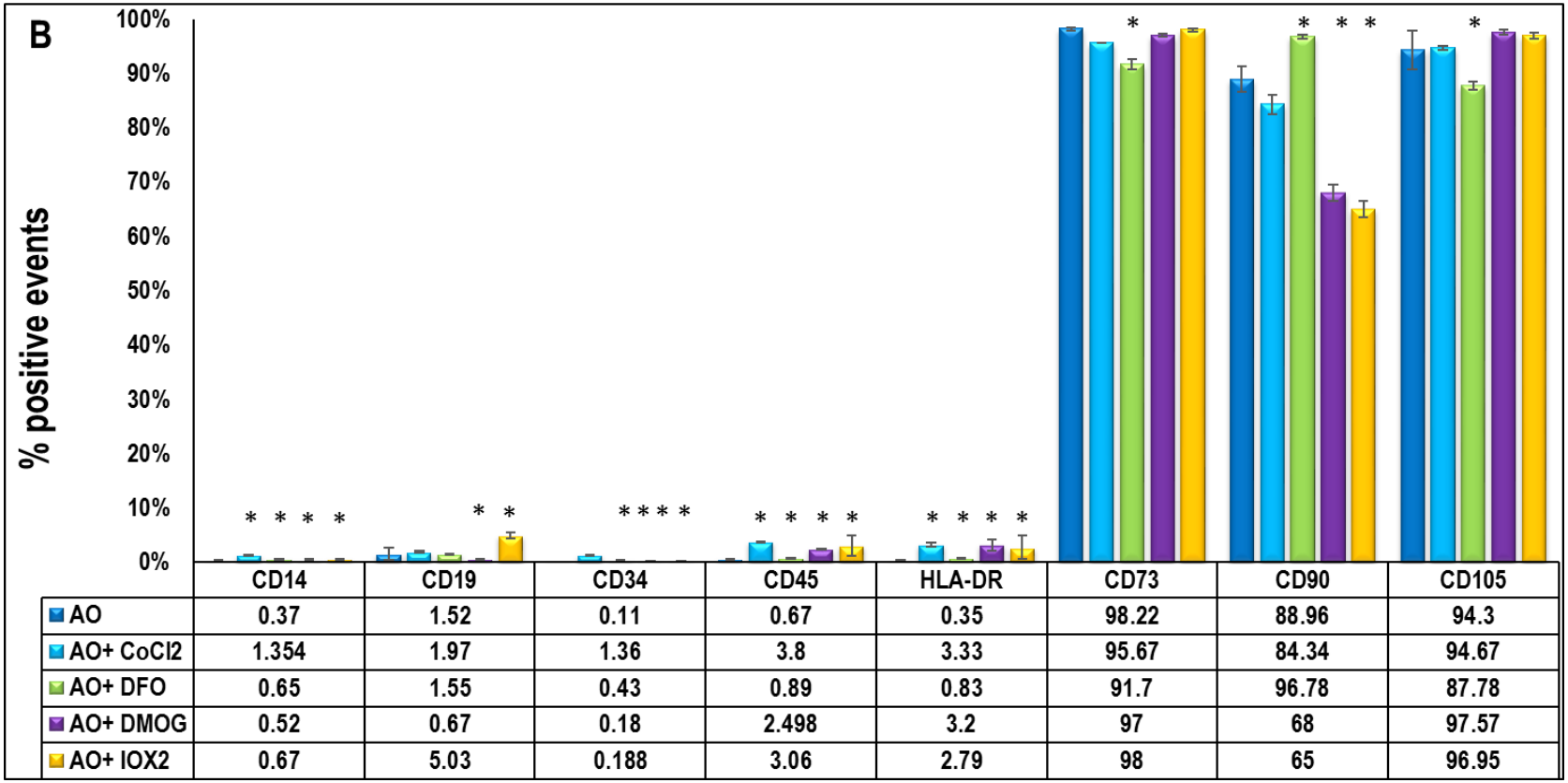

	CD14	CD19	CD34	CD45	HLA-DR	CD73	CD90	CD105
AO	0.37	1.52	0.11	0.67	0.35	98.22	88.96	94.3
AO+ CoCl2	1.354	1.97	1.36	3.8	3.33	95.67	84.34	94.67
AO+ DFO	0.65	1.55	0.43	0.89	0.83	91.7	96.78	87.78
AO+ DMOG	0.52	0.67	0.18	2.498	3.2	97	68	97.57
AO+ IOX2	0.67	5.03	0.188	3.06	2.79	98	65	96.95

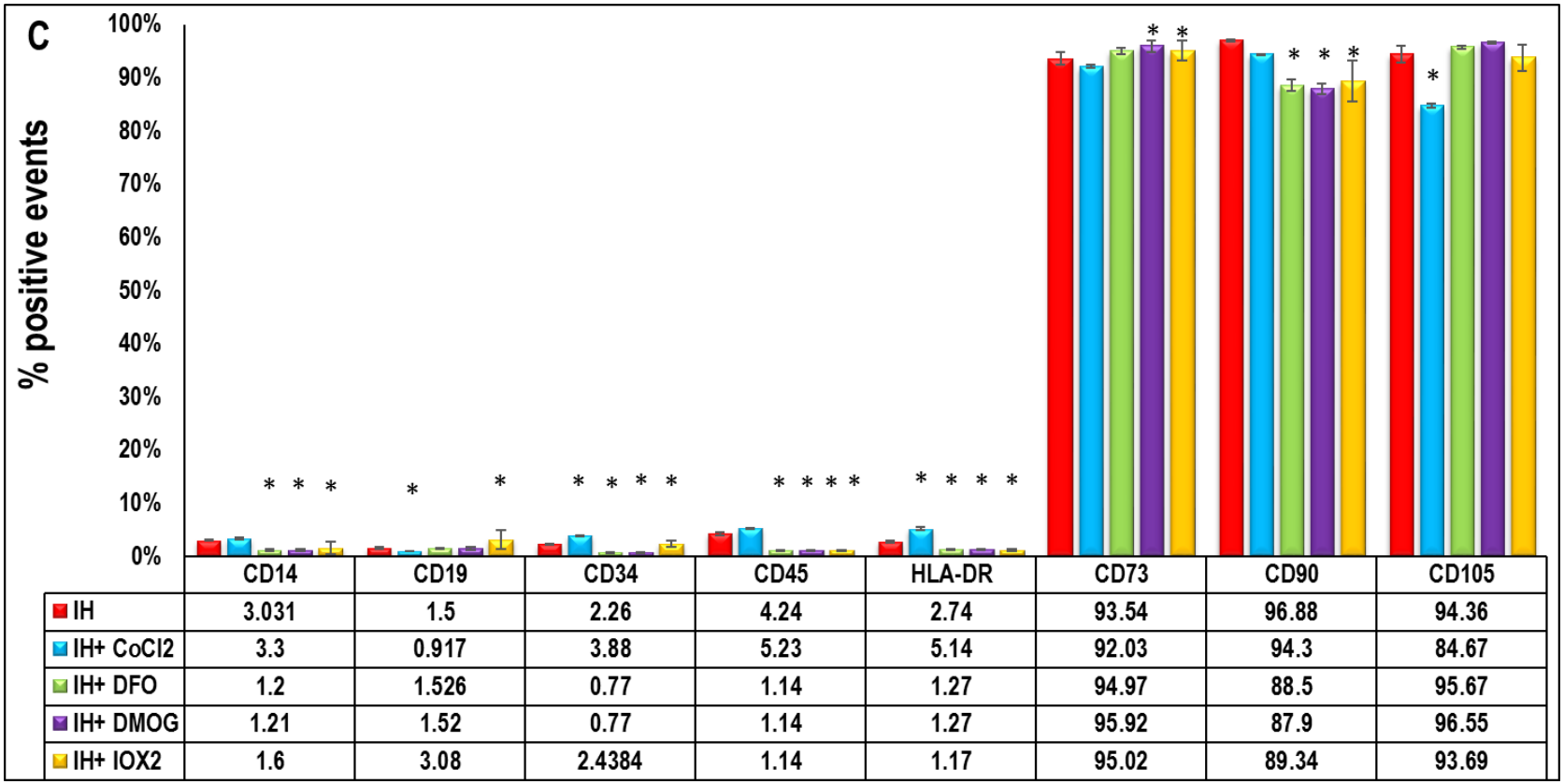

	CD14	CD19	CD34	CD45	HLA-DR	CD73	CD90	CD105
IH	3.031	1.5	2.26	4.24	2.74	93.54	96.88	94.36
IH+ CoCl2	3.3	0.917	3.88	5.23	5.14	92.03	94.3	84.67
IH+ DFO	1.2	1.526	0.77	1.14	1.27	94.97	88.5	95.67
IH+ DMOG	1.21	1.52	0.77	1.14	1.27	95.92	87.9	96.55
IH+ IOX2	1.6	3.08	2.4384	1.14	1.17	95.02	89.34	93.69

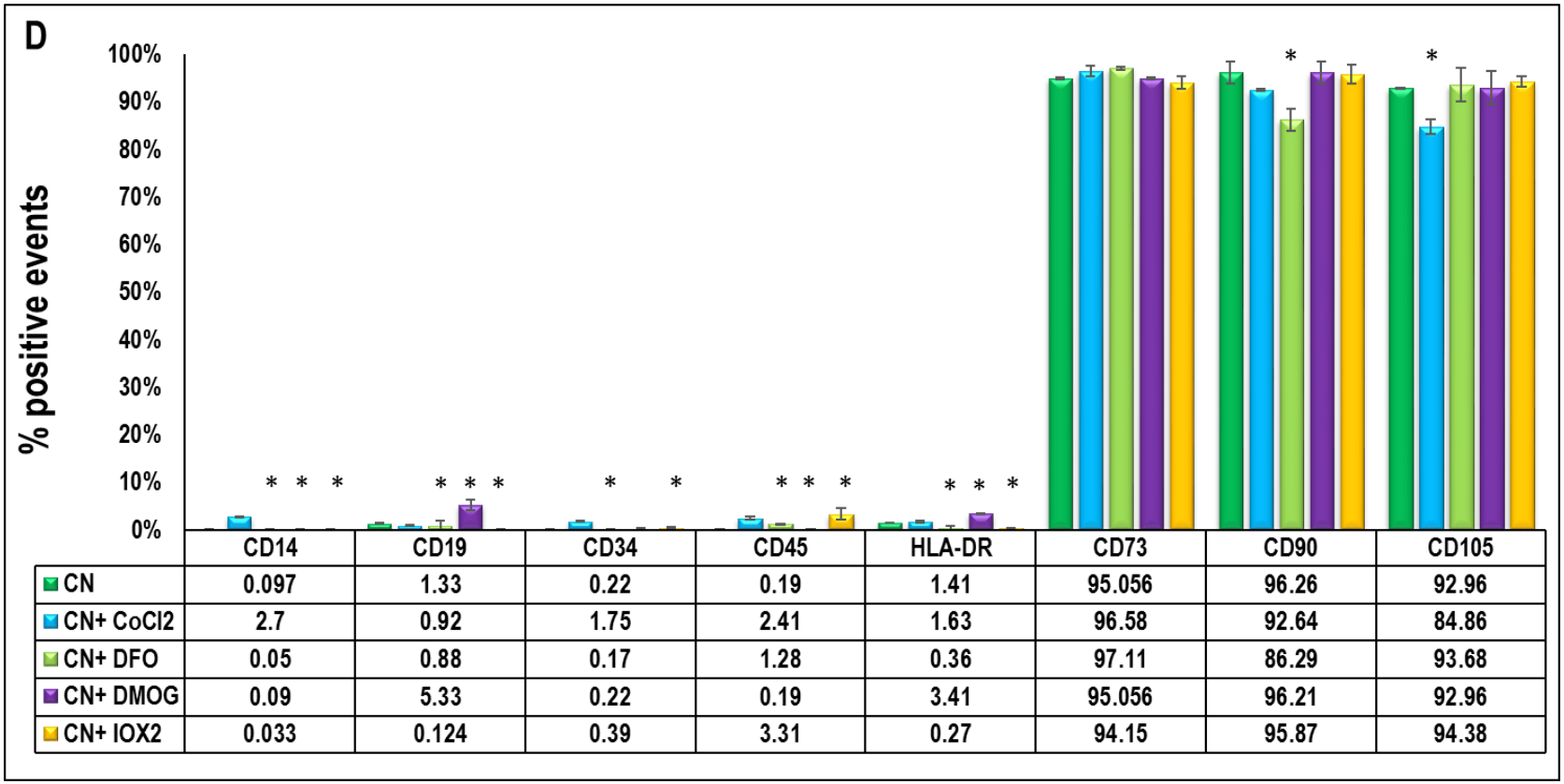

	CD14	CD19	CD34	CD45	HLA-DR	CD73	CD90	CD105
CN	0.097	1.33	0.22	0.19	1.41	95.056	96.26	92.96
CN+ CoCl2	2.7	0.92	1.75	2.41	1.63	96.58	92.64	84.86
CN+ DFO	0.05	0.88	0.17	1.28	0.36	97.11	86.29	93.68
CN+ DMOG	0.09	5.33	0.22	0.19	3.41	95.056	96.21	92.96
CN+ IOX2	0.033	0.124	0.39	3.31	0.27	94.15	95.87	94.38

Figure 4.15. Immunophenotype of BM-hMSCs after treatment with HMAs

*BM-derived hMSCs were recovered in three oxygen conditions (A), AO + HMAs (B), IH + HMAs (C) and CN + HMAs (D). Histograms showed mean surface marker expression in AO, IH and CN culture conditions with and without HMA treatment. X-axis represents surface markers. Y-axis represents % of positive events. n=3, * indicates significant difference when compared to the control for each oxygen culture condition ($p < 0.01$).*

4.3.5. Effect of hypoxia mimetic agents on BM-hMSCs apoptosis

Exploring the mechanism of BM-hMSCs apoptosis in hypoxia and after treatment with hypoxia mimetic agents is important for improving of the efficiency of cell therapy. Research has suggested that hypoxia and growth factor withdrawal caused apoptosis via a caspase-dependent manner in transplanted BM-hMSCs (Zhu *et al.,* 2006). However, the molecular mechanisms of BM-hMSCs have not been fully elucidated, as there are many apoptosis-inducing factors in the microenvironment of BM-hMSCs. Two pathways of apoptosis have been delineated in BM-hMSCs (Abdelwahid *et al.,* 2016). The first is the mitochondrial pathway which involves the release of proteins, such as cytochrome c from the mitochondria to cytosol (Galluzzi *et al.,* 2012). Cytochrome c release is usually associated with regulation of mitochondrial membrane proteins, such as the Bcl-2 family and results in activation of the caspase family (Martinou & Youle, 2011). The second pathway is the extrinsic pathway which includes activation of Fas (or CD95-L) and its receptor. However, many studies have shown that Fas-pathway seemed not to be involved in apoptosis of BM-hMSCs, as a Fas mAb agonist did not induce apoptosis of BM-hMSCs (Akiyama *et al.,* 2012). Meanwhile, we presume that other pathways may play a vital role in induction of apoptosis of BM-hMSCs, such as extracellular signal-regulated kinase (ERK), Akt, HIF and VEGF at hypoxia condition. HIF is activated when a cell is exposed to shortage in oxygen and HIF then stimulates the release of VEGF, ERK and Akt pathway (Fan *et al.,* 2015).

An evaluation of BM-hMSCs spontaneous apoptosis frequency identified that IH displayed a slight increase in early apoptosis and necrosis and a larger increase in late apoptosis abundance while reduction in necrosis was also noted in CN cultured cells in comparison to AO ($p<0.01$) (Figure 4.16.A).

Under AO $CoCl_2$, DFO and DMOG produced a shared apoptotic induction profile with significant increases in early apoptosis and decreases in late apoptosis and necrosis ($p<0.01$). In contrast, IOX2 reduced both early apoptosis and necrosis and increased late

apoptosis after HMAs treatment ($p<0.01$) (Figure 4.16.B). The overall apoptosis pattern induced by HMAs did not resemble the pattern observed in AO culture.

IH culture supplemented with HMAs resulted in a broadly identical response profile (Figure 4.16.C). Necrosis was reduced in all supplements vs. IH control ($p<0.01$). Early and late apoptosis were similarly reduced following HMA supplementation with the exceptions of DFO (early apoptosis) and IOX2 (late apoptosis) ($p<0.01$) (Figure 4.16.C). Again, the overall apoptosis pattern induced by HMAs did not resemble the pattern observed under the IH culture condition.

CN culture supplemented with HMAs resulted in broadly consistent patterns where reductions in early apoptosis and increases in late apoptosis were noted ($p<0.01$). Necrosis displayed more variability with decreases observed with $CoCl_2$ and DMOG and increases with DFO and IOX2 ($p<0.01$) (Figure 4.16). In summary IH and CN culture with HMAs reduced the frequency of cells in early apoptosis and necrosis. HMAs reduced late apoptosis at AO and IH with significant elevation at CN in some conditions. HMA exposure does not replicate the pattern of apoptosis observed in either CN or IH culture.

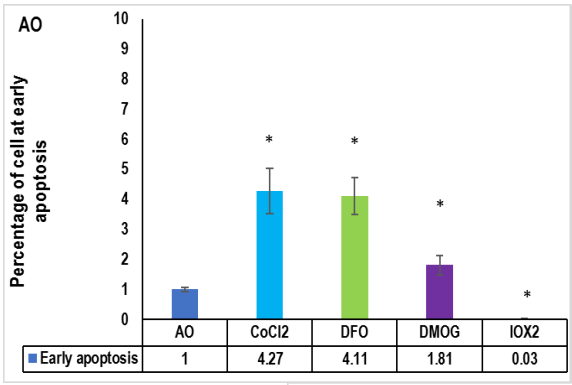
AO
Percentage of cell at early apoptosis
10
9
8
7
6
5
4
3
2
1
0
AO
CoCl2
DFO
DMOG
IOX2
Early apoptosis
1
4.27
4.11
1.81
0.03

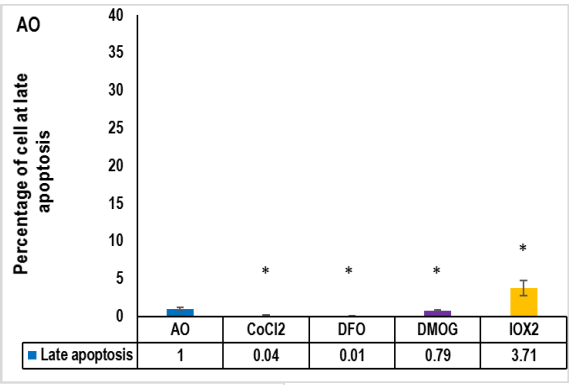
AO
Percentage of cell at late apoptosis
40
35
30
25
20
15
10
5
0
AO
CoCl2
DFO
DMOG
IOX2
Late apoptosis
1
0.04
0.01
0.79
3.71

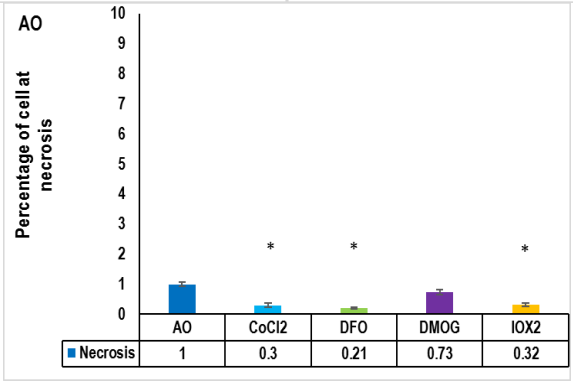
AO
Percentage of cell at necrosis
10
9
8
7
6
5
4
3
2
1
0
AO
CoCl2
DFO
DMOG
IOX2
Necrosis
1
0.3
0.21
0.73
0.32

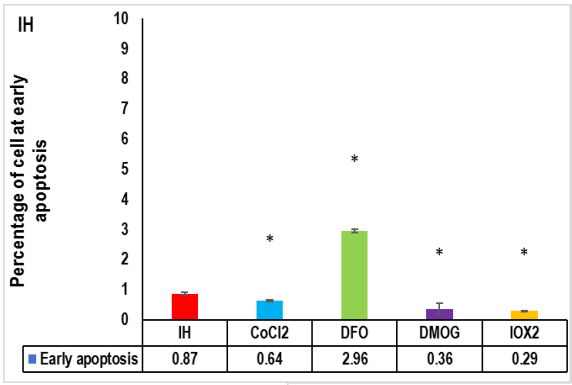
IH
Percentage of cell at early apoptosis
10
9
8
7
6
5
4
3
2
1
0
IH
CoCl2
DFO
DMOG
IOX2
Early apoptosis
0.87
0.64
2.96
0.36
0.29

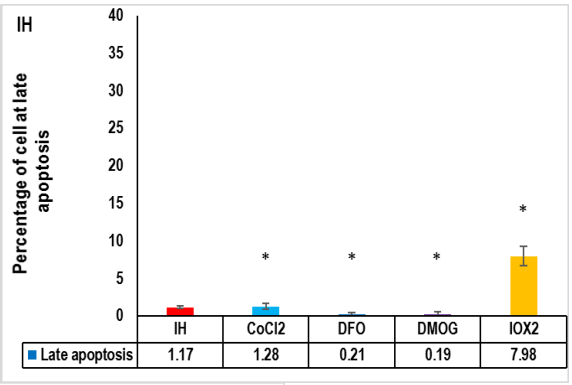
IH
Percentage of cell at late apoptosis
40
35
30
25
20
15
10
5
0
IH
CoCl2
DFO
DMOG
IOX2
Late apoptosis
1.17
1.28
0.21
0.19
7.98

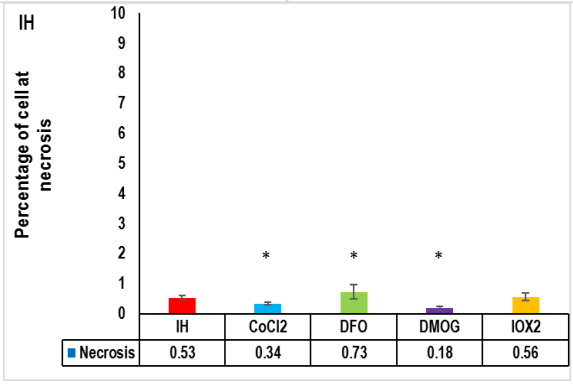
IH
Percentage of cell at necrosis
10
9
8
7
6
5
4
3
2
1
0
IH
CoCl2
DFO
DMOG
IOX2
Necrosis
0.53
0.34
0.73
0.18
0.56

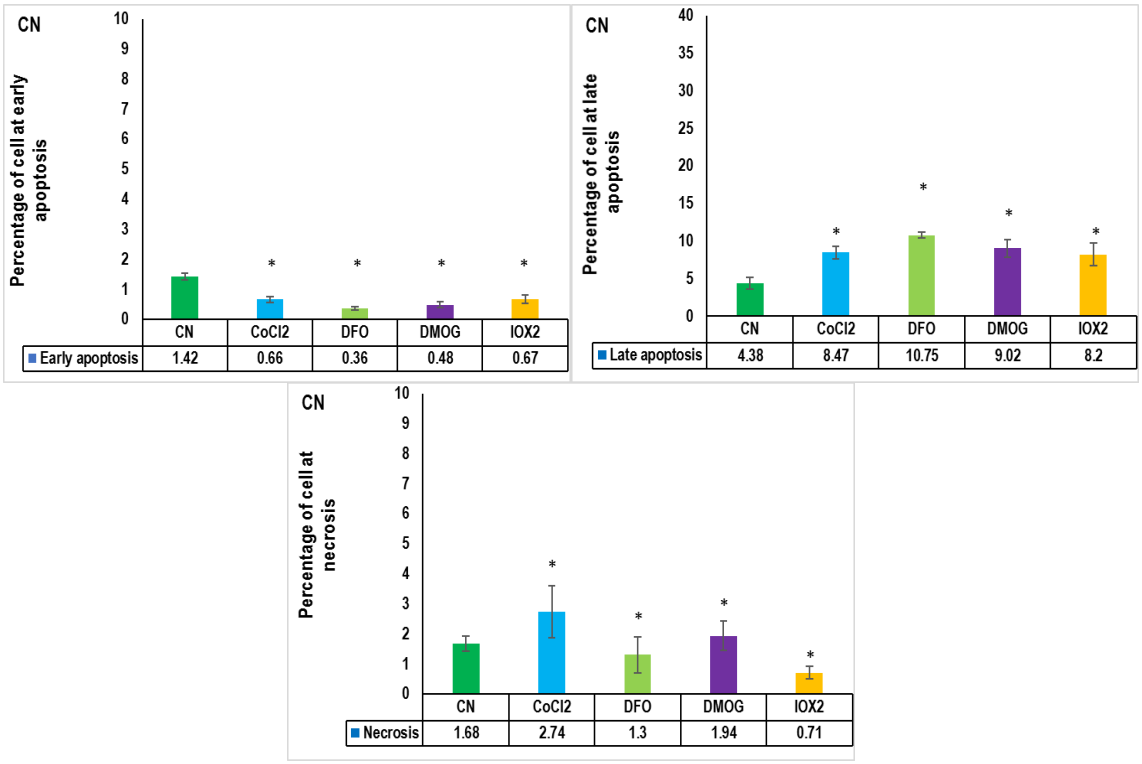

Figure 4.16. Effect of hypoxia mimetic agents on BM-hMSCs

*Following exposure to either 50 µM $CoCl_2$, 50 µM DFO, 100 µM DMOG, or 50 nM IOX2 for 14 days early apoptosis, late apoptosis and necrosis at AO culture, IH culture and CN culture, respectively, were measured. Cells treated with HMAs at AO. Cells treated with HMAs at IH. Cells treated with HMAs at CN. X-axis represents different treatment. Y-axis represent percentage of cells at each stage of cell death. Data are presented as mean of percentage of the cell at each stage ± standard deviation (SD). n=1 triplicate, * Indicates significant difference in comparison to control at each culture condition (p<0.01).*

4.3.6. Effect of hypoxia mimetic agents on BM-hMSCs cell cycle

Oxygen levels modify the expression of many molecules that are directly or indirectly involved in cell proliferation and survival (Mohyeldin *et al.,* 2010). The expression of many cell cycle molecules is regulated by HIF-1α including p21, anti-apoptotic factors, such as Bcl-2, and pro-apoptotic proteins, such as p53 (Velletri *et al.,* 2016). Consequently, BM-hMSCs show significant difference in proliferation rates when expanded under hypoxia compared to those expanded under air oxygen culture (Ranera *et al.,* 2012).

Using FACS analysis of BM-hMSCs we established a consistent baseline pattern of cell cycle characteristics. AO BM-hMSCs stocks were used to initiate all experiments and were measured to establish at zero-time baseline pattern. We noted that AO and IH culture conditions has no effect on G0-G1 phase, while CN significantly lower S phase and elevated G2-M phase in comparison to baseline ($p<0.01$) (Figure 4.18.A).

We next sought to evaluate if AO supplementation with HMAs would mimic either IH or CN behaviour. Overall HMAs significantly increased the percentage of cells in G0/G1 phase when compared to control AO culture ($p<0.05$). Cells at S-phase showed either a significant decrease ($p<0.01$) after supplementation with $CoCl_2$, DFO and DMOG (19%, 13% and 21% respectively) or no change (IOX2) when compared to control AO culture. G2-M displayed a significant increase ($p<0.05$) after supplementation with $CoCl_2$, DFO and DMOG (8%, 6% and 5% respectively) while no effect was noticed after IOX2 treatment (Figures 4.17.A and 18.B).

In IH culture DFO and IOX2 supplementation elevated the percentage of cells in G0/G1 phase (16% and 28% respectively) ($p<0.01$), no significant effect was noticed after DMOG, and a significant reduction noted with $CoCl_2$ versus control IH. S phase increases were only noted with $CoCl_2$ (13%) while in contrast DFO and IOX2 were reduced (20%) ($p<0.01$) and DMOG unchanged when compared to control IH. All HMAs resulted in a significant decrease in G2-M phase values ($p<0.01$) (Figures 4.17.B and 18.C).

CN culture also resulted in an overall significant increase in G0/G1 composition following HMA supplementation ($p<0.01$). DFO and DMOG significantly elevated S phase values while $CoCl_2$ and IOX2 had no effect. Finally, all HMAs down-regulated G2-M phase when compared to CN control ($p<0.05$) (Figures 4.17.C and 18.D).

In summary, HMAs showed no resemblance in cell cycle pattern to any pattern we found under the three-oxygen culture. Where HMAs under AO trapped MSCs at G0/G1 phase and drop in S-phase after treatment with HMAs (except IOX2). Again, under IH culture

condition, HMAs (except $CoCl_2$) elevated G0/G1 phase and drop in G2-M. Under CN culture condition, HMAs trapped cells again in G0/G1 phase with drop in S-phase.

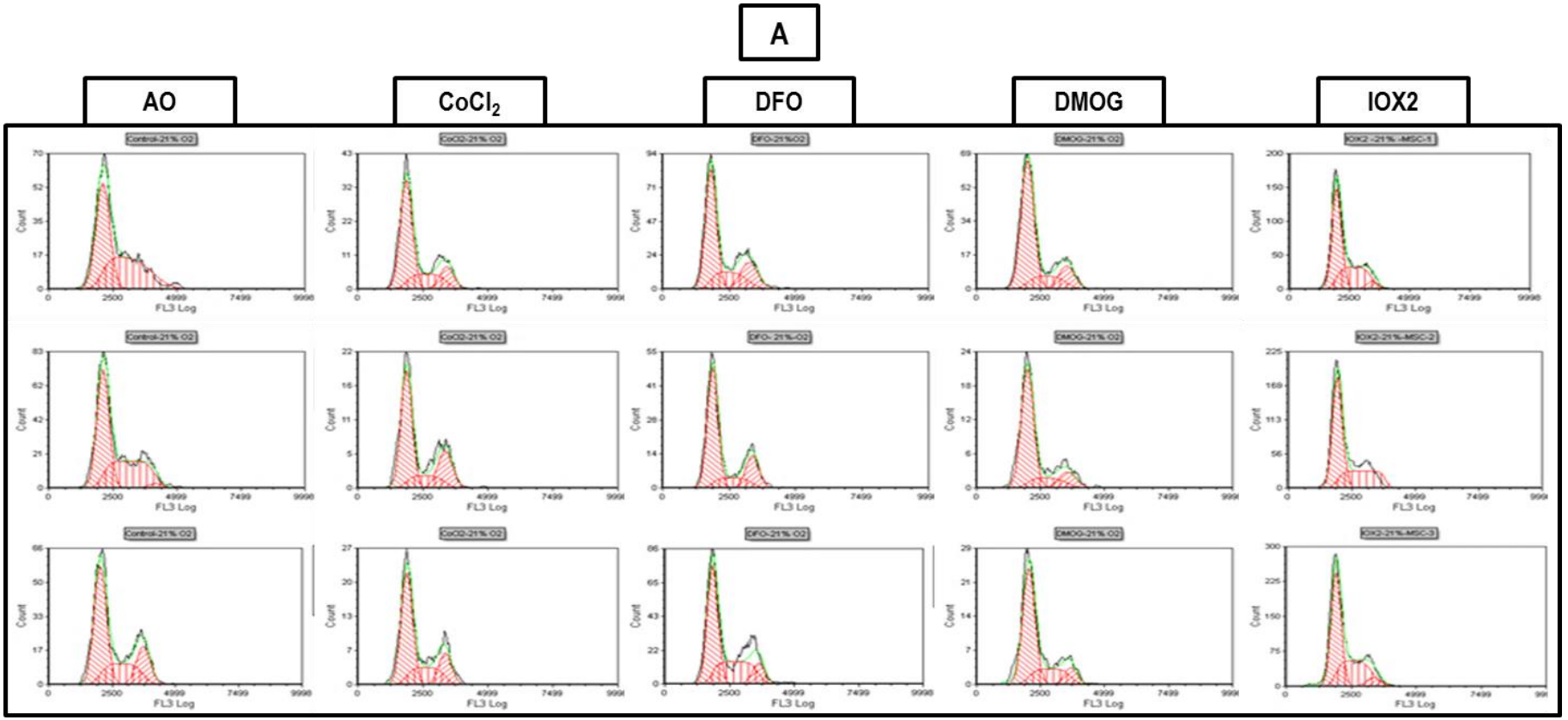
A
AO
CoCl2
DFO
DMOG
IOX2
Count
FL3 Log

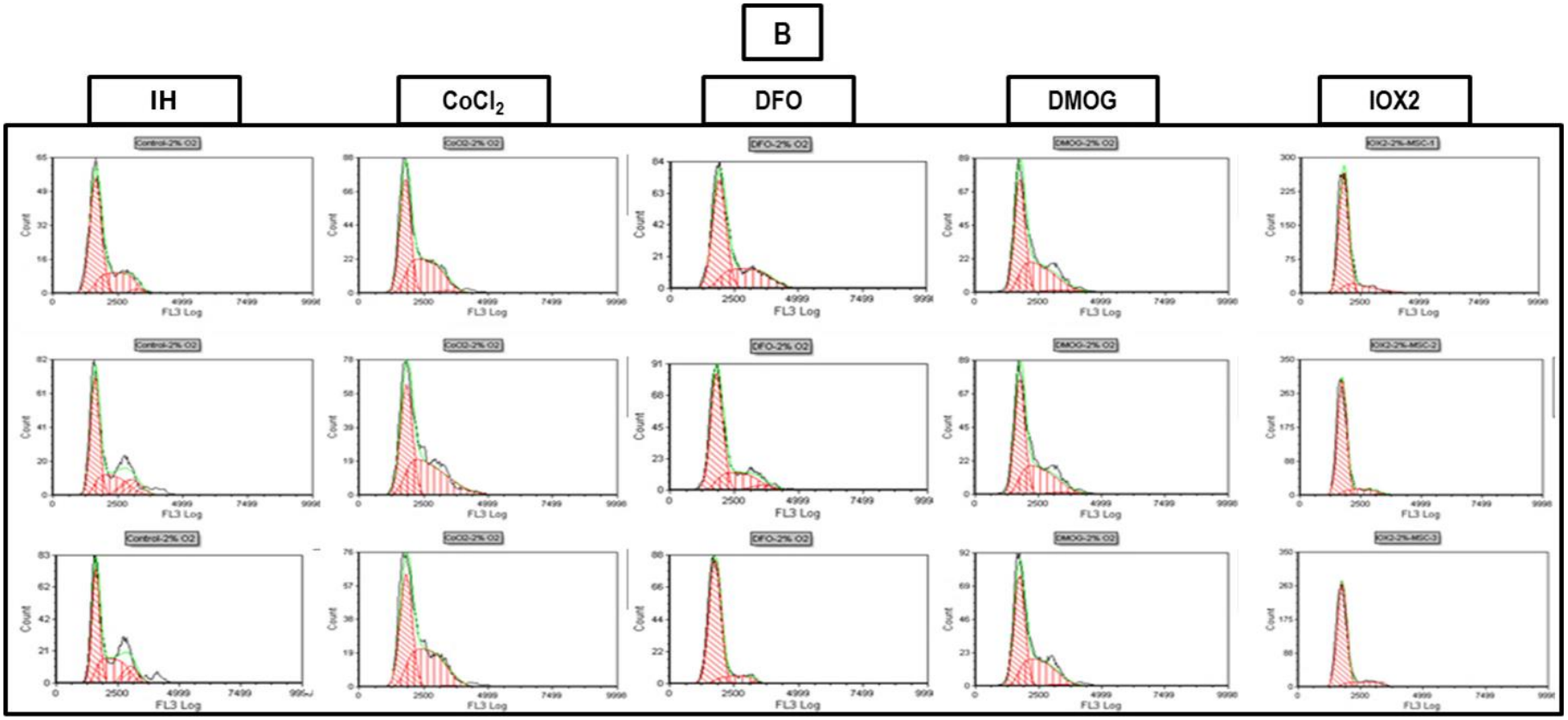
B
IH
CoCl2
DFO
DMOG
IOX2
Count
FL3 Log

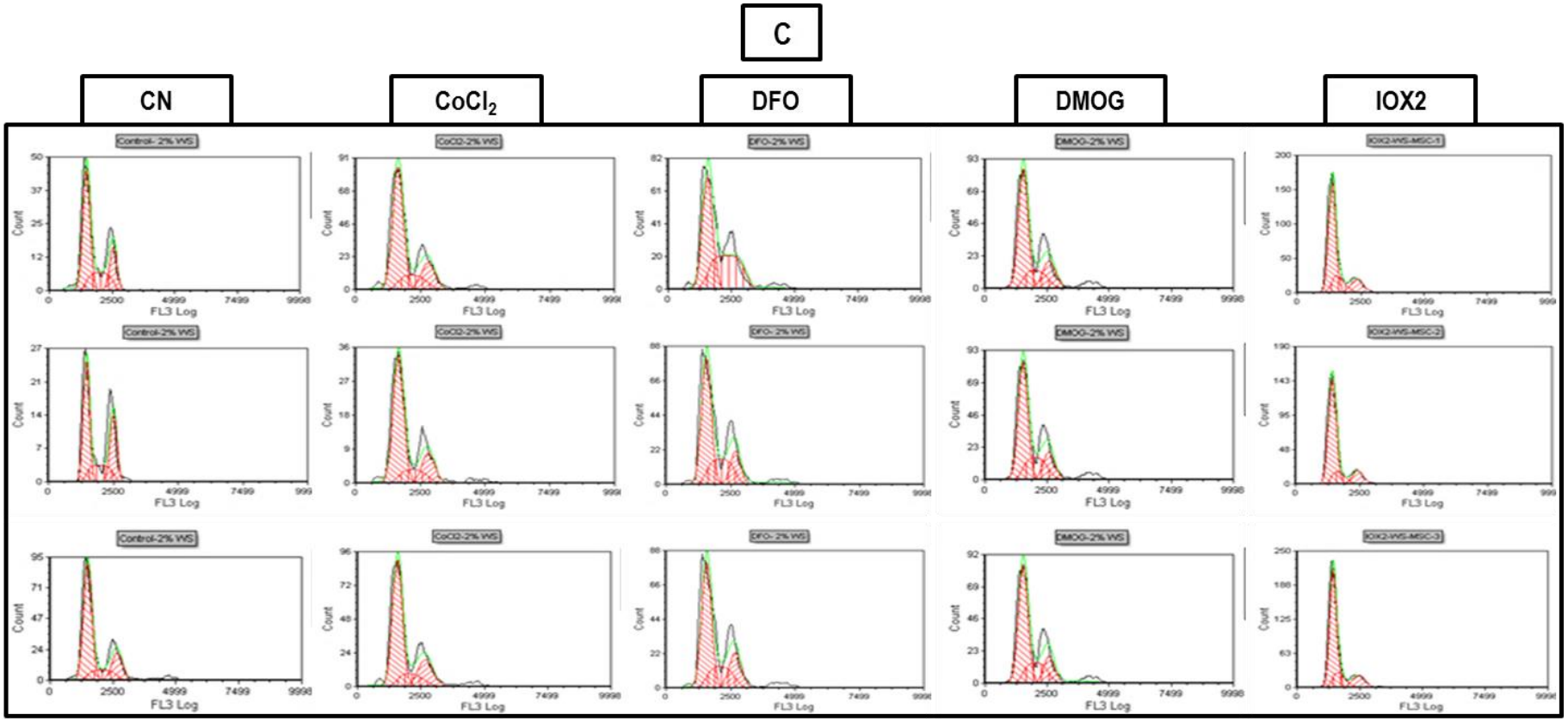

Figure 4.17. Cell cycle analysis

Representative DNA fluorescence histograms of PI stained cells and the peaks indicated G0/G1, S and G2-M (Figure 2.7). BM-hMSCs cultured in AO (A), IH (B) and CN (C) following exposure to either 50 µM $CoCl_2$, 50 µM DFO, 100 µM DMOG or 50 nM IOX2 for 14 days assessed by flow cytometry. Untreated BM-hMSCs are included for control purposes.

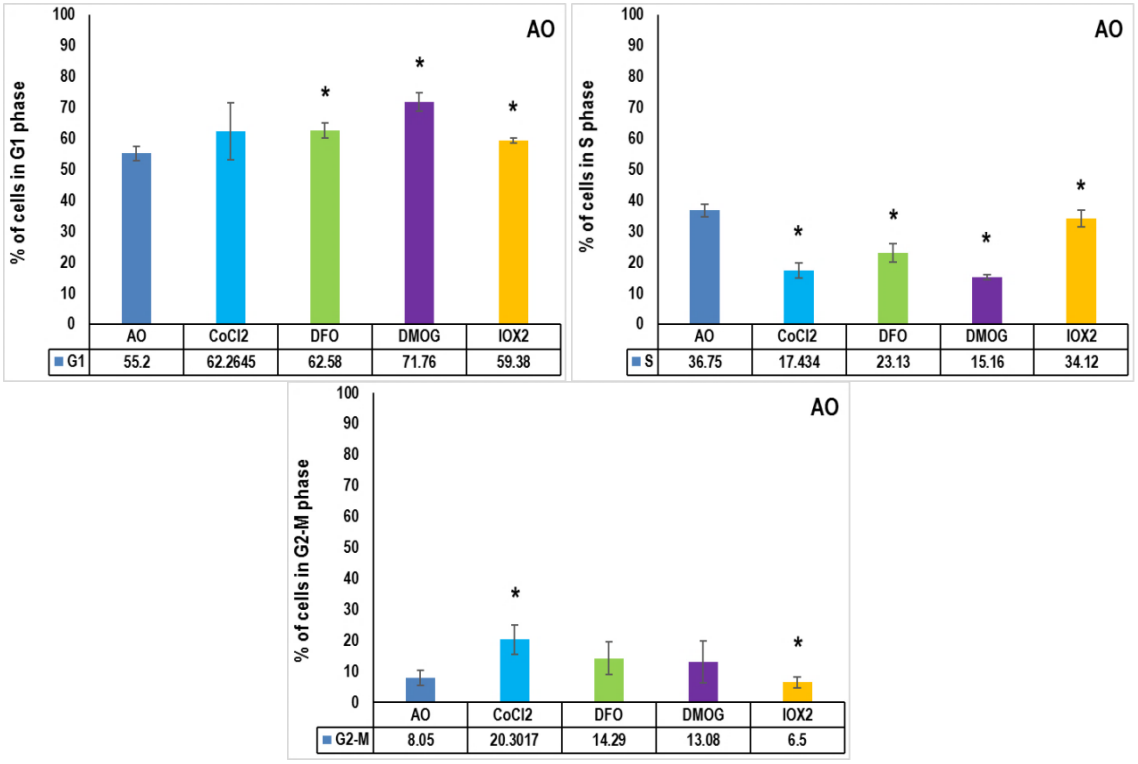
AO
% of cells in G1 phase
AO CoCl2 DFO DMOG IOX2
G1 55.2 62.2645 62.58 71.76 59.38
AO
% of cells in S phase
AO CoCl2 DFO DMOG IOX2
S 36.75 17.434 23.13 15.16 34.12
AO
% of cells in G2-M phase
AO CoCl2 DFO DMOG IOX2
G2-M 8.05 20.3017 14.29 13.08 6.5

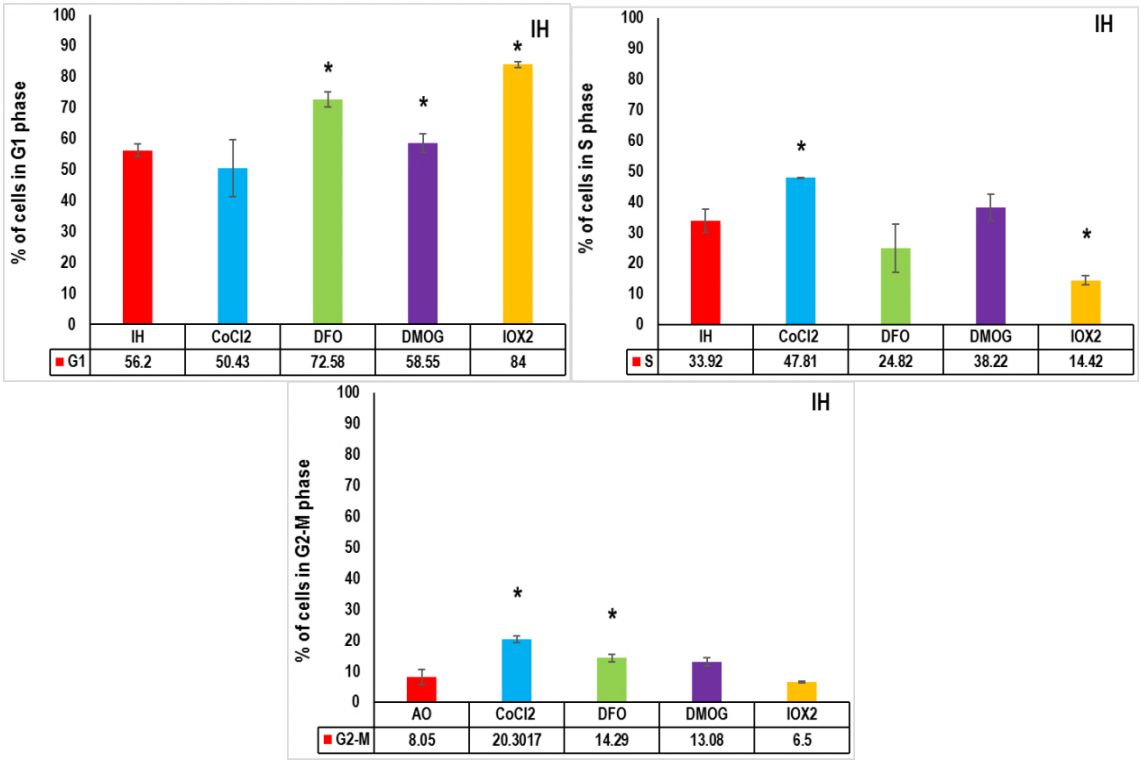
IH
% of cells in G1 phase
IH CoCl2 DFO DMOG IOX2
G1 56.2 50.43 72.58 58.55 84
IH
% of cells in S phase
IH CoCl2 DFO DMOG IOX2
S 33.92 47.81 24.82 38.22 14.42
IH
% of cells in G2-M phase
AO CoCl2 DFO DMOG IOX2
G2-M 8.05 20.3017 14.29 13.08 6.5

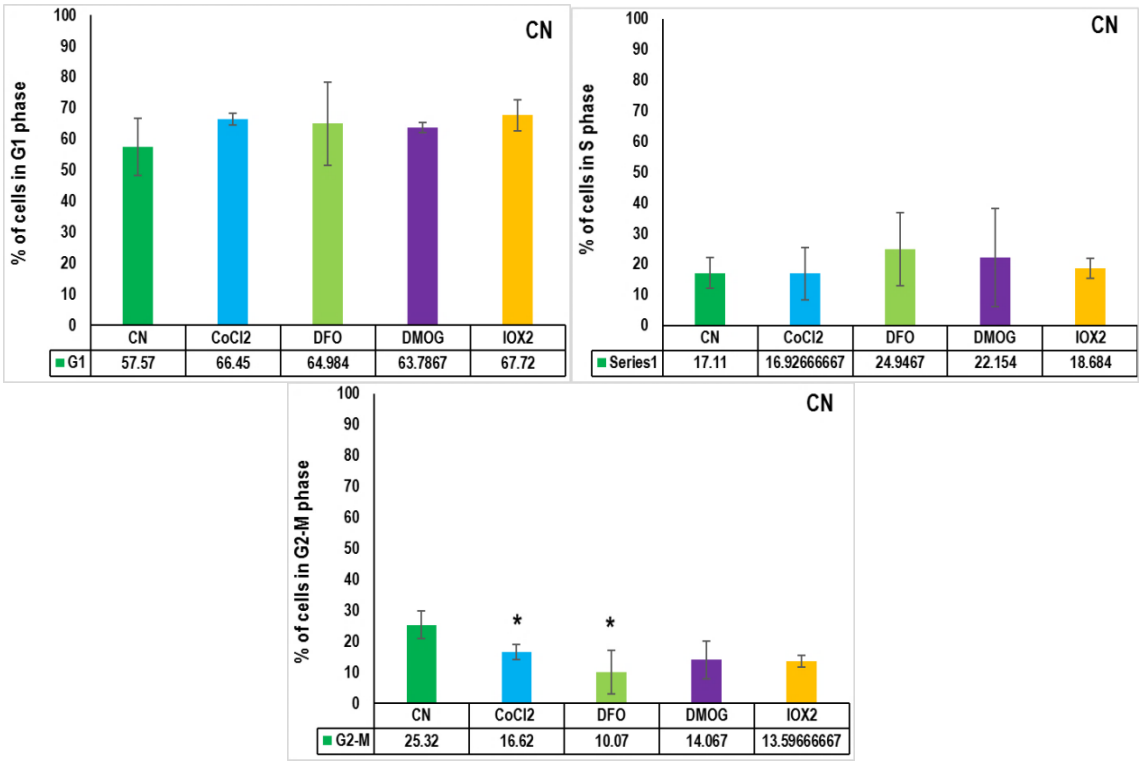

Figure 4.18. Effect of hypoxia mimetic agents on BM-MSCs cell cycle cultured in three oxygen culture conditions

*Following exposure to either 50 µM $CoCl_2$, 50 µM DFO, 100 µM DMOG or 50 nM IOX2 for 14 days, the percentage of cells in each cycle phase at AO, IH and CN culture was determined. Control BM-hMSCs in three alternate oxygen conditions. MSCs treated with HMAs in AO. MSCs treated with HMAs in IH. MSCs treated with HMAs in CN. X-axis indicates different treatment groups. Y-axis represents percentage of cells in each cycle phase. Data are presented as mean of the percentage of cells in each phase ± standard deviation (SD). n=1 triplicate, * indicates significant difference in comparison to control at each oxygen condition (p<0.05).*

Under CN significantly reduced percentage of cells in S-phase with elevation in G2-M phase and this may relate to the alteration in the expression of several G2 checkpoint regulators, in particular Cyclin B with reduction phosphorylation of a Cyclin dependent kinase (CDK) target in G2 phase cells after hypoxia, suggesting decreased CDK activity. HMAs under AO and IH trapped cells at G1 phase PHD1 depletion caused accumulation of cells in G2/M phase in AO and IH (Moser *et al.,* 2013).

4.3.7 Effect of hypoxia mimetic agents on ROS formation and nitroreductase activity of BM-hMSCs

Oxidative stress results in deregulated production and/or scavenging of reactive oxygen and nitrogen species (ROS and RNS, respectively) (Baird *et al.,* 2014). ROS are mainly generated from mitochondrial complexes I and III and NADPH oxidase (Schröder *et al.,* 2009). The accumulation of these radicals will seriously damage many biomolecules such as protein, lipids and DNA. Elevation in ROS/RNS levels can cause cellular dysfunction and cell death. Basal ROS levels are important in the maintenance of cellular proliferation, differentiation, and survival (D'Autréaux & Toledano, 2007; Sena & Chandel, 2012). There are conflicting reports about if BM-hMSCs have low baseline ROS levels or high levels or high level of cellular antioxidant (e.g. Glutathione) (Valle-Prieto & Conget 2010; Rodrigues *et al.,* 2012; Haque *et al.,* 2013; Mumaw *et al.,* 2015; Maraldi *et al.,* 2015). In BM-hMSCs, excess ROS impaired differentiation capacity, and proliferation (Ho *et al.,* 2013; Zhang *et al.,* 2015; Denu & Hematti, 2016) while increased antioxidants activities or levels, stimulated MSC proliferation (Zhou *et al.,* 2014). However, it is important to note that studies on the effect of HMAs on ROS/RNS formation are usually carried out in air oxygen.

FACS analysis of suspensions of BM-hMSCs established that AO cultured cells displayed a consistent baseline pattern of ROS formation, BM-hMSCs stocks used to initiate all experiments and were measured to establish at baseline (BL) pattern. ROS formation was increased in both IH and CN (29% and 80%) ($p<0.01$) vs. control AO (Figure 4.19.A). DFO, DMOG and IOX2 significantly elevated ROS formation after incubation at AO ($p<0.01$) while $CoCl_2$ had no effect (Figure 4.19.B). At IH culture $CoCl_2$ and DFO treatment reduced ROS formation when compared to control IH ($p<0.01$) while IOX2 elevated ROS formation and no effect was noticed after DMOG treatment. Incubation of BM-hMSCs in CN supplemented with HMAs (except $CoCl_2$) displayed a significant reduction in ROS

formation when compared to control CN (Figure 4.19). In summary HMAs do not possess similar pattern to that of MSCs incubated under AO, IH and CN.

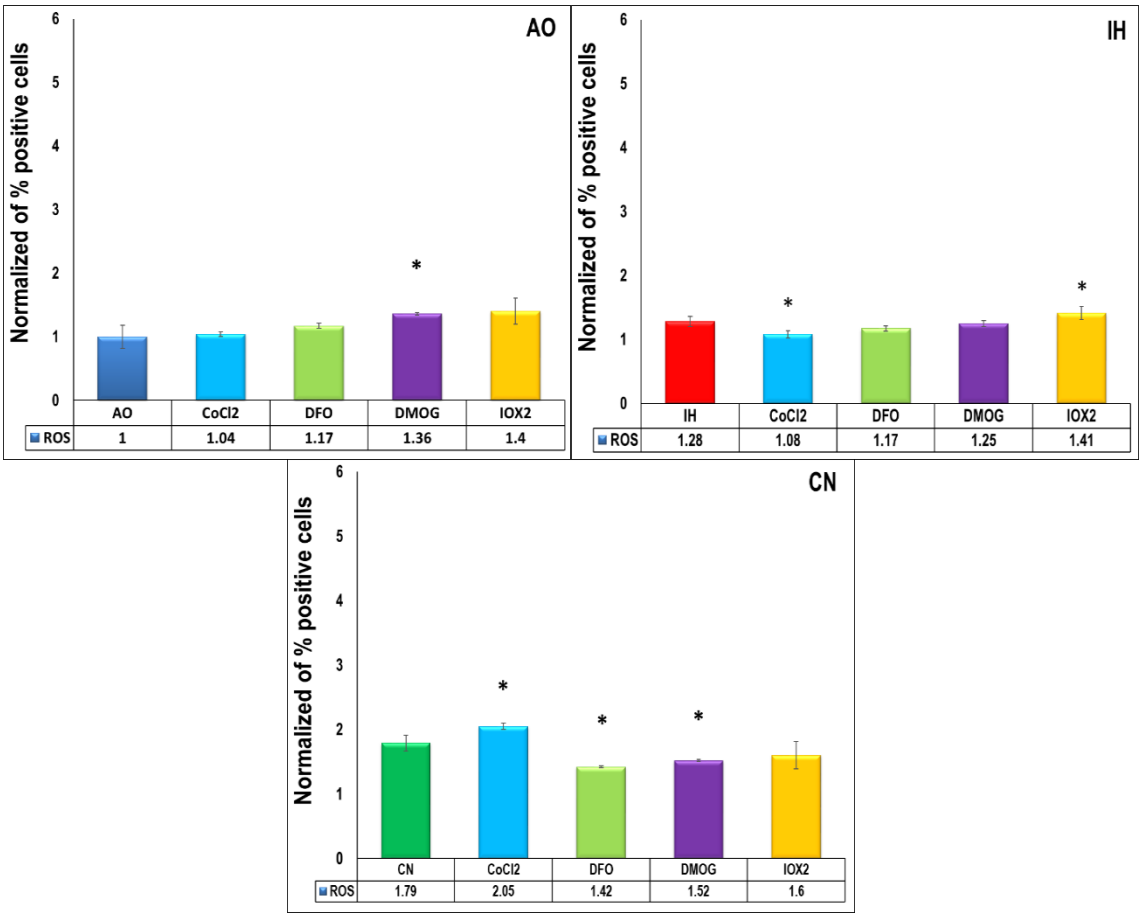

Figure 4.19. Effect of hypoxia mimetic agents on ROS formation in BM-hMSCs

*Histogram of normalized ROS-positive BM-hMSCs after labelling with ROS-ID® Hypoxia/Oxidative stress detection reagent. BM-hMSCs were exposed to either 50 µM $CoCl_2$, 50 µM DFO, 100 µM DMOG or and 50 nM IOX2) for 14 days and incubated under either AO, IH or CN. BM-hMSCs in three oxygen culture conditions (A). MSCs treated with HMAs at AO (B). MSCs treated with HMAs at IH (C). MSCs treated with HMAs at CN (D). Data are presented as mean of normalized value ± standard deviation (SD). n=1 triplicate, * indicates significant difference in comparison to control at each oxygen condition (p<0.05).*

Nitroreductases activity (NTR) was elevated after 14 day incubation in both IH (slight) and CN in comparison to control at AO (P<0.01). Under AO culture, $CoCl_2$, DFO and IOX2 supplementation significantly reduced NTR activity while DMOG treatment elevated NTR. Though significant the AO differences were slight. In IH culture slight, though significant,

reductions in NTR activity were noted for both $CoCl_2$ and DFO when compared to control IH while IOX2 displayed elevated NTR activity. Reductions in NTR were noted for all HMAs (except $CoCl_2$) in CN, significant for DFO, DMOG and IOX2 ($p<0.01$) (Figure 4.20). In summary, Iron chelating and Iron competitive inhibitor HMAs reduce NTR at all oxygen culture conditions. 2-oxoglutarate HMAs have variable effect with different oxygen culture conditions.

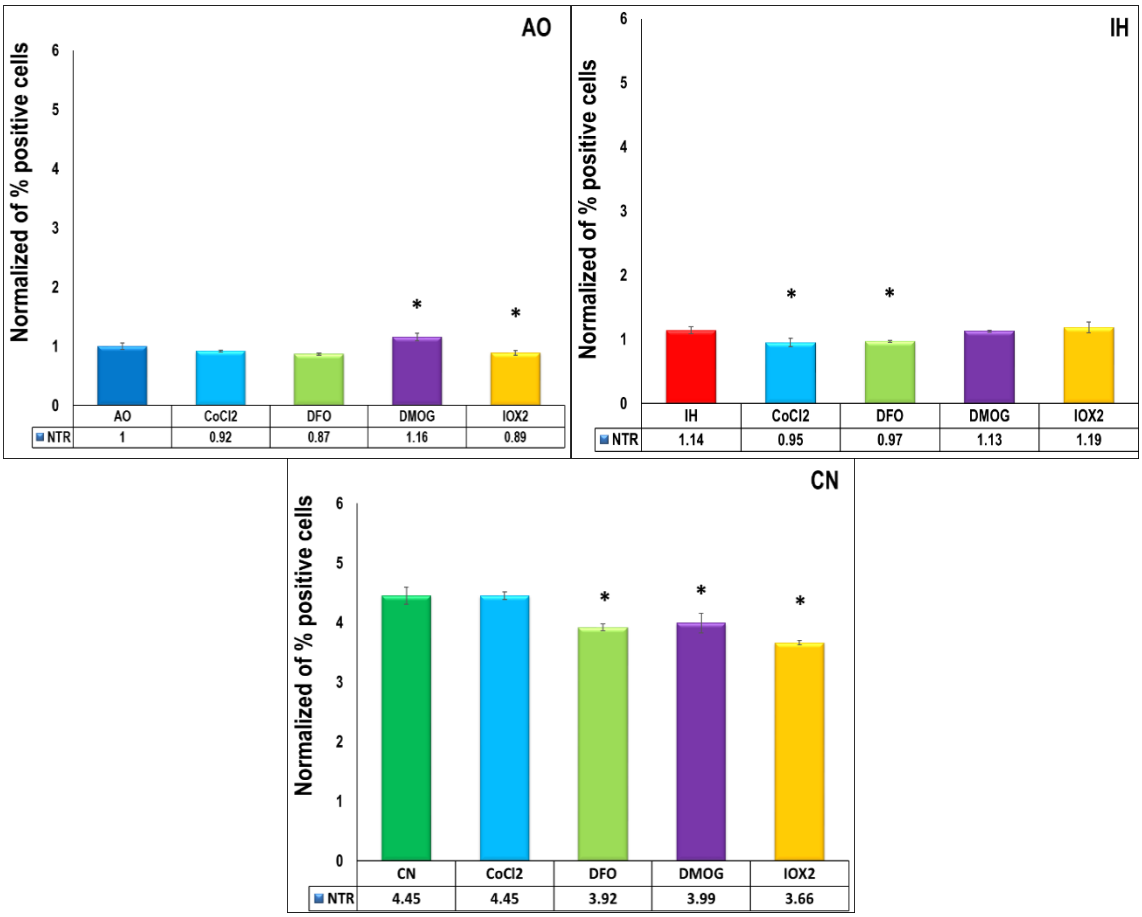

Figure 4.20. Effect of hypoxia mimetic agents on the nitroreductase activity of BM-hMSCs

*Histogram of normalized positive BM-hMSCs after labelling with ROS-ID® Hypoxia/Oxidative stress detection reagent as for BM-hMSCs at three oxygen culture condition (A). MSCs treated with HMAs at AO (B). MSCs treated with HMAs at IH (C). MSCs treated with HMAs at CN (D). Data are presented as mean of normalized value ± standard deviation (SD). n=1 triplicate, * indicates significant difference in comparison to control at each oxygen condition ($p<0.05$).*

Both IH and CN significantly elevate ROS formation may relate to elevation NADPH oxidase-mediated reactive oxygen species production ERK pathway under control of HIF-1 (Chung *et al.,* 2014).

4.4. Discussion

BM-hMSCs isolated from bone marrow have unique properties which suggest that BM-hMSCs are suitable for cell therapy application in a series of pathological conditions. In addition to being relatively easy to isolate and expand *in vitro*, they have strong immunomodulatory effect making them a promising tool for treating auto and alloimmune conditions including inflammatory disease, rheumatic diseases, lupus erythematosus and type I diabetes. BM-hMSCs used in regenerative medicine also have the ability of differentiation and restoration of tissue homeostasis. They also possess a high migratory capacity to sites of injury with very low immunogenicity (Sohni & Verfaillie, 2013; Becker & Riet, 2016). The major problem facing the clinical trials is the inadequate number of cells for clinical use without prior in vitro expansion (Shi *et al.,* 2011). Most BM-hMSCs expansion procedures are conducted under ambient oxygen concentration where cells are exposed to 21 % O_2, which is 4-10 fold higher than their natural niche (Mohyeldin *et al.,* 2010).

The last 10 years have seen a significant increase in the number of studies into how culture conditions affect cell behaviour and function, among these factors is the oxygen tensions utilised for culture. The influence of oxygen tension in morphology, phenotype, proliferative capacity, and functionality of BM-hMSCs has been increasingly studied with controversial results. Such controversies could be related to the different culture conditions such as use of HMAs or use of hypoxic chambers (Boyette *et al.,* 2014; Liu *et al.,* 2015; Zhang *et al.,* 2015).

In this chapter, we explored the effect of hypoxia mimetic agents on cell viability, apoptosis, and the cell cycle. BM-hMSCs (viability, apoptosis, and cell cycle, ROS

formation and NTR activity) were measured and compared these changes to the changes in HIFs expression. In this study, we tested the response of BM-hMSCs to different hypoxia mimetic agents under three oxygen culture conditions to (1) establish BM-hMSCs behaviour under different oxygen culture conditions and (2) determine if hypoxia mimetic agents mimic any of the oxygen culture behaviour in BM-hMSCs. After screening we selected the doses 50 µM, 50 µM, 100 µM and 50 nM of $CoCl_2$, DFO, DMOG and IOX2, respectively that caused minimal change on cell count and MTT activity.

In this work, we found some variations between cell count and MTT activity of the cells that treated hypoxia mimetic agents under both CN and IH culture condition. To define if chosen concentrations still act as hypoxia mimetic agents (induce HIFs) BM-hMSCs cells were treated with chosen concentrations and incubated in the three oxygen conditions. This is the first report of the use of low concentrations of HMAs to induce HIF expression. Previous studies have relied on higher concentrations for shorter times (Guo *et al.,* 2006; Genetos *et al.,* 2010; Zeng *et al.,* 2011). The results show that HIF-1α expression is significantly increased in IH versus both AO and CN where the later may be related to the ability of the cell to reset HIF mechanism to improve cell adaptation (Prabhakar & Semenza, 2007; Yuan *et al.,* 2014). HIF-2α expression was up regulated under IH culture condition, this result was in agreement with Rane *et al.,* (2009) who correlate the increase in HIF-2α expression to increase Sirtuin (SIRT1) activity. SIRT1 have the ability to inhibits transcription of EGLN1 gene (gene responsible of encoding of prolyl hydroxylase PHD2) leading to significant reduction of HIF-1α and HIF-2α degradation (Rane et al. 2009). Under AO culture, HIF-2α expression elevated by HMAs, this may be related to increase Sirtuin (SIRT1) activity and this result was in agreement with Wang *et al.,* (2016). Under IH and CN culture condition, HMAs either slightly reduced or have no effect on HIF-2α expression.

CFU-F recovery from bone marrow aspirate significantly increased in CN and IH conditions and AO culture supplemented with HMA did not achieve CN or IH CFU-F

levels. In addition to above, HMAs inhibited CFU-F isolation when used in conjunction with either IH or CN. There are contradicting reports about the effect of hypoxia mimetic agent on BM-hMSCs differentiation (Zeng *et al.,* 2011; Boyette *et al.,* 2014; Esfahani *et al.,* 2015). These results showed that the hypoxia mimetic agents have no additive advantageous effect over other cultured cells. The study of the effect of HMAs on cell death revealed that $CoCl_2$, DFO and DMOG significantly increased early apoptosis (Das *et al.,* 2010; Zeng *et al.,* 2011) in AO culture and late apoptosis only in CN culture condition which is perhaps related to the reported alteration in caspase 3/7 and inhibition of anti-apoptotic protein Bax / Bak or stabilisation of p53 by HIF-1α independent pathway (Ejtehadifar *et al.,* 2015). In contrast Ge *et al.,* (2016) stated that DMOG significantly reduce early apoptosis without clarifying the effects on late apoptosis and necrosis. This is the first report that suggests that IOX2 significantly reduces early apoptosis increases late apoptosis in BM-hMSCs over all oxygen culture conditions. The cell cycle analysis revealed that BM-hMSCs treated with HMAs in AO and CN became over-represented in G0/G1. A marked contrast was noted in G2-M between AO, IH and CN were the former was increase the later reduced.

ROS formation showed significant increases after CN culture and after DMOG treatment in both AO and IH conditions while in CN culture DFO, DMOG and IOX2 reduced ROS formation. Nitroreductases activity significantly increased under CN only with no significant effect observed under IH culture condition. DFO at AO and DFO DMOG and IOX2 at CN culture reduce NTR activity and this may have related to the effect of these agent on NRF2 (Loboda *et al.,* 2009; Chung *et al.,* 2014). From all results above, we can easily realise that mitochondrial function was affected by hypoxia and HMAs and in the further work we will focus on mitochondrial biogenesis, shape and function.

4.5. Conclusion

This study confirms the ability of individual hypoxia mimetic agents to induce HIF-1α expression which related to significant changes in apoptosis and cycle arrest at G0/G1 phase that associated with changes ROS formation and nitroreductases activity in BM-hMSCs in all three oxygen conditions that does not recapture any pattern that was noticed at IH or CN culture condition.

Chapter 5 : Effects of hypoxia mimetic agents on mitochondrial dynamics of PC12 and hMSCs

5.1. Introduction

Mitochondria are central to the life and death of the cell and as the major source of ATP in eukaryotic cells containing the machinery for both the Krebs cycle and fatty acid oxidation (Stein and Imai, 2012). In addition, mitochondria represent the heart of intermediary metabolism impacting on processes other than the direct supply of ATP, for instance Krebs cycle intermediates can have regulatory roles in cytosolic processes such as hypoxia sensing and altering epigenetic modifications to the nuclear genome (Masson & Ratcliffe, 2014). Moreover, mitochondria have biosynthetic roles such as in the assembly of Fe-S centres and haem biosynthesis. Mitochondria represent the largest consumers of oxygen and are the site of the electron transport chain (ETC) which is the main source of ROS produced in tissues (Zorov *et al.,* 2014). Mitochondrial respiration accounts for approximately 90% of cellular oxygen uptake, and as much as 3% of the oxygen consumed is converted to ROS (Marchi *et al.,* 2011). This ROS production contributes cell signalling from the organelle to the rest of the cell and to a wide range of pathologies (Dröge, 2002; Balaban *et al.,* 2005). There are a limited number of studies investigating the effect of different oxygen culture regimes and HMAs on mitochondrial functions such as burden, action potential, mitochondrial genome copy number and changes to mitochondrial morphology. The primary aim of this study was to assess the *in vitro* effect of HMAs on mitochondrial dynamics under AO, IH and CN conditions.

5.2. Methods

5.2.1. Materials

Analytical grade reagents and deionised water (Sigma, UK) were used. All chemicals employed are listed in Chapter 2, Section 2.1.

5.2.2. Cell models

The BM-hMSCs were recovered after culture of MNC from commercially obtained bone marrow aspirate as outlined in Chapter 2. Cells were maintained in an incubator at an atmosphere of 37°C and 5% CO_2 under either AO, IH and CN culture conditions. PC12 were cultured as described in Chapter 2.

5.3. Results

5.3.1. Effect of hypoxia mimetic agents on PC12 on mitochondrial dynamic

Mitochondrial are the most abundant oxygen modulating organelle inside the cell representing the largest consumer of oxygen. Any changes in the oxygen level reflect directly on different aspects of mitochondrial presence, shape and activity. HIF plays many vital roles by induction of a glycolytic phenotyping in energy production through modifying transcription to upregulate genes that encode glucose transporting proteins and glycolytic enzymes (Semenza, 2010). These can modify lactate metabolism, divert pyruvate away from mitochondria and inhibit hypoxic mitochondrial respiration thereby reducing the amount of ROS generated by inefficient respiration (Kim *et al.,* 2006; Papandreou *et al.,* 2006). It is also clear that optimising respiration efficiency via elevation of cytochrome c oxidase (COX) subunit IV isoform 2 (COX4-2) and the mitochondrial protease LONP1, which degrades the less efficient COX4-1 (Fukuda *et al.,* 2007) and HIF-1α-mediated inhibition of MYC and PGC-1 results in reduced mitochondrial mass and biogenesis (Shoag & Arany, 2010). Previous studies have described the effect of oxygen level modulation and HMAs on both PC12 (Crispo *et al.,* 2011; Lan *et al.,* 2011; Guo *et al.,* 2012; Kolamunne *et al.,* 2013; Zheng *et al.,* 2015) and MSCs (Sena & Chandel 2012; Schönenberger & Kovacs, 2015; Wanet *et al.,* 2015; Lin *et al.,* 2017).

These studies results rise the need to establish baseline effects in the two cell models, evaluate the impact of the three oxygen culture conditions, and then study the effect of HMAs on mitochondria.

5.3.1.1. PC12 mitochondrial burden

5.3.1.1.1. Determination of PC12 mitochondrial burden after incubation in different oxygen conditions.

Mitochondrial burden can be applied as a relative measure of mitochondrial mass. PC12 were cultured and stained as stated in Chapter 2 (2.2.1.11). Before collecting measurements, the MitoTracker® Green optimal concentration was established and the flow cytometry machine optimised by compensation to FL channels to avoid channel bleeding.

AO cultured cells displayed a consistent baseline fluorescence. PC12 cells used to initiate all experiments were measured to establish control levels and this is represented as the x-axis intersection with the y-axis and all values normalized to this value. IH significantly elevated mitochondrial burden over 96 hrs in contrast to CN where there was no change in burden except significant reduction significant after 72 hrs in comparison to control AO.

5.3.1.1.2. Determination of PC12 mitochondrial burden after $CoCl_2$ treatment in different oxygen conditions.

AO cultured PC12 were exposed to 50 µM $CoCl_2$ which increased mitochondrial burden after 24 hrs (13%) in comparison to control AO ($p<0.05$). In IH culture there were significant reductions in mitochondria burden after over 24 hrs, 48 hrs, 72 hrs and 96 hrs (60%, 55%, 70% and 55% respectively) in comparison to control IH. Mitochondrial burden reduced after after 72 hrs of $CoCl_2$ supplementation (38%) in comparison to control CN (Figure 5.1).

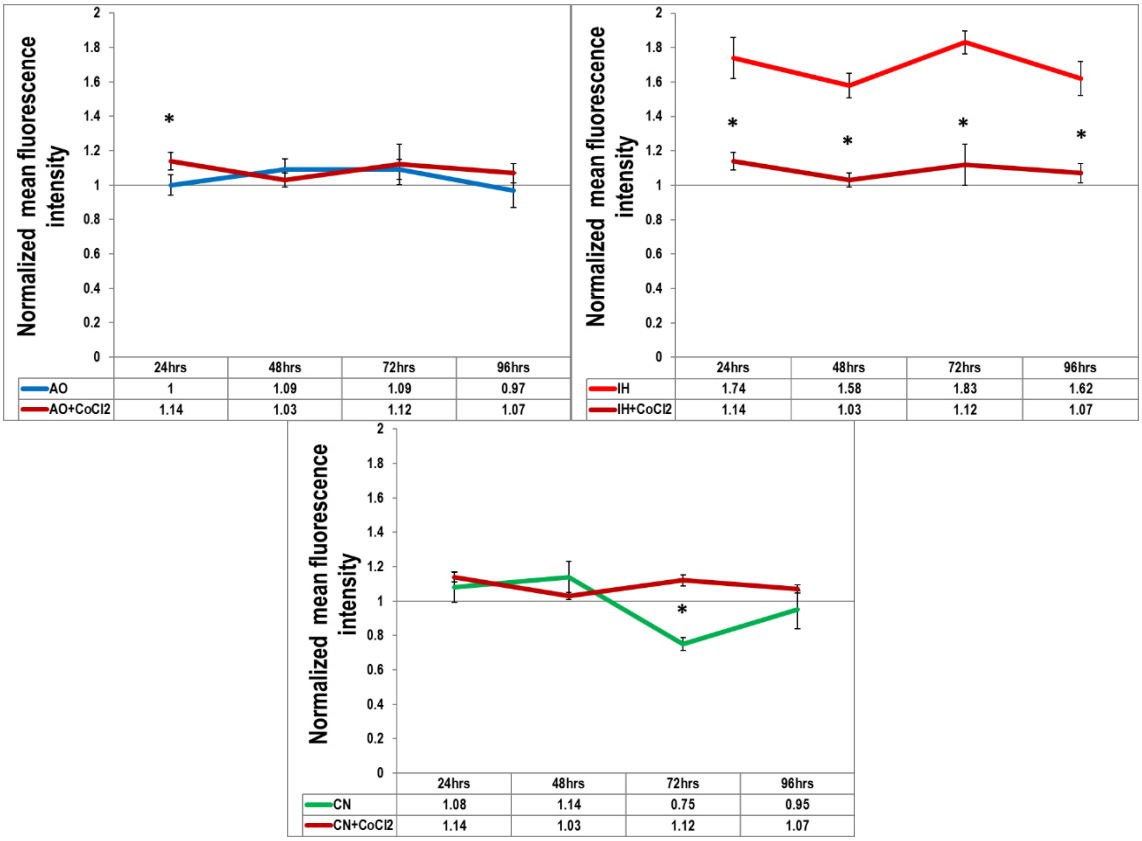

Figure 5.1. Mitochondrial burden of PC12 cultured with $CoCl_2$ in three different oxygen culture conditions

*Incubation of PC12 with $CoCl_2$ for 24 hrs, 48 hrs, 72 hrs and 96 hrs in either air oxygen (AO), intermittent hypoxia (IH), or continuous normoxia (CN). MitoTracker® Green fluorescence was measured as indicated earlier. X-axis represent normalized mean fluorescence intensity. Y-axis represent different time points. Data are presented as normalized mean fluorescence intensity ± standard deviation (SD). n=1 triplicate, * indicates significant difference in comparison to control at each time point under each oxygen culture condition ($p<0.01$).*

5.3.1.1.3. Determination of PC12 mitochondrial burden after DFO treatment in different oxygen conditions.

Under AO PC12 were exposed to 50 µM DFO which significantly elevated mitochondrial burden after both 24 (38%) in comparison to control with significant reduction noted after 72 hrs (22%) ($p<0.05$). In IH there were significant elevation after 48 hrs (18%) with reductions after 72 and 96 hrs (77% and 72%) in comparison to control IH. Incubation in CN with DFO also resulted in significant elevation after 24 hrs and 96 hrs (23% and 23% respectively) with significant reduction after 48 hrs (21%) (Figure 5.2).

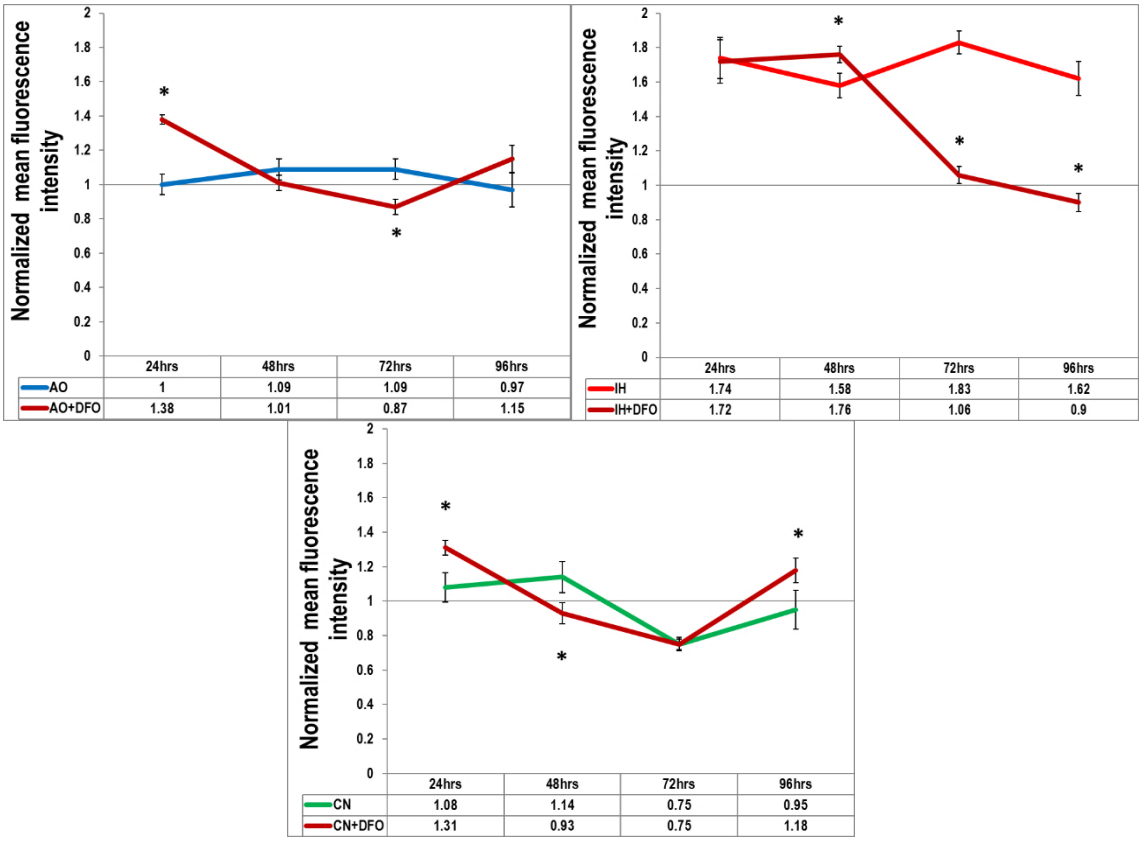

5.2. Mitochondrial burden of PC12 cultured with DFO in three different oxygen culture conditions

PC12 incubated with DFO for 24 hrs, 48 hrs, 72 hrs and 96 hrs in either air oxygen (AO), intermittent hypoxia (IH), or continuous normoxia (CN). MitoTracker® Green fluorescence was measured as before. X-axis represent normalized mean fluorescence intensity. Y- axis represent different time points. Data are presented as normalized mean fluorescence intensity ± standard

*deviation (SD). n=1 triplicate, * indicates significant difference in comparison to control at each time point under each oxygen culture condition (p<0.01).*

5.3.1.1.4. Determination of PC12 mitochondrial burden after DMOG treatment in different oxygen conditions.

Under AO culture condition cells exposed to 100 µM DMOG significantly elevated their mitochondrial burden after 24 hrs and 96 hrs (40% and 26%) compared to control AO with significant dropping noted (26%) after 72 hrs, while under IH culture reductions were noted after 24 hrs, 72 hrs and 96 hrs (66%, 53% and 64%, respectively) in comparison to control IH (p<0.01). Significant elevation in mitochondrial burden was also noted after 24 incubations at CN with DMOG (33% and 16%) (Figure 5.3).

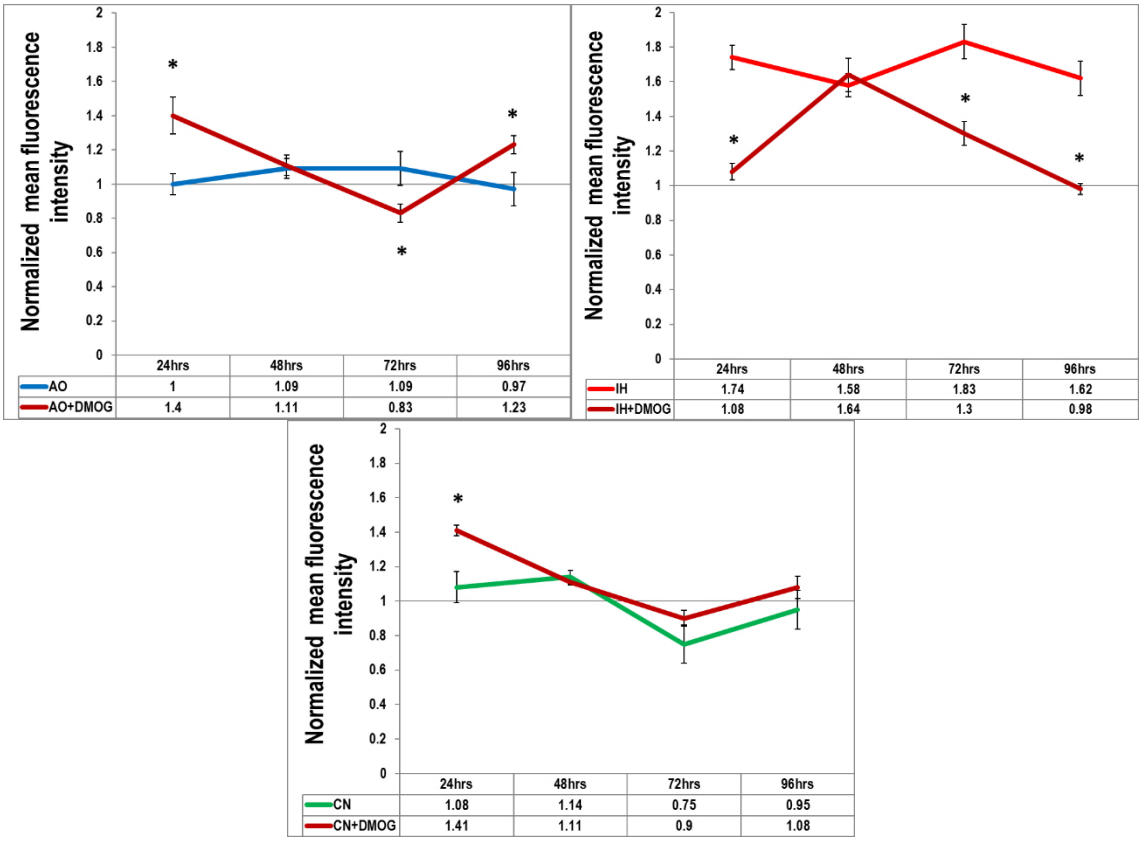

Figure 5.3. Mitochondrial burden of PC12 cultured with DMOG in three different oxygen culture conditions

PC12 incubated with DMOG for 24 hrs, 48 hrs, 72 hrs and 96 hrs in either air oxygen (AO), intermittent hypoxia (IH), or continuous normoxia (CN). MitoTracker® Green fluorescence was measured as before. X-axis represent normalized mean fluorescence intensity. Y- axis represent different time points. Data are presented as normalized mean fluorescence intensity ± standard

*deviation (SD). n=1 triplicate, * indicates significant difference in comparison to control at each time point under each oxygen culture condition (p<0.01).*

5.3.1.1.5. Determination of PC12 mitochondrial burden after IOX2 treatment in different oxygen conditions.

AO cultured PC12 cells exposed to 50 nM IOX2 displayed a significantly elevated mitochondrial burden after both 24 hrs and 96 hrs (40% and 68%) in comparison to control AO (p<0.01) while after 72 hrs significant reduction (26%) was noticed. IH culture resulted significant reductions 24 hrs, 72 hrs and 96 hrs (40%, 50% and 64%) in comparison to control IH (p<0.01). Significant elevation was also noted after 72 hrs and 96 hrs incubation in CN with IOX2 where elevation was noted after 72 hrs and 96 hrs (43% and 24%) (Figure 5.4).

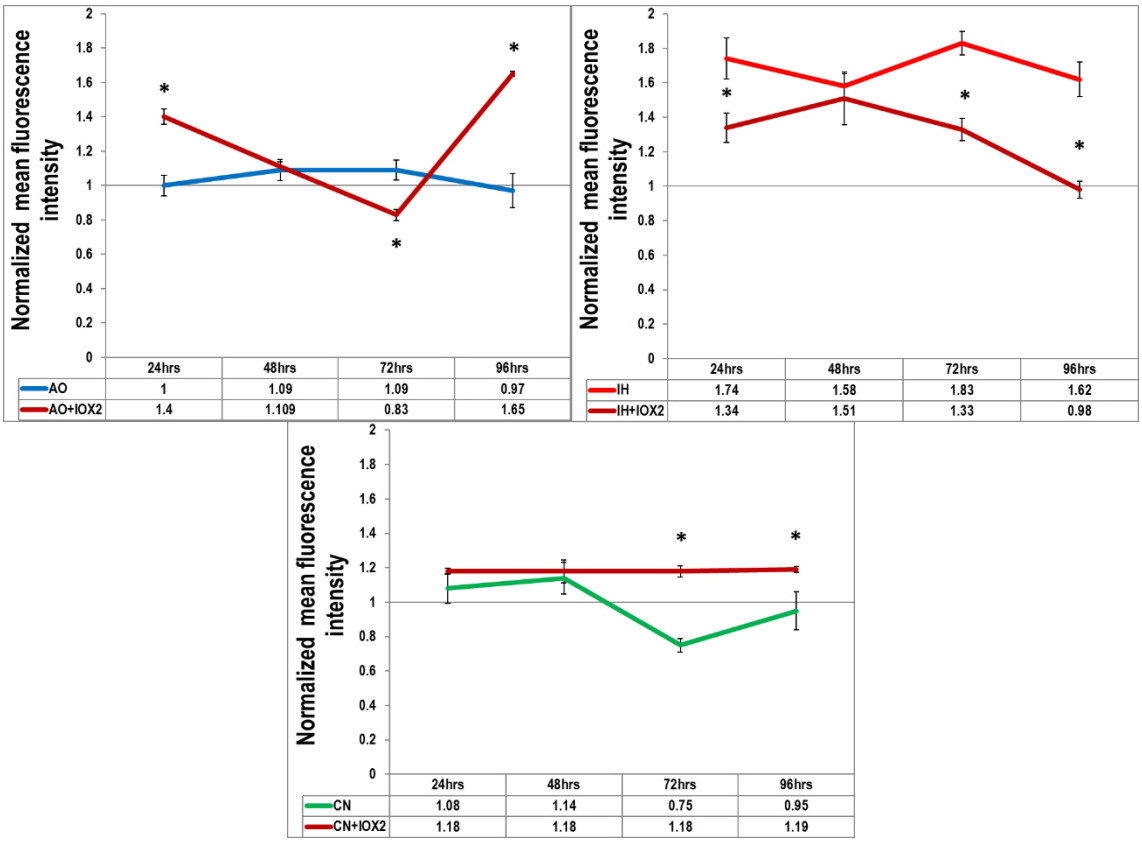

Figure 5.4. Mitochondrial burden of PC12 cultured with IOX2 at three different oxygen culture conditions

PC12 incubated with IOX2 for 24 hrs, 48 hrs, 72 hrs and 96 hrs in either air oxygen (AO), intermittent hypoxia (IH), or continuous normoxia (CN). MitoTracker® Green fluorescence was

*measured as before. X-axis represent normalized mean fluorescence intensity. Y- axis represent different time points. Data are presented as normalized mean fluorescence intensity ± standard deviation (SD). n=1 triplicate, * indicates significant difference in comparison to control at each time point under each oxygen culture condition (p<0.01).*

To sum up, IH increase mitochondrial burden in comparison to control AO over 96 hrs. while CN cause significant reduction after 72 hrs in comparison to control AO. HMAs undre AO significantly elevated burden after 24 hrs while under IH, HMAs reduced burden after 72 hrs and 96 hrs. Under CN culture condition, HMAs (except $CoCl_2$) significantly elevated burden after 24 hrs in comparison to control CN. HMAs fail to replicate cells behaviour under all culture conditions. These changes may relate to the activation of peroxisome proliferator activated receptor γ coactivator-1α (PGC-1α) which is the main regulator of mitochondrial biogenesis. It initiates the transcription of nuclear encoded mitochondrial proteins such as nuclear respiratory factors 1 and 2 (NRF1 and NRF2), oestrogen related receptor α (ERRα), forkhead box class-o (Foxo-1), and peroxisome proliferator activated receptors (PPARs) (Puigserver & Spiegelman, 2003) where expression of these proteins leads to the eventual increase in mitochondrial mass (Dillon et al., 2012).

5.3.1.2. PC12 mitochondrial action potential

5.3.1.2.1. Determination of PC12 mitochondrial action potential after incubation in different oxygen conditions.

Mitochondrial action potential (mt-AP) plays a vital role in cellular activity. PC12 were cultured and stained as stated in Chapter 2 (2.2.1.11). MitoTracker® Red optimal concentration was first defined and the flow cytometry machine optimised to avoid bleeding across the FL channels. AO cultured cells displayed a consistent baseline fluorescence. PC12 cells used to initiate all experiments were first measured to establish

control levels and are represented as the x-axis intersection with the y-axis and all values normalized to this value. Both IH and CN culture significantly elevated mt-AP over 96 hrs ($p<0.01$) in comparison to AO.

5.3.1.2.2. Determination of PC12 mitochondrial action potential after treatment with $CoCl_2$ at different oxygen conditions.

AO cultured PC12 cells exposed to 50 µM $CoCl_2$ displayed no significantly effect on mt-AP, while IH cultured PC12 displayed significant reductions after 24 hrs, 72 hrs and 96 hrs (56%, 90% and 30% respectively) in comparison to IH control ($p<0.01$). Significant reductions in mt-AP were also noted after incubation in CN with $CoCl_2$ after 48 hrs, 72 hrs and 96 hrs (49%, 75% and 74% respectively) (Figure 5.5).

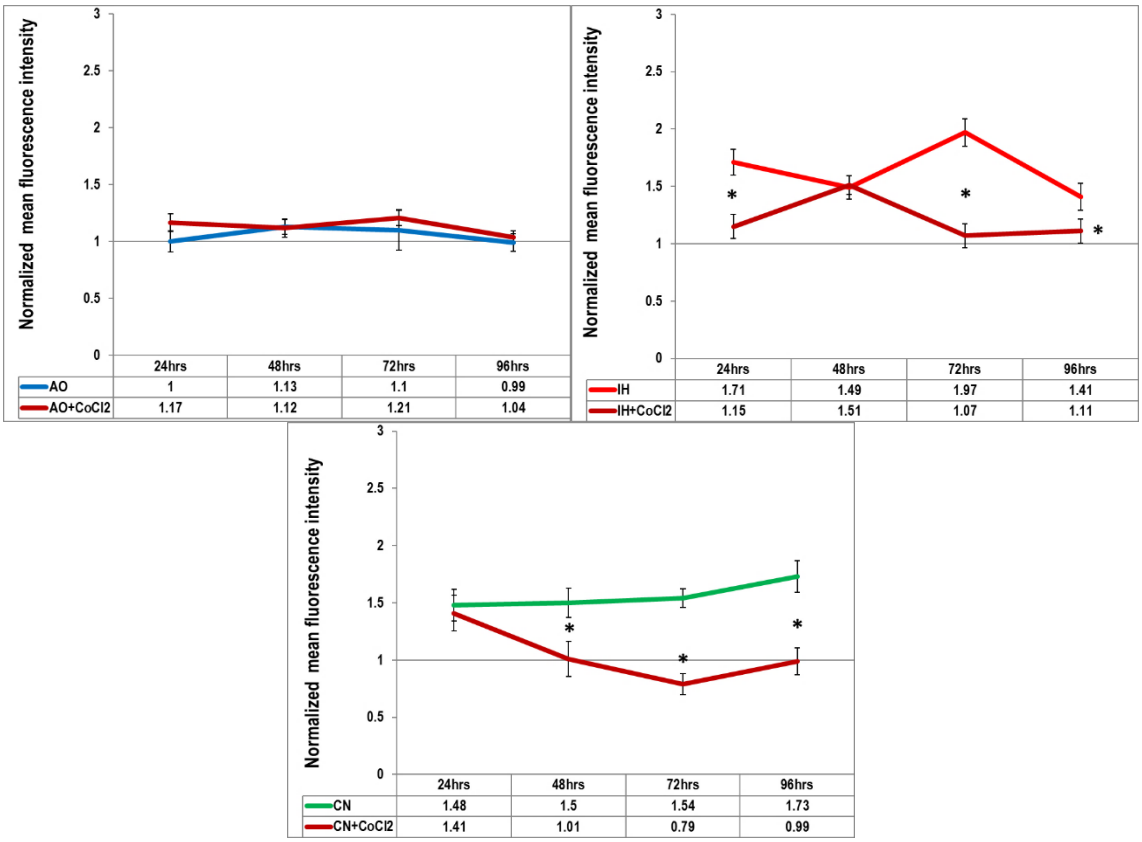

Figure 5.5. Mitochondrial action potential of PC12 cultured with $CoCl_2$ at three different oxygen culture conditions

*PC12 incubated with $CoCl_2$ for 24 hrs, 48 hrs, 72 hrs and 96 hrs in either air oxygen (AO), intermittent hypoxia (IH), or continuous normoxia (CN). MitoTracker® Red fluorescence was measured as described earlier. X-axis represents normalised fluorescence intensity values. Y-axis represent time points (hrs). Data are presented as normalized mean fluorescence intensity ± standard deviation (SD). n=1 triplicate, * indicates significant difference in comparison to control at each time point under each oxygen culture condition (p<0.01).*

5.3.1.2.3. Determination of PC12 mitochondrial action potential after treatment with DFO at different oxygen conditions.

AO cultured PC12 cells exposed to 50 µM DFO significantly increased mt-AP after 24 hrs only (36%) in comparison to control AO ($p<0.01$), while under IH culture there were significant reductions after 24 hrs, 72 hrs and 96 hrs (50%, 82% and 52%) in comparison to control IH ($p<0.01$) with an increase after 48 hrs (107%) ($p<0.001$). Reductions were noted after incubation at CN where DFO reduced mt-AP after 48 hrs,72 hrs and 96 hrs (50 %, 71% and 55% respectively) (Figure 5.6).

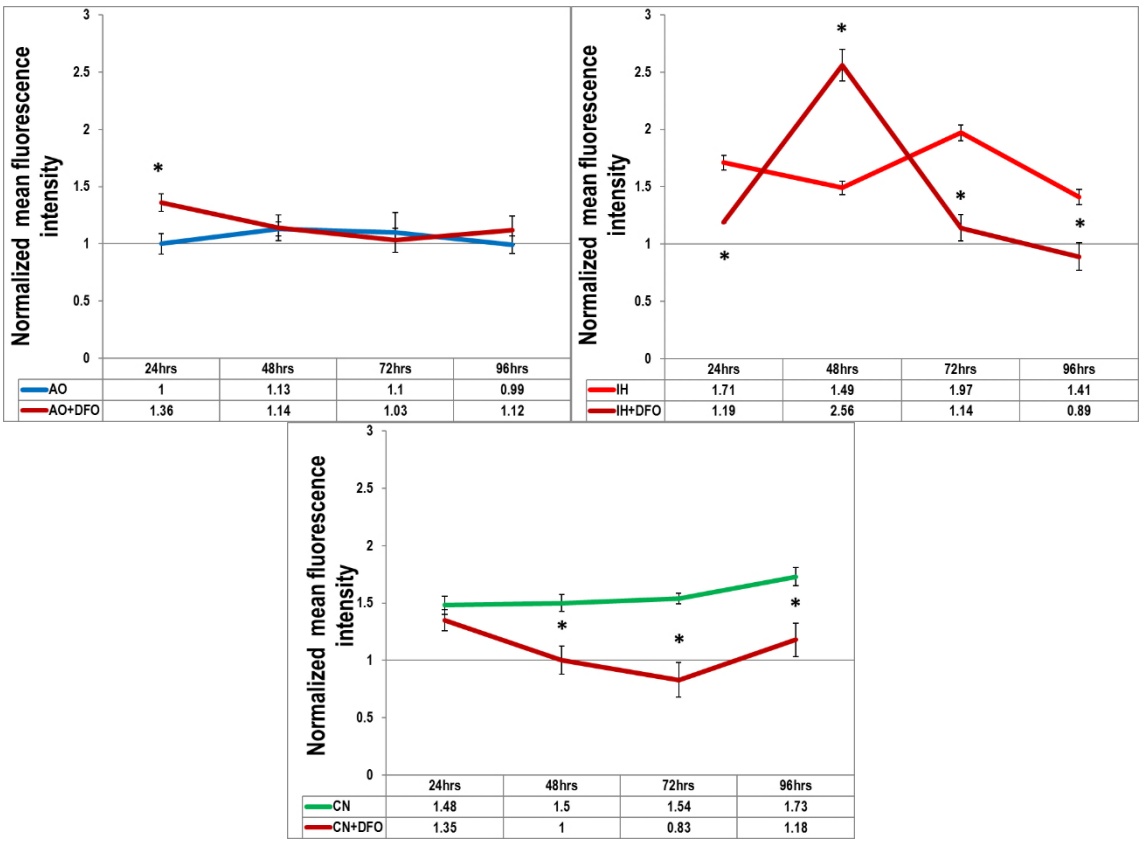

Figure 5.6. Mitochondrial action potential of PC12 cultured with DFO in three different oxygen culture conditions

*PC12 incubated with DFO for 24 hrs, 48 hrs, 72 hrs and 96 hrs in either air oxygen (AO), intermittent hypoxia (IH), or continuous normoxia (CN). MitoTracker® Red fluorescence was measured as indicated previously. X-axis represents normalised fluorescence intensity values. Y-axis represent time points (hrs). Data are presented as normalized mean fluorescence intensity ± standard deviation (SD). n=1 triplicate, * indicates significant difference in comparison to control at each time point under each oxygen culture condition (p<0.01).*

5.3.1.2.4. Determination of PC12 mitochondrial action potential after treatment with DMOG at different oxygen conditions.

AO cultured PC12 cells exposed to 100 µM DMOG significantly elevated mt-AP after 24 hrs (45%) with significant reduction (27%) in comparison to control AO, while under IH culture there were significant reduction after 24 hrs, 72 hrs and 96 hrs (53%, 65% and 43%) in comparison to control IH. Significant reductions were noted after incubation at CN where DMOG reduced mt-AP after 48 hrs, 72 hrs and 96hrs (39%, 61% and 63% respectively) (Figure 5.7).

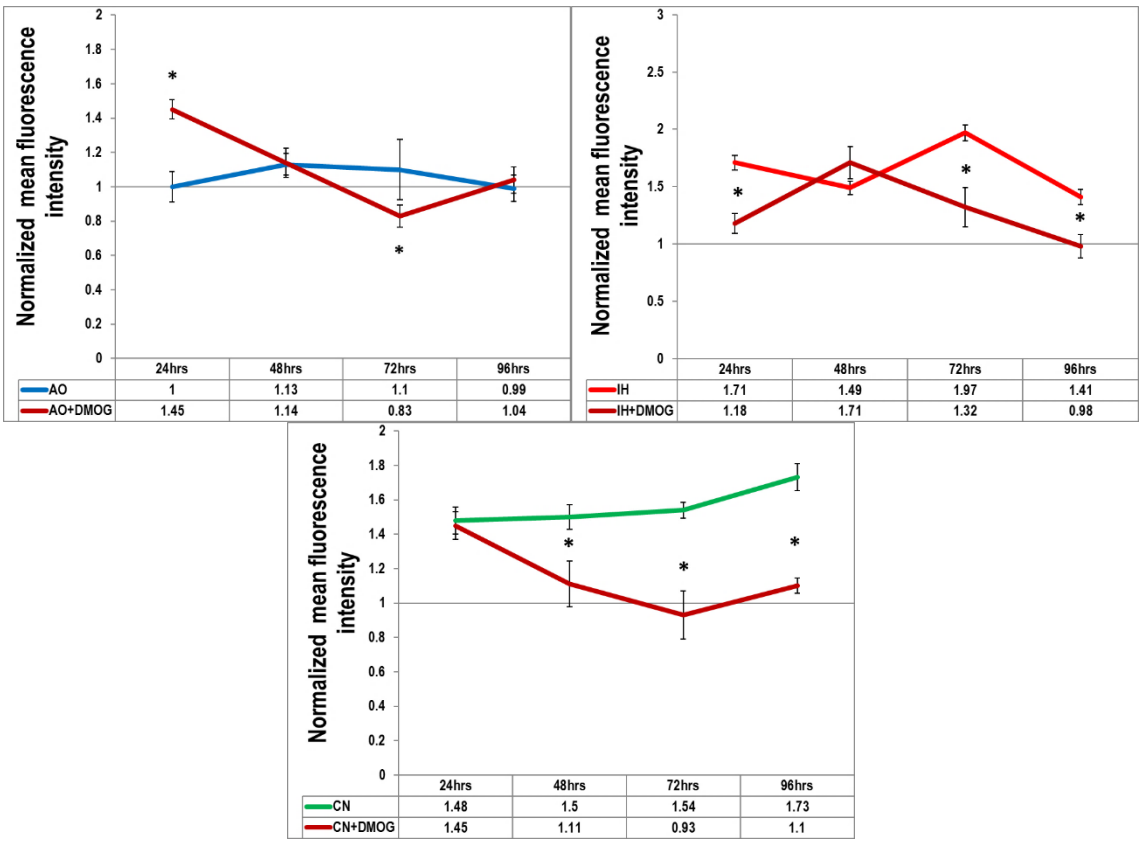

Figure 5.7. Mitochondrial action potential of PC12 cultured with DMOG in three different oxygen culture conditions

*PC12 incubated with DMOG for 24 hrs, 48 hrs, 72 hrs and 96 hrs in either air oxygen (AO), intermittent hypoxia (IH), or continuous normoxia (CN). MitoTracker® Red fluorescence was measured following labelling and incubation via FACS. X-axis represents normalised fluorescence intensity values. Y-axis represent time points (hrs). Data are presented as normalized mean fluorescence intensity ± standard deviation (SD). n=1 triplicate, * indicates significant difference in comparison to control at each time point under each oxygen culture condition (p<0.01).*

5.3.1.2.5. Determination of PC12 mitochondrial action potential after treatment with IOX2 at different oxygen conditions.

AO cultured PC12 cells exposed to 50 nM IOX2 have no significant effect on mt-AP, while under IH culture there were significant reductions after 24 hrs, 72 hrs and 96 hrs (56%, 90% and 30% respectively) in comparison to control IH with no significant effect was noted after 48 hrs. mt-AP reductions were noted after 48 hrs, 72 hrs and 96 hrs of IOX2 supplementation at CN (49%, 74% and 74% respectively) (p<0.01) (Figure 5.8).

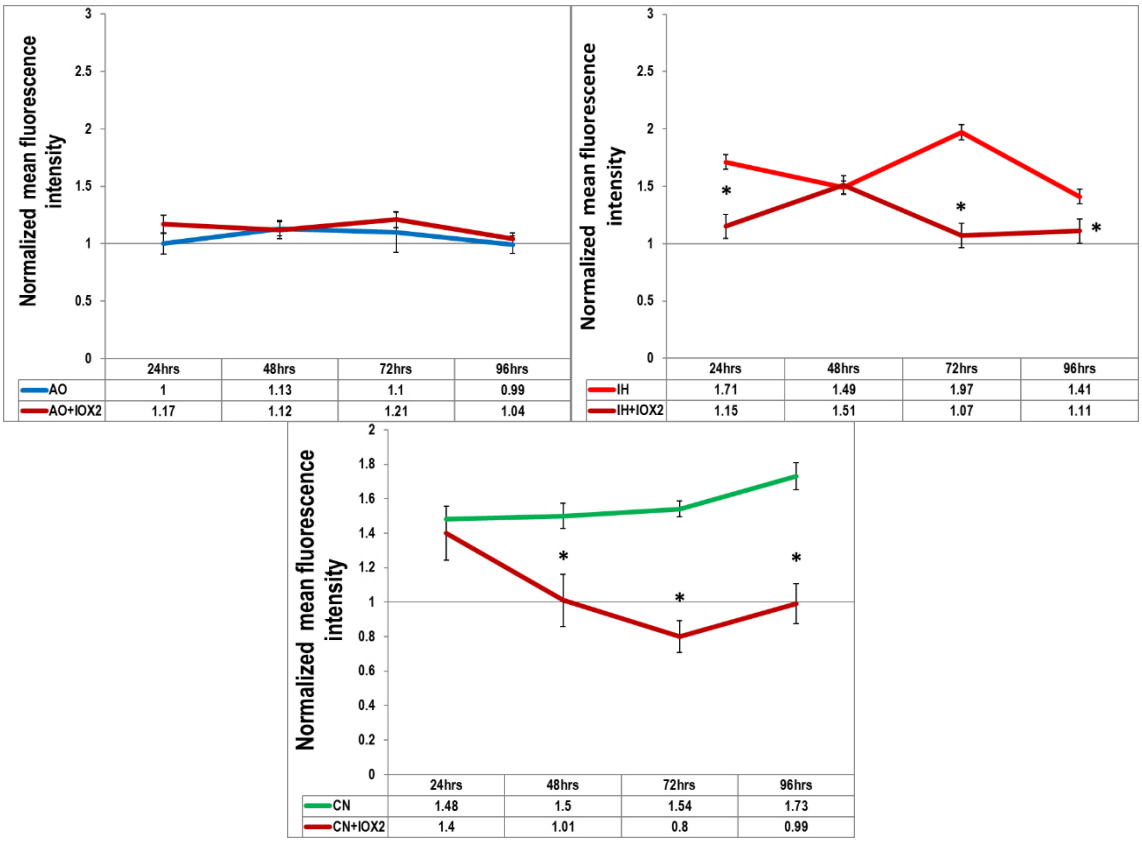

Figure 5.8. Mitochondrial action potential of PC12 cultured with IOX2 in three different oxygen culture conditions

*PC12 incubated with IOX2 for 24 hrs, 48 hrs, 72 hrs and 96 hrs in either air oxygen (AO), intermittent hypoxia (IH), or continuous normoxia (CN). MitoTracker® Red fluorescence was measured as before. X-axis represents normalised fluorescence intensity values. Y-axis represent time points (hrs). Data are presented as normalized mean fluorescence intensity ± standard deviation (SD). n=1 triplicate, * indicates significant difference in comparison to control at each time point under each oxygen culture condition (p<0.01).*

To sum up, mitochondrial action potential elevated over the 96 hrs in IH and CN. Where after HMAs at IH and CN significantly reduced action potential after 48 hrs, 72 hrs and 96hrs. While under AO culture condition, little or no significant effect on action potential. HMAs treatment again fail to recapture mitochondrial action potential pattern on all culture conditions and these changes may relate to fission/ fussion process Mfn-2 regulates mitochondrial mass, membrane potential, and glucose oxidation. Mfn-2 induces aggregation of small mitochondrial clusters of fragmented mitochondria (Kawalec et al., 2015).

5.3.1.3. PC12 mitochondrial genome copy number

There is strong association between mitochondrial function and the quantity of mitochondrial DNA (mtDNA) (Xu *et al.,* 2013). Elevated levels of ROS formation lead to mtDNA oxidative damage, which is associated with multisystem disorders, mainly affecting energy dependent functions e.g. central nervous system. Mitochondria play a vital role in the regulation of synaptic formation and function and any mitochondrial dysfunction may underlie neurological changes under hypoxia. The mechanisms that underlie potential mtDNA copy alterations observed under different oxygen levels have not been fully elucidated. Mitochondrial copy number changes can trigger many damaging processes including apoptosis, oxidative stress and autophagy, which are tightly regulated pathways (Guha & Avadhani, 2013). We hypothesised that HMAs and/or may IH/CN change the number of mitochondria. Mitochondrial DNA were extracted from PC12 cells as described in Chapter 2 (2.4.1) and used for detection of the changes in mitochondrial genome copy number.

There was significant elevation in mitochondrial copy number were noted following $2^{\wedge\Delta\Delta Ct}$ qPCR methodology after incubation in IH (while under CN culture conditions there was significant reduction in comparison to the baseline AO (Figure 5.9).

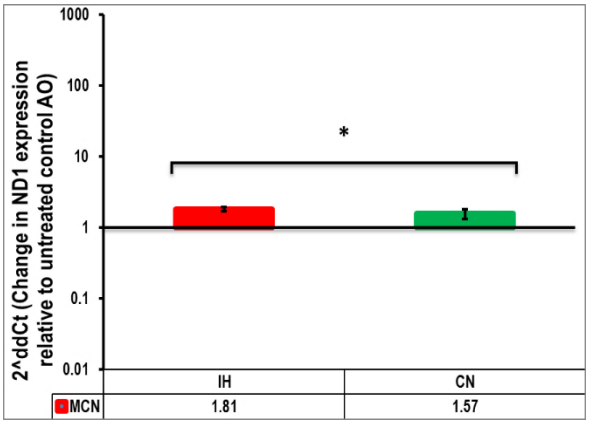

Figure 5.9. Mitochondrial genome copy number changes after incubation under different oxygen culture conditions

PC12 were incubated for 24 hrs in either air oxygen (AO), intermittent hypoxia (IH), or continuous normoxia (CN) before DNA was extracted. X-axis represents different oxygen culture condition. Y-

axis represent fold change in ND1 relative to AO. qPCR assessment of mtDNA using the mt-ND1 gene locus. β actin gene is used as genomic copy number housekeeping gene. Error bars represent ± one standard deviation from the mean.

After supplementation with $CoCl_2$ in AO the mitochondrial genome copy number was significantly elevated after both 48 hrs and 72hrs (5 and 4 fold respectively) but dropped below significance after 96 hrs. No significant change in the mitochondrial genome copy number was noticed after IH culture condition over 96 hrs while only slight, though significant, reductions were noted in CN after 48 hrs and 72 hrs (0.27 and 0.56 fold respectively) in comparison to the baseline AO (Figure 5.10).

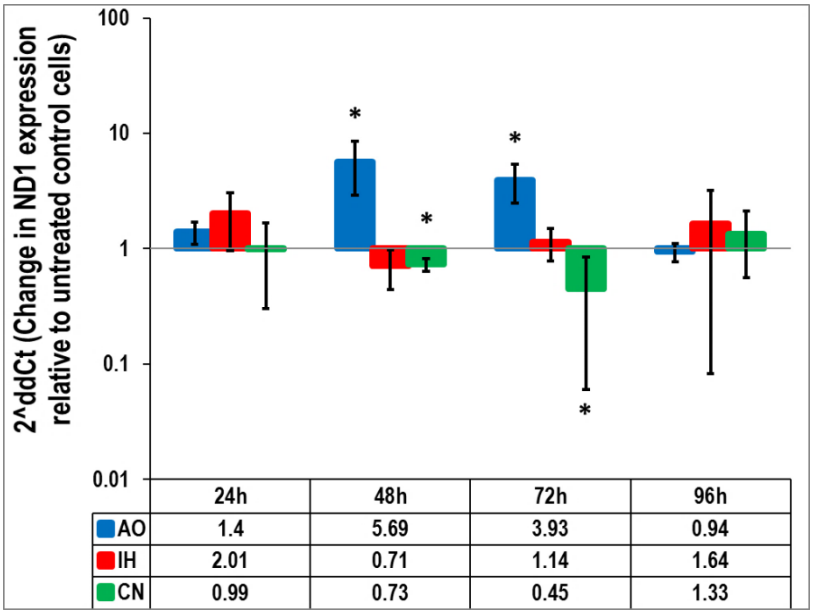

	24h	48h	72h	96h
AO	1.4	5.69	3.93	0.94
IH	2.01	0.71	1.14	1.64
CN	0.99	0.73	0.45	1.33

Figure 5.10. Mitochondrial genome copy number changes after CoCl2 incubation under different oxygen culture conditions

Mitochondrial genome copy number changes after treatment with $CoCl_2$ in either AO, IH, or CN. qPCR assessment of mtDNA using the mt-ND1 gene locus. β-actin gene is used as housekeeping gene. X-axis represents different time points. Y-axis represents relative changes in $2^{\wedge\Delta\Delta Ct}$ of treated cell to untreated control. The fold change above or below is normalized to mt-ND1 control untreated cells at each oxygen condition. Error bars represent ± one standard deviation from the mean.

Supplementation of PC12 cells with DFO in AO resulted in a significant elevation of mitochondrial genome copy number after 48 hrs and 72 hrs (1.7 and 0.7 fold) followed by a significant reduction (0.5 fold) after 96 hrs. Under IH a significant elevation in mitochondrial genome copy number was observed 24 hrs, 48 hrs and 72 hrs (0.73, 14.5, 0.5 fold respectively) followed by reduction (0.63 fold). In contrast, no significant change was noticed with CN in comparison to the baseline AO (Figure 5.11).

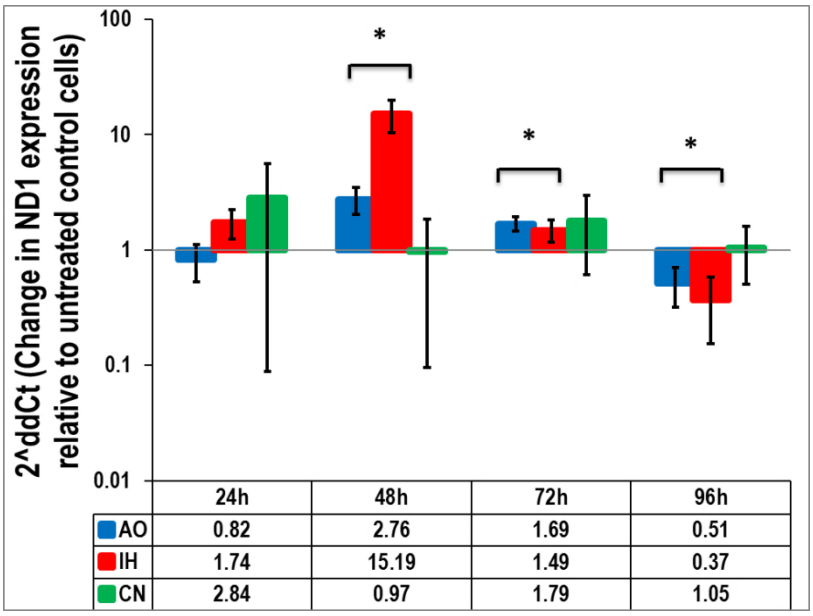

	24h	48h	72h	96h
AO	0.82	2.76	1.69	0.51
IH	1.74	15.19	1.49	0.37
CN	2.84	0.97	1.79	1.05

Figure 5.11. Mitochondrial genome copy number changes after DFO incubation under different oxygen culture conditions

Mitochondrial genome copy number changes after treatment with DFO in either air oxygen (AO), intermittent hypoxia (IH), or continuous normoxia (CN). qPCR assessment of mtDNA using the mt-ND1 gene locus. β-actin gene is used as housekeeping gene. X-axis represents different time points. Y-axis represents relative changes in $2^{\wedge\Delta\Delta Ct}$ *of treated cell to untreated control. The fold change above or below is normalized to mt-ND1 control untreated cells at each oxygen condition. Error bars represent ± one standard deviation from the mean*.

PC12 supplementation with DMOG in AO resulted in a significant elevation of mitochondrial genome copy number after 24 hrs, 48 hrs and 72 hrs (0.39, 2.26 and 0.73 fold). Under IH culture significant elevation of mitochondrial genome copy number occurred after 24 hrs (4 fold) followed another elevation after 72 hrs (15 fold). In contrast, significant reduction was noted after both 48 hrs and 72 hrs (0.35 and 0.44 fold) in CN in comparison to the baseline AO (Figure 5.12).

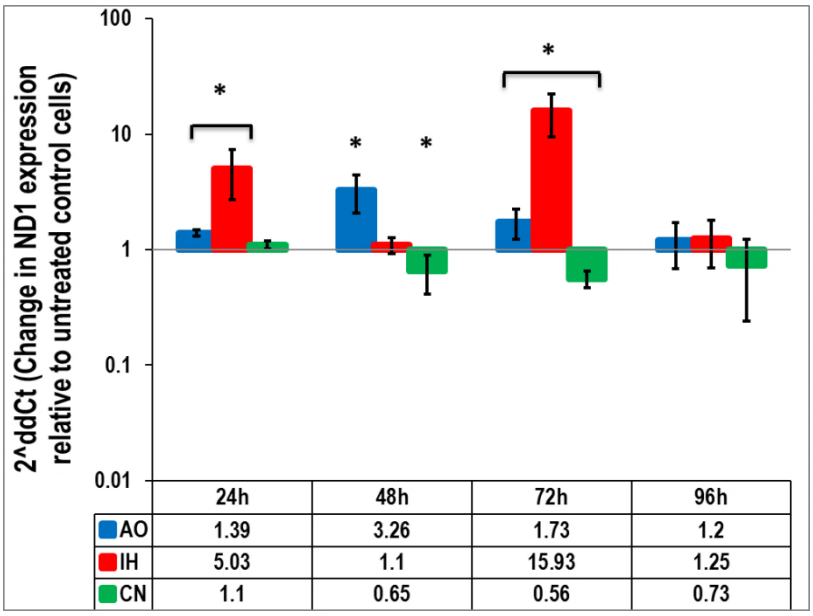

Figure 5.12. Mitochondrial genome copy number changes after DMOG incubation under different oxygen culture conditions

Mitochondrial genome copy number changes after treatment with DMOG in either air oxygen (AO), intermittent hypoxia (IH), or continuous normoxia (CN). qPCR assessment of mtDNA using the mt-ND1 gene locus. β-actin gene is used as housekeeping gene. X-axis represents different time points. Y-axis represents relative changes in $2^{\wedge\Delta\Delta Ct}$ *of treated cell to untreated control. The fold change above or below is normalized to mt-ND1 control untreated cells at each oxygen condition. Error bars represent ± one standard deviation from the mean.*

PC12 supplementation with IOX2 in AO resulted in a significant elevation of mitochondrial genome copy number after 24 hrs and 96 hrs (5 and 95 fold). Under IH significant reduction in mitochondrial genome copy number were noted after both 24 hrs (0.38 fold). Significant elevation was noticed after 48 hrs and 96 hrs (8 and 0.5 fold) in CN in comparison to the baseline (Figure 5.13).

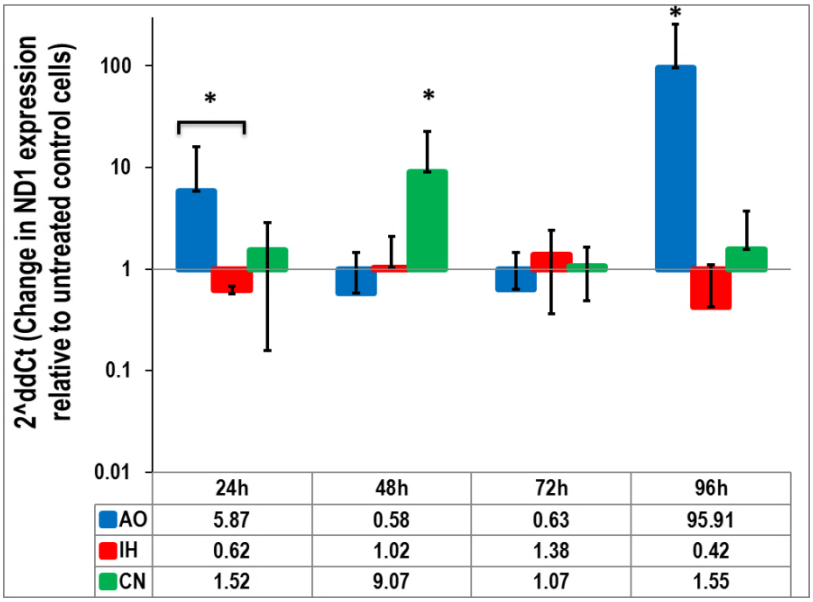

	24h	48h	72h	96h
AO	5.87	0.58	0.63	95.91
IH	0.62	1.02	1.38	0.42
CN	1.52	9.07	1.07	1.55

Figure 5.13. Mitochondrial genome copy number changes after IOX2 incubation under different oxygen culture conditions

Mitochondrial genome copy number changes after treatment with IOX2 in either air oxygen (AO), intermittent hypoxia (IH), or continuous normoxia (CN). qPCR assessment of mtDNA using the mt-ND1 gene locus. β-actin gene is used as housekeeping gene. X- axis represents different time points. Y-axis represents relative changes in $2^{\wedge\Delta\Delta Ct}$ of treated cell to untreated control. The fold change above or below is normalized to mt-ND1 control untreated cells at each oxygen condition. Error bars represent ± one standard deviation from the mean.

To sum up, $CoCl_2$ increase mitochondrial genome copy number after 48, 72 hrs in AO and reduced the copy number after 72 hrs in CN. DFO increase mitochondrial genome copy number after 48, 72 hrs in AO and 24, 48, 72 hrs in IH with significant reduction after 96 hrs in IH. DMOG increase mitochondrial genome copy number after 24, 48, 72 hrs in AO and 24, 72 hrs in IH with significant reduction noted after 48 and 96 hrs. finally IOX2

increase mitochondrial genome copy number after 24, 96 hrs in AO and 48, 96 hrs with significant reduction after 24 hrs in IH.

In conclusion, IH increase mitochondrial burden and action potential without affecting mitochondrial genome copy number. HMAs supplementation under all conditions induce distinctive pattern of mitochondrial dynamic different than that noted under IH and CN, thus HMAs fail to mimic effect of oxygen modulation on mitochondrial level.

5.3.2. Effect of hypoxia mimetic agents on BM-hMSCs mitochondrial dynamic

5.3.2.1. BM-hMSCs mitochondrial burden

Mitochondrial burden can be applied as a relative measure of mitochondrial mass. MSCs were cultured and stained as stated in Chapter 2 (2.2.2.9) and optimisation performed as described previously for PC12. An evaluation of AO cultured MSCs used to initiate all experiments was performed to establish baseline fluorescence and this is represented as the x-axis intersection with the y-axis and all values normalized to this value. IH culture conditions caused significant reduction on burden in comparison to AO control.

Under AO culture condition, supplementation of media with either $CoCl_2$, DFO or DMOG significantly reduced burden (23%, 51% and 24%) in comparison to control AO (Figure 5.14).

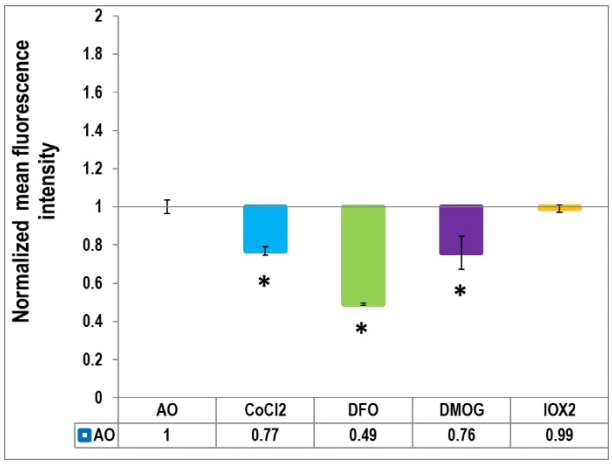

Figure 5.14. Mitochondrial burden of hMSCs cultured with HMAs in air oxygen culture condition

*hMSCs were incubated for 14 days in air oxygen supplemented with either $CoCl_2$, DFO, DMOG, or IOX2 after which mitochondrial burden was assayed. MitoTracker® Green was measured as indicated previously. X-axis represents normalized mean fluorescence intensity. Y-axis represent different treatment. Data are presented as normalized mean fluorescence intensity ± standard deviation (SD). n=3, * indicates significant difference in comparison to control AO (p<0.01).*

Under IH supplementation of media with DFO and DMOG significantly reduced burden (50% and 10%) in comparison to control IH. In contrast IOX2 significantly increase burden (23%) in comparison to control IH (Figure 5.15).

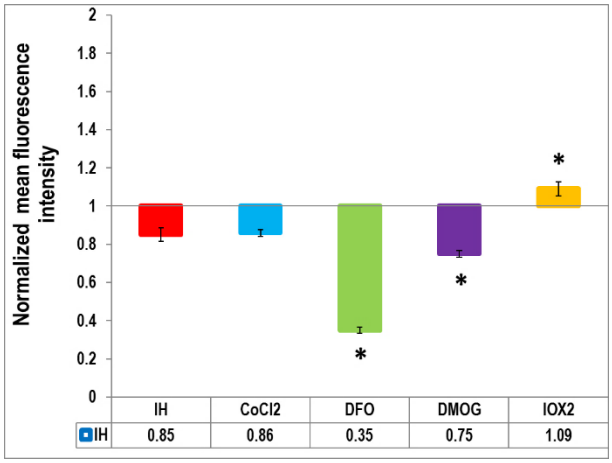

Figure 5.15. Mitochondrial burden of hMSCs cultured with HMAs at intermittent hypoxia culture condition

*hMSCs were incubated for 14 days in intermittent hypoxia supplemented with either $CoCl_2$, DFO, DMOG, or IOX2 after which mitochondrial burden was assayed. MitoTracker® Green was measured as indicated previously. X-axis represents normalized mean fluorescence intensity. Y-axis represent different treatment. Data are presented as normalized mean fluorescence intensity ± standard deviation (SD). n=1 triplicate, * indicates significant difference in comparison to control IH (p<0.01).*

Under CN supplementation of media with HMAs significantly reduced burden after $CoCl_2$, DFO, DMOG and IOX2 (17%, 60%, 17% and 21% respectively) in comparison to control CN. (Figure 5.16).

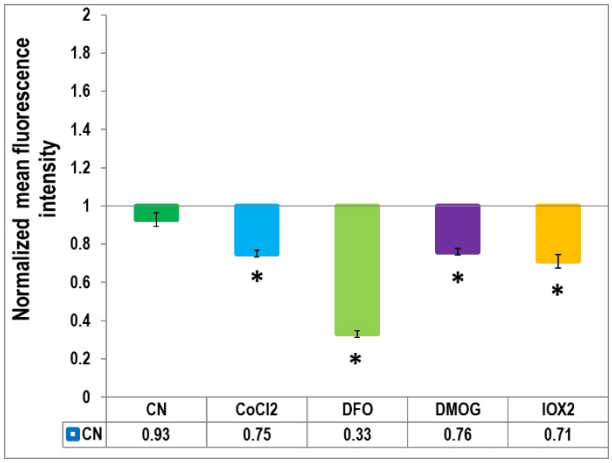

Figure 5.16. Mitochondrial burden of hMSCs cultured with HMAs in continuous normoxia culture condition

*hMSCs were incubated for 14 days in continuous supplemented with either $CoCl_2$, DFO, DMOG, or IOX2 after which mitochondrial burden was assayed. MitoTracker® Green was measured as indicated previously. X-axis represents normalized mean fluorescence intensity. Y-axis represent different treatment. Data are presented as normalized mean fluorescence intensity ± standard deviation (SD). n=1 triplicate, * indicates significant difference in comparison to control CN ($p<0.01$).*

To sum up, hMSCs mitochondrial burden reduced under IH. $CoCl_2$, DFO and DMOG significantly reduce mitochondrial burden in AO. Under IH culture DFO and DMOG reduced mitochondrial burden with elevation noted after IOX2. All HMAs reduce mitochondrial burden in CN. HMAs recapture mitochondrial burden pattern only with IOX2 under AO and $CoCl_2$ under IH.

5.3.2.2. BM-hMSCs mitochondrial action potential.

Mitochondrial action potential (mt-AP) plays a vital role in cellular activity. hMSCs cultured and stained as stated in Chapter 2 (2.2.1.11). AO cultured cells displayed a consistent baseline fluorescence. MSCs used to initiate all experiments were first measured to establish control levels and are represented as the x-axis intersection with the y-axis and all values normalized to this value. IH significantly elevate mt-AP in comparison to AO with no significant effect was noted with CN.

Under AO culture condition, supplementation media with $CoCl_2$ and DMOG significantly reduced mt-AP (18% and 26%) in comparison to control AO with significant elevation was noted after IOX2 supplementation (70%) (Figure 5.17).

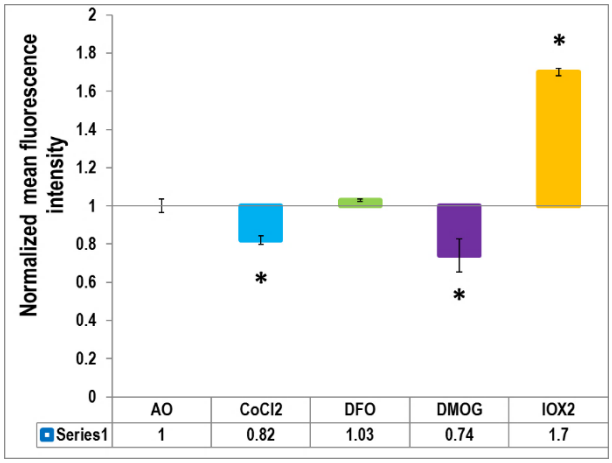

Figure 5.17. Mitochondrial action potential of hMSCs cultured with HMAs in air oxygen culture condition

*hMSCs were incubated for 14 days in air oxygen supplemented with either $CoCl_2$, DFO, DMOG, or IOX2 after which mitochondrial burden was assayed. MitoTracker® Red was measured as indicated previously. X-axis represents normalized mean fluorescence intensity. Y-axis represent different treatment. Data are presented as normalized mean fluorescence intensity ± standard deviation (SD). n=1 triplicate, * indicates significant difference in comparison to control AO ($p<0.01$).*

Under IH culture condition, supplementation media with DFO and DMOG significantly reduced mt-AP (63% and 33%) in comparison to control IH. In contrast IOX2 significantly elevated mt-AP (50%) in comparison to control IH (Figure 5.18).

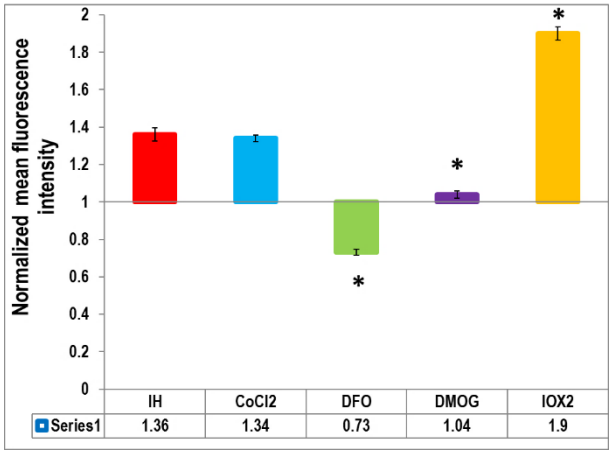

Figure 5.18. Mitochondrial action potential of hMSCs cultured with HMAs in intermittent hypoxia culture condition

*hMSCs were incubated for 14 days in intermittent hypoxia supplemented with either $CoCl_2$, DFO, DMOG, or IOX2 after which mitochondrial burden was assayed. MitoTracker® Red was measured as indicated previously. X-axis represents normalized mean fluorescence intensity. Y-axis represent different treatment. Data are presented as normalized mean fluorescence intensity ± standard deviation (SD). n=1 triplicate, * indicates significant difference in comparison to control IH ($p<0.01$).*

Under CN culture condition supplementation media with $CoCl_2$ and DFO significantly reduced burden (28% and 38%) in comparison to control CN with significant elevation was noticed after IOX2 supplementation (35%) in comparison to control CN (Figure 5.19).

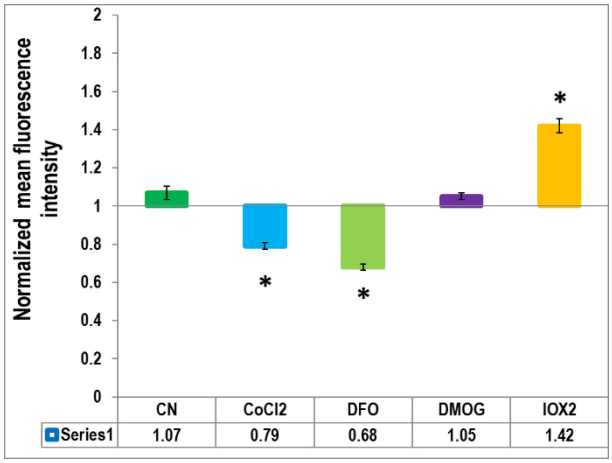

Figure 5.19. Mitochondrial action potential of hMSCs cultured with HMAs in continuous culture condition

*hMSCs were incubated for 14 days in continuous normoxia supplemented with either $CoCl_2$, DFO, DMOG, or IOX2 after which mitochondrial burden was assayed. MitoTracker® Red was measured as indicated previously. X-axis represents normalized mean fluorescence intensity. Y-axis represent different treatment. Data are presented as normalized mean fluorescence intensity ± standard deviation (SD). n=1 triplicate, * indicates significant difference in comparison to control CN (p<0.01).*

To sum up, hMSCs mitochondrial action potential increase in IH. $CoCl_2$ and DFO reduced mitochondrial action potential under AO with significant increase noted after IOX2 supplementation. Under IH culture DFO and DMOG reduced mitochondrial the action potential with elevation noted after IOX2. $CoCl_2$ and DFO reduce mitochondrial action potential in CN with significant elevation after IOX2 supplementation. HMAs recapture mitochondrial burden pattern only with IOX2 under AO and $CoCl_2$ under IH.

5.3.2.3. BM-hMSCs mitochondrial genome copy number

Mitochondria are sites of energy production in human cells which usually contain 100s to 1000s of mitochondria/cell and each mitochondrion contain 2–10 mitochondrial DNA (mtDNA) copies that form the mitochondrial network (Gilkerson *et al.,* 2013). The amount of energy produced is related to the number of mtDNA copies and the abundance of mitochondria under different physiological conditions (Trinei *et al.,* 2006). The human mtDNA is a circular DNA with 16,569 bp (Berdanier, 2005). It encodes only for 13 polypeptides that are essential for the assembly of respiratory enzyme complexes I, III, IV, and V. The remaining ~90 polypeptides constituting the respiratory enzyme complexes are encoded in nuclear DNA (nDNA) (Lin & Wang, 2013). The complex II subunits are totally encoded in nDNA. mtDNA replication and transcription regulated by number of proteins such as mitochondrial transcription factor A (TFAM) which play dual roles in mtDNA replication and transcription by interaction to the noncoding D-loop region. TFAM plays an important role in the regulation of mitochondrial biogenesis under different oxygen level (Holt & Reyes, 2012). Limited studies have discussed the role of HMAs on mitochondrial genome copy number in BM-hMSCs.

Following the procedures outlined previously DNA was extracted from hMSC and qPCR performed for ND1 and ACTB to establish an indicator of mt genome copy number. Both IH and CN displayed a significantly elevation in mitochondrial genome copy number in BM-hMSCs in comparison to AO with no significant effect was noted with CN (Figure 5.20).

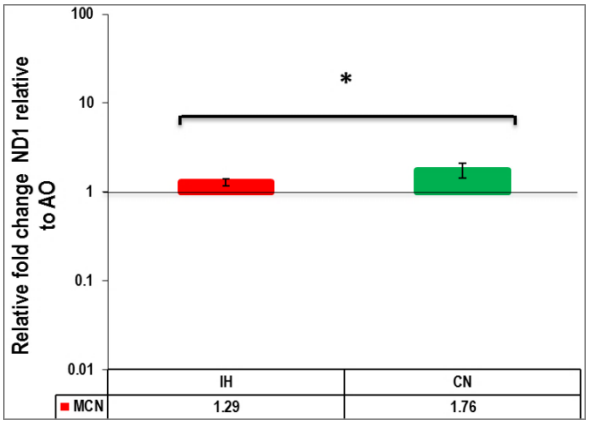

Figure 5.20. Mitochondrial genome copy number changes after incubation under different oxygen culture conditions

*Following incubation of BM-hMSCs for 14 days in either air oxygen (AO), intermittent hypoxia (IH), or continuous normoxia (CN) DNA was extracted and qPCR performed. X-axis represents different oxygen culture condition. Y-axis represent fold change in ND1 relative to AO. qPCR assessment of mtDNA using the mt-ND1 gene locus. β-actin gene is used as housekeeping gene. The mean normalized to control AO. Error bars represent ± one standard deviation from the mean. * indicates significant difference in comparison to baseline (p<0.01).*

Under AO cultured BM-hMSC supplemented with either $CoCl_2$, DFO, or IOX2 significantly elevated ND1 (11, 2, and 1.5 fold) in comparison to baseline was observed, no significant effect was noted with DMOG (Figure 5.21).

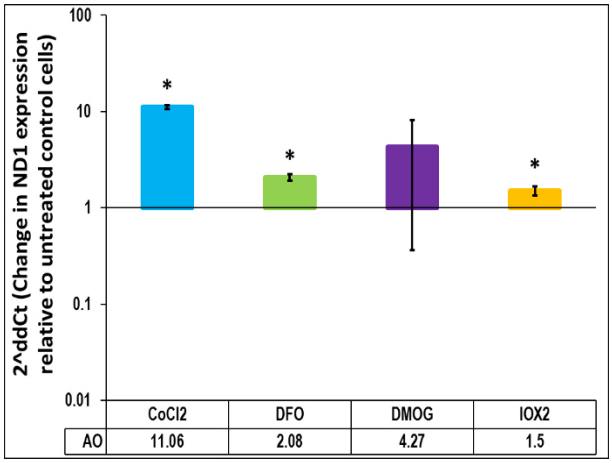

Figure 5.21. Mitochondrial genome copy number changes after incubation with HMAs under air oxygen culture condition

*Mitochondrial genome copy number changes after treatment with either $CoCl_2$, DFO, DMOG, or IOX2 in AO culture. X-axis represents individuals HMAs. Y-axis represent fold change in ND1 relative to AO. qPCR assessment of mtDNA using the mt-ND1 gene locus. β-actin gene is used as housekeeping gene. The fold change above or below is normalized to mt-ND1 control untreated cells at each oxygen condition. Error bars represent ± one standard deviation from the mean, * indicates significant difference in comparison to baseline (p<0.01).*

Under IH culture condition, DFO and DMOG significantly elevated ND1 (2.83 and 7.15 fold, respectively) with a significant reduction noted after either $CoCl_2$ (0.26 fold) or IOX2 (0.87 fold) treatment compare to baseline (Figure 5.22).

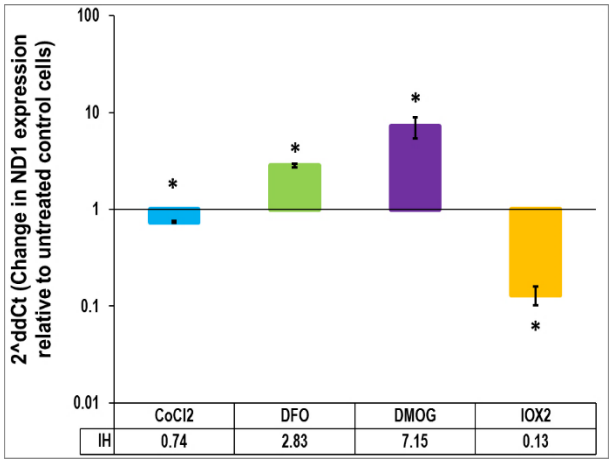

Figure 5.22. Mitochondrial genome copy number changes after incubation with HMAs under intermittent hypoxia culture condition

*Mitochondrial genome copy number changes after treatment with either $CoCl_2$, DFO, DMOG, or IOX2 in IH culture. X-axis represents individuals HMAs. Y-axis represent fold change in ND1 relative to IH. qPCR assessment of mtDNA using the mt-ND1 gene locus. β-actin gene is used as housekeeping gene. The fold change above or below is normalized to mt-ND1 control untreated cells at each oxygen condition. Error bars represent ± one standard deviation from the mean, * indicates significant difference in comparison to baseline (p<0.01).*

Under CN culture condition $CoCl_2$, DFO and DMOG significantly elevated ND1 (4.25, 1.97, and 13.8 fold respectively). In contrast, a significant reduction was noted after IOX2 treatment when compared to baseline (0.47) (Figure 5.23).

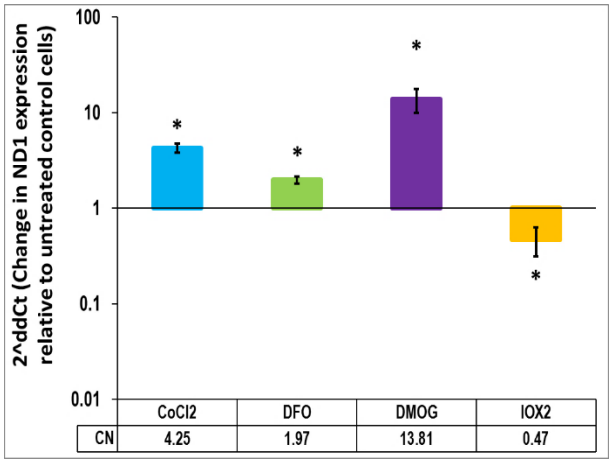

Figure 5.23. Mitochondrial genome copy number changes after incubation with HMAs under continuous normoxia culture condition

*Mitochondrial genome copy number changes after treatment with either $CoCl_2$, DFO, DMOG, or IOX2 in CN culture. X-axis represents individuals HMAs. Y-axis represent fold change in ND1 relative to CN. qPCR assessment of mtDNA using the mt-ND1 gene locus. β-actin gene is used as housekeeping gene. The fold change above or below is normalized to mt-ND1 control untreated cells at each oxygen condition. Error bars represent ± one standard deviation from the mean, * indicates significant difference in comparison to baseline (p<0.01).*

To sum up with exception of DMOG in AO, HMAs induced significant change in mitochondrial genome number which not mimics any of patterns seen under the three oxygen culture conditions.

In conclusion. IH decrease both mitochondrial burden and mitochondrial genome copy number with increase in action potential. HMAs supplementation of under all conditions induce distinctive pattern of mitochondrial dynamic different than that noted under IH, thus HMAs fail to mimic effect of oxygen modulation preconditioning on mitochondrial level.

Now it is clear that HMAs does not mimic any pattern that was noticed under all studied oxygen culture conditions. We still need to determine the effect of different oxygen level on MSCs ultrastructure in order connect these effect with previous finding.

5.3.3. Effect of different oxygen level on BM-hMSCs ultrastructure

Mitochondria play a number of important cellular role including ATP production, homeostasis of intracellular Ca^{2+}, reactive oxygen species formation, and the release of cytochrome c (Perier & Vila, 2012). Moreover, they play a major role in triggering programmed cell death (apoptosis) (Carmona-Gutierrez *et al.,* 2010). Mitochondrial dysfunction has been described as playing a part in many physiological conditions such as aging and pathological conditions as neurodegenerative disorders for example Parkinson's disease (Uttara *et al.,* 2009). Mitochondrial dysfunction is associated with accumulation of misfolded or unfolded proteins which relate to endoplasmic reticulum (ER) stress (Cao & Kaufman, 2014). Mitochondria may undergo various morphological alterations reflective of different physiological and pathological conditions (Sasaki, 2010). The TEM remains the most effective tool to study morphological changes of mitochondrial and other ultrastructural changes. The changes in these organelles are reflected as changes in mitochondrial mass, action potential and oxidative stress.

Under AO culture, BM-hMSCs cells have an ultrastructure that is held in common across animal cells. Cells have polymorphic nuclei with clear border, deep invaginations, euchromatin, and conspicuous nucleoli. The cytoplasm possesses well-developed cisternae of rough endoplasmic reticulum and cytoskeleton filaments with areas of depleted cytoplasm. The cells have branched plasma membranes which resemble filopodia that served in attaching to the surface. Mitochondria are rod–like structure and distributed around and near to the nucleus. Cytoplasm there are well-developed cisternae of rough endoplasmic reticulum and cytoskeleton filaments expanded within areas of depleted cytoplasm (black arrow). We also observed that mitochondria appeared branched close proximity/near attachment to each other and located very close to the ER. This may be reflective of the fusion process described by Van der Bliek *et al.,* (2013) (Figure 5.26). (Figure 5.24, 25 and 26).

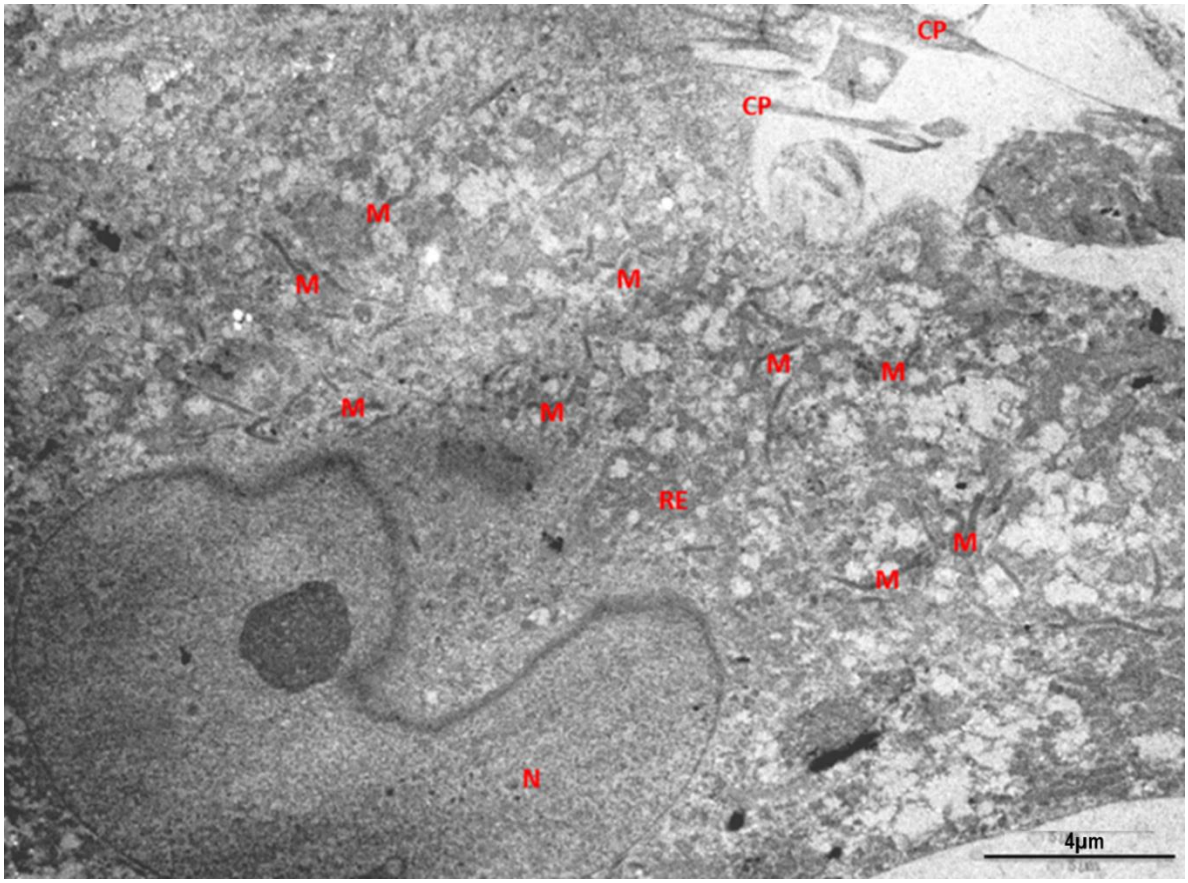

Figure 5.24. BM-hMSCs ultrastructure after incubation in air oxygen

TEM image of BM-hMSCs after 14 days incubation in AO. Cells have well defined nucleus (N). The cytoplasm has a well-developed endoplasmic reticulum (ER) and cytoskeleton filaments within areas of depleted cytoplasm. Mitochondria (M) show as dark-road-shape structures. MSCs have cytoplasm processes (CP). Scale= 4 µm.

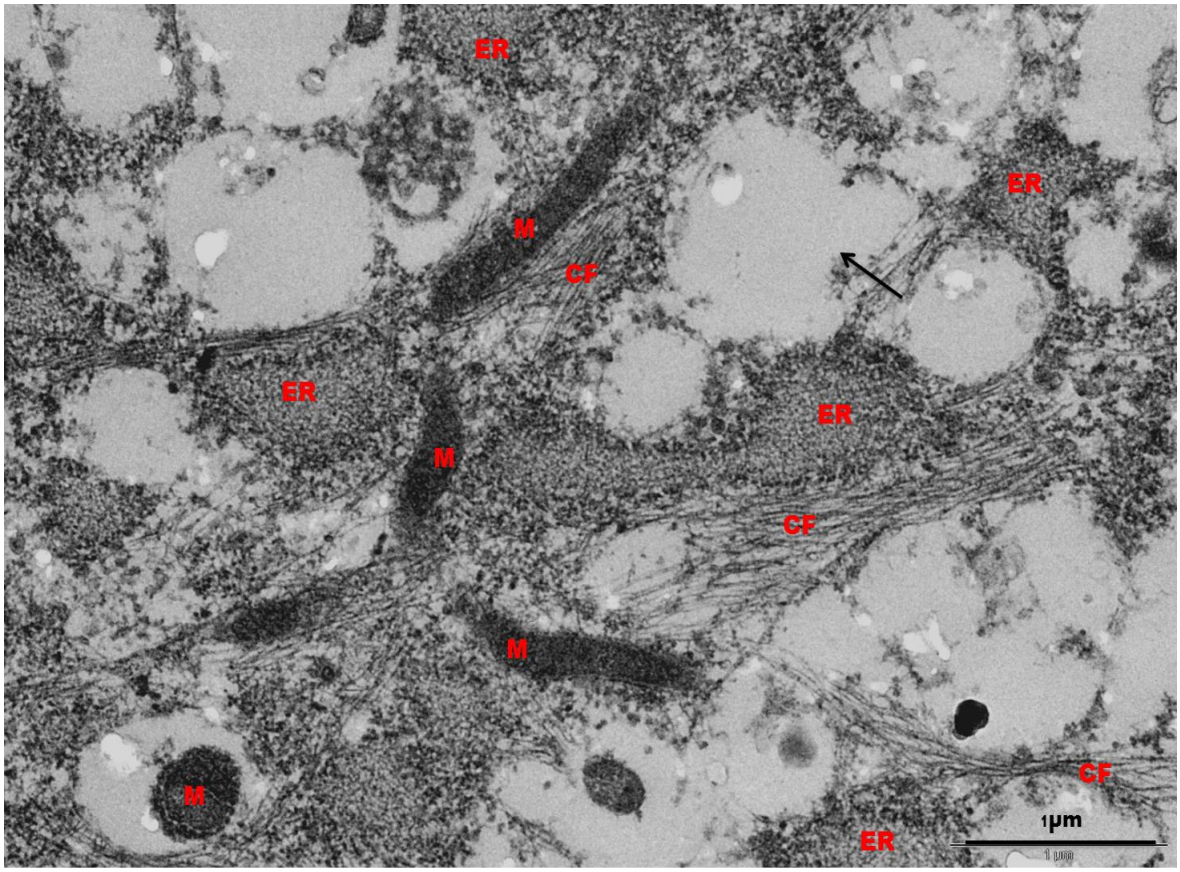

Figure 5.25. Mitochondria in air oxygen culture condition

TEM image of BM-hMSCs after 14-days incubation in AO. Cells display an expanded endoplasmic reticulum (ER) and cytoskeleton filaments (CF) with areas of depleted cytoplasm. Mitochondria (M) have well defined crista. Scale= 1 µm.

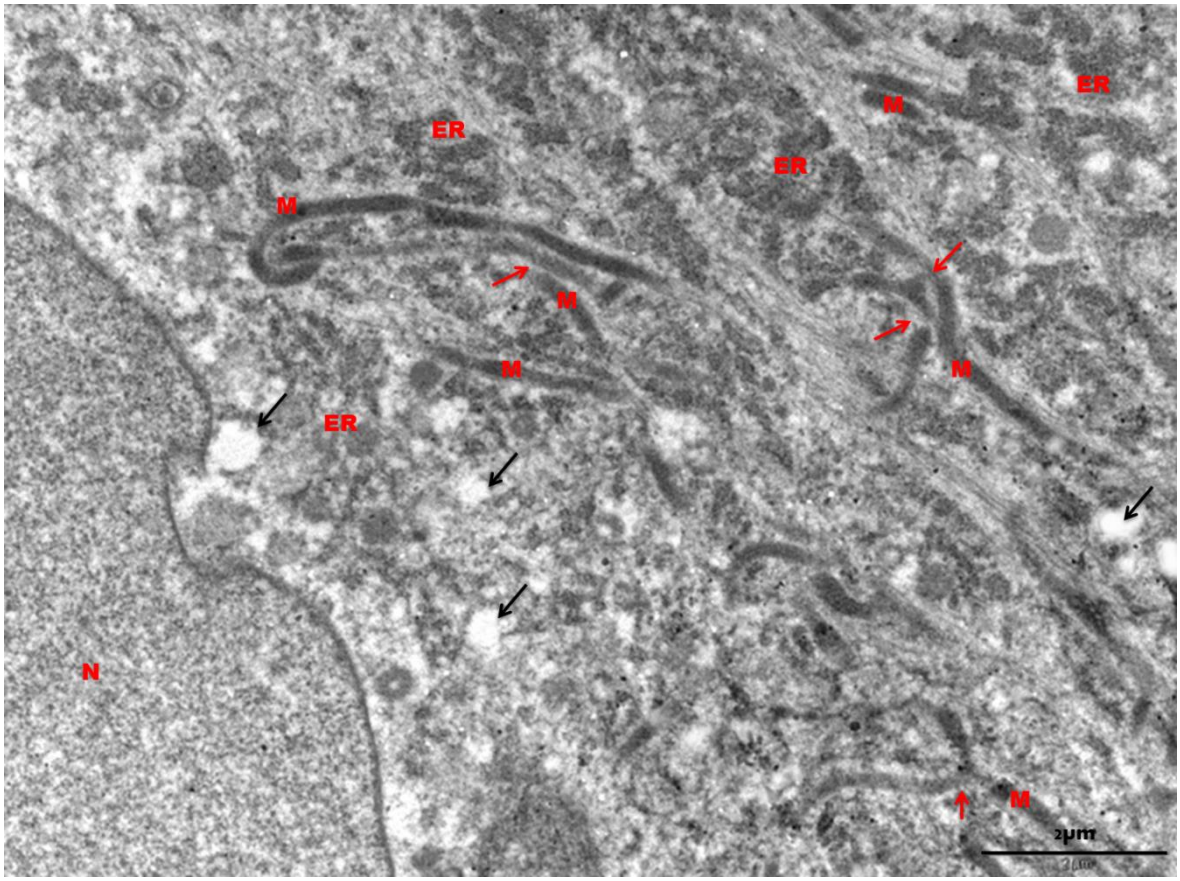

Figure 5.26. BM-hMSCs ultrastructure during incubation in air oxygen

TEM image of BM-hMSCs after 14-days incubation in AO culture cells shows cell have well defined nucleus (N). Cytoplasm is well-developed with depleted areas (black arrow), and endoplasmic reticulum (ER). Mitochondria (M) are dark-road-shape structures that look branched and apparently bind to each other in some points (red arrow). Scale= 2 µm.

Under IH culture, mitochondria are shorter than that in AO and distributed near to the nucleus. More gaps in cytoplasm were noticed near to both the mitochondria and ER in comparison to that noted in AO and areas of parallel microfilaments appeared expanded in comparison to that noted in AO. We also observed that mitochondria were divided into defined portions at specific sites (red arrow) and this may reflect an ongoing fusion/ fission process (Van der Bliek *et al.,* 2013) (Figure 5.27).

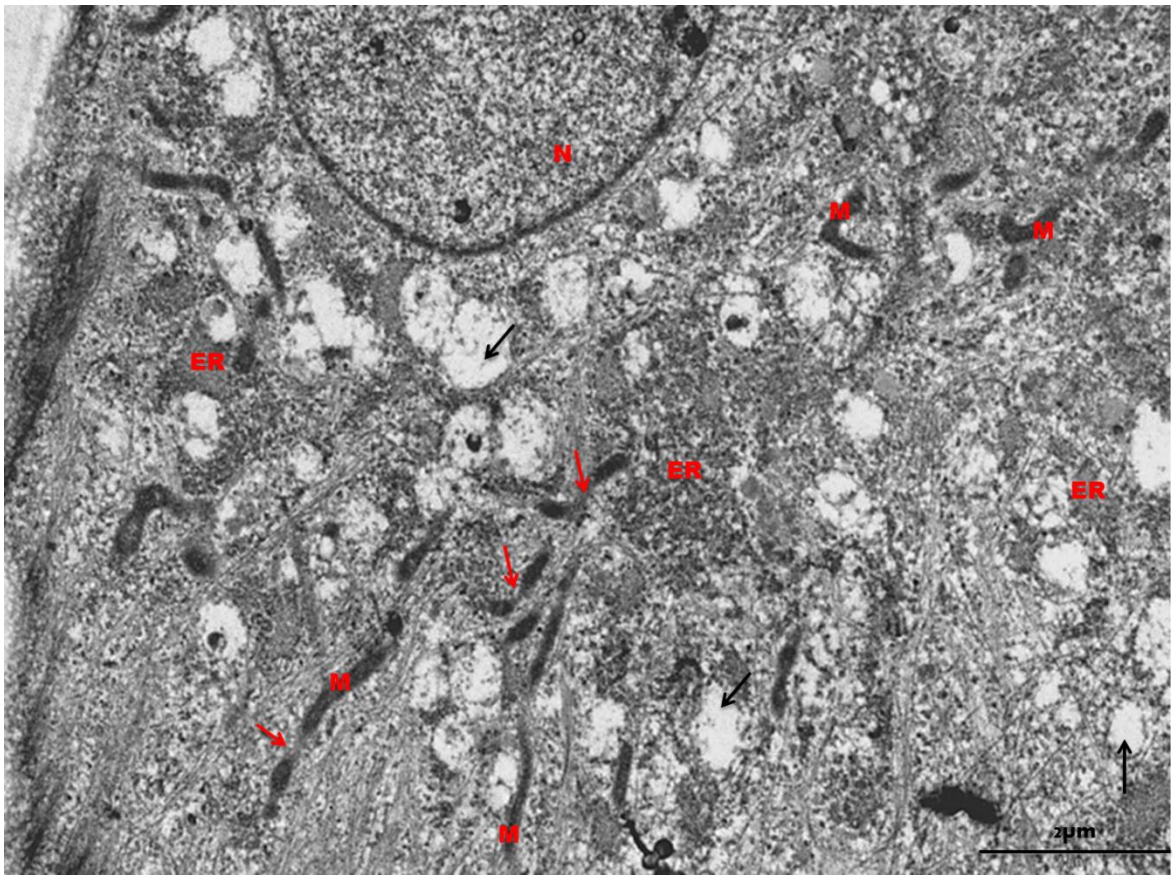

Figure 5.27. BM-hMSCs ultrastructure after incubation under intermittent hypoxia

TEM image of BM-hMSCs after 14 days incubation in IH culture. Cells have well defined nucleus (N). A Cytoplasm with a high number of depleted areas (black arrow) and an expanded endoplasmic reticulum (ER). Mitochondria (M) show as short dark-road-shape structures with structural thinning on occasion (red arrow). Scale= 2 µm.

Under CN culture a quite distinct morphology was observed where mitochondria clustered in globular structures. A highly dense cytoplasm made endoplasmic reticulum (ER) and cytoskeleton filaments (CF) not evident with very small areas of depleted cytoplasm (Figure 5.28).

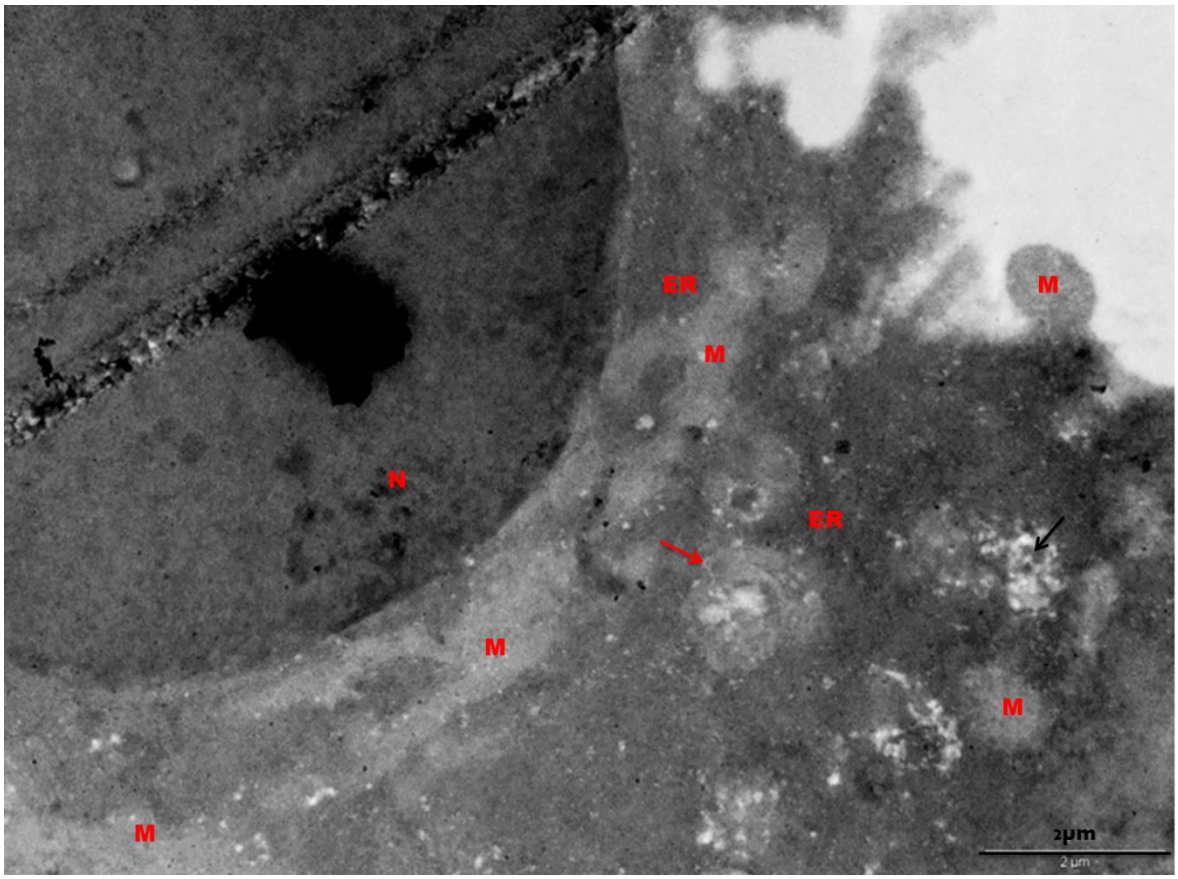

Figure 5.28. BM-hMSCs ultrastructure after incubation under continuous normoxia

TEM image of BM-hMSCs after 14-days incubation in CN. Cells have a well define nucleus (N) and a cytoplasm with very small depleted areas. Endoplasmic reticulum (ER) was not evident due to dense cytoplasm. Mitochondria (M) are evident with a faint-grey colour structure (red arrow). Scale= 2 µm.

TEM image analysis revealed that mitochondrial volume fraction (which obtained by dividing mitochondrial area in section on total area of the section using analysSIS® software) which represent by the (percentage of mitochondria volume) / cell. No significant change after IH culture, while significant elevation was noticed after CN culture ($p<0.001$) in comparison to AO cultured cells (Figure 5.29).

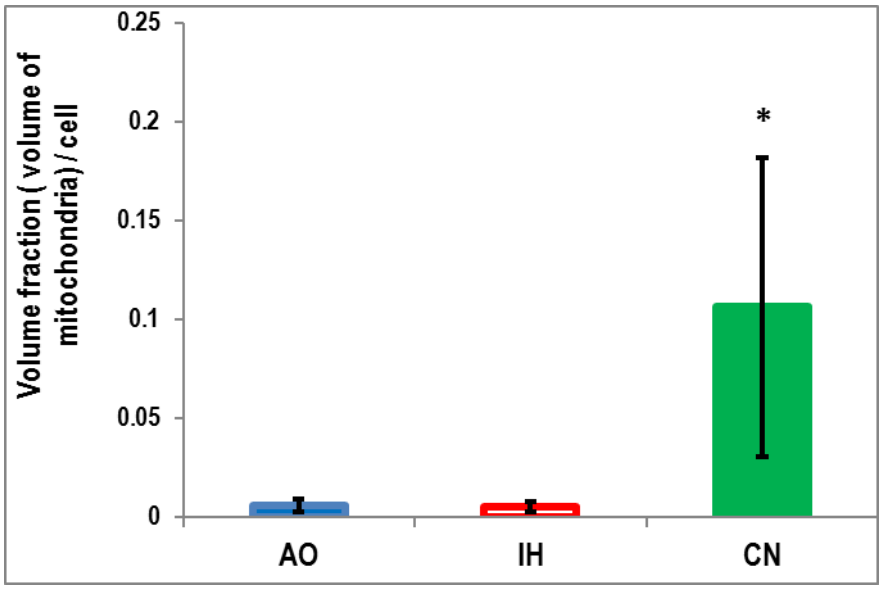

Figure 5.29. Mitochondrial volume fraction of BM-hMSCs after incubation under three different oxygen culture conditions

*BM-hMSCs after 14-days incubation in three alternate oxygen culture conditions. TEM images were taken and analysed using TEM software. The histogram represents mitochondrial volume fraction represented by the percentage of mitochondrial volume/cell. X-axis represents different oxygen treatment. Y-axis represents mitochondrial volume fraction. Error bars represent ± one standard deviation from the mean. n=3, * indicated significant difference in comparison to BM-hMSCs cultured in AO.*

In contrast, mitochondrial density that obtained by dividing number of mitochondria in section / area of the section showed significant elevation only after IH culture ($p<0.001$) in comparison to AO culture (Figure 5.30).

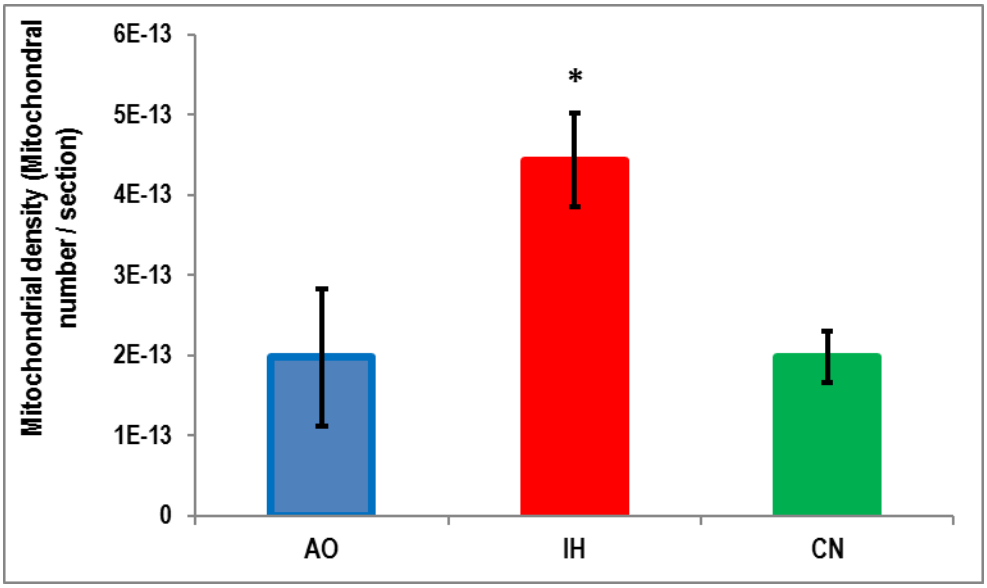

Figure 5.30. Mitochondrial density of BM-hMSCs after incubation under three different oxygen culture conditions

*BM-hMSCs after 14-days incubation in either of three alternate oxygen culture conditions. TEM images were taken and analysed using analysSIS® software. The histogram represents mitochondrial density represented by the number of mitochondrial volume/total cytoplasm area. X-axis represents different oxygen treatment. Y-axis represents mitochondrial density/ section. Error bars represent ± one standard deviation from the mean. n=3, * indicated significant difference in comparison to BM-hMSCs cultured in AO.*

Moreover, the TEM study revealed that IH culture condition induced a resemblance to a scenario observed in apoptosis with an electron-dense nucleus with nuclear fragmentation, and intact cell membrane even late in the cell disintegration phase, disorganised cytoplasmic organelles with apoptotic bodies, and large clear vacuoles that may bleb out of the cell as described by Elmore (2007) (Figure 5.31). In addition, IH cultured cells possess feature like features of mitophagy (Gomes *et al.,* 2011) where mitochondria are engulfed by double-membrane-delimited vesicles and condensed to a circular structure with vesicles merged to form larger structures (Figure 5.32).

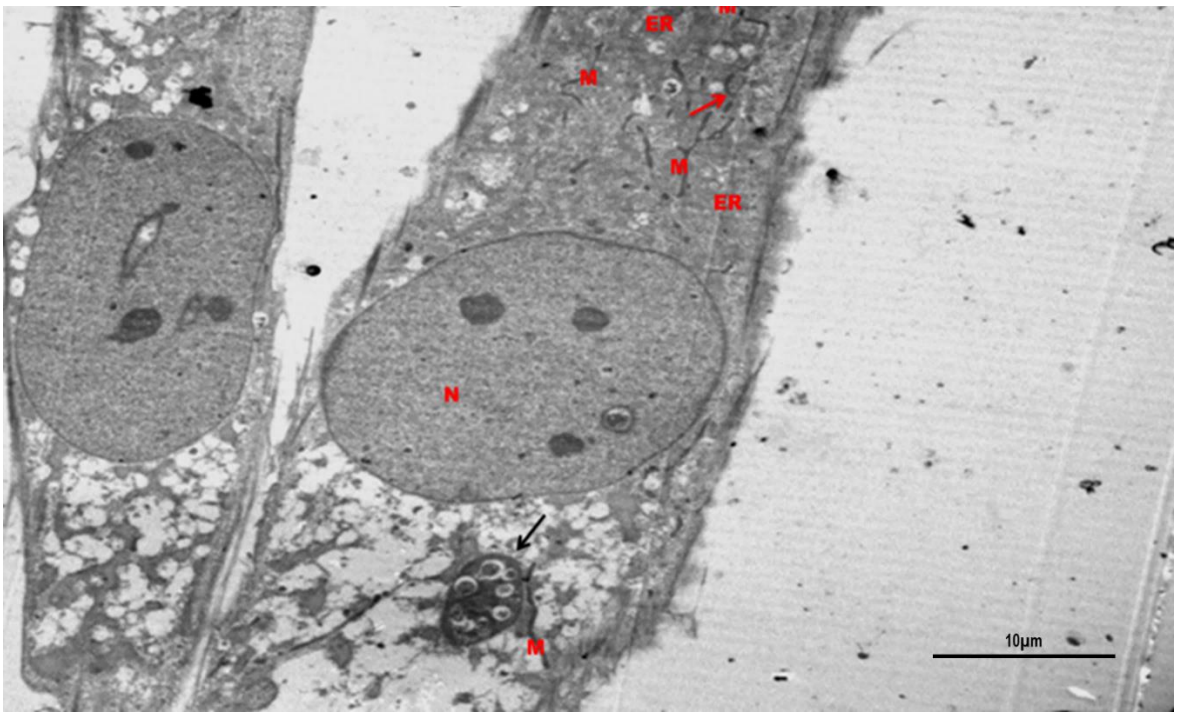

Figure 5.31. BM-hMSCs after incubation under IH culture condition

BM-hMSCs after 14 day incubation at IH culture. TEM image was taken and analysed using TEM software. The image revealed that MSCs have an intact cell membrane with a depleted cytoplasm and disorganised cytoplasmic organelles with apoptotic bodies and large clear vacuoles. Scale= 10 µm.

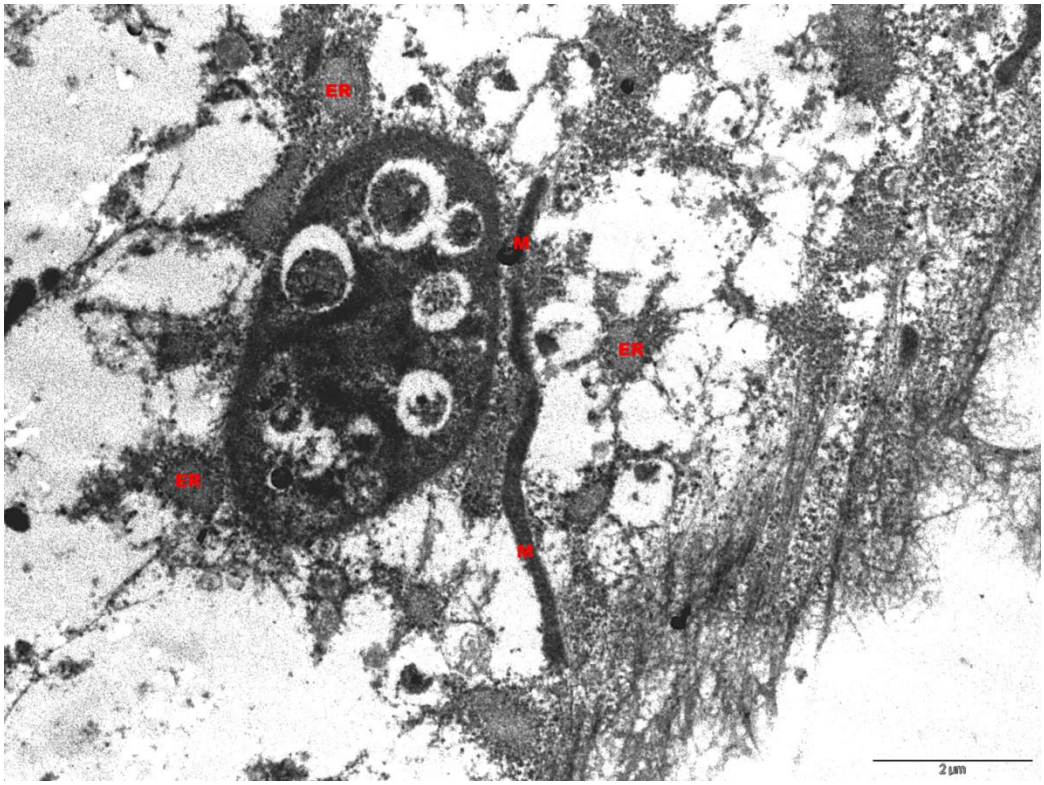

Figure 5.32. BM-hMSCs possess feature like mitophagy after incubation under IH culture condition

BM-hMSCs after 14-days incubation at IH culture. TEM images were taken and analysed using TEM software. The image revealed that mitochondria were engulfed by double-membrane-delimited vesicles and the condensed to circular structure and the vesicles merged to form lager structure. Scale= 2 µm.

5.4. Discussion

Mitochondria are the most dynamic organelles inside the cell that response to different cell's demand such as energy production, oxygen presence and ROS status. Mitochondria continuously undergo structural remodelling and this dynamic activity plays major role in regulation of several vital cellular activities such as cell cycle, autophagy, and age-related diseases. In PC12 cells IH significantly reduce mitochondrial burden with significant increase in mitochondrial genome copy number that result increase in mitochondrial action potential this agree with results obtained by Onyango *et al.,* (2010) but disagree with Li *et al.,* (2015) who described significant reduction in mitochondrial mass and action potential. Many studies discussed the possible mechanisms of this effect. Oxygen level changes suppress mitochondrial biogenesis, so reduce mitochondrial mass. Suppression of mitochondrial biogenesis involve replication of the mtDNA and harmonise expression of many nuclear/ mitochondrial encoded genes such PGC-1α. PGC-1α is the master regulator of all mitochondrial biogenesis aspects, as it regulate respiratory chain and fatty acid oxidation genes, increased mitochondrial number, mtDNA replication, and augmentation of mitochondrial respiratory capacity by direct interaction with and co-activation of PPARs, the nuclear respiratory factors NRFs, and estrogen-related receptors ERRs (Scarpulla *et al.,* 2012). PGC-1α activity is control by oxygen, and cellular energy balance at both the transcriptional and posttranslational level (Dominy *et al.,* 2010). In addition, PGC-1β and PRC have the similar role on mitochondrial biogenesis (Scarpulla *et al.,* 2012). Low oxygen also reduces mitochondrial ROS formation by optimising respiration efficiency through inducing cytochrome c oxidase (COX) subunit IV isoform 2 (COX4-2) and the mitochondrial protease LONP1, which degrades the less efficient COX4-1 (Fukuda *et al.,* 2007)

Our results revealed that despite the HMAs does not follow the hypoxia pattern, but they have no effect on mitochondrial mass and copy number with significant reduction in

mitochondrial action potential and this agree with (Neitemeier *et al.,* 2016; Niatsetskaya *et al.,* 2010).

Bone marrow-derived mesenchymal stem cells present good therapeutic tool in treatment in many disease conditions. Oxygen level changes lead to reduction in mitochondrial mass and genome copy number with compensatory elevation in mitochondrial action potential and may be related to reduction in Mfn-2 activity. Mfn-2 is the regulator of mitochondrial mass, membrane potential, and glucose oxidation. Mfn-2 induces aggregation of small mitochondrial clusters of fragmented mitochondria (Kawalec *et al.,* 2015) which is functionally impaired and release cytochrome c to the cytosol, thus leading to apoptotic cell death and this agree with Wang *et al.,* (2016) and disagree with Stab *et al.,* (2016). HMAs (except IOX2) reduced mitochondrial mass and action potential under all oxygen culture condition with increase in mitochondrial genome copy number and this may be related also to the reduction Mfn-2 activity that reduced mitochondrial mass, membrane potential, and glucose oxidation (Wang *et al.,* 2016) lead to production of non-functional mitochondria and this result disagree with Zhang *et al.,* (2014).

We found that mitochondrial potential directly correlated to HIF-1α changes and this may have related to inhibition of the mitochondrial F_0 F_1-ATPase leads to an increase in the mitochondrial membrane potential and slowing down of electron transport (Gong & Agani ,2005; Hagen, 2012). The number of mitochondria per cell change according to the energy demands, oxygen availability and oxidative stress inside the cell, so the copy number of mitochondrial DNA (mtDNA) can vary depending upon the energy needs of a cell (Shay *et al.,* 1990) and oxidative stress conditions (Lee & Wei, 2005). HMAs change mitochondrial genome copy number in way not matches any oxygen culture condition and this different mechanism of action.

Now we can have stated that HMAs does not mimic effect different oxygen culture condition, thus further work will focus on the effect of changes in oxygen culture condition

on MSCs ultrastructure and as we previously proposed that HIF-α signaling affects mitochondrial biogenesis, shape, size and function.

In this study, we described the effect of different oxygen culture condition on ultrastructure of BM-hMSCs the results revealed that with HIF-1α change is directly related to mitochondria density/ cell, this result was in line with Mason *et al.,* (2004) study. In addition, the AO and IH culture significantly lower mitochondrial volume fraction that reflecting in the images.

5.5. Conclusion

This study suggested that each hypoxia mimetic agents induced significantly different pattern of mitochondrial burden, action potential and genome copy number from that seen at three oxygen culture condition. In addition, preconditioning MSCs cell with 2% IH produce more serious damage that was noticed with CN.

Keele University

Chapter 6 : Summative discussion, conclusions and future works

6.1. Summative discussion

During the review of literature and the practical laboratory work in this thesis we are facing many controversies in the terminology or definition of oxygen culture condition. Many studies described 21% oxygen as normoxia (Höhler *et al.,* 1999; Tai *et al.,* 2009; Naranjo-Suarez *et al.,* 2012; Boyette *et al.,* 2014; Teixeira *et al.* 2015), whereas, oxygen culture condition lower than 21% oxygen defined as hypoxia (Mohyeldin *et al.,* 2010; Ejtehadifar *et al.,* 2015; Widowati *et al.,* 2015; El-Moataz *et al.,* 2016;). Cells grow *in vivo* at oxygen level much lower than 21%, thus, hypoxia definition is inapplicable. In this work, air oxygen culture term used to describe the 21% oxygen culture condition. Throughout this work, air oxygen culture induced some changes on specific cellular activities different from that we find at continuous 2% oxygen culture, which mimics the native in vivo growth environment. *In vivo, cells* are exposed to different oxygen concentrations and this depends on many factors, such as location, vasculaturisation and cell function. In order to mimic an *in vivo* environment, *in vitro* conditions should have the similar oxygen levels. BM-hMSCs grow in 1.4 - 4.2% oxygen level (Spencer *et al.,* 2014) *in vivo*, hence *in vitro* oxygen levels should be comparable. We have used a continuous control oxygen workstation in the form of an hypoxic incubator to generate useful information about cell survival and behaviour under continuous 2% oxygen culture, referred to throughout this thesis as continuous normoxia (CN). IH also represents cell growth at 2% oxygen, however oxygen levels under this condition change as result of the incubator door opening (not more 5 min./ open). This condition aimed to mimic hypoxia/reoxygenation found after ischaemia *in vivo*.

From early 1970s, Ian Richter *et al.,* (1972), Packer and Fuehr (1978) described the effect of low oxygen on the plating efficiency (which is reflect the number of colonies originating from single cells) and lifespan of human cells. Since that time, researchers continued to focus more on the biology of physiological oxygen concentration and how it affects cells, despite that, low oxygen culture conditions have not received much attention.

The term hypoxia mimetic agents does not really reflect the role of these chemical agents in cell behaviour as these agents may induce HIF-1α expression. However, they induce variable expression of HIF-2α and change many other cellular activities including; attenuating cell proliferation, apoptosis, interruption of the cell cycle, changes in ROS production and changes in mitochondrial biogenesis. Based on this, it would be more logical to call them HIF-1α inducer rather than hypoxia mimetic, as the results from this thesis suggest that HMAs donot recapture all aspects of hypoxia response that we have noticed under both IH and CN.

Preconditioning is another term used to describe exposing cells to brief hypoxia or anoxia, which makes cells more resistant to subsequent oxygen stress. this helps to enhance the effectiveness of transplantation therapies by improving cell survival, increasing the production of paracrine factors and a reducing the inflammatory gene expression (Kloner *et al.,* 2006; Haider & Ashraf, 2008; Wei *et al.,* 2016;). Pharmacological hypoxia of cells with hypoxia mimetic agents does not fit the principle of preconditioning, as this work found that these agents did not recapture patterns that we noticed at IH or CN culture conditions. Our results demonstrate that HMAs reduce proliferation, induced cell apoptosis and changed both cell cycle and ROS formation. This is in agreement with a number of literature sources (Guo *et al.,* 2006; Yang *et al.,* 2008; Lopez-Sánchez *et al.,* 2014; Mansfield *et al.,* 2005; Correia & Moreira, 2010).

After dose screening for HMAs and HIF analyses by flow cytometer, the outcome of the PC12 model, showed that HIF-1α expression was induced in much lower doses than stated in majority of works that involve HMAs for treatment of cultured cells (Boorn, 2010; Najafi & Sharifi, 2013; Peng *et al.,* 2014; Wu *et al.,* 2014; Ciavarella *et al.,* 2015; Liu *et al.,* 2015). Interstingly, even at these lower doses adverse effect on cellular viability and metabolic activity is comparable with that reported in the literature. We suggest that HMAs at used concentraton does not activite the full spectrum of hypoxia response and this may explain adverse effect of these on cellular viability and metabolic activity. This study also

showed that HMAs induce HIF-1α expression under both AO and CN culture conditions. In addition, HMAs induced HIF-2α after 96 hrs under all oxygen culture condition, and this related to the ability of these agents to inhibit PHD activity (section 4.3.2). This is also in good agreement with previous work studying these pathways (Gao *et al.,* 2004; Tai *et al.,* 2009; Yuan *et al.,* 2014; Choi *et al.,* 2016; Wigerup *et al.,* 2016).

Additionally, HMAs appeared to affect apoptosis under all culture conditions. This may be related to the elevation in HIF-1α expression, which initiates hypoxia-mediated-apoptosis by enhancing the expression of Bcl-2 binding proteins (BNIP-3 and NIX) Tai *et al.,* (2009), Zeno *et al.* (2012), Hashimoto-Torii *et al.,* (2014) and Neitemeier *et al.,* (2017). Under all culture conditions, HMAs trapped cells in G0/G1 phase, effectivly reducing the number of cells in G2-M phase. This may be related HIF-1α stabilised p53 activating p21, a pro-apoptotic protein (Holzwarth *et al.,* 2010; Zeng *et al.,* 2011).

HMAs increased electron leak from the ETC, leading to an elevation in ROS formation (Khan *et al.,* 2012). This suggests that under IH culture, HMAs induce ROS formation and nitroreductase activity. This could be due to up regulation of activator protein-1 (AP-1) or nuclear factor kappa B (NF-κB) that harmonise the expression and function of cell cycle regulators cyclin D1, p53 and p21 (Toffoli & Michiels, 2008).

The major problem facing the clinical implementation of MSCs is the low yield of these cells from bone marrow aspirates. Based on our findings, *in vitro* expansion under continuous normoxia, or alternatively using HMAs could improve the expansion capacity and quality of therapeutic cells doses (section 4.3.3).

After the initial work studying PC12, we repeated dose screening experiments in BM-hMSCs, ensuring that the doses used did not adversely cell viability but still induced HIF-1α expression. These results showed that HIF-1α was induced in much lower doses than that stated in the literature (Boorn, 2010; Najafi & Sharifi, 2013; Wu *et al.,* 2013; Peng *et al.,* 2014; Liu *et al.,* 2015; Ciavarella *et al.,* 2016; Yoo *et al.,* 2016). Our results reflect the

effect of higher doses used in these studies, which showed dose-dependent adverse effect pattren on cellular viability and biological activities. Our results showed that MSCs cultured under IH, CN and HMAs at AO culture enhance the recovery (section 4.3.3) and this is in agreement with a recent similar study (Ge *et al.,* 2016) Prolonging MSCs survival after transplantation has been shown to be important for potential treatments of the ischemic heart (Hu et al. 2008; Wang *et al.,* 2008) and ischemic brain (Theus *et al.,* 2008). Our results are also in agreement with Yang *et al.,* (2011) who described the recovery enhancement of BM-MSCs aspirates upon exposure to IH and CN conditions, compared with AO culture. This may be related to HIF-1α increases the proliferation of MSCs through the enhancement of TWIST expression, which downregulates the E2A-p21 pathway. Moreover HIF-1α maintain MSCs survival by activating glucose 6-phosphate transporter (G6PT) to increase their metabolic flexibility (Yang *et al.,* 2011).

Iron dependent HMAs ($CoCl_2$ and DFO) reduced MSCs proliferation when compared with 2-OG (2-oxoglutarate) analogues, which had no effect on MSCs proliferation (section 4.3.1). This may be related to the iron-dependent mechanism of action of these drugs, which reduces many iron-dependent enzymes involved in the critical citric acid cycle enzyme aconitase via a translational mechanism involving iron regulatory protein activity, thus influencing the citric acid cycle and oxidative phosphorylation (Oexle *et al.,* 1999).

This study also identified a difference between cell count and MTT activity of the cells grown at IH and CN. Such effects may be related to the inhibition of mitochondrial activity by HIF-1α stabilisation during changes in oxygen levels. This has been shown to affect the production of NAD(P)H which plays an important role in MTT reagent reduction in NAD(P)H-dehydrogenase (Natarajan and Becker, 2012). Under IH conditions, expression of HIF-1α increased, which is commonly reported in the literature (Semenza, 2007; Kaelin *et al.,* 2008; Ježek *et al.,* 2010). HIF-1 upregulates numerous downstream target genes, including those whose products phosphorylate and downregulate the activity of the pyruvate dehydrogenase complex (PDC) (Kim *et al.,* 2006; Papandreou *et al.,* 2006;

Semenza, 2007; Lu *et al.,* 2008). The inhibition of PDC is a key regulator of mitochondrial oxidative metabolism depression under IH (Kim *et al.,* 2006; Papandreou *et al.,* 2006; Ježek *et al.,* 2010). Interestingly, more variation was noticed after treatment with HMAs and this may be related to the different mechanism of action of these agents as those who replace or chelate iron could also affect many downstream events such as mitochondrial pyruvate dehydrogenase (Borcar *et al.,* 2013). Based on these findings, the use of HMAs could not be a viable alternative to engineered control oxygen technique. However, if there no other option, drug selection will require stringent quality control assesment to thoroughly evaluate cell behaviour. HMA treated cells showed more distinct changes in metabolic activity compared with cells cultured under both CN and IH conditions. This may have related to the inhibition of mitochondrial activity by HIF-1α stabilisation which showed higher elevation at IH during changes in oxygen levels. This will affect the production of NAD(P)H, which as stated previously, plays important role in MTT reagent reduction (Yuan *et al.,* 2011).

Following the metabolic profiling of our different treatments, we sought to clarify how the differentiation potential of BM-MSCs was affected. This was assessed using histological and immunostaining methods. The results of this study showed that HMAs + AO and CN inhibited osteogenesis in BM-hMSCs after 21 days (section 4.3.4) This could be due to HIF elevation inhibit the osteogenic differentiation of MSCs by decreasing the expression of RUNX2. (Yang *et al.,* 2011). Our result was in agreement with Park *et al.,* (2009) study. Our results then showed that both CN and HMAs under all culture conditions (except IH) increased adipogenesis. This could be due to upregulation of the signalling from Wnt and Rho, shown to be important in the initiation of adipogenic differentiation (Ge *et al.,* 2016). Terminal differentiation of preadipocytes is induced by activation of peroxisome proliferator-activated receptor-γ (PPARγ) which is in coordination with CCAAT/enhancer-binding protein transcription factor, which maintains adipocyte gene expression (Cristancho & Lazar, 2011). Finally, we showed an elevation in chondrogenesis after

culture in CN even after treatment with HMAs in comparison to control AO. No significant effect of HMAs was seen at AO and IH culture condition (except IOX2 at IH). Under CN culture condition HMAs had no significant effect on chondrogenesis (except DFO) and this disagree with Lee *et al.,* (2015) who have shown hypoxia-enhanced chondrogenesis of BM-MSCs occurs via activation of the mitogen-activated protein kinase p38 pathway.

Many studies have focused on the possible mechanisms involved in HMAs-induced early apoptosis in MSCs under AO culture condition (Sermeus & Michiels, 2011; Zeng *et al.,* 2011; Tang *et al.,* 2014; Ge *et al.,* 2016; Li *et al.,* 2017). HMAs affect an array of proapoptotic proteins by activating the dissociation p53/murine double minute 2 (MDM2) complex, enabling p53 binding to pro-apoptotic proteins, including PUMA, NOXA, CD95, Apaf-1, Bax, Bid and caspases (Green & Kroemer 2009). In addition, p53 has the ability to induce autophagy by activation of damage-regulated autophagy modulator (DRAM). In agreement with our results, these studies have confirmed that HMAs affect apoptosis, possible through a p53-dependent mechanism. In IH and CN cultures, HMAs significant reduction in early apoptosis and cellular necrosis. This may be related to survivin expression (Semenza, 2010) and downregulation of Bax, Bid and caspases. Moreover, p53 induces autophagy by DRAM and upregulation of beclin-1, BNIP-3 and NIX (Mazure & Pouysségur, 2010). TEM imaging confirmed apoptosis in hMSCs, which could be related phosphatidylinositol `3-kinase PI3K/Akt/mTOR cascade (Zhang *et al.,* 2016; Zhou *et al.,* 2011).

Cell cycle analysis showed that under CN culture condition S phase was reduced and G2-M phase was elevated with no significant effect on G0/G1 phase and this may have related to inactivation of enzymes responsible for nucleotide synthesis, ultimately inhibiting DNA replication (Semenza *et al.,* 1994). In contrast HMAs trapped cells in G0/G1 phase and this may have related to induces cell cycle arrest that may exert a markerbiliy different pattern of regulation at various cell cycle checkpoint genes such as ataxia telangiectasia mutated (ATM), ataxia telangiectasia and Rad3 related (ATR), p53,

p21, p27 and p21 (Chen *et al.,* 2013) another possible mechanism is modulation of p53 activity. p53 plays an important role in regulating cell cycle progression at G1 and G2 checkpoints. Specifically, in response to DNA damage, activation of molecular pathways regulated by p53, leads to cell cycle arrest at G0/G1 (Obacz *et al.,* 2013). Furthermore, more recently it has been reported that expression of a p53 is involved in cell cycle arrest at G2 in response to different cell stress conditions, including endoplasmic reticulum stress, unfolded protein response and hypoxia (Obacz *et al.,* 2013).

Our results suggestes showed that ROS formation significantly increased after CN culture and after DMOG treatment in both AO and IH conditions. while in CN culture DFO, DMOG and IOX2 reduced ROS formation (Loboda *et al.,* 2009; Chung *et al.,* 2014). Controversies was noticed in the studies related to ROS formation in hypoxia, in which some studies showed a significant increase in ROS formation (Loboda *et al.,* 2009; Chung *et al.,* 2014Bell *et al.,* 2007), while other works showed a decrease in ROS formation (Vaux *et al.,* 2001; Agani *et al.,* 2000; Callapina *et al.,* 2005). The elevation in HIF-1α expression contributes to ROS formation specifically the mitochondrial ROS (Agani *et al.,* 2000). However, other studies have demonstrated a CN decrease in HIF-1α with increasing ROS and this was in agreement with our results and this may be related to induction of superoxide generator which elevate ROS formation, HIF-1 is downregulated, as PHD activity is upregulated (Wartenberg *et al.,* 2003; Callapina *et al.,* 2005) and this can be representing feed-forward loop, where ROS reduce HIF-1 by upregulation of PHD2 or by donating oxygen in hypoxic condition. HMAs under AO culture condition significantly increase ROS formation and this may be related to the inhibit PHD activity and induce mitochondrial changes that lead to produce more H_2O_2 due to electron leaking from respiratory chain (Granger & Kvietys, 2015).

Under IH condition, iron-dependent HMAs ($CoCl_2$ and DFO) reduced ROS formation and this may be related to an iron-dependent mechanism; in contrast to 2-oxoglutarat analogue (DMOG and IOX2) which elevated ROS formation. This was disagreeing with

Boorn (2010) study. Under CN culture condition, HMAs reduced ROS formation and this may be related to the reduction in mitochondrial mass, as these agents increase mitochondrial autophagy when it combined with adaptive response to chronic hypoxia. This was in agreement with Prabhakar & Semenza (2012) and Schönenberger & Kovacs (2015) studies.

Nitroreductases are a family of flavin-dependent enzymes which facilitate the conversion of nitro-groups to amines or hydroxylamines, depending on NAD(P)H as an electron donor and as hypoxia upregulate number of genes that results a redox potential shift by switch from oxidative phosphorylation to glycolysis with increase in NAD(P)H production (Wheaton & Chandel, 2011; Brocato *et al.,* 2014) that cause significantly elevated reductive stress, causing upregulation in nitroreductase activity (Krohn *et al.,* 2008; Li *et al.,* 2013) and this was in agreement with the results of our study.

Mitochondrial dynamic analysis showed that IH reduced mitochondrial burden and mitochondrial genome copy number in comparison to AO cultured cells and this may be related elevation in autophagic activity (Mathew *et al.,* 2013, Chen *et al.,* 2014) and this result agreed with Rocheteau *et al.,* (2015). HMAs (except IOX2) under AO culture condition, reduced mitochondrial burden but not mitochondrial genome copy number and this may be related to production of inactive mitochondria (Bigarella *et al.,* 2014).

our result also showed that under AO condition HMAs decreasing mitochondrial membrane potential and this associated with increases the ROS production is which is commonly reported in the literature (Sena & Chandel, 2012; Cai *et al.,* 2016; Yang *et al.,* 2015). From all above, IH and HMAs induced morphology changes of mitochondria with lower metabolic activity, as determined by lower mitochondrial burden and action potential and this agree with results obtained by Simsek *et al.,* (2010). The novel HMA (IOX2) at used concentration follow same path of the other HMAs in changing the measured parameter.

6.2. Conclusions

The results presented in this thesis demonstrate that continuous normoxia has a positive impact on the growth profiles of multipotent stem cells and that attenuation of ROS production increases cell proliferation even further. Different avenues were explored to test the hypothesis that HMAs mimic oxygen control engineering. HMAs induced both HIF-1α and HIF-2α under AO culture even with low doses that were used in this work. These agents elevate MSCs proliferation but lower than does with CN. These agents change apoptosis, cell cycle patterns and mitochondrial dynamic and morphology. HMAs fail to recapture the biology activities that found in IH. Rely on the above evidence, application of these agents on cells associated with no additive but many adverse effects in comparison to oxygen control culture. In addition, culture of multipotent stem cells with 2% oxygen IH cause significant damage in comparison to CN and this create an obstacle in clinical application of multipotent stem cells in degenerative medicine.

6.3. Future perspectives

The results of this thesis raised many considerations for the future work as detailed below. In order to ensure a successful preconditioning for cultured MSCs. Future study can focus on the difference between oxygen cultured cells and these cultured by HMAs in animal model to obtained better knowledge of how these cells behave inside live system and what are the main difference between the two methods of preconditioning. More work can be done on effect of HMAs on inducing MSCs neurogenic differentiation *in vitro* and *in vivo* model which will help in treatment of many neurological disorder. Further work also

can examine the effects of HMAs on the mitochondria morphology using TEM (which was stopped due to limitations in time and finance) with addition of more autophagic markers. Moreover, future work can focus on the effects of each preconditioning technique on MSCs secretome which is considered new option as immunomodulator in treatment of autoimmune diseases. The current experience with hypoxia using oxygen control engineering will help in developing unbiased model for obesity and metabolic syndrome using cell culture. Moreover, this work gives a base for future work that explain the role of HIF pathway activation by iron chelating agents in patient with thalassemia major a condition that common in Mediterranean area.

The preconditioning of MSCs in 2% oxygen CN represents the best method for preconditioning in comparison to IH preconditioning which is the method use for preconditioning in many centres around the world.

Keele University

References

Abdelwahid, E., Kalvelyte, A., Stulpinas, A., de Carvalho, K. A. T., Guarita-Souza S., *et al.* (2016) 'Stem cell death and survival in heart regeneration and repair.', Apoptosis: an international journal on programmed cell death. NIH Public Access, 21(3), pp. 252–68. doi: 10.1007/s10495-015-1203-4.

Abdollahi, A., Hahnfeldt, P., Maercker, C., Gröne, H.-J., Debus, J., *et al.* (2004) 'Endostatin's antiangiogenic signaling network.', Molecular cell, 13(5), pp. 649–63. Available at: http://www.ncbi.nlm.nih.gov/pubmed/15023336 (Accessed: 26 July 2017).

Agani, F. H., Pichiule, P., Chavez, J. C. and LaManna, J. C. (2000) 'The Role of Mitochondria in the Regulation of Hypoxia-inducible Factor 1 Expression during Hypoxia', Journal of Biological Chemistry, 275(46), pp. 35863–35867. doi: 10.1074/jbc.M005643200.

Ahmad, T., Kumar, M., Mabalirajan, U., Pattnaik, B., Aggarwal, S., *et al.* (2012) 'Hypoxia Response in Asthma', American Journal of Respiratory Cell and Molecular Biology, 47(1), pp. 1–10. doi: 10.1165/rcmb.2011-0203OC.

Akiyama, K., Chen, C., Wang, D., Xu, X., Qu, C., *et al.* (2012) 'Mesenchymal-stem-cell-induced immunoregulation involves FAS-ligand-/FAS-mediated T cell apoptosis.', Cell stem cell. NIH Public Access, 10(5), pp. 544–55. doi: 10.1016/j.stem.2012.03.007.

Allen, J. W. A. (2011) 'Cytochrome c biogenesis in mitochondria - Systems III and V', FEBS Journal, 278(22), pp. 4198–4216. doi: 10.1111/j.1742-4658.2011.08231.x.

Aloe, L., Calissano, P., Levi-Montalcini, R. and Micera, A. (1982) 'Effects of oral administration of nerve growth factor and of its antiserum on sympathetic ganglia of neonatal mice', Developmental Brain Research. BioMed Central, 4(1), pp. 31–34. doi: 10.1016/0165-3806(82)90094-3.

Alonso, M., Melani, M., Converso, D., Jaitovich, A., Paz, C., *et al.* (2004) 'Mitochondrial extracellular signal-regulated kinases 1/2 (ERK1/2) are modulated during brain development', Journal of Neurochemistry. Blackwell Science Ltd, 89(1), pp. 248–256. doi: 10.1111/j.1471-4159.2004.02323.x.

Anderson, S., Bankier, A. T., Barrell, B. G., de Bruijn, M. H., Coulson, A. R., *et al.* (1981) 'Sequence and organization of the human mitochondrial genome.', Nature, 290(5806), pp. 457–65. Available at: http://www.ncbi.nlm.nih.gov/pubmed/7219534 (Accessed: 25 July 2017).

Ang, S. O., Chen, H., Hirota, K., Gordeuk, V. R., Jelinek, J., *et al*. (2002) 'Disruption of oxygen homeostasis underlies congenital Chuvash polycythemia', Nature Genetics. Nature Publishing Group, 32(4), pp. 614–621. doi: 10.1038/ng1019.

Antico Arciuch, V. G., Elguero, M. E., Poderoso, J. J. and Carreras, M. C. (2012) 'Mitochondrial regulation of cell cycle and proliferation.', Antioxidants & redox signaling. Mary Ann Liebert, Inc., 16(10), pp. 1150–80. doi: 10.1089/ars.2011.4085.

Aprelikova, O., Wood, M., Tackett, S., Chandramouli, G. V. R. and Barrett, J. C. (2006) 'Role of ETS Transcription Factors in the Hypoxia-Inducible Factor-2 Target Gene Selection', Cancer Research, 66(11).

Aragonés, J., Schneider, M., Van Geyte, K., Fraisl, P., Dresselaers, T., *et al.* (2008) 'Deficiency or inhibition of oxygen sensor Phd1 induces hypoxia tolerance by reprogramming basal metabolism', Nature Genetics. Nature Publishing Group, 40(2), pp. 170–180. doi: 10.1038/ng.2007.62.

Avramovich-Tirosh, Y., Amit, T., Bar-Am, O., Zheng, H., Fridkin, M., *et al.* (2007) 'Therapeutic targets and potential of the novel brain- permeable multifunctional iron chelator? monoamine oxidase inhibitor drug, M-30, for the treatment of Alzheimer's disease', Journal of Neurochemistry. Blackwell Publishing Ltd, 100(2), pp. 490–502. doi: 10.1111/j.1471-4159.2006.04258.x.

Baracca A, Barogi S, Paolini S, Lenaz G, Solaini G. (2002) Fluorescence resonance energy transfer between coumarin-derived mitochondrial F(1)-ATPase gamma subunit and pyrenylmaleimide-labelled fragments of IF(1) and c subunit. Biochem J [Internet]. 2002 Feb 15 [cited 2017 Aug 22];362(Pt 1):165–71. Available from: http://www.ncbi.nlm.nih.gov/pubmed/11829753

Balaban, R. S., Nemoto, S. and Finkel, T. (2005) 'Mitochondria, Oxidants, and Aging', Cell, 120(4), pp. 483–495. doi: 10.1016/j.cell.2005.02.001.

Baradaran, R., Berrisford, J. M., Minhas, G. S. and Sazanov, L. A. (2013) 'Crystal structure of the entire respiratory complex I.', Nature. Europe PMC Funders, 494(7438), pp. 443–8. doi: 10.1038/nature11871.

Baranova, O., Miranda, L. F., Pichiule, P., Dragatsis, I., Johnson, R. S. *et al*. (2007) 'Neuron-Specific Inactivation of the Hypoxia Inducible Factor 1α Increases Brain Injury in a Mouse Model of Transient Focal Cerebral Ischemia', Journal of Neuroscience, 27(23). Available at: http://www.jneurosci.org/content/27/23/6320 (Accessed: 24 July 2017).

Baird, L., Swift, S., Llères, D. and Dinkova-Kostova, A. T. (2014) 'Monitoring Keap1-Nrf2 interactions in single live cells.', Biotechnology advances. Elsevier, 32(6), pp. 1133–44. doi: 10.1016/j.biotechadv.2014.03.004.

Barnabas, O., Wang, H. and Gao, X.-M. (2013) 'Role of estrogen in angiogenesis in cardiovascular diseases', Journal of Geriatric Cardiology 377−382 J Geriatr Cardiol, 10(10), pp. 377–382. doi: 10.3969/j.issn.1671-5411.2013.04.008.

Bartels, K., Grenz, A. and Eltzschig, H. K. (2013) 'Hypoxia and inflammation are two sides of the same coin.', Proceedings of the National Academy of Sciences of the United States of America. National Academy of Sciences, 110(46), pp. 18351–2. doi: 10.1073/pnas.1318345110.

Basciano, L., Nemos, C., Foliguet, B., De Isla, N., De Carvalho, M., *et al.* (2011) 'Long term culture of mesenchymal stem cells in hypoxia promotes a genetic program maintaining their undifferentiated and multipotent status'. doi: 10.1186/1471-2121-12-12.

Bell, E. L., Klimova, T. A., Eisenbart, J., Schumacker, P. T. and Chandel, N. S. (2007) 'Mitochondrial reactive oxygen species trigger hypoxia-inducible factor-dependent extension of the replicative life span during hypoxia.', Molecular and cellular biology. American Society for Microbiology (ASM), 27(16), pp. 5737–45. doi: 10.1128/MCB.02265-06.

Berdanier, C. (ed.) (2005) Mitochondria in Health and Disease. CRC Press (Oxidative Stress and Disease). doi: 10.1201/9781420028843.

Berniakovich, I. and Giorgio, M. (2013) 'Low Oxygen Tension Maintains Multipotency, Whereas Normoxia Increases Differentiation of Mouse Bone Marrow Stromal Cells', International Journal of Molecular Sciences, 14(1), pp. 2119–2134. doi: 10.3390/ijms14012119.

Betz, C., Stracka, D., Prescianotto-Baschong, C., Frieden, M., Demaurex, N. and Hall, M. N. (no date) 'mTOR complex 2-Akt signaling at mitochondria- associated

endoplasmic reticulum membranes (MAM) regulates mitochondrial physiology'. doi: 10.1073/pnas.1302455110.

Bhattacharyya, A., Chattopadhyay, R., Mitra, S. and Crowe, S. E. (2014) 'Oxidative stress: an essential factor in the pathogenesis of gastrointestinal mucosal diseases.', Physiological reviews. American Physiological Society, 94(2), pp. 329–54. doi: 10.1152/physrev.00040.2012.

Bigarella, C. L., Liang, R. and Ghaffari, S. (2014) 'Stem cells and the impact of ROS signaling.', Development (Cambridge, England). Company of Biologists, 141(22), pp. 4206–18. doi: 10.1242/dev.107086.

Blagosklonny, M. V. and Pardee, A. B. (2013) 'The Restriction Point of the Cell Cycle'. Landes Bioscience. Available at: https://www.ncbi.nlm.nih.gov/books/NBK6318/ (Accessed: 26 July 2017).

Boddy, J. L., Fox, S. B., Han, C., Campo, L., Turley, H., Kanga, S., Malone, P. R. and Harris, A. L. (2005) 'The Androgen Receptor Is Significantly Associated with Vascular Endothelial Growth Factor and Hypoxia Sensing via Hypoxia-Inducible Factors HIF-1a, HIF-2a, and the Prolyl Hydroxylases in Human Prostate Cancer', Clinical Cancer Research, 11(21).

Bogdanova, A., Petrushanko, I. Y., Hernansanz-Agustín, P. and Martínez-Ruiz, A. (2016) '& quot; Oxygen Sensing & quot; by Na, K-ATPase: These Miraculous Thiols.', Frontiers in physiology. Frontiers Media SA, 7, p. 314. doi: 10.3389/fphys.2016.00314.

Bolisetty, S. and Jaimes, E. A. (2013) 'Mitochondria and reactive oxygen species: physiology and pathophysiology.', International journal of molecular sciences. Multidisciplinary Digital Publishing Institute (MDPI), 14(3), pp. 6306–44. doi: 10.3390/ijms14036306.

Boorn, L. S. (2010) 'The role of reactive oxygen species in the stabilisation of hypoxia-inducible factor-1α (HIF-1α)'. Available at: http://discovery.ucl.ac.uk/758259/1/758259.pdf (Accessed: 28 June 2017).

Borcar, A., Menze, M. A., Toner, M. and Hand, S. C. (2013) 'Metabolic Preconditioning of Mammalian Cells: Mimetic Agents for Hypoxia Lack Fidelity in Promoting Phosphorylation of Pyruvate Dehydrogenase'. doi: 10.1007/s00441-012-1517-2.

Bordoli, M. R., Stiehl, D. P., Borsig, L., Kristiansen, G., Hausladen, S., *et al.* (2011) 'Prolyl-4-hydroxylase PHD2- and hypoxia-inducible factor 2-dependent regulation of amphiregulin contributes to breast tumorigenesis', Oncogene. Nature Publishing Group, 30(5), pp. 548–560. doi: 10.1038/onc.2010.433.

Boregowda, S. V, Krishnappa, V., Chambers, J. W., Lograsso, P. V, Lai, W.-T., *et al.* (2012) 'Atmospheric oxygen inhibits growth and differentiation of marrow-derived mouse mesenchymal stem cells via a p53-dependent mechanism: implications for long-term culture expansion.', Stem cells (Dayton, Ohio). NIH Public Access, 30(5), pp. 975–87. doi: 10.1002/stem.1069.

Bosetti F, Brizzi F, Barogi S, Mancuso M, Siciliano G, *et al.* (2002) Cytochrome c oxidase and mitochondrial F1F0-ATPase (ATP synthase) activities in platelets and brain from patients with Alzheimer's disease. Neurobiol Aging [Internet]. [cited 2017 Aug 22];23(3):371–6. Available from: http://www.ncbi.nlm.nih.gov/pubmed/11959398

Bossy-Wetzel, E., Talantova, M. V, Lee, W. D., Schölzke, M. N., Harrop, A., *et al.* (2004) 'Crosstalk between Nitric Oxide and Zinc Pathways to Neuronal Cell Death Involving

Mitochondrial Dysfunction and p38-Activated K+ Channels', Neuron, 41(3), pp. 351–365. doi: 10.1016/S0896-6273(04)00015-7.

Boyette, L. B., Creasey, O. A., Guzik, L., Lozito, T. and Tuan, R. S. (2014) 'Human bone marrow-derived mesenchymal stem cells display enhanced clonogenicity but impaired differentiation with hypoxic preconditioning.', Stem cells translational medicine. Wiley-Blackwell, 3(2), pp. 241–54. doi: 10.5966/sctm.2013-0079.

Bradley, T. R., Hodgson, G. S. and Rosendaal, M. (1978) 'The effect of oxygen tension on haemopoietic and fibroblast cell proliferation in vitro', Journal of Cellular Physiology. Wiley Subscription Services, Inc., A Wiley Company, 97(3), pp. 517–522. doi: 10.1002/jcp.1040970327.

Brand, M. D. (2010) 'The sites and topology of mitochondrial superoxide production.', Experimental gerontology. NIH Public Access, 45(7–8), pp. 466–72. doi: 10.1016/j.exger.2010.01.003.

Brocato, J., Chervona, Y. and Costa, M. (2014) 'Molecular responses to hypoxia-inducible factor 1α and beyond.', Molecular pharmacology. American Society for Pharmacology and Experimental Therapeutics, 85(5), pp. 651–7. doi: 10.1124/mol.113.089623.

Brown, G. C. (2001) 'Regulation of mitochondrial respiration by nitric oxide inhibition of cytochrome c oxidase', Biochimica et Biophysica Acta (BBA) - Bioenergetics, 1504(1), pp. 46–57. doi: 10.1016/S0005-2728(00)00238-3.

Brown, T. A., Tkachuk, A. N., Shtengel, G., Kopek, B. G., Bogenhagen, D. F., *et al.* (2011) 'Superresolution fluorescence imaging of mitochondrial nucleoids reveals their spatial range, limits, and membrane interaction.', Molecular and cellular biology. American Society for Microbiology (ASM), 31(24), pp. 4994–5010. doi: 10.1128/MCB.05694-11.

Bruick, R. K. and McKnight, S. L. (2001) 'A Conserved Family of Prolyl-4-Hydroxylases That Modify HIF', Science, 294(5545), pp. 1337–1340. doi: 10.1126/science.1066373.

Brunori M, Giuffrè A, Forte E, Mastronicola D, Barone MC, *et al.* (2003) Control of cytochrome c oxidase activity by nitric oxide. Biochim Biophys Acta - Bioenerg [Internet]. 2004 Apr [cited 2017 Aug 22]; 1655:365–71. Available from: http://linkinghub.elsevier.com/retrieve/pii/S0005272803002093.

Burgering, B. M. and Kops, G. J. P. (2002) 'Cell cycle and death control: long live Forkheads', Trends in Biochemical Sciences, 27(7), pp. 352–360. doi: 10.1016/S0968-0004(02)02113-8.

Bürmann, F., Sawant, P. and Bramkamp, M. (2012) 'Identification of interaction partners of the dynamin-like protein DynA from Bacillus subtilis'. doi: 10.4161/cib.20215.

Cai, J., Wang, J., Huang, Y., Wu, H., Xia, T., *et al.* (2016) 'ERK/Drp1-dependent mitochondrial fission is involved in the MSC-induced drug resistance of T-cell acute lymphoblastic leukemia cells', Cell Death and Disease. Nature Publishing Group, 7(11), p. e2459. doi: 10.1038/cddis.2016.370.

Cai, Y., Yang, L., Hu, G., Chen, X., Niu, F., *et al.* (2016) 'Regulation of morphine-induced synaptic alterations: Role of oxidative stress, ER stress, and autophagy', The Journal of Cell Biology, 215(2), pp. 245–258. doi: 10.1083/jcb.201605065.

Campisi, J., Medrano, E. E., Morreo, G. and Pardeet, A. B. (1982) 'Restriction point control of cell growth by a labile protein: Evidence for increased stability in

transformed cells (animal cells/transformation/protein degradation/cell cycle/growth control)', Cell Biology, 79, pp. 436–440. Available at: http://www.pnas.org/content/79/2/436.full.pdf (Accessed: 25 July 2017).

Cantó, C. and Auwerx, J. (2010) 'AMP-activated protein kinase and its downstream transcriptional pathways', Cellular and Molecular Life Sciences. SP Birkhäuser Verlag Basel, 67(20), pp. 3407–3423. doi: 10.1007/s00018-010-0454-z.

Carmona-Gutierrez, D., Eisenberg, T., Büttner, S., Meisinger, C., Kroemer, G. *et al.* (2010) 'Apoptosis in yeast: triggers, pathways, subroutines', Cell Death and Differentiation. Nature Publishing Group, 17(5), pp. 763–773. doi: 10.1038/cdd.2009.219.

Carreau A, Hafny-Rahbi B El, Matejuk A, Grillon C, Kieda C. (2011) Why is the partial oxygen pressure of human tissues a crucial parameter? Small molecules and hypoxia. J Cell Mol Med [Internet]. 2011 Jun [cited 2017 Aug 26];15(6):1239–53. Available from: http://www.ncbi.nlm.nih.gov/pubmed/21251211

Cartee, T. V, White, K. J., Newton-West, M. and Swerlick, R. A. (2012) 'Hypoxia and hypoxia mimetics inhibit TNF-dependent VCAM1 induction in the 5A32 endothelial cell line via a hypoxia inducible factor dependent mechanism.', Journal of dermatological science. NIH Public Access, 65(2), pp. 86–94. doi: 10.1016/j.jdermsci.2011.10.003.

Chan, D. A. and Giaccia, A. J. (2007) 'Hypoxia, gene expression, and metastasis', Cancer and Metastasis Reviews. Kluwer Academic Publishers-Plenum Publishers, 26(2), pp. 333–339. doi: 10.1007/s10555-007-9063-1.

Chan, D. A., Sutphin, P. D., Denko, N. C. and Giaccia, A. J. (2002) 'Role of prolyl hydroxylation in oncogenically stabilized hypoxia-inducible factor-1alpha.', The Journal of biological chemistry. American Society for Biochemistry and Molecular Biology, 277(42), pp. 40112–7. doi: 10.1074/jbc.M206922200.

Chang, C.-R. and Blackstone, C. (2010) 'Dynamic regulation of mitochondrial fission through modification of the dynamin-related protein Drp1', Annals of the New York Academy of Sciences, 1201(1), pp. 34–39. doi: 10.1111/j.1749-6632.2010.05629.x.

Chang, K.-C. and Hung, S.-C. (2016) 'Hypoxia-preconditioned allogeneic mesenchymal stem cells can be used for myocardial repair in non-human primates.', Journal of thoracic disease. AME Publications, 8(7), pp. E593-5. doi: 10.21037/jtd.2016.05.46.

Chavez, J. C., Baranova, O., Lin, J. and Pichiule, P. (2006) 'The Transcriptional Activator Hypoxia Inducible Factor 2 (HIF-2/EPAS-1) Regulates the Oxygen-Dependent Expression of Erythropoietin in Cortical Astrocytes', Journal of Neuroscience, 26(37).

Chen, R., Jiang, T., She, Y., Xu, J., Li, C., *et al.* (2017) 'Effects of Cobalt Chloride, a Hypoxia-Mimetic Agent, on Autophagy and Atrophy in Skeletal C2C12 Myotubes.', BioMed research international. Hindawi, 2017, p. 7097580. doi: 10.1155/2017/7097580.

Chen, T.-I., Chiu, H.-W., Pan, Y.-C., Hsu, S.-T., Lin, J.-H. *et al.* (no date) 'Intermittent hypoxia-induced protein phosphatase 2A activation reduces PC12 cell proliferation and differentiation'. doi: 10.1186/1423-0127-21-46.

Chen H, Chomyn A, Chan DC. (2005) Disruption of Fusion Results in Mitochondrial Heterogeneity and Dysfunction. J Biol Chem [Internet]. 2005 Jul 15 [cited 2017 Aug 22];280(28):26185–92. Available from: http://www.ncbi.nlm.nih.gov/pubmed /15899 901

Cho, D.-H., Nakamura, T., Fang, J., Cieplak, P., Godzik, A., *et al.* (2009) 'S-Nitrosylation of Drp1 Mediates β-Amyloid–Related Mitochondrial Fission and Neuronal Injury'. doi: 10.1126/science.1171091.

Choi, J. H., Lee, Y. Bin, Jung, J., Hwang, S. G., Oh, I.-H. *et al.* (2016) 'Hypoxia Inducible Factor-1 α Regulates the Migration of Bone Marrow Mesenchymal Stem Cells via Integrin α 4', Stem Cells International. Hindawi, 2016, pp. 1–11. doi: 10.1155/2016/7932185.

Choi, S.-W., Lee, K.-S., Lee, J. H., Kang, H. J., Lee, M. J., *et al.* (2016) 'Suppression of Akt-HIF-1α signaling axis by diacetyl atractylodiol inhibits hypoxia-induced angiogenesis.', BMB reports. Korean Society for Biochemistry and Molecular Biology, 49(9), pp. 508–13. doi: 10.5483/bmbrep.2016.49.9.069.

Chowdhury, R., Candela-Lena, J. I., Chan, M. C., Greenald, D. J., Yeoh, K. K., *et al.* (2013) 'Selective Small Molecule Probes for the Hypoxia Inducible Factor (HIF) Prolyl Hydroxylases', ACS Chemical Biology, 8(7), pp. 1488–1496. doi: 10.1021/cb400088q.

Chowdhury, R., Yeoh, K. K., Tian, Y.-M., Hillringhaus, L., Bagg, E. A., *et al.* (2011) 'The oncometabolite 2-hydroxyglutarate inhibits histone lysine demethylases.', EMBO reports. European Molecular Biology Organization, 12(5), pp. 463–9. doi: 10.1038/embor.2011.43.

Chung, J., Song, M., Ha, C.-W., Kim, J.-A., Lee, C.-H. *et al.* (2014) 'Comparison of articular cartilage repair with different hydrogel-human umbilical cord blood-derived mesenchymal stem cell composites in a rat model', Stem Cell Research & Therapy, 5(2), p. 39. doi: 10.1186/scrt427.

Chuang J-H, Lin T-K, Tai M-H, Liou C-W, Huang S-T, *et al.* (2012) Preferential involvement of mitochondria in Toll-like receptor 3 agonist-induced neuroblastoma cell apoptosis, but not in inhibition of cell growth. Apoptosis [Internet]. 2012 Apr 21 [cited 2017 Aug 22];17(4):335–48. Available from: http://www.ncbi.nlm.nih.gov/pubmed/22187010

Churchill, E. N. and Mochly-Rosen, D. (2007) 'The roles of PKCδ and ϵ isoenzymes in the regulation of myocardial ischaemia/reperfusion injury: Figure 1', Biochemical Society Transactions, 35(5), pp. 1040–1042. doi: 10.1042/BST0351040.

Ciavarella, C., Fittipaldi, S., Pedrini, S., Vasuri, F., Gallitto, E., *et al.* (2015) 'In vitro alteration of physiological parameters do not hamper the growth of human multipotent vascular wall-mesenchymal stem cells.', Frontiers in cell and developmental biology. Frontiers Media SA, 3, p. 36. doi: 10.3389/fcell.2015.00036.

Cioffi, C. L., Qin Liu, X., Kosinski, P. A., Garay, M. and Bowen, B. R. (2003) 'Differential regulation of HIF-1α prolyl-4-hydroxylase genes by hypoxia in human cardiovascular cells', Biochemical and Biophysical Research Communications, 303(3), pp. 947–953. doi: 10.1016/S0006-291X(03)00453-4.

Circu, M. L. and Aw, T. Y. (2010) 'Reactive oxygen species, cellular redox systems, and apoptosis.', Free radical biology & medicine. NIH Public Access, 48(6), pp. 749–62. doi: 10.1016/j.freeradbiomed.2009.12.022.

Claerhout, S., Decraene, D., Van Laethem, A., Van Kelst, S., Agostinis, P. *et al.* (2007) 'AKT Delays the Early-Activated Apoptotic Pathway in UVB-Irradiated Keratinocytes Via BAD Translocation', Journal of Investigative Dermatology, 127(2), pp. 429–438. doi: 10.1038/sj.jid.5700533.

Clanton, T. L. (2007) 'Hypoxia-induced reactive oxygen species formation in skeletal muscle', Journal of Applied Physiology, 102(6).

Coller, H. A., Khrapko, K., Bodyak, N. D., Nekhaeva, E., Herrero-Jimenez, P. and Thilly, W. G. (2001) 'High frequency of homoplasmic mitochondrial DNA mutations in human tumors can be explained without selection', Nature Genetics. Nature Publishing Group, 28(2), pp. 147–150. doi: 10.1038/88859.

Comino-Mendez, I., de Cubas, A. A., Bernal, C., Alvarez-Escola, C., Sanchez-Malo, C., *et al.* (2013) 'Tumoral EPAS1 (HIF2A) mutations explain sporadic pheochromocytoma and paraganglioma in the absence of erythrocytosis', Human Molecular Genetics. Oxford University Press, 22(11), pp. 2169–2176. doi: 10.1093/hmg/ddt069.

Connett, R. J., Honig, C. R., Gayeski, T. E. and Brooks, G. A. (1990) 'Defining hypoxia: a systems view of VO2, glycolysis, energetics, and intracellular PO2', Journal of Applied Physiology, 68(3). Available at: http://jap.physiology.org/content/68/3/833 (Accessed: 24 July 2017).

Cook, E. H. (2010) 'Reduction of increased repetitive self-grooming in ASD mouse model by metabotropic 5 glutamate receptor antagonism; randomized controlled trial of early start denver model', Autism Research. John Wiley & Sons, Inc., 3(1), pp. 40–42. doi: 10.1002/aur.118.

Corcoran, A., O 'connor, J. J., Corcoran, A. and O 'connor, J. (2013) 'Title Hypoxia-inducible factor signaling mechanisms in the central nervous system Hypoxia inducible factor signalling mechanisms in the central nervous system', Acta Physiologica, 208(4), pp. 298–310. doi: 10.1111/apha.12117.

Correia, S. C. and Moreira, P. I. (2010) 'Hypoxia-inducible factor 1: a new hope to counteract neurodegeneration?', Journal of Neurochemistry. Blackwell Publishing Ltd, 112(1), pp. 1–12. doi: 10.1111/j.1471-4159.2009.06443.x.

Crewe, C., An, Y. A. and Scherer, P. E. (2017) 'The ominous triad of adipose tissue dysfunction: inflammation, fibrosis, and impaired angiogenesis', Journal of Clinical Investigation, 127(1), pp. 74–82. doi: 10.1172/JCI88883.

Crispo, J. A. G., Ansell, D. R., Ubriaco, G. and Tai, T. C. (2011) 'Role of reactive oxygen species in the neural and hormonal regulation of the PNMT gene in PC12 cells.', Oxidative medicine and cellular longevity. Hindawi Publishing Corporation, 2011, p. 756938. doi: 10.1155/2011/756938.

Cristancho, A. G. and Lazar, M. A. (2011) 'Forming functional fat: a growing understanding of adipocyte differentiation', Nature Reviews Molecular Cell Biology. Nature Publishing Group, 12(11), pp. 722–734. doi: 10.1038/nrm3198.

Cummins, E. P., Berra, E., Comerford, K. M., Ginouves, A., Fitzgerald, K. T., *et al.* (2006) 'Prolyl hydroxylase-1 negatively regulates IkappaB kinase-beta, giving insight into hypoxia-induced NFkappaB activity.', Proceedings of the National Academy of Sciences of the United States of America. National Academy of Sciences, 103(48), pp. 18154–9. doi: 10.1073/pnas.0602235103.

D'Autréaux, B. and Toledano, M. B. (2007) 'ROS as signalling molecules: mechanisms that generate specificity in ROS homeostasis', Nature Reviews Molecular Cell Biology. Nature Publishing Group, 8(10), pp. 813–824. doi: 10.1038/nrm2256.

Dabrowska, A., Venero, J. L., Iwasawa, R., Hankir, M.-K., Rahman, S., *et al.* (2015) 'PGC-1α controls mitochondrial biogenesis and dynamics in lead-induced neurotoxicity.', Aging. Impact Journals, LLC, 7(9), pp. 629–47. doi: 10.18632/aging.100790.

Dagda, R. K. and Das Banerjee, T. (2015) 'Role of protein kinase A in regulating mitochondrial function and neuronal development: implications to neurodegenerative diseases', Reviews in the Neurosciences. De Gruyter, 26(3), pp. 359–370. doi: 10.1515/revneuro-2014-0085.

Das, R., Jahr, H., van Osch, G. J. V. M. and Farrell, E. (2010) 'The Role of Hypoxia in Bone Marrow–Derived Mesenchymal Stem Cells: Considerations for Regenerative Medicine Approaches', Tissue Engineering Part B: Reviews. Mary Ann Liebert, Inc. 140 Huguenot Street, 3rd Floor New Rochelle, NY 10801 USA, 16(2), pp. 159–168. doi: 10.1089/ten.teb.2009.0296.

Dendorfer, A., Heidbreder, M., Hellwig-Bqrgel, T., Jfhren, O., Qadri, F. *et al*. (2004) 'Deferoxamine induces prolonged cardiac preconditioning via accumulation of oxygen radicals'. doi: 10.1016/j.freeradbiomed.2004.10.015.

Dengler, V. L., Galbraith, M. D. and Espinosa, J. M. (2014) 'Transcriptional regulation by hypoxia inducible factors.', Critical reviews in biochemistry and molecular biology. NIH Public Access, 49(1), pp. 1–15. doi: 10.3109/10409238.2013.838205.

Denu, R. A. and Hematti, P. (2016) 'Effects of Oxidative Stress on Mesenchymal Stem Cell Biology.', Oxidative medicine and cellular longevity. Hindawi, 2016, p. 2989076. doi: 10.1155/2016/2989076.

Dillon, L. M., Williams, S. L., Hida, A., Peacock, J. D., Prolla, T. A., Lincoln, J. and Moraes, C. T. (2012) 'Increased mitochondrial biogenesis in muscle improves aging phenotypes in the mtDNA mutator mouse', Human Molecular Genetics, 21(10), pp. 2288–2297. doi: 10.1093/hmg/dds049.

Di Meo, S., Reed, T. T., Venditti, P. and Victor, V. M. (2016) 'Harmful and Beneficial Role of ROS', Oxidative Medicine and Cellular Longevity, 2016, pp. 1–3. doi: 10.1155/2016/7909186.

Dominy, J. E., Lee, Y., Gerhart-Hines, Z. and Puigserver, P. (2010) 'Nutrient-dependent regulation of PGC-1α's acetylation state and metabolic function through the enzymatic activities of Sirt1/GCN5', Biochimica et Biophysica Acta (BBA) - Proteins and Proteomics, 1804(8), pp. 1676–1683. doi: 10.1016/j.bbapap.2009.11.023.

De Marchi, U., Santo-Domingo, J., Castelbou, C., Sekler, I., Wiederkehr, A. *et al.* (2014) 'NCLX regulates Ca 2+ -driven mitochondrial matrix redox signaling NCLX, but not LETM1, mediates mitochondrial Ca 2+ extrusion thereby limiting Ca 2+ -induced NAD(P)H production and modulating matrix redox state*'. doi: 10.1074/jbc.M113.540898.

Dominy, J. E. and Puigserver, P. (2013) 'Mitochondrial biogenesis through activation of nuclear signaling proteins.', Cold Spring Harbor perspectives in biology. Cold Spring Harbor Laboratory Press, 5(7). doi: 10.1101/cshperspect. a015008.

Dröge, W. (2002) 'Free Radicals in the Physiological Control of Cell Function', Physiological Reviews, 82(1), pp. 47–95. doi: 10.1152/physrev.00018.2001.

Du, Z., Tong, X. and Ye, X. (2013) 'Cyclin D1 promotes cell cycle progression through enhancing NDR1/2 kinase activity independent of cyclin-dependent kinase 4.', The Journal of biological chemistry. American Society for Biochemistry and Molecular Biology, 288(37), pp. 26678–87. doi: 10.1074/jbc.M113.466433.

Duarte, A., Castillo, A. F., Podestá, E. J. and Poderoso, C. (2014) 'Mitochondrial fusion and ERK activity regulate steroidogenic acute regulatory protein localization in mitochondria.', PloS one. Public Library of Science, 9(6), p. e100387. doi: 10.1371/journal.pone.0100387.

Duke, T. (1999) 'Dysoxia and lactate', Archives of Disease in Childhood, 81(4), pp. 343–350. doi: 10.1136/adc.81.4.343.

Duronio, R. J. and Xiong, Y. (2013) 'Signaling pathways that control cell proliferation.', Cold Spring Harbor perspectives in biology. Cold Spring Harbor Laboratory Press, 5(3), p. a008904. doi: 10.1101/cshperspect. a008904.

Eckel, R. H. and Cornier, M.-A. (2014) 'Update on the NCEP ATP-III emerging cardiometabolic risk factors'. Available at: https://bmcmedicine.biomedcentral .com/track/pdf/10.1186/1741-7015-12-115?site=bmcmedicine.biomedcentral.com (Accessed: 24 July 2017).

Eckle, T., Kohler, D., Lehmann, R., El Kasmi, K. C. and Eltzschig, H. K. (2008) 'Hypoxia-Inducible Factor-1 Is Central to Cardioprotection: A New Paradigm for Ischemic Preconditioning', Circulation, 118(2), pp. 166–175. doi: 10.1161/CIRCULATIONAHA.107.758516.

Efremov, R., Rozbehbaradaran and Sazanov, & leonida (2010) 'The architecture of respiratory complex I'. doi: 10.1038/nature09066.

Eisner, V., Cupo, R. R., Gao, E., Csordás, G., Slovinsky, W. S., *et al*. (2017) 'Mitochondrial fusion dynamics is robust in the heart and depends on calcium oscillations and contractile activity.', Proceedings of the National Academy of Sciences of the United States of America. National Academy of Sciences, p. 201617288. doi: 10.1073/pnas.1617288114.

Ejtehadifar, M., Shamsasenjan, K., Movassaghpour, A., Akbarzadehlaleh, P., Dehdilani, N., *et al.* (2015) 'The effect of hypoxia on mesenchymal stem cell biology', Advanced Pharmaceutical Bulletin. doi: 10.15171/apb.2015.021.

El-Moataz, N., Ahmed, B., Murakami, M., Kaneko, S. and Nakashima, M. (2016) 'The effects of hypoxia on the stemness properties of human dental pulp stem cells (DPSCs)'. doi: 10.1038/srep35476.

Elgass, K., Pakay, J., Ryan, M. T. and Palmer, C. S. (2013) 'Recent advances into the understanding of mitochondrial fission', Biochimica et Biophysica Acta (BBA) - Molecular Cell Research, 1833(1), pp. 150–161. doi: 10.1016/j.bbamcr.2012.05.002.

Elmore, S. (2007) 'Apoptosis: a review of programmed cell death.', Toxicologic pathology. NIH Public Access, 35(4), pp. 495–516. doi: 10.1080/01926230701320337.

Ema, M., Taya, S., Yokotani, N., Sogawa, K., Matsuda, Y. *et al.* (1997) 'A novel bHLH-PAS factor with close sequence similarity to hypoxia-inducible factor 1␣ regulates the VEGF expression and is potentially involved in lung and vascular development', Biochemistry, 94, pp. 4273–4278.

Emelyanov, V. V (2003) 'Mitochondrial connection to the origin of the eukaryotic cell.', European journal of biochemistry, 270(8), pp. 1599–618. Available at: http://www.ncbi.nlm.nih.gov/pubmed/12694174 (Accessed: 24 July 2017).

Epstein, C. B., Waddle, J. A., Hale, W., Dave, V., Thornton, J., *et al.* (2001) 'Genome-wide Responses to Mitochondrial Dysfunction', Molecular Biology of the Cell, 12(2), pp. 297–308. doi: 10.1091/mbc.12.2.297.

Erez, N., Milyavsky, M., Eilam, R., Shats, I., Goldfinger, N., *et al.* (2003) 'Expression of Prolyl-Hydroxylase-1 (PHD1/EGLN2) Suppresses Hypoxia Inducible Factor-1α Activation and Inhibits Tumor Growth', Cancer Research, 63(24).

Escobar-Henriques, M. and Langer, T. (2014) 'Dynamic survey of mitochondria by ubiquitin.', EMBO reports. European Molecular Biology Organization, 15(3), pp. 231–43. doi: 10.1002/embr.201338225.

Esfahani, M., Karimi, F., Afshar, S., niknazar, S., Sohrabi, S. *et al.* (2015) 'Prolyl hydroxylase inhibitors act as agents to enhance the efficiency of cell therapy', Expert Opinion on Biological Therapy, 15(12), pp. 1739–1755. doi: 10.1517/14712598.2015.1084281.

Espinosa-Diez, C., Miguel, V., Mennerich, D., Kietzmann, T., Sánchez-Pérez, P., *et al.* (2015) 'Antioxidant responses and cellular adjustments to oxidative stress.', Redox biology. Elsevier, 6, pp. 183–97. doi: 10.1016/j.redox.2015.07.008.

Fan, L., Li, J., Yu, Z., Dang, X. and Wang, K. (2014) 'The hypoxia-inducible factor pathway, prolyl hydroxylase domain protein inhibitors, and their roles in bone repair and regeneration.', BioMed research international. Hindawi, 2014, p. 239356. doi: 10.1155/2014/239356.

Fan, S., Zhang, B., Luan, P., Gu, B., Wan, Q., *et al.* (2015) 'PI3K/AKT/mTOR/p70S6K Pathway Is Involved in A β 25-35-Induced Autophagy', BioMed Research International. Hindawi, 2015, pp. 1–9. doi: 10.1155/2015/161020.

Fan, Y., Wang, L., Liu, C., Zhu, H., Zhou, L., *et al.* (2015) 'Local renin-angiotensin system regulates hypoxia-induced vascular endothelial growth factor synthesis in mesenchymal stem cells.', International journal of clinical and experimental pathology. e-Century Publishing Corporation, 8(3), pp. 2505–14. Available at: http://www.ncbi.nlm.nih.gov/pubmed/26045756 (Accessed: 29 March 2017).

Feldmann, M. (2002) 'Timeline: Development of anti-TNF therapy for rheumatoid arthritis', Nature Reviews Immunology. Nature Publishing Group, 2(5), pp. 364–371. doi: 10.1038/nri802.

Fernandez-Marcos, P. J. and Auwerx, J. (2011) 'Regulation of PGC-1, a nodal regulator of mitochondrial biogenesis', American Journal of Clinical Nutrition, 93(4), p. 884S–890S. doi: 10.3945/ajcn.110.001917.

Figueroa-Romero, C., Iniguez-Lluhi, J. A., Stadler, J., Chang, C.-R., Arnoult, D., *et al.* (2009) 'SUMOylation of the mitochondrial fission protein Drp1 occurs at multiple nonconsensus sites within the B domain and is linked to its activity cycle', The FASEB Journal, 23(11), pp. 3917–3927. doi: 10.1096/fj.09-136630.

Finkel, T. (2011) 'Signal transduction by reactive oxygen species.', The Journal of cell biology. The Rockefeller University Press, 194(1), pp. 7–15. doi: 10.1083/jcb.201102095.

Finn, R. S., Aleshin, A. and Slamon, D. J. (2016) 'Targeting the cyclin-dependent kinases (CDK) 4/6 in estrogen receptor-positive breast cancers.', Breast cancer research: BCR. BioMed Central, 18(1), p. 17. doi: 10.1186/s13058-015-0661-5.

Fong, G.-H. and Takeda, K. (2008) 'Role and regulation of prolyl hydroxylase domain proteins', Cell Death and Differentiation. Nature Publishing Group, 15(4), pp. 635–641. doi: 10.1038/cdd.2008.10.

Fontanesi, F., Soto, I. C. and Barrientos, A. (2008) 'Cytochrome c oxidase biogenesis: New levels of regulation', IUBMB Life. Wiley Subscription Services, Inc., a Wiley company, 60(9), pp. 557–568. doi: 10.1002/iub.86.

Forsyth, N. R., Evans, A. P., Shay, J. W. and Wright, W. E. (2003) 'Developmental differences in the immortalization of lung fibroblasts by telomerase.', Aging cell, 2(5),

pp. 235–43. Available at: http://www.ncbi.nlm.nih.gov/pubmed/14570231 (Accessed: 2 April 2017).

Forsyth, N. R., Musio, A., Vezzoni, P., Simpson, A. H. R. W., Noble, B. S. *et al.* (2006) 'Physiologic Oxygen Enhances Human Embryonic Stem Cell Clonal Recovery and Reduces Chromosomal Abnormalities', Cloning and Stem Cells, 8(1), pp. 16–23. doi: 10.1089/clo.2006.8.16.

Foster, D. A., Yellen, P., Xu, L. and Saqcena, M. (2010) 'Regulation of G1 Cell Cycle Progression: Distinguishing the Restriction Point from a Nutrient-Sensing Cell Growth Checkpoint(s).', Genes & cancer. Impact Journals, LLC, 1(11), pp. 1124–31. doi: 10.1177/1947601910392989.

Fox, S. B., Generali, D., Berruti, A., Brizzi, M. P., Campo, L., *et al*. (2011) 'The prolyl hydroxylase enzymes are positively associated with hypoxia-inducible factor-1α and vascular endothelial growth factor in human breast cancer and alter in response to primary systemic treatment with epirubicin and tamoxifen.', Breast cancer research: BCR. BioMed Central, 13(1), p. R16. doi: 10.1186/bcr2825.

Fraisl, P., Aragonés, J. and Carmeliet, P. (2009) 'Inhibition of oxygen sensors as a therapeutic strategy for ischaemic and inflammatory disease', Nature Reviews Drug Discovery. Nature Publishing Group, 8(2), pp. 139–152. doi: 10.1038/nrd2761.

Franke, T. F., Kaplan, D. R. and Cantley, L. C. (1997) 'PI3K: Downstream AKTion Blocks Apoptosis', Cell, 88(4), pp. 435–437. doi: 10.1016/S0092-8674(00)81883-8.

Fu, X., Fang, L., Li, X., Cheng, B. and Sheng, Z. (2006) 'Enhanced wound-healing quality with bone marrow mesenchymal stem cells autografting after skin injury', Wound Repair and Regeneration, 14(3), pp. 325–335. doi: 10.1111/j.1743-6109.2006.00128.x.

Fukuda, R., Zhang, H., Kim, J., Shimoda, L., Dang, C. V. *et al.* (2007) 'HIF-1 Regulates Cytochrome Oxidase Subunits to Optimize Efficiency of Respiration in Hypoxic Cells', Cell, 129(1), pp. 111–122. doi: 10.1016/j.cell.2007.01.047.

Gaber, T., Dziurla, R., Tripmacher, R., Burmester, G. R. and Buttgereit, F. (2005) 'Hypoxia inducible factor (HIF) in rheumatology: low O2! See what HIF can do!', Annals of the rheumatic diseases. BMJ Publishing Group Ltd and European League Against Rheumatism, 64(7), pp. 971–80. doi: 10.1136/ard.2004.031641.

Galluzzi, L., Kepp, O., Trojel-Hansen, C. and Kroemer, G. (2012) 'Non-apoptotic functions of apoptosis-regulatory proteins.', EMBO reports. European Molecular Biology Organization, 13(4), pp. 322–30. doi: 10.1038/embor.2012.19.

Galkin A, Higgs A, Moncada S. (2007) Nitric oxide and hypoxia. Essays Biochem [Internet]. 2007 [cited 2017 Aug 22]; 43:29–42. Available from: http://www.ncbi.nlm.nih.gov/pubmed/17705791

Ge, T., Yu, Q., Liu, W., Cong, L., Liu, L., *et al.* (2016) Molecular medicine reports., Molecular Medicine Reports. D.A. Spandidos. Available at: https://www.spandidos-publications.com/10.3892/mmr.2016.4945 (Accessed: 27 July 2017).

Genetos, D. C., Cheung, W. K., Decaris, M. L. and Leach, J. K. (2010) 'Oxygen tension modulates neurite outgrowth in PC12 cells through a mechanism involving HIF and VEGF.', Journal of molecular neuroscience: MN. Springer, 40(3), pp. 360–6. doi: 10.1007/s12031-009-9326-0.

Genetos, D. C., Rao, R. R. and Vidal, M. A. (2010) 'Betacellulin inhibits osteogenic differentiation and stimulates proliferation through HIF-1alpha.', Cell and tissue research. Springer, 340(1), pp. 81–9. doi: 10.1007/s00441-010-0929-0.

Gerald, D., Berra, E., Frapart, Y. M., Chan, D. A., Giaccia, A. J., *et al.* (2004) 'JunD Reduces Tumor Angiogenesis by Protecting Cells from Oxidative Stress', Cell, 118(6), pp. 781–794. doi: 10.1016/j.cell.2004.08.025.

Ghafourifar, P. and Cadenas, E. (2005) 'Mitochondrial nitric oxide synthase', Trends in Pharmacological Sciences, 26(4), pp. 190–195. doi: 10.1016/j.tips.2005.02.005.

Giacinti, C. and Giordano, A. (2006) 'RB and cell cycle progression', Oncogene, 25(38), pp. 5220–5227. doi: 10.1038/sj.onc.1209615.

Giansanti, V., Rodriguez, G. E. V., Savoldelli, M., Gioia, R., Forlino, A., *et al.* (2013) 'Characterization of stress response in human retinal epithelial cells.', Journal of cellular and molecular medicine. Wiley-Blackwell, 17(1), pp. 103–15. doi: 10.1111/j.1582-4934.2012. 01652.x.

Gilkerson, R., Bravo, L., Garcia, I., Gaytan, N., Herrera, A., *et al.* (2013) 'The Mitochondrial Nucleoid: Integrating Mitochondrial DNA into Cellular Homeostasis'. doi: 10.1101/cshperspect. a011080.

Ginsberg, M. D., Feliciello, A., Jones, J. K., Avvedimento, E. V and Gottesman, M. E. (2003) 'PKA-dependent binding of mRNA to the mitochondrial AKAP121 protein.', Journal of molecular biology, 327(4), pp. 885–97. Available at: http://www.ncbi.nlm.nih.gov/pubmed/12654270 (Accessed: 26 July 2017).

Giralt, A. and Villarroya, F. (2012) 'SIRT3, a pivotal actor in mitochondrial functions: metabolism, cell death and aging', Biochem. J, 444, pp. 1–10. doi: 10.1042/BJ20120030.

Gomes, L. C., Di Benedetto, G. and Scorrano, L. (2011) 'During autophagy mitochondria elongate, are spared from degradation and sustain cell viability.', Nature cell biology. Europe PMC Funders, 13(5), pp. 589–98. doi: 10.1038/ncb2220.

Gong, Y. and Agani, F. H. (2005) 'Oligomycin inhibits HIF-1 expression in hypoxic tumor cells', AJP: Cell Physiology, 288(5), pp. C1023–C1029. doi: 10.1152/ajpcell.00443.2004.

Gonzalez, E. and McGraw, T. E. (2009) 'The Akt kinases: isoform specificity in metabolism and cancer.', Cell cycle (Georgetown, Tex.). NIH Public Access, 8(16), pp. 2502–8. doi: 10.4161/cc.8.16.9335.

Granger, D. N. and Kvietys, P. R. (2015) 'Reperfusion injury and reactive oxygen species: The evolution of a concept', Redox Biology, 6, pp. 524–551. doi: 10.1016/j.redox.2015.08.020.

Gray, M. W. (2012) 'Mitochondrial evolution.', Cold Spring Harbor perspectives in biology. Cold Spring Harbor Laboratory Press, 4(9), p. a011403. doi: 10.1101/cshperspect. a011403.

Grayson, W. L., Zhao, F., Bunnell, B. and Ma, T. (2007) 'Hypoxia enhances proliferation and tissue formation of human mesenchymal stem cells', Biochemical and Biophysical Research Communications, 358(3), pp. 948–953. doi: 10.1016/j.bbrc.2007.05.054.

Green, D. R. and Kroemer, G. (2009) 'Cytoplasmic functions of the tumour suppressor p53', Nature. Nature Publishing Group, 458(7242), pp. 1127–1130. doi: 10.1038/nature07986.

Greene, L. A. and Tischler, A. S. (1976) 'Establishment of a noradrenergic clonal line of rat adrenal pheochromocytoma cells which respond to nerve growth factor.', Proceedings of the National Academy of Sciences of the United States of America, 73(7), pp. 2424–8. Available at: http://www.ncbi.nlm.nih.gov/pubmed/1065897 (Accessed: 26 July 2017).

Greijer, A. E. and van der Wall, E. (2004) 'The role of hypoxia inducible factor 1 (HIF-1) in hypoxia induced apoptosis.', Journal of clinical pathology, 57(10), pp. 1009–14. doi: 10.1136/jcp.2003.015032.

Griendling, K. K. and FitzGerald, G. A. (2003) 'Oxidative Stress and Cardiovascular Injury Part I: Basic Mechanisms and In Vivo Monitoring of ROS', Circulation, 108(16), pp. 1912–1916. doi: 10.1161/01.CIR. 0000093660.86242.BB.

Guha, M. and Avadhani, N. G. (2013) 'Mitochondrial retrograde signaling at the crossroads of tumor bioenergetics, genetics and epigenetics.', Mitochondrion. NIH Public Access, 13(6), pp. 577–91. doi: 10.1016/j.mito.2013.08.007.

Guo, F. F., Yang, W., Jiang, W., Geng, S., Peng, T. *et al.* (2012) 'Magnetosomes eliminate intracellular reactive oxygen species in Magnetospirillum gryphiswaldense MSR-1', Environmental Microbiology. Blackwell Publishing Ltd, 14(7), pp. 1722–1729. doi: 10.1111/j.1462-2920.2012. 02707.x.

Guo S, Bragina O, Xu Y, Cao Z, Chen H, *et al.* (2008) Glucose up-regulates HIF-1 alpha expression in primary cortical neurons in response to hypoxia through maintaining cellular redox status. J Neurochem [Internet]. 2008 Jun [cited 2017 Aug 22];105(5):1849–60. Available from: http://doi.wiley.com/10.1111/j.1471-4159.2008.05287.x

Guo, M., Song, L.-P., Jiang, Y., Liu, W., Yu, Y. *et al*. (2006) 'Hypoxia-mimetic agents desferrioxamine and cobalt chloride induce leukemic cell apoptosis through different hypoxia-inducible factor-1α independent mechanisms', Apoptosis, 11(1), pp. 67–77. doi: 10.1007/s10495-005-3085-3.

Gupte, T. M. (2015) 'Mitochondrial Fragmentation Due to Inhibition of Fusion Increases Cyclin B through Mitochondrial Superoxide Radicals.', PloS one. Public Library of Science, 10(5), p. e0126829. doi: 10.1371/journal.pone.0126829.

Hagen, T. (2012) 'Oxygen versus Reactive Oxygen in the Regulation of HIF-1α: The Balance Tips.', Biochemistry research international. Hindawi, 2012, p. 436981. doi: 10.1155/2012/436981.

Haider, H. K. and Ashraf, M. (2008) 'Strategies to promote donor cell survival: Combining preconditioning approach with stem cell transplantation', Journal of Molecular and Cellular Cardiology, 45(4), pp. 554–566. doi: 10.1016/j.yjmcc.2008.05.004.

Hamacher-Brady A, Brady NR, Logue SE, Sayen MR, Jinno M, *et al.* (2007) Response to myocardial ischemia/reperfusion injury involves Bnip3 and autophagy. Cell Death Differ [Internet]. 2007 Jan 28 [cited 2017 Aug 22];14(1):146–57. Available from: http://www.ncbi.nlm.nih.gov/pubmed/16645637

Hammond EM, Dorie MJ, Giaccia AJ. (2003) ATR/ATM targets are phosphorylated by ATR in response to hypoxia and ATM in response to reoxygenation. J Biol Chem [Internet]. 2003 Apr 4 [cited 2017 Aug 22];278(14):12207–13. Available from: http://www.ncbi.nlm.nih.gov/pubmed/12519769

Haque, N., Rahman, M. T., Abu Kasim, N. H. and Alabsi, A. M. (2013) 'Hypoxic culture conditions as a solution for mesenchymal stem cell based regenerative therapy.', TheScientificWorldJournal. Hindawi, 2013, p. 632972. doi: 10.1155/2013/632972.

Harrison, J. S., Rameshwar, P., Chang, V. and Bandari, P. (2002) 'Oxygen saturation in the bone marrow of healthy volunteers', Blood, 99(1). Available at: http://www.bloodjournal.org/content/99/1/394.long?sso-checked=true (Accessed: 26 July 2017).

Hasselmann, V., Oesch, P., Fernandez-Luque, L. and Bachmann, S. (2015) 'Are exergames promoting mobility an attractive alternative to conventional self-regulated exercises for elderly people in a rehabilitation setting? Study protocol of a randomized controlled trial', BMC Geriatrics, 15. doi: 10.1186/s12877-015-0106-0.

Hausenloy, D. J., Yellon, D. M., Stone, G., Kloner, R., Alexander, R. *et al*. (2013) 'Myocardial ischemia-reperfusion injury: a neglected therapeutic target.', The Journal of clinical investigation. American Society for Clinical Investigation, 123(1), pp. 92–100. doi: 10.1172/JCI62874.

Hawlitschek, G., Schneider, H., Schmidt, B., Tropschug, M., Hartl, F. U., *et al*. (1988) 'Mitochondrial protein import: identification of processing peptidase and of PEP, a processing enhancing protein.', Cell. Academic Press, New York, 53(5), pp. 795–806. doi: 10.1016/0092-8674(88)90096-7.

Henze, A.-T., Riedel, J., Diem, T., Wenner, J., Flamme, I., *et al.* (2010) 'Prolyl Hydroxylases 2 and 3 Act in Gliomas as Protective Negative Feedback Regulators of Hypoxia-Inducible Factors', Cancer Research, 70(1).

Heyman, S. N., Rosen, S. and Rosenberger, C. (2011) 'Hypoxia-inducible factors and the prevention of acute organ injury.', Critical care (London, England). BioMed Central, 15(2), p. 209. doi: 10.1186/cc9991.

Heywood, H. K. and Lee, D. A. (2016) 'Bioenergetic reprogramming of articular chondrocytes by exposure to exogenous and endogenous reactive oxygen species and its role in the anabolic response to low oxygen', Journal of Tissue Engineering and Regenerative Medicine, p. n/a-n/a. doi: 10.1002/term.2126.

Hirsilä, M., Koivunen, P., Günzler, V., Kivirikko, K. I. and Myllyharju, J. (2003) 'Characterization of the human prolyl 4-hydroxylases that modify the hypoxia-inducible factor.', The Journal of biological chemistry. American Society for Biochemistry and Molecular Biology, 278(33), pp. 30772–80. doi: 10.1074/jbc.M304982200.

Ho, K. K., Myatt, S. S. and Lam, E. W.-F. (2008) 'Many forks in the path: cycling with Foxo', Oncogene. Nature Publishing Group, 27(16), pp. 2300–2311. doi: 10.1038/onc.2008.23.

Ho, P.-J., Yen, M.-L., Tang, B.-C., Chen, C.-T. and Yen, B. L. (2013) 'H2O2 accumulation mediates differentiation capacity alteration, but not proliferative decline, in senescent human fetal mesenchymal stem cells.', Antioxidants & redox signaling. Mary Ann Liebert, Inc., 18(15), pp. 1895–905. doi: 10.1089/ars.2012.4692.

Höhler, B., Lange, B., Holzapfel, B., Goldenberg, A., Hänze, J., *et al*. (1999) 'Hypoxic upregulation of tyrosine hydroxylase gene expression is paralleled, but not induced, by increased generation of reactive oxygen species in PC12 cells', FEBS Letters, 457(1), pp. 53–56. doi: 10.1016/S0014-5793(99)00999-0.

Holt, I. J. and Reyes, A. (2012) 'Human mitochondrial DNA replication.', Cold Spring Harbor perspectives in biology. Cold Spring Harbor Laboratory Press, 4(12). doi: 10.1101/cshperspect. a012971.

Holzwarth, C., Vaegler, M., Gieseke, F., Pfister, S. M., Handgretinger, *et al.* (2010) 'Low physiologic oxygen tensions reduce proliferation and differentiation of human

multipotent mesenchymal stromal cells', BMC Cell Biology, 11(1), p. 11. doi: 10.1186/1471-2121-11-11.

Hopkins, C., Li, J., Rae, F. and Little, M. (2009) 'Stem cell options for kidney disease', The Journal of Pathology, 217(2), pp. 265–281. doi: 10.1002/path.2477.

Hoppins, S., Edlich, F., Cleland, M. M., Banerjee, S., McCaffery, J. M., *et al*. (2011) 'The soluble form of Bax regulates mitochondrial fusion via MFN2 homotypic complexes.', Molecular cell. NIH Public Access, 41(2), pp. 150–60. doi: 10.1016/j.molcel.2010.11.030.

Hsieh, M. M., Linde, N. S., Wynter, A., Metzger, M., Wong, C., *et al*. (2007) 'HIF prolyl hydroxylase inhibition results in endogenous erythropoietin induction, erythrocytosis, and modest fetal hemoglobin expression in rhesus macaques.', Blood. American Society of Hematology, 110(6), pp. 2140–7. doi: 10.1182/blood-2007-02-073254.

Hu, C., Fan, L., Cen, P., Chen, E., Jiang, Z., *et al.* (2016) 'Energy Metabolism Plays a Critical Role in Stem Cell Maintenance and Differentiation.', International journal of molecular sciences. Multidisciplinary Digital Publishing Institute (MDPI), 17(2), p. 253. doi: 10.3390/ijms17020253.

Hu, Y., Liu, J. and Huang, H. (2013) 'Recent agents targeting HIF-1α for cancer therapy', Journal of Cellular Biochemistry. Wiley Subscription Services, Inc., A Wiley Company, 114(3), pp. 498–509. doi: 10.1002/jcb.24390.

Hubbi ME, Luo W, Baek JH, Semenza GL. (2011) MCM proteins are negative regulators of hypoxia-inducible factor 1. Mol Cell [Internet]. 2011 Jun 10 [cited 2017 Aug 22];42(5):700–12. Available from: http://www.ncbi.nlm.nih.gov/pubmed/21658608

Huang, J., Wu, S., Barrera, J., Matthews, K., Pan, D., *et al.* (2005) 'The Hippo signaling pathway coordinately regulates cell proliferation and apoptosis by inactivating Yorkie, the Drosophila Homolog of YAP.', Cell. Cold Spring Harbor Laboratory Press, Plainview, New York, 122(3), pp. 421–34. doi: 10.1016/j.cell.2005.06.007.

Huang, L. E., Bindra, R. S., Glazer, P. M. and Harris, A. L. (2007) 'Hypoxia-induced genetic instability—a calculated mechanism underlying tumor progression', Journal of Molecular Medicine. Springer-Verlag, 85(2), pp. 139–148. doi: 10.1007/s00109-006-0133-6.

Huerta-Yepez, S., Baay-Guzman, G. J., Bebenek, I. G., Hernandez-Pando, R., Vega, M. I., *et al*. (2011) 'Hypoxia Inducible Factor promotes murine allergic airway inflammation and is increased in asthma and rhinitis', Allergy, 66(7), pp. 909–918. doi: 10.1111/j.1398-9995.2011. 02594.x.

Hutton, J. J., Kaplan, A. and Udenfriend, S. (1967) 'Conversion of the amino acid sequence Gly-Pro-Pro in protein to Gly-Pro-Hyp by collagen proline hydroxylase', Archives of Biochemistry and Biophysics, 121(2), pp. 384–391. doi: 10.1016/0003-9861(67)90091-4.

Hyde, B. B., Twig, G. and Shirihai, O. S. (2010) 'Organellar vs cellular control of mitochondrial dynamics', Seminars in Cell & Developmental Biology, 21(6), pp. 575–581. doi: 10.1016/j.semcdb.2010.01.003.

Iglesias, P., Fraga, M. and Costoya, J. A. (2013) 'Defining hypoxic microenvironments by non-invasive functional optical imaging', European Journal of Cancer, 49(1), pp. 264–271. doi: 10.1016/j.ejca.2012.06.001.

Isaacs, J. S., Jung, Y. J., Mole, D. R., Lee, S., Torres-Cabala, C., *et al.* (2005) 'HIF overexpression correlates with biallelic loss of fumarate hydratase in renal cancer:

Novel role of fumarate in regulation of HIF stability', Cancer Cell, 8(2), pp. 143–153. doi: 10.1016/j.ccr.2005.06.017.

Ivan, M., Kondo, K., Yang, H., Kim, W., Valiando, J., *et al*. (2001) 'HIFα Targeted for VHL-Mediated Destruction by Proline Hydroxylation: Implications for O2 Sensing', Science, 292(5516).

Jaakkola, P., Mole, D. R., Tian, Y.-M., Wilson, M. I., Gielbert, J., *et al*. (2001) 'Targeting of HIF-α to the von Hippel-Lindau Ubiquitylation Complex by O2-Regulated Prolyl Hydroxylation', Science, 292(5516).

Järviluoma, A., Child, E. S., Sarek, G., Sirimongkolkasem, P., Peters, G., *et al.* (2006) 'Phosphorylation of the cyclin-dependent kinase inhibitor p21Cip1 on serine 130 is essential for viral cyclin-mediated bypass of a p21Cip1-imposed G1 arrest.', Molecular and cellular biology. American Society for Microbiology, 26(6), pp. 2430–40. doi: 10.1128/MCB.26.6.2430-2440.2006.

Jezek, P., Plecit-Hlavat, L., Smolkov, K. and Rossignol, R. (2009) 'Distinctions and similarities of cell bioenergetics and the role of mitochondria in hypoxia, cancer, and embryonic development', The International Journal of Biochemistry & Cell Biology, 42(5), pp. 604–622. doi: 10.1016/j.biocel.2009.11.008.

Jenkins, C. L. and Raines, R. T. (2002) 'Insights on the conformational stability of collagen'. doi: 10.1039/a903001h.

Ježek P, Plecitá-Hlavatá L. (2009) Mitochondrial reticulum network dynamics in relation to oxidative stress, redox regulation, and hypoxia. Int J Biochem Cell Biol [Internet]. 2009 Oct [cited 2017 Aug 22];41(10):1790–804. Available from: http://www.ncbi.nlm.nih.gov/pubmed/19703650

Jiang, B., Semenza, G. L., Bauer, C., Mart, H. H. and Marti, H. H. (1996) 'Hypoxia-inducible factor 1 levels vary exponentially over a physiologically relevant range of O2 tension'.

Jin, K., Mao, X. O., Zhu, Y. and Greenberg, D. A. (2002) 'MEK and ERK protect hypoxic cortical neurons via phosphorylation of Bad', Journal of Neurochemistry. Blackwell Science, Ltd, 80(1), pp. 119–125. doi: 10.1046/j.0022-3042.2001. 00678.x.

Jokilehto, T., Rantanen, K., Luukkaa, M., Heikkinen, P., Grenman, R., *et al*. (2006) 'Overexpression and nuclear translocation of hypoxia-inducible factor prolyl hydroxylase PHD2 in head and neck squamous cell carcinoma is associated with tumor aggressiveness.', Clinical Cancer Research, 12(4).

Kaelin, W. G. and Ratcliffe, P. J. (2008) 'Oxygen Sensing by Metazoans: The Central Role of the HIF Hydroxylase Pathway', Molecular Cell, 30(4), pp. 393–402. doi: 10.1016/j.molcel.2008.04.009.

Kalucka, J., Ettinger, A., Franke, K., Mamlouk, S., Singh, R. P., *et al*. (2013) 'Loss of Epithelial Hypoxia-Inducible Factor Prolyl Hydroxylase 2 Accelerates Skin Wound Healing in Mice', Molecular and Cellular Biology, 33(17), pp. 3426–3438. doi: 10.1128/MCB.00609-13.

Kao, S., Jaiswal, R. K., Kolch, W. and Landreth, G. E. (2001) 'Identification of the mechanisms regulating the differential activation of the mapk cascade by epidermal growth factor and nerve growth factor in PC12 cells.', The Journal of biological chemistry. American Society for Biochemistry and Molecular Biology, 276(21), pp. 18169–77. doi: 10.1074/jbc.M008870200.

Karin, M. and Greten, F. R. (2005) 'NF-κB: linking inflammation and immunity to cancer development and progression', Nature Reviews Immunology. Nature Publishing Group, 5(10), pp. 749–759. doi: 10.1038/nri1703.

Karuppagounder, S. S. and Ratan, R. R. (2012) 'Hypoxia-inducible factor prolyl hydroxylase inhibition: robust new target or another big bust for stroke therapeutics?', Journal of cerebral blood flow and metabolism: official journal of the International Society of Cerebral Blood Flow and Metabolism. Nature Publishing Group, 32(7), pp. 1347–61. doi: 10.1038/jcbfm.2012.28.

Kasuya, K., Tsuchida, A., Nagakawa, Y., Suzuki, M., Abe, Y., *et al.* (2011) 'Hypoxia-inducible factor-1?? expression and gemcitabine chemotherapy for pancreatic cancer', Oncology Reports, 26(6), pp. 1399–1406. doi: 10.3892/or.2011.1457.

Kawalec, M., Boratyńska-Jasińska, A., Beręsewicz, M., Dymkowska, D., Zabłocki, K. *et al.* (2015) 'Mitofusin 2 Deficiency Affects Energy Metabolism and Mitochondrial Biogenesis in MEF Cells'. doi: 10.1371/journal.pone.0134162.

Ke, Q. and Costa, M. (2006) 'Hypoxia-Inducible Factor-1 (HIF-1)', Molecular Pharmacology, 70(5).

Kempf, V. A. J., Lebiedziejewski, M., Alitalo, K., Ehehalt, U., Ehehalt U., *et al*. (2005) 'Activation of hypoxia-inducible factor-1 in bacillary angiomatosis: Evidence for a role of hypoxia-inducible factor-1 in bacterial infections', Circulation, 111(8), pp. 1054–1062. doi: 10.1161/01.CIR. 0000155608.07691.B7.

Khan, M. I., Mohammad, A., Patil, G., Naqvi, S. A. H., Chauhan, L. K. S. *et al.* (2012) 'Induction of ROS, mitochondrial damage and autophagy in lung epithelial cancer cells by iron oxide nanoparticles', Biomaterials, 33(5), pp. 1477–1488. doi: 10.1016/j.biomaterials.2011.10.080.

Kim, J., Tchernyshyov, I., Semenza, G. L. and Dang, C. V. (2006) 'HIF-1-mediated expression of pyruvate dehydrogenase kinase: A metabolic switch required for cellular adaptation to hypoxia', Cell Metabolism, 3(3), pp. 177–185. doi: 10.1016/j.cmet.2006.02.002.

Kim JW, Tchernyshyov I, Semenza GL, Dang C V. (2006) HIF-1-mediated expression of pyruvate dehydrogenase kinase: A metabolic switch required for cellular adaptation to hypoxia. Cell Metab [Internet]. 2006 Mar [cited 2017 Aug 22];3(3):177–85. Available from: http://linkinghub.elsevier.com/retrieve/pii/S1550413106000623

Kirichok, Y., Krapivinsky, G. and Clapham, D. E. (2004) 'The mitochondrial calcium uniporter is a highly selective ion channel', Nature. Nature Publishing Group, 427(6972), pp. 360–364. doi: 10.1038/nature02246.

KLONER, R., REZKALLA, S. and I., L. (2006) 'Preconditioning, postconditioning and their application to clinical cardiology', Cardiovascular Research. Oxford University Press, 70(2), pp. 297–307. doi: 10.1016/j.cardiores.2006.01.012.

Knott, A. B., Perkins, G., Schwarzenbacher, R. and Bossy-Wetzel, E. (2008) 'Mitochondrial fragmentation in neurodegeneration', Nature Reviews Neuroscience. Nature Publishing Group, 9(7), pp. 505–518. doi: 10.1038/nrn2417.

Koivunen, P., Hirsilä, M., Remes, A. M., Hassinen, I. E., Kivirikko, K. I. *et al.* (2007) 'Inhibition of hypoxia-inducible factor (HIF) hydroxylases by citric acid cycle intermediates: possible links between cell metabolism and stabilization of HIF.', The Journal of biological chemistry. American Society for Biochemistry and Molecular Biology, 282(7), pp. 4524–32. doi: 10.1074/jbc.M610415200.

Koivunen, P., Lee, S., Duncan, C. G., Lopez, G., Lu, G., *et al.* (2012) 'Transformation by the (R)-enantiomer of 2-hydroxyglutarate linked to EGLN activation', Nature. Nature Research, 483(7390), pp. 484–488. doi: 10.1038/nature10898.

Kolamunne, R. T., Dias, I. H., Vernallis, A. B., Grant, M. M. and Griffiths, H. R. (2013) 'Nrf2 activation supports cell survival during hypoxia and hypoxia/reoxygenation in cardiomyoblasts; the roles of reactive oxygen and nitrogen species', Redox Biology, 1(1), pp. 418–426. doi: 10.1016/j.redox.2013.08.002.

Koong, A. C., Chen, E. Y. and Giaccia, A. J. (1994) 'Hypoxia Causes the Activation of Nuclear Factor κB through the Phosphorylation of IκBα on Tyrosine Residues', Cancer Research, 54(6).

Kotake-Nara, E. and Saida, K. (2007) 'Characterization of CoCl2-induced reactive oxygen species (ROS): Inductions of neurite outgrowth and endothelin-2/vasoactive intestinal contractor in PC12 cells by CoCl2 are ROS dependent, but those by MnCl2 are not', Neuroscience Letters, 422(3), pp. 223–227. doi: 10.1016/j.neulet.2007.06.026.

Kotake-Nara, E., Takizawa, S., Quan, J., Wang, H. and Saida, K. (2005) 'Cobalt chloride induces neurite outgrowth in rat pheochromocytoma PC-12 cells through regulation of endothelin-2/vasoactive intestinal contractor', Journal of Neuroscience Research. Wiley Subscription Services, Inc., A Wiley Company, 81(4), pp. 563–571. doi: 10.1002/jnr.20568.

Kotch, L. E., Iyer, N. V, Laughner, E. and Semenza, G. L. (1999) 'Defective Vascularization of HIF-1-Null Embryos Is Not Associated with VEGF Deficiency but with Mesenchymal Cell Death'.

Krohn, K. A., Link, J. M. and Mason, R. P. (2008) 'Molecular Imaging of Hypoxia', Journal of Nuclear Medicine, 49(Suppl_2), p. 129S–148S. doi: 10.2967/jnumed.107.045914.

Krtolica A, Krucher NA, Ludlow JW. (1998) Hypoxia-induced pRB hypophosphorylation results from downregulation of CDK and upregulation of PP1 activities. Oncogene [Internet]. 1998 Oct 10 [cited 2017 Aug 22];17(18):2295–304. Available from: http://www.ncbi.nlm.nih.gov/pubmed/9811460

Kühlbrandt, W. (2015) 'Structure and function of mitochondrial membrane protein complexes'. doi: 10.1186/s12915-015-0201-x.

Kumar, G. K., Kim, D.-K., Lee, M.-S., Ramachandran, R., Prabhakar, *et al*. (2003) 'Activation of tyrosine hydroxylase by intermittent hypoxia: involvement of serine phosphorylation', Journal of Applied Physiology. BioMed Central, 95(2), pp. 536–544. doi: 10.1152/japplphysiol.00186.2003.

Kurland, C. G., Andersson, S. G. E., Zomorodipour, A., Andersson, J. O., Sicheritz-Pontén, *et al.* (1998) 'The genome sequence of Rickettsia prowazekii and the origin ofmitochondria', Nature. Nature Publishing Group, 396(6707), pp. 133–140. doi: 10.1038/24094.

Kussmaul, L. and Hirst, J. (2006) 'The mechanism of superoxide production by NADH: ubiquinone oxidoreductase (complex I) from bovine heart mitochondria', Proceedings of the National Academy of Sciences, 103(20), pp. 7607–7612. doi: 10.1073/pnas.0510977103.

Laitala, A., Aro, E., Walkinshaw, G., Mäki, J. M., Rossi, M., *et al*. (2012) 'Transmembrane prolyl 4-hydroxylase is a fourth prolyl 4-hydroxylase regulating EPO production and erythropoiesis', Blood, 120(16).

Lan, A., Liao, X., Mo, L., Yang, C., Yang, Z., *et al.* (2011) 'Hydrogen Sulfide Protects against Chemical Hypoxia- Induced Injury by Inhibiting ROS-Activated ERK1/2 and p38MAPK Signaling Pathways in PC12 Cells'. doi: 10.1371/journal.pone.0025921.

Lando, D., Peet, D. J., Gorman, J. J., Whelan, D. A., Whitelaw, M. L. *et al.* (2002) 'FIH-1 is an asparaginyl hydroxylase enzyme that regulates the transcriptional activity of hypoxia-inducible factor.', Genes & development. Cold Spring Harbor Laboratory Press, 16(12), pp. 1466–71. doi: 10.1101/gad.991402.

Lando, D., Peet, D. J., Whelan, D. A., Gorman, J. J. and Whitelaw, M. L. (2002) 'Asparagine Hydroxylation of the HIF Transactivation Domain: A Hypoxic Switch', Science, 295(5556).

Langlois, A. and Duval, D. (1997) 'Differentiation of the human NT2 cells into neurons and glia', Methods in Cell Science. Kluwer Academic Publishers, 19(3), pp. 213–219. doi: 10.1023/A:1009731707443.

Lavrentieva, A., Majore, I., Kasper, C. and Hass, R. (2010) 'Effects of hypoxic culture conditions on umbilical cord-derived human mesenchymal stem cells.', Cell communication and signaling: CCS. BioMed Central, 8, p. 18. doi: 10.1186/1478-811X-8-18.

Lee, D. M., Kiener, H. P., Agarwal, S. K., Noss, E. H., Watts, G. F. M., *et al*. (2007) 'Cadherin-11 in synovial lining formation and pathology in arthritis.', Science (New York, N.Y.), 315(5814), pp. 1006–10. doi: 10.1126/science.1137306.

Lee, H.-C. and Wei, Y.-H. (2005) 'Mitochondrial biogenesis and mitochondrial DNA maintenance of mammalian cells under oxidative stress', The International Journal of Biochemistry & Cell Biology, 37(4), pp. 822–834. doi: 10.1016/j.biocel.2004.09.010.

Lee, J., Eschen-Lippold, L., Lassowskat, I., Böttcher, C. and Scheel, D. (2015) 'Cellular reprogramming through mitogen-activated protein kinases.', Frontiers in plant science. Frontiers Media SA, 6, p. 940. doi: 10.3389/fpls.2015.00940.

Lee, S., Nakamura, E., Yang, H., Wei, W., Linggi, M. S., *et al.* (2005) 'Neuronal apoptosis linked to EGlN3 prolyl hydroxylase and familial pheochromocytoma genes: developmental culling and cancer.', Cancer cell. Elsevier, 8(2), pp. 155–67. doi: 10.1016/j.ccr.2005.06.015.

Lee, Y., Jeong, S.-Y., Karbowski, M., Smith, C. L. and Youle, R. J. (2004) 'Roles of the mammalian mitochondrial fission and fusion mediators Fis1, Drp1, and Opa1 in apoptosis.', Molecular biology of the cell. American Society for Cell Biology, 15(11), pp. 5001–11. doi: 10.1091/mbc. E04-04-0294.

Ley, R., Balmanno, K., Hadfield, K., Weston, C. and Cook, S. J. (2003) 'Activation of the ERK1/2 signaling pathway promotes phosphorylation and proteasome-dependent degradation of the BH3-only protein, Bim.', The Journal of biological chemistry. American Society for Biochemistry and Molecular Biology, 278(21), pp. 18811–6. doi: 10.1074/jbc.M301010200.

Li, W., Saud, S. M., Young, M. R., Chen, G. and Hua, B. (2015) 'Targeting AMPK for cancer prevention and treatment.', Oncotarget. Impact Journals, LLC, 6(10), pp. 7365–78. doi: 10.18632/oncotarget.3629.

Li, Y., Padmanabha, D., Gentile, L. B., Dumur, C. I., Beckstead, R. B. *et al.* (2013) 'HIF- and Non-HIF-Regulated Hypoxic Responses Require the Estrogen-Related Receptor in Drosophila melanogaster', PLoS Genetics. Edited by E. Rulifson. Public Library of Science, 9(1), p. e1003230. doi: 10.1371/journal.pgen.1003230.

Liao, D. and Johnson, R. S. (2007) 'Hypoxia: A key regulator of angiogenesis in cancer', Cancer and Metastasis Reviews. Kluwer Academic Publishers-Plenum Publishers, 26(2), pp. 281–290. doi: 10.1007/s10555-007-9066-y.

Liesa, M. and Shirihai, O. S. (2013) 'Mitochondrial Dynamics in the Regulation of Nutrient Utilization and Energy Expenditure', Cell Metabolism, 17(4), pp. 491–506. doi: 10.1016/j.cmet.2013.03.002.

Liew, Y.-F. and Shaw, N.-S. (2005) 'Mitochondrial cysteine desulfurase iron-sulfur cluster S and aconitase are post-transcriptionally regulated by dietary iron in skeletal muscle of rats.', The Journal of nutrition, 135(9), pp. 2151–8. Available at: http://www.ncbi.nlm.nih.gov/pubmed/16140891 (Accessed: 25 July 2017).

Lim, S., Smith, K. R., Lim, S.-T. S., Tian, R., Lu, J. *et al*. (2016) 'Regulation of mitochondrial functions by protein phosphorylation and dephosphorylation', Cell & Bioscience, 6(1), p. 25. doi: 10.1186/s13578-016-0089-3.

Lin, W., Xu, L., Zwingenberger, S., Gibon, E., Goodman, S. B. *et al.* (2017) 'Mesenchymal stem cells homing to improve bone healing', Journal of Orthopaedic Translation, 9, pp. 19–27. doi: 10.1016/j.jot.2017.03.002.

Liu, J., Hao, H., Xia, L., Ti, D., Huang, H., *et al.* (2015) 'Hypoxia Pretreatment of Bone Marrow Mesenchymal Stem Cells Facilitates Angiogenesis by Improving the Function of Endothelial Cells in Diabetic Rats with Lower Ischemia', PLOS ONE. Edited by G. Camussi. Public Library of Science, 10(5), p. e0126715. doi: 10.1371/journal.pone.0126715.

Liu, L., Marti, G. P., Wei, X., Zhang, X., Zhang, H., *et al.* (2009) 'NIH Public Access', 217(2), pp. 319–327. doi: 10.1002/jcp.21503.Age-dependent.

Liu, Y. and Chen, X. J. (2013) 'Adenine Nucleotide Translocase, Mitochondrial Stress, and Degenerative Cell Death', Oxidative Medicine and Cellular Longevity, 2013, pp. 1–10. doi: 10.1155/2013/146860.

Loboda, A., Stachurska, A., Florczyk, U., Rudnicka, D., Jazwa, A., *et al.* (2009) 'HIF-1 Induction Attenuates Nrf2-Dependent IL-8 Expression in Human Endothelial Cells', Antioxidants & Redox Signaling, 11(7), pp. 1501–1517. doi: 10.1089/ars.2008.2211.

Loenarz, C. and Schofield, C. J. (2008) 'Expanding chemical biology of 2-oxoglutarate oxygenases', Nature Chemical Biology. Nature Publishing Group, 4(3), pp. 152–156. doi: 10.1038/nchembio0308-152.

Loiacono, L. A., Shapiro, D. S., Gili, G. *et al.* (2010) 'Detection of hypoxia at the cellular level.', Critical care clinics. Churchill Livingstone, New York, 26(2), p. 409–21, table of contents. doi: 10.1016/j.ccc.2009.12.001.

Lopez-Sánchez, L. M., Jimenez, C., Valverde, A., Hernandez, V., Peñarando, J., *et al.* (2014) 'CoCl2, a Mimic of Hypoxia, Induces Formation of Polyploid Giant Cells with Stem Characteristics in Colon Cancer', PLoS ONE. Edited by C. G. Maki. Public Library of Science, 9(6), p. e99143. doi: 10.1371/journal.pone.0099143.

Loschen, G. and Azzi, A. (1975) 'On the formation of hydrogen peroxide and oxygen radicals in heart mitochondria.', Recent advances in studies on cardiac structure and metabolism, 7, pp. 3–12. Available at: http://www.ncbi.nlm.nih.gov/pubmed/179119 (Accessed: 25 July 2017).

Lukashev, D., Ohta, A. and Sitkovsky, M. (2007) 'Hypoxia-dependent anti-inflammatory pathways in protection of cancerous tissues', Cancer and Metastasis Reviews.

Kluwer Academic Publishers-Plenum Publishers, 26(2), pp. 273–279. doi: 10.1007/s10555-007-9054-2.

Lum JJ, Bui T, Gruber M, Gordan JD, DeBerardinis RJ, *et al.* (2007) The transcription factor HIF-1 plays a critical role in the growth factor-dependent regulation of both aerobic and anaerobic glycolysis. Genes Dev [Internet]. 2007 Apr 16 [cited 2017 Aug 22];21(9):1037–49. Available from: http://www.ncbi.nlm.nih.gov/pubmed/17437992

Luo, W., Hu, H., Chang, R., Zhong, J., Knabel, M., *et al.* (2011) 'Pyruvate Kinase M2 Is a PHD3-Stimulated Coactivator for Hypoxia-Inducible Factor 1', Cell, 145(5), pp. 732–744. doi: 10.1016/j.cell.2011.03.054.

Luukkaa, M., Jokilehto, T., Kronqvist, P., Vahlberg, T., Grénman, R., *et al.* (2009) 'Expression of the cellular oxygen sensor PHD2 (EGLN-1) predicts radiation sensitivity in squamous cell cancer of the head and neck', International Journal of Radiation Biology, 85(10), pp. 900–908. doi: 10.1080/09553000903074104.

Madji Hounoum, B., Blasco, H., Emond, P. and Mavel, S. (2016) 'Liquid chromatography–high-resolution mass spectrometry-based cell metabolomics: Experimental design, recommendations, and applications', TrAC Trends in Analytical Chemistry, 75, pp. 118–128. doi: 10.1016/j.trac.2015.08.003.

Majmundar, A. J., Wong, W. J. and Simon, M. C. (2010) 'Hypoxia-Inducible Factors and the Response to Hypoxic Stress', Molecular Cell, 40(2), pp. 294–309. doi: 10.1016/j.molcel.2010.09.022.

Makino, Y., Cao, R., Svensson, K., Bertilsson, G., Asman, M., *et al.* (2001) 'Inhibitory PAS domain protein is a negative regulator of hypoxia-inducible gene expression', Nature. Nature Publishing Group, 414(6863), pp. 550–554. doi: 10.1038/35107085.

Malumbres, M. (2014) 'Cyclin-dependent kinases.', Genome biology. BioMed Central, 15(6), p. 122. doi: 10.1186/gb4184.

Mansfield, K. D., Guzy, R. D., Pan, Y., Young, R. M., Cash, T. P., *et al.* (2005) 'Mitochondrial dysfunction resulting from loss of cytochrome c impairs cellular oxygen sensing and hypoxic HIF-alpha activation.', Cell metabolism. Howard Hughes Medical Institute, 1(6), pp. 393–9. doi: 10.1016/j.cmet.2005.05.003.

Maraldi, T., Angeloni, C., Giannoni, E. and Sell, C. (2015) 'Reactive Oxygen Species in Stem Cells.', Oxidative medicine and cellular longevity. Hindawi, 2015, p. 159080. doi: 10.1155/2015/159080.

Marchi, S., Giorgi, C., Suski, J. M., Agnoletto, C., Bononi, A., *et al.* (2011) 'Mitochondria-Ros Crosstalk in the Control of Cell Death and Aging', Journal of Signal Transduction. Hindawi, 2012. doi: 10.1155/2012/329635.

Margulis, L. (1971) 'The Origin of Plant and Animal Cells: The serial symbiosis view of the origin of higher cells suggests that the customary division of living things into two kingdoms should be reconsidered', American Scientist. Sigma Xi, The Scientific Research Society, 59, pp. 230–235. doi: 10.2307/27829542.

Marin, J. J. G., Lozano, E. and Perez, M. J. (2016) 'Lack of mitochondrial DNA impairs chemical hypoxia-induced autophagy in liver tumor cells through ROS-AMPK-ULK1 signaling dysregulation independently of HIF-1α'. doi: 10.1016/j.freeradbiomed.2016.09.025.

Markham, A., Bains, R., Franklin, P. and Spedding, M. (2014) 'Changes in mitochondrial function are pivotal in neurodegenerative and psychiatric disorders: how important is

BDNF?', British journal of pharmacology. Wiley-Blackwell, 171(8), pp. 2206–29. doi: 10.1111/bph.12531.

Martínez-Diez, M., Santamaría, G., Ortega, Á. D. and Cuezva, J. M. (2006) 'Biogenesis and Dynamics of Mitochondria during the Cell Cycle: Significance of 3′UTRs', PLoS ONE. Edited by J. Bähler, 1(1), p. e107. doi: 10.1371/journal.pone.0000107.

Martinou, J.-C. and Youle, R. J. (2011) 'Mitochondria in apoptosis: Bcl-2 family members and mitochondrial dynamics.', Developmental cell. NIH Public Access, 21(1), pp. 92–101. doi: 10.1016/j.devcel.2011.06.017.

Masson, N., Willam, C., Maxwell, P. H., Pugh, C. W. and Ratcliffe, P. J. (2001) 'Independent function of two destruction domains in hypoxia-inducible factor-α chains activated by prolyl hydroxylation', The EMBO Journal, 20(18), pp. 5197–5206. doi: 10.1093/emboj/20.18.5197.

Matés, J. M. (2000) 'Effects of antioxidant enzymes in the molecular control of reactive oxygen species toxicology', Toxicology, 153, pp. 83–104. Available at: www.elsevier.com/locate/toxicol (Accessed: 25 July 2017).

Matsuura, B., Nunoi, H., Miyake, T., Hiasa, Y. and Onji, M. (2013) 'Obesity and gastrointestinal liver disorders in Japan', Journal of Gastroenterology and Hepatology, 28, pp. 48–53. doi: 10.1111/jgh.12238.

Maxwell, P. and Salnikow, K. (2004) 'HIF-1: an oxygen and metal responsive transcription factor.', Cancer biology & therapy, 3(1), pp. 29–35. Available at: http://www.ncbi.nlm.nih.gov/pubmed/14726713 (Accessed: 22 January 2017).

Maynard, M. A., Evans, A. J., Hosomi, T., Hara, S., Jewett, M. A. S. *et al.* (2005) 'Human HIF-3alpha4 is a dominant-negative regulator of HIF-1 and is down-regulated in renal cell carcinoma.', FASEB journal: official publication of the Federation of American Societies for Experimental Biology. Federation of American Societies for Experimental Biology, 19(11), pp. 1396–406. doi: 10.1096/fj.05-3788com.

Masson N, Ratcliffe PJ. (2014) Hypoxia signaling pathways in cancer metabolism: the importance of co-selecting interconnected physiological pathways. Cancer Metab. 2014;2:3

Mazure, N. M. and Pouysségur, J. (2010) 'Hypoxia-induced autophagy: cell death or cell survival?', Current Opinion in Cell Biology, 22(2), pp. 177–180. doi: 10.1016/j.ceb.2009.11.015.

Medina PP, Slack FJ. (2008) MicroRNAs and cancer: An overview. Cell Cycle [Internet]. 2008 Aug 15 [cited 2017 Aug 22];7(16):2485–92. Available from: http://www.ncbi.nlm.nih.gov/pubmed/18719380

Meini, A., Sticozzi, C., Massai, L. and Palmi, M. (2008) 'A nitric oxide/Ca $^{(2+)}$/calmodulin/ERK1/2 mitogen-activated protein kinase pathway is involved in the mitogenic effect of IL-1beta in human astrocytoma cells.', British journal of pharmacology. Wiley-Blackwell, 153(8), pp. 1706–17. doi: 10.1038/bjp.2008.40.

Meloche, S. and Pouysseur, J. (2007) 'The ERK1/2 mitogen-activated protein kinase pathway as a master regulator of the G1-to S-phase transition', Oncogene, 26, pp. 3227–3239. doi: 10.1038/sj.onc.1210414.

Meyer, J. (2008) 'Iron–sulfur protein folds, iron–sulfur chemistry, and evolution', JBIC Journal of Biological Inorganic Chemistry. Springer-Verlag, 13(2), pp. 157–170. doi: 10.1007/s00775-007-0318-7.

Michailidou, Z., Jensen, M. D., Dumesic, D. A., Chapman, K. E., Seckl, J. R., *et al.* (2007) 'Omental 11β-hydroxysteroid Dehydrogenase 1 Correlates with Fat Cell Size Independently of Obesity'. Available at: http://s3.amazonaws.com/academia.edu.documents/40069790/Omental11-hydroxysteroid_Dehydrogenas20151116-22647-ltjh4x.pdf?AWSAccessKeyId=AKIAIWOWYYGZ2Y53UL3A&Expires=1500920878&Signature=D7UPKTkrdEVGXnTYivlxNIoRRMw%3D&response-content-disposition=inline%3Bfilename%3DOmental_11-hydroxysteroid_Dehydrogenase.pdf (Accessed: 24 July 2017).

Michiels, C., Minet, E., Mottet, D. and Raes, M. (2002) 'Regulation of gene expression by oxygen: NF-κB and HIF-1, two extremes', Free Radical Biology and Medicine, 33(9), pp. 1231–1242. doi: 10.1016/S0891-5849(02)01045-6.

Mitra, K., Wunder, C., Roysam, B., Lin, G. and Lippincott-Schwartz, J. (2009) 'A hyperfused mitochondrial state achieved at G1-S regulates cyclin E buildup and entry into S phase.', Proceedings of the National Academy of Sciences of the United States of America. National Academy of Sciences, 106(29), pp. 11960–5. doi: 10.1073/pnas.0904875106.

Moeller, B. J., Richardson, R. A. and Dewhirst, M. W. (2007) 'Hypoxia and radiotherapy: opportunities for improved outcomes in cancer treatment', Cancer and Metastasis Reviews. Kluwer Academic Publishers-Plenum Publishers, 26(2), pp. 241–248. doi: 10.1007/s10555-007-9056-0.

Moniz, S., Bandarra, D., Biddlestone, J., Campbell, K. J., Komander, D., *et al.* (2015) 'Cezanne regulates E2F1-dependent HIF2α expression.', Journal of cell science. Company of Biologists, 128(16), pp. 3082–93. doi: 10.1242/jcs.168864.

Moore, S. F., Hunter, R. W. and Hers, I. (2011) 'mTORC2 protein complex-mediated Akt (Protein Kinase B) Serine 473 Phosphorylation is not required for Akt1 activity in human platelets [corrected].', The Journal of biological chemistry. American Society for Biochemistry and Molecular Biology, 286(28), pp. 24553–60. doi: 10.1074/jbc.M110.202341.

Morrish, F. and Hockenbery, D. (2014) 'MYC and mitochondrial biogenesis.', Cold Spring Harbor perspectives in medicine. Cold Spring Harbor Laboratory Press, 4(5). doi: 10.1101/cshperspect. a014225.

Moser, S. C., Bensaddek, D., Ortmann, B., Maure, J.-F., Mudie, S., *et al.* (2013) 'PHD1 links cell-cycle progression to oxygen sensing through hydroxylation of the centrosomal protein Cep192.', Developmental cell. Elsevier, 26(4), pp. 381–92. doi: 10.1016/j.devcel.2013.06.014.

Muchnik, E. and Kaplan, J. (2011) 'HIF prolyl hydroxylase inhibitors for anemia', Expert Opinion on Investigational Drugs, 20(5), pp. 645–656. doi: 10.1517/13543784.2011.566861.

Muller, F. L., Liu, Y. and Van Remmen, H. (2004) 'Complex III releases superoxide to both sides of the inner mitochondrial membrane.', The Journal of biological chemistry. American Society for Biochemistry and Molecular Biology, 279(47), pp. 49064–73. doi: 10.1074/jbc.M407715200.

Mumaw, J. L., Schmiedt, C. W., Breidling, S., Sigmund, A., Norton, N. A., *et al.* (2015) 'Feline mesenchymal stem cells and supernatant inhibit reactive oxygen species production in cultured feline neutrophils'. doi: 10.1016/j.rvsc.2015.09.010.

Murphy, L. O. and Blenis, J. (2006) 'MAPK signal specificity: the right place at the right time', Trends in Biochemical Sciences, 31(5), pp. 268–275. doi: 10.1016/j.tibs.2006.03.009.

Murphy, M. P. (2009) 'How mitochondria produce reactive oxygen species.', The Biochemical journal. Portland Press Ltd, 417(1), pp. 1–13. doi: 10.1042/BJ20081386.

Myllyharju, J. and Kivirikko, K. I. (2004) 'Collagens, modifying enzymes and their mutations in humans, flies and worms', Trends in Genetics, 20(1), pp. 33–43. doi: 10.1016/j.tig.2003.11.004.

Natarajan, S. and Becker, D. (2012) 'Role of apoptosis-inducing factor, proline dehydrogenase, and NADPH oxidase in apoptosis and oxidative stress', Cell health and cytoskeleton. (4) pp: 11-27.

Nagel, S., Papadakis, M., Chen, R., Hoyte, L. C., Brooks, K. J., *et al.* (2011) 'Neuroprotection by Dimethyloxalylglycine following Permanent and Transient Focal Cerebral Ischemia in Rats', Journal of Cerebral Blood Flow & Metabolism, 31(1), pp. 132–143. doi: 10.1038/jcbfm.2010.60.

Najafi, R. and Sharifi, A. M. (2013) 'Deferoxamine preconditioning potentiates mesenchymal stem cell homing in vitro and in streptozotocin-diabetic rats', Expert Opinion on Biological Therapy, 13(7), pp. 959–972. doi: 10.1517/14712598.2013.782390.

Nakamura, T., Tu, S., Akhtar, W., Sunico, C. R., Okamoto, S.-I. *et al*. (no date) 'Aberrant Protein S-Nitrosylation in Neurodegenerative Diseases'. doi: 10.1016/j.neuron.2013.05.005.

Naranjo-Suarez, S., Carlson, B. A., Tsuji, P. A., Yoo, M.-H., Gladyshev, V. N. *et al.* (2012) 'HIF-Independent Regulation of Thioredoxin Reductase 1 Contributes to the High Levels of Reactive Oxygen Species Induced by Hypoxia', PLoS ONE. Edited by M. Koritzinsky. Public Library of Science, 7(2), p. e30470. doi: 10.1371/journal.pone.0030470.

Neitemeier, S., Jelinek, A., Laino, V., Hoffmann, L., Eisenbach, I., *et al.* (2017) 'BID links ferroptosis to mitochondrial cell death pathways', Redox Biology, 12, pp. 558–570. doi: 10.1016/j.redox.2017.03.007.

Nekanti, U., Dastidar, S., Venugopal, P., Totey, S. and Ta, M. (2010) 'Increased proliferation and analysis of differential gene expression in human Wharton's jelly-derived mesenchymal stromal cells under hypoxia.', International journal of biological sciences. Ivyspring International Publisher, 6(5), pp. 499–512. Available at: http://www.ncbi.nlm.nih.gov/pubmed/20877435 (Accessed: 26 July 2017).

Nery, A. A., Nascimento, I. C., Glaser, T., Bassaneze, V., Krieger, J. E. *et al.* (2013) 'Human mesenchymal stem cells: From immunophenotyping by flow cytometry to clinical applications', Cytometry Part A. Wiley Subscription Services, Inc., A Wiley Company, 83A(1), pp. 48–61. doi: 10.1002/cyto.a.22205.

Newsholme, P., Rebelato, E., Abdulkader, F., Krause, M., Carpinelli, A. *et al.* (2012) 'REVIEW Reactive oxygen and nitrogen species generation, antioxidant defenses, and b-cell function: a critical role for amino acids', Journal of Endocrinology, 214, pp. 11–20. doi: 10.1530/JOE-12-0072.

Nojima, H. (1997) 'Cell cycle checkpoints, chromosome stability and the progression of cancer.', Human cell, 10(4), pp. 221–30. Available at: http://www.ncbi.nlm.nih.gov/pubmed/9573481 (Accessed: 25 July 2017).

Obacz, J., Pastorekova, S., Vojtesek, B. and Hrstka, R. (2013) 'Cross-talk between HIF and p53 as mediators of molecular responses to physiological and genotoxic stresses', Molecular Cancer, 12(1), p. 93. doi: 10.1186/1476-4598-12-93.

Ockaili, R., Natarajan, R., Salloum, F., Fisher, B. J., Jones, D., *et al.* (2005) 'HIF-1 activation attenuates postischemic myocardial injury: role for heme oxygenase-1 in modulating microvascular chemokine generation', AJP: Heart and Circulatory Physiology, 289(2), pp. H542–H548. doi: 10.1152/ajpheart.00089.2005.

Oexle, H., Gnaiger, E. and Weiss, G. (1999) 'Iron-dependent changes in cellular energy metabolism: influence on citric acid cycle and oxidative phosphorylation.', Biochimica et biophysica acta, 1413(3), pp. 99–107. Available at: http://www.ncbi.nlm.nih.gov/pubmed/10556622 (Accessed: 3 July 2017).

Osellame, L. D. and Duchen, M. R. (2014) 'Quality control gone wrong: mitochondria, lysosomal storage disorders and neurodegeneration.', British journal of pharmacology. Wiley-Blackwell, 171(8), pp. 1958–72. doi: 10.1111/bph.12453.

Otera, H., Ishihara, N. and Mihara, K. (2013) 'New insights into the function and regulation of mitochondrial fission', Biochimica et Biophysica Acta (BBA) - Molecular Cell Research, 1833(5), pp. 1256–1268. doi: 10.1016/j.bbamcr.2013.02.002.

Owusu-Ansah, E., Yavari, A., Mandal, S. and Banerjee, U. (2008) 'Distinct mitochondrial retrograde signals control the G1-S cell cycle checkpoint', Nature Genetics. Nature Publishing Group, 40(3), pp. 356–361. doi: 10.1038/ng.2007.50.

Pagel-Langenickel, I., Bao, J., Joseph, J. J., Schwartz, D. R., Mantell, B. S., *et al.* (2008) 'PGC-1α Integrates Insulin Signaling, Mitochondrial Regulation, and Bioenergetic Function in Skeletal Muscle', Journal of Biological Chemistry, 283(33), pp. 22464–22472. doi: 10.1074/jbc.M800842200.

Papandreou, I., Cairns, R. A., Fontana, L., Lim, A. L. and Denko, N. C. (2006) 'HIF-1 mediates adaptation to hypoxia by actively downregulating mitochondrial oxygen consumption', Cell Metabolism, 3(3), pp. 187–197. doi: 10.1016/j.cmet.2006.01.012.

Papanicolaou, K. N., Ngoh, G. A., Dabkowski, E. R., O'Connell, K. A., Ribeiro, R. F., *et al.* (2012) 'Cardiomyocyte deletion of mitofusin-1 leads to mitochondrial fragmentation and improves tolerance to ROS-induced mitochondrial dysfunction and cell death.', American journal of physiology. Heart and circulatory physiology. American Physiological Society, 302(1), pp. H167-79. doi: 10.1152/ajpheart.00833.2011.

Paradkar, P. N., Zumbrennen, K. B., Paw, B. H., Ward, D. M. and Kaplan, J. (2009) 'Regulation of mitochondrial iron import through differential turnover of mitoferrin 1 and mitoferrin 2.', Molecular and cellular biology. American Society for Microbiology, 29(4), pp. 1007–16. doi: 10.1128/MCB.01685-08.

Park, M.-T., Choi, J.-A., Kim, M.-J., Um, H.-D., Bae, S., *et al.* (2003) 'Suppression of extracellular signal-related kinase and activation of p38 MAPK are two critical events leading to caspase-8- and mitochondria-mediated cell death in phytosphingosine-treated human cancer cells.', The Journal of biological chemistry. American Society for Biochemistry and Molecular Biology, 278(50), pp. 50624–34. doi: 10.1074/jbc.M309011200.

Parrish, A. B., Freel, C. D. and Kornbluth, S. (2013) 'Cellular mechanisms controlling caspase activation and function.', Cold Spring Harbor perspectives in biology. Cold Spring Harbor Laboratory Press, 5(6). doi: 10.1101/cshperspect. a008672.

Peng, Y.-J., Yuan, G., Khan, S., Nanduri, J., Makarenko, V. V, Reddy, V. D., Vasavda, C., Kumar, G. K., Semenza, G. L. and Prabhakar, N. R. (2014) 'Regulation of hypoxia-

inducible factor-α isoforms and redox state by carotid body neural activity in rats.', The Journal of physiology. Wiley-Blackwell, 592(17), pp. 3841–58. doi: 10.1113/jphysiol.2014.273789.

Pennock, S. and Wang, Z. (2003) 'Stimulation of cell proliferation by endosomal epidermal growth factor receptor as revealed through two distinct phases of signaling.', Molecular and cellular biology, 23(16), pp. 5803–15. Available at: http://www.ncbi.nlm.nih.gov/pubmed/12897150 (Accessed: 26 July 2017).

Perier, C. and Vila, M. (2012) 'Mitochondrial biology and Parkinson's disease.', Cold Spring Harbor perspectives in medicine. Cold Spring Harbor Laboratory Press, 2(2), p. a009332. doi: 10.1101/cshperspect. a009332.

Perrone-Bizzozero, N. I., Sower, A. C., Bird, E. D., Benowitz, L. I., Ivins, K. J. *et al.* (1996) 'Levels of the growth-associated protein GAP-43 are selectively increased in association cortices in schizophrenia.', Proceedings of the National Academy of Sciences of the United States of America. National Academy of Sciences, 93(24), pp. 14182–7. Available at: http://www.ncbi.nlm.nih.gov/pubmed/8943081 (Accessed: 23 April 2017).

Peterson, K. M., Aly, A., Lerman, A., Lerman, L. O. and Rodriguez-Porcel, M. (2011) 'Improved survival of mesenchymal stromal cell after hypoxia preconditioning: Role of oxidative stress', Life Sci. January, 3(8812), pp. 65–73. doi: 10.1016/j.lfs.2010.10.023.

Peurala, E., Koivunen, P., Bloigu, R., Haapasaari, K.-M. and Jukkola-Vuorinen, A. (2012) 'Expressions of individual PHDs associate with good prognostic factors and increased proliferation in breast cancer patients', Breast Cancer Research and Treatment. Springer US, 133(1), pp. 179–188. doi: 10.1007/s10549-011-1750-5.

Pfaff, E. and Klingenberg, M. (1968) 'Adenine Nucleotide Translocation of Mitochondria. 1. Specificity and Control', European Journal of Biochemistry. Blackwell Publishing Ltd, 6(1), pp. 66–79. doi: 10.1111/j.1432-1033.1968.tb00420.x.

Pfaller, R., Pfanners, N. and Neupert, W. (1989) 'THE JOURNAL OF BIOLOGICAL CHEMISTRY Mitochondrial Protein Import BYPASS OF PROTEINACEOUS SURFACE RECEPTORS CAN OCCUR WITH LOW SPECIFICITY AND EFFICIENCY*', 264(1), pp. 34–39. Available at: http://www.jbc.org/content/264/1/34.full.pdf (Accessed: 24 July 2017).

Phillips, N. R., Sprouse, M. L. and Roby, R. K. (2014) 'Simultaneous quantification of mitochondrial DNA copy number and deletion ratio: A multiplex real-time PCR assay'. doi: 10.1038/srep03887.

Ponting, C. P. and Aravind, L. (1997) 'PAS: a multifunctional domain family comes to light.', Current biology: CB, 7(11), pp. R674-7. Available at: http://www.ncbi.nlm.nih.gov/pubmed/9382818 (Accessed: 21 January 2017).

Pugazhenthi, S., Nesterova, A., Sable, C., Heidenreich, K. A., Boxer, L. M., *et al.* (2000) 'Akt/protein kinase B up-regulates Bcl-2 expression through cAMP-response element-binding protein.', The Journal of biological chemistry. American Society for Biochemistry and Molecular Biology, 275(15), pp. 10761–6. doi: 10.1074/JBC.275.15.10761.

Puigserver, P. and Spiegelman, B. M. (2003) 'Peroxisome Proliferator-Activated Receptor-γ Coactivator 1α (PGC-1α): Transcriptional Coactivator and Metabolic Regulator', Endocrine Reviews, 24(1), pp. 78–90. doi: 10.1210/er.2002-0012.

Puigserver, P., Wu, Z., Park, C. W., Graves, R., Wright, M. *et al.* (1998) 'A cold-inducible coactivator of nuclear receptors linked to adaptive thermogenesis.', Cell, 92(6), pp. 829–39. Available at: http://www.ncbi.nlm.nih.gov/pubmed/9529258 (Accessed: 24 July 2017).

Poyton RO, Ball KA, Castello PR. (2009) Mitochondrial generation of free radicals and hypoxic signaling. Trends Endocrinol Metab [Internet]. 2009 Sep [cited 2017 Aug 22];20(7):332–40. Available from: http://www.ncbi.nlm.nih.gov/pubmed/19733481

Rahal, A., Kumar, A., Singh, V., Yadav, B., Tiwari, R., *et al.* (2014) 'Oxidative stress, prooxidants, and antioxidants: the interplay.', BioMed research international. Hindawi Publishing Corporation, 2014, p. 761264. doi: 10.1155/2014/761264.

Rahman, K. (2007) 'Studies on free radicals, antioxidants, and co-factors.', Clinical interventions in aging. Dove Press, 2(2), pp. 219–36. Available at: http://www.ncbi.nlm.nih.gov/pubmed/18044138 (Accessed: 26 July 2017).

Rahtu-Korpela, L., Karsikas, S., Horkko, S., Blanco Sequeiros, R., Lammentausta, E., *et al*. (2014) 'HIF Prolyl 4-Hydroxylase-2 Inhibition Improves Glucose and Lipid Metabolism and Protects Against Obesity and Metabolic Dysfunction', Diabetes, 63(10), pp. 3324–3333. doi: 10.2337/db14-0472.

Ramos, T. L., Sánchez-Abarca, L. I., Muntión, S., Preciado, S., Puig, N., *et al*. (2016) 'MSC surface markers (CD44, CD73, and CD90) can identify human MSC-derived extracellular vesicles by conventional flow cytometry.', Cell communication and signaling: CCS. BioMed Central, 14, p. 2. doi: 10.1186/s12964-015-0124-8.

Rane, S., He, M., Sayed, D., Vashistha, H., Malhotra, A., *et al*. (2009) 'Downregulation of MiR-199a Derepresses Hypoxia-Inducible Factor-1 and Sirtuin 1 and Recapitulates Hypoxia Preconditioning in Cardiac Myocytes', Circulation Research, 104(7), pp. 879–886. doi: 10.1161/CIRCRESAHA.108.193102.

Ranera, B., Remacha, A. R., Álvarez-Arguedas, S., Romero, A., Vázquez, F. J., *et al*. (2012) 'Effect of hypoxia on equine mesenchymal stem cells derived from bone marrow and adipose tissue.', BMC veterinary research. BioMed Central, 8, p. 142. doi: 10.1186/1746-6148-8-142.

Raval, R. R., Lau, K. W., Tran, M. G. B., Sowter, H. M., Mandriota, S. J., *et al*. (2005) 'Contrasting properties of hypoxia-inducible factor 1 (HIF-1) and HIF-2 in von Hippel-Lindau-associated renal cell carcinoma.', Molecular and cellular biology. American Society for Microbiology, 25(13), pp. 5675–86. doi: 10.1128/MCB.25.13.5675-5686.2005.

Ravenna, L., Salvatori, L. and Russo, M. A. (2016) 'HIF3α: the little we know', FEBS Journal, 283(6), pp. 993–1003. doi: 10.1111/febs.13572.

Rhind, N. and Russell, P. (2012) 'Signaling pathways that regulate cell division.', Cold Spring Harbor perspectives in biology. Cold Spring Harbor Laboratory Press, 4(10), p. a005942. doi: 10.1101/cshperspect. a005942.

Richter, A., Sanford, K. K. and Evans, V. J. (1972) 'Influence of Oxygen and Culture Media on Plating Efficiency of Some Mammalian Tissue Cells', JNCI: Journal of the National Cancer Institute. Oxford University Press, 49(6), pp. 1705–1712. doi: 10.1093/jnci/49.6.1705.

Ripoli, M., D 'aprile, A., Quarato, G., Sarasin-Filipowicz, M., Gouttenoire, J., *et al*. (2010) 'Hepatitis C Virus-Linked Mitochondrial Dysfunction Promotes Hypoxia-Inducible Factor 1␣-Mediated Glycolytic Adaptation', JOURNAL OF VIROLOGY, 84(1), pp. 647–660. doi: 10.1128/JVI.00769-09.

ROBINSON-WHITE, A. and STRATAKIS, C. A. (2002) 'Protein Kinase A Signaling', Annals of the New York Academy of Sciences. Blackwell Publishing Ltd, 968(1), pp. 256–270. doi: 10.1111/j.1749-6632.2002. tb04340.x.

Rocheteau, P., Chatre, L., Briand, D., Mebarki, M., Jouvion, G., *et al*. (2015) 'ARTICLE Sepsis induces long-term metabolic and mitochondrial muscle stem cell dysfunction amenable by mesenchymal stem cell therapy', Nature Communications, 6. doi: 10.1038/ncomms10145.

Rodrigues, M., Turner, O., Stolz, D., Griffith, L. G. and Wells, A. (2012) 'Production of Reactive Oxygen Species by Multipotent Stromal Cells/Mesenchymal Stem Cells upon Exposure to Fas Ligand', Cell Transplantation, 21(10), pp. 2171–2187. doi: 10.3727/096368912X639035.

Rodrigues, M., Turner, O., Stolz, D., Griffith, L. G. and Wells, A. (2012) 'Production of reactive oxygen species by multipotent stromal cells/mesenchymal stem cells upon exposure to fas ligand.', Cell transplantation. NIH Public Access, 21(10), pp. 2171–87. doi: 10.3727/096368912X639035.

Rodríguez-Jiménez, F. J., Moreno-Manzano, V., Lucas-Dominguez, R. and Sánchez-Puelles, J.-M. (2008) 'Hypoxia Causes Downregulation of Mismatch Repair System and Genomic Instability in Stem Cells', Stem Cells. John Wiley & Sons, Ltd., 26(8), pp. 2052–2062. doi: 10.1634/stemcells.2007-1016.

Rossoll, W. and Bassell, G. J. (2009) 'Spinal Muscular Atrophy and a Model for Survival of Motor Neuron Protein Function in Axonal Ribonucleoprotein Complexes', in Results and problems in cell differentiation, pp. 87–107. doi: 10.1007/400_2009_4.

Rossow, P. W., Riddle, V. G. H. and Pardee, A. B. (1979) 'Synthesis of labile, serum-dependent protein in early G1 controls animal cell growth (3T3 cells/restriction point/cycloheximide/cell cycle/protein synthesis)', Cell Biology, 76(9), pp. 4446–4450. Available at: http://www.pnas.org/content/76/9/4446.full.pdf (Accessed: 25 July 2017).

Roy, M., Reddy, P. H., Iijima, M. and Sesaki, H. (2015) 'Mitochondrial division and fusion in metabolism.', Current opinion in cell biology. NIH Public Access, 33, pp. 111–8. doi: 10.1016/j.ceb.2015.02.001.

Ruthenborg, R. J., Ban, J.-J., Wazir, A., Takeda, N. and Kim, J.-W. (2014) 'Regulation of wound healing and fibrosis by hypoxia and hypoxia-inducible factor-1.', Molecules and cells. Korean Society for Molecular and Cellular Biology, 37(9), pp. 637–43. doi: 10.14348/molcells.2014.0150.

Sakamaki, T., Casimiro, M. C., Ju, X., Quong, A. A., Katiyar, S., *et al*. (2006) 'Cyclin D1 determines mitochondrial function in vivo.', Molecular and cellular biology. American Society for Microbiology (ASM), 26(14), pp. 5449–69. doi: 10.1128/MCB.02074-05.

Saqcena, M., Menon, D., Patel, D., Mukhopadhyay, S., Chow, V. *et al*. (2013) 'Amino acids and mTOR mediate distinct metabolic checkpoints in mammalian G1 cell cycle.', PloS one. Public Library of Science, 8(8), p. e74157. doi: 10.1371/journal.pone.0074157.

Saraswati, S., Guo, Y., Atkinson, J. and Young, P. P. (2015) 'Prolonged hypoxia induces monocarboxylate transporter-4 expression in mesenchymal stem cells resulting in a secretome that is deleterious to cardiovascular repair.', Stem cells (Dayton, Ohio). NIH Public Access, 33(4), pp. 1333–44. doi: 10.1002/stem.1935.

Sarbassov, D. D. (2005) 'Phosphorylation and Regulation of Akt/PKB by the Rictor-mTOR Complex', Science, 307(5712), pp. 1098–1101. doi: 10.1126/science.1106148.

Santore MT, McClintock DS, Lee VY, Budinger GRS, Chandel NS.(2002) Anoxia-induced apoptosis occurs through a mitochondria-dependent pathway in lung epithelial cells. Am J Physiol - Lung Cell Mol Physiol [Internet]. 2002 Apr 1 [cited 2017 Aug 22];282(4):L727–34. Available from: http://www.ncbi.nlm.nih.gov/pubmed/11880298

Scarpulla, R. C., Vega, R. B. and Kelly, D. P. (2012) 'Transcriptional integration of mitochondrial biogenesis.', Trends in endocrinology and metabolism: TEM. NIH Public Access, 23(9), pp. 459–66. doi: 10.1016/j.tem.2012.06.006.

Schneider, M., Van Geyte, K., Fraisl, P., Kiss, J., Aragonés, J., *et al*. (2010) 'Loss or Silencing of the PHD1 Prolyl Hydroxylase Protects Livers of Mice Against Ischemia/Reperfusion Injury', Gastroenterology, 138(3), p. 1143–1154.e2. doi: 10.1053/j.gastro.2009.09.057.

Schofield, C. J. and Ratcliffe, P. J. (2004) 'Oxygen sensing by HIF hydroxylases', Nature Reviews Molecular Cell Biology. Nature Publishing Group, 5(5), pp. 343–354. doi: 10.1038/nrm1366.

Schönenberger, M. J. and Kovacs, W. J. (2015) 'Hypoxia signaling pathways: modulators of oxygen-related organelles', Frontiers in Cell and Developmental Biology. Frontiers, 3, p. 42. doi: 10.3389/fcell.2015.00042.

Schröder, K., Wandzioch, K., Helmcke, I. and Brandes, R. P. (2009) 'Nox4 Acts as a Switch Between Differentiation and Proliferation in Preadipocytes', Arteriosclerosis, Thrombosis, and Vascular Biology, 29(2). Available at: http://atvb.ahajournals.org/content/29/2/239.long (Accessed: 11 April 2017).

Schroeter, H., Boyd, C. S., Ahmed, R., Spencer, J. P. E., Duncan, R. F., *et al*. (2003) 'c-Jun N-terminal kinase (JNK)-mediated modulation of brain mitochondria function: new target proteins for JNK signalling in mitochondrion-dependent apoptosis', Biochem. J, 372, pp. 359–369. Available at: https://www.ncbi.nlm.nih.gov/pmc/articles/PMC1223409/pdf/12614194.pdf (Accessed: 26 July 2017).

Schwartz, R. S., Eltzschig, H. K. and Carmeliet, P. (2011) 'Hypoxia and Inflammation', New England Journal of Medicine, 364(7), pp. 656–665. doi: 10.1056/NEJMra0910283.

Sclafani, R. A. and Holzen, T. M. (2007) 'Cell Cycle Regulation of DNA Replication', Annual Review of Genetics, 41(1), pp. 237–280. doi: 10.1146/annurev.genet.41.110306.130308.

Scortegagna, M., Ding, K., Oktay, Y., Gaur, A., Thurmond, F., *et al*. (2003) 'Multiple organ pathology, metabolic abnormalities and impaired homeostasis of reactive oxygen species in Epas1−/− mice', Nature Genetics. Nature Publishing Group, 35(4), pp. 331–340. doi: 10.1038/ng1266.

Scott, I. and Youle, R. J. (2010) 'Mitochondrial fission and fusion.', Essays in biochemistry. NIH Public Access, 47, pp. 85–98. doi: 10.1042/bse0470085.

Semenza, G. L. (1999) 'Regulation of Mammalian O 2 Homeostasis by Hypoxia-Inducible Factor 1', Annual Review of Cell and Developmental Biology, 15(1), pp. 551–578. doi: 10.1146/annurev.cellbio.15.1.551.

Semenza, G. L. (2000) 'HIF-1: mediator of physiological and pathophysiological responses to hypoxia', Journal of Applied Physiology, 88(4).

Semenza, G. L. (2007) 'HIF-1 mediates the Warburg effect in clear cell renal carcinoma', Journal of Bioenergetics and Biomembranes, 39(3), pp. 231–234. doi: 10.1007/s10863-007-9081-2.

Semenza, G. L. (2010) 'HIF-1: upstream and downstream of cancer metabolism', Current Opinion in Genetics & Development, 20(1), pp. 51–56. doi: 10.1016/j.gde.2009.10.009.

Semenza, G. L. and Prabhakar, N. R. (2007) 'HIF-1-dependent respiratory, cardiovascular, and redox responses to chronic intermittent hypoxia.', Antioxidants & redox signaling. Mary Ann Liebert Inc., 9(9), pp. 1391–6. doi: 10.1089/ars.2007.1691.

Semenza, G. L. and Prabhakar, N. R. (2012) 'The role of hypoxia-inducible factors in oxygen sensing by the carotid body.', Advances in experimental medicine and biology. NIH Public Access, 758, pp. 1–5. doi: 10.1007/978-94-007-4584-1_1.

Semenza, G. L., Roth, P. H., Fang, H. M. and Wang, G. L. (1994) 'Transcriptional regulation of genes encoding glycolytic enzymes by hypoxia-inducible factor 1.', The Journal of biological chemistry, 269(38), pp. 23757–63. Available at: http://www.ncbi.nlm.nih.gov/pubmed/8089148 (Accessed: 6 July 2017).

Semenza, G. L. and Wang, G. L. (1992) 'A nuclear factor induced by hypoxia via de novo protein synthesis binds to the human erythropoietin gene enhancer at a site required for transcriptional activation.', Molecular and cellular biology. American Society for Microbiology (ASM), 12(12), pp. 5447–54. Available at: http://www.ncbi.nlm.nih.gov/pubmed/1448077 (Accessed: 20 January 2017).

Sena, L. A. and Chandel, N. S. (2012) 'Physiological Roles of Mitochondrial Reactive Oxygen Species', Molecular Cell, 48(2), pp. 158–167. doi: 10.1016/j.molcel.2012.09.025.

Senetta, R., Stella, G., Pozzi, E., Sturli, N., Massi, D. *et al*. (2013) 'Caveolin-1 as a promoter of tumour spreading: when, how, where and why', Journal of Cellular and Molecular Medicine, 17(3), pp. 325–336. doi: 10.1111/jcmm.12030.

Sermeus, A. and Michiels, C. (2011) 'Reciprocal influence of the p53 and the hypoxic pathways', Cell Death and Disease. Nature Publishing Group, 2(5), p. e164. doi: 10.1038/cddis.2011.48.

Shalaby, S. M., El-Shal, A. S., Zidan, H. E., Mazen, N. F., Abd El-Haleem, M. R. *et al*. (2016) 'Comparing the effects of MSCs and CD34+ cell therapy in a rat model of myocardial infarction', IUBMB Life, 68(5), pp. 343–354. doi: 10.1002/iub.1487.

Shamas-Din, A., Kale, J., Leber, B. and Andrews, D. W. (2013) 'Mechanisms of action of Bcl-2 family proteins.', Cold Spring Harbor perspectives in biology. Cold Spring Harbor Laboratory Press, 5(4), p. a008714. doi: 10.1101/cshperspect. a008714.

Sharma, P., Jha, A. B., Dubey, R. S. and Pessarakli, M. (2012) 'Reactive Oxygen Species, Oxidative Damage, and Antioxidative Defense Mechanism in Plants under Stressful Conditions', Journal of Botany. Hindawi, 2012, pp. 1–26. doi: 10.1155/2012/217037.

Sasaki, S. (2010) Determination of Altered Mitochondria Ultrastructure by Electron Microscopy. In Humana Press, Totowa, NJ, pp. 279–290. Available at: http://link.springer.com/10.1007/978-1-60761-756-3_19.

Shay, J. W., Pierceli, D. J. and Werbin, H. (1991) 'Mitochondrial DNA Copy Number Is Proportional to Total Cell DNA under a Variety of Growth Conditions*', THE

JOURNAL. OF BIOLOGICAL CHEMISTRY, 265(25), pp. 14802–14807. Available at: http://www.jbc.org/content/265/25/14802.full.pdf (Accessed: 29 May 2017).

Sheftel, A. D. and Lill, R. (2009) 'The power plant of the cell is also a smithy: The emerging role of mitochondria in cellular iron homeostasis', Annals of Medicine, 41(2), pp. 82–99. doi: 10.1080/07853890802322229.

Sheng, Z.-H. and Cai, Q. (2012) 'Mitochondrial transport in neurons: impact on synaptic homeostasis and neurodegeneration', Nature Reviews Neuroscience. Nature Publishing Group, 13(2), p. 77. doi: 10.1038/nrn3156.

Shi, D. and Gu, W. (2012) 'Dual Roles of MDM2 in the Regulation of p53: Ubiquitination Dependent and Ubiquitination Independent Mechanisms of MDM2 Repression of p53 Activity.', Genes & cancer. Impact Journals, LLC, 3(3–4), pp. 240–8. doi: 10.1177/1947601912455199.

Shi, D., Liao, L., Zhang, B., Liu, R., Dou, X., Li, J., Zhu, X., Yu, L., Chen, D. and Zhao, R. C. H. (2011) 'Human adipose tissue−derived mesenchymal stem cells facilitate the immunosuppressive effect of cyclosporin A on T lymphocytes through Jagged-1−mediated inhibition of NF-κB signaling', Experimental Hematology, 39(2), p. 214–224.e1. doi: 10.1016/j.exphem.2010.10.009.

Shoag, J. and Arany, Z. (2010) 'Regulation of Hypoxia-Inducible Genes by PGC-1', Arteriosclerosis, Thrombosis, and Vascular Biology, 30(4), pp. 662–666. doi: 10.1161/ATVBAHA.108.181636.

Shoubridge, E. A. and Wai, T. (2007) 'Mitochondrial DNA and the Mammalian Oocyte', in Current topics in developmental biology, pp. 87–111. doi: 10.1016/S0070-2153(06)77004-1.

Simon, M. C. and Keith, B. (2008) 'The role of oxygen availability in embryonic development and stem cell function', Nature Reviews Molecular Cell Biology. Nature Publishing Group, 9(4), pp. 285–296. doi: 10.1038/nrm2354.

Simsek, T., Kocabas, F., Zheng, J., Deberardinis, R. J., Mahmoud, A. I., *et al.* (2010) 'The distinct metabolic profile of hematopoietic stem cells reflects their location in a hypoxic niche.', Cell stem cell. NIH Public Access, 7(3), pp. 380–90. doi: 10.1016/j.stem.2010.07.011.

Skroblin, P., Grossmann, S., Schäfer, G., Rosenthal, W. and Klussmann, E. (2010) 'Mechanisms of Protein Kinase A Anchoring', in, pp. 235–330. doi: 10.1016/S1937-6448(10)83005-9.

Snell, C. E., Turley, H., McIntyre, A., Li, D., Masiero, M., *et al.* (2014) 'Proline-Hydroxylated Hypoxia-Inducible Factor 1α (HIF-1α) Upregulation in Human Tumours', PLoS ONE. Edited by S. A. Aziz. Public Library of Science, 9(2), p. e88955. doi: 10.1371/journal.pone.0088955.

Sohni, A. and Verfaillie, C. M. (2013) 'Mesenchymal stem cells migration homing and tracking.', Stem cells international. Hindawi, 2013, p. 130763. doi: 10.1155/2013/130763.

Solaini, G., Baracca, A., Lenaz, G. and Sgarbi, G. (2010) 'Hypoxia and mitochondrial oxidative metabolism', BBA - Bioenergetics, 1797, pp. 1171–1177. doi: 10.1016/j.bbabio.2010.02.011.

Spees, J. L., Lee, R. H. and Gregory, C. A. (no date) 'Mechanisms of mesenchymal stem/stromal cell function'. doi: 10.1186/s13287-016-0363-7.

Spencer, J. A., Ferraro, F., Roussakis, E., Klein, A., Wu, J., *et al.* (2014) 'Direct measurement of local oxygen concentration in the bone marrow of live animals', Nature, 508(7495), pp. 269–273. doi: 10.1038/nature13034.

Stein LR and Imai S. (2012) The dynamic regulation of NAD metabolism in mitochondria. Trends Endocrinol Metab [Internet]. 2012 Sep [cited 2017 Aug 29];23(9):420–8. Available from: http://www.ncbi.nlm.nih.gov/pubmed/22819213.

Steinberg, S. F. (2008) 'Structural Basis of Protein Kinase C Isoform Function', Physiological Reviews, 88(4), pp. 1341–1378. doi: 10.1152/physrev.00034.2007.

Su, Y., Loos, M., Giese, N., Metzen, E., Büchler, M. W., *et al.* (2012) 'Prolyl hydroxylase-2 (PHD2) exerts tumor-suppressive activity in pancreatic cancer', Cancer, 118(4), pp. 960–972. doi: 10.1002/cncr.26344.

Suen, D.-F., Norris, K. L. and Youle, R. J. (2008) 'Mitochondrial dynamics and apoptosis.', Genes & development. Cold Spring Harbor Laboratory Press, 22(12), pp. 1577–90. doi: 10.1101/gad.1658508.

Sun, Q., Chen, X., Ma, J., Peng, H., Wang, F., *et al.* (2011) 'Mammalian target of rapamycin up-regulation of pyruvate kinase isoenzyme type M2 is critical for aerobic glycolysis and tumor growth.', Proceedings of the National Academy of Sciences of the United States of America. National Academy of Sciences, 108(10), pp. 4129–34. doi: 10.1073/pnas.1014769108.

Swietach, P., Vaughan-Jones, R. D. and Harris, A. L. (2007) 'Regulation of tumor pH and the role of carbonic anhydrase 9', Cancer and Metastasis Reviews. Kluwer Academic Publishers-Plenum Publishers, 26(2), pp. 299–310. doi: 10.1007/s10555-007-9064-0.

Taanman, J.-W. (1999) 'The mitochondrial genome: structure, transcription, translation and replication', Biochimica et Biophysica Acta (BBA) - Bioenergetics, 1410(2), pp. 103–123. doi: 10.1016/S0005-2728(98)00161-3.

Tai, T. C., Wong-Faull, D. C., Claycomb, R. and Wong, D. L. (2009) 'Hypoxic stress-induced changes in adrenergic function: role ï¿½ of HIF1α', Journal of Neurochemistry. Blackwell Publishing Ltd, 109(2), pp. 513–524. doi: 10.1111/j.1471-4159.2009.05978.x.

Tait, S. W. G. and Green, D. R. (2012) 'Mitochondria and cell signalling.', Journal of cell science. Company of Biologists, 125(Pt 4), pp. 807–15. doi: 10.1242/jcs.099234.

Takeda, K., Ho, V. C., Takeda, H., Duan, L.-J., Nagy, A. *et al.* (2006) 'Placental but not heart defects are associated with elevated hypoxia-inducible factor alpha levels in mice lacking prolyl hydroxylase domain protein 2.', Molecular and cellular biology. American Society for Microbiology, 26(22), pp. 8336–46. doi: 10.1128/MCB.00425-06.

Tamama, K., Kawasaki, H., Kerpedjieva, S. S., Guan, J., Ganju, R. K. *et al.* (2011) 'Differential roles of hypoxia inducible factor subunits in multipotential stromal cells under hypoxic condition', Journal of Cellular Biochemistry. Wiley Subscription Services, Inc., A Wiley Company, 112(3), pp. 804–817. doi: 10.1002/jcb.22961.

Tang, S., Halberg, M. C., Floyd, K. C. and Wang, J. (2012) 'Analysis of Common Mitochondrial DNA Mutations by Allele-Specific Oligonucleotide and Southern Blot Hybridization', in Methods in molecular biology (Clifton, N.J.), pp. 259–279. doi: 10.1007/978-1-61779-504-6_18.

Teixeira, F. G., Panchalingam, K. M., Anjo, S. I., Manadas, B., *et al.* (2015) 'Do hypoxia/normoxia culturing conditions change the neuroregulatory profile of Wharton Jelly mesenchymal stem cell secretome?', Stem Cell Research & Therapy. BioMed Central, 6(1), p. 133. doi: 10.1186/s13287-015-0124-z.

Theus, M. H., Wei, L., Cui, L., Francis, K., Hu, X., *et al.* (2008) 'In vitro hypoxic preconditioning of embryonic stem cells as a strategy of promoting cell survival and functional benefits after transplantation into the ischemic rat brain', Experimental Neurology, 210(2), pp. 656–670. doi: 10.1016/j.expneurol.2007.12.020.

Thoms, H. C., Dunlop, M. G. and Stark, L. A. (2007) 'p38-Mediated Inactivation of Cyclin D1/Cyclin-Dependent Kinase 4 Stimulates Nucleolar Translocation of RelA and Apoptosis in Colorectal Cancer Cells', Cancer Res, 67(4), pp. 1660–9. doi: 10.1158/0008-5472.CAN-06-1038.

Thorburn, D. R. and Rahman, S. (1993) Mitochondrial DNA-Associated Leigh Syndrome and NARP, University of Washington, Seattle. Available at: http://www.ncbi.nlm .nih.gov/pubmed/20301352

Tian, H., McKnight, S. L. and Russell, D. W. (1997) 'Endothelial PAS domain protein 1 (EPAS1), a transcription factor selectively expressed in endothelial cells.', Genes & development. Cold Spring Harbor Laboratory Press, 11(1), pp. 72–82. doi: 10.1101/GAD.11.1.72.

Toffoli, S. and Michiels, C. (2008) 'Intermittent hypoxia is a key regulator of cancer cell and endothelial cell interplay in tumours', FEBS Journal. Blackwell Publishing Ltd, 275(12), pp. 2991–3002. doi: 10.1111/j.1742-4658.2008.06454.x.

Trinei, M., Berniakovich, I., Pelicci, P. G. and Giorgio, M. (2006) 'Mitochondrial DNA copy number is regulated by cellular proliferation: A role for Ras and p66Shc', Biochimica et Biophysica Acta (BBA) - Bioenergetics, 1757(5), pp. 624–630. doi: 10.1016/j.bbabio.2006.05.029.

Tsukihara, T., Aoyama, H., Yamashita, E., Tomizaki, T., Yamaguchi, H., *et al.* (1996) 'The whole structure of the 13-subunit oxidized cytochrome c oxidase at 2.8 A.', Science (New York, N.Y.), 272(5265), pp. 1136–44. Available at: http://www.ncbi.nlm.nih.gov/pubmed/8638158 (Accessed: 25 July 2017).

Ullah, I., Subbarao, R. B. and Rho, G. J. (2015) 'Human mesenchymal stem cells - current trends and future prospective.', Bioscience reports. Portland Press Ltd, 35(2). doi: 10.1042/BSR20150025.

Uttara, B., Singh, A. V, Zamboni, P. and Mahajan, R. T. (2009) 'Oxidative stress and neurodegenerative diseases: a review of upstream and downstream antioxidant therapeutic options.', Current neuropharmacology. Bentham Science Publishers, 7(1), pp. 65–74. doi: 10.2174/157015909787602823.

Valero, T. (2014) 'Mitochondrial biogenesis: pharmacological approaches.', Current pharmaceutical design, 20(35), pp. 5507–9. Available at: http://www.ncbi.nlm.nih.gov/pubmed/24606795 (Accessed: 25 July 2017).

Valko, M., Leibfritz, D., Moncol, J., Cronin, M. T. D., Mazur, M. *et al.* (2007) 'Free radicals and antioxidants in normal physiological functions and human disease', The International Journal of Biochemistry & Cell Biology, 39(1), pp. 44–84. doi: 10.1016/j.biocel.2006.07.001.

Valle-Prieto, A. and Conget, P. A. (2010) 'Human Mesenchymal Stem Cells Efficiently Manage Oxidative Stress', Stem Cells and Development. Mary Ann Liebert, Inc.

140 Huguenot Street, 3rd Floor New Rochelle, NY 10801 USA, 19(12), pp. 1885–1893. doi: 10.1089/scd.2010.0093.

Van der Bliek, A., Shen, Q., Kawajiri S. (2013) 'Mechanisms of Mitochondrial Fission and Fusion', Cold Spring Harb Perspect Biol., 5(6), a011072. doi: 10.1101/cshperspect.a011072

Vanhorebeek, I., De Vos, R., Mesotten, D., Wouters, P. J., De Wolf-Peeters, C. *et al.* (2005) 'Protection of hepatocyte mitochondrial ultrastructure and function by strict blood glucose control with insulin in critically ill patients', The Lancet, 365(9453), pp. 53–59. doi: 10.1016/S0140-6736(04)17665-4.

Vasandan, A. B., Jahnavi, S., Shashank, C., Prasad, P., Kumar, A. *et al.* (2016) 'Human Mesenchymal stem cells program macrophage plasticity by altering their metabolic status via a PGE 2 -dependent mechanism'. doi: 10.1038/srep38308.

Vaux, E. C., Metzen, E., Yeates, K. M. and Ratcliffe, P. J. (2001) 'Regulation of hypoxia-inducible factor is preserved in the absence of a functioning mitochondrial respiratory chain', Blood, 98(2). Available at: http://www.bloodjournal.org/content/98/2/296?sso-checked=true (Accessed: 27 July 2017).

Velletri, T., Xie, N., Wang, Y., Huang, Y., Yang, Q., *et al.* (2016) 'P53 functional abnormality in mesenchymal stem cells promotes osteosarcoma development', Cell Death and Disease. Nature Publishing Group, 7(1), p. e2015. doi: 10.1038/cddis.2015.367.

Viollet, B., Guigas, B., Leclerc, J., Hébrard, S., Lantier, L., *et al.* (2009) 'AMP-activated protein kinase in the regulation of hepatic energy metabolism: from physiology to therapeutic perspectives', Acta Physiologica. Blackwell Publishing Ltd, 196(1), pp. 81–98. doi: 10.1111/j.1748-1716.2009.01970.x.

Wanet, A., Arnould, T., Najimi, M. and Renard, P. (2015) 'Connecting Mitochondria, Metabolism, and Stem Cell Fate.', Stem cells and development. Mary Ann Liebert, Inc., 24(17), pp. 1957–71. doi: 10.1089/scd.2015.0117.

Wang, C., Li, Z., Lu, Y., Du, R., Katiyar, S., *et al.* (2006) 'Cyclin D1 repression of nuclear respiratory factor 1 integrates nuclear DNA synthesis and mitochondrial function.', Proceedings of the National Academy of Sciences of the United States of America. National Academy of Sciences, 103(31), pp. 11567–72. doi: 10.1073/pnas.0603363103.

Wang, H.-J., Hsieh, Y.-J., Cheng, W.-C., Lin, C.-P., Lin, Y., *et al.* (2014) 'JMJD5 regulates PKM2 nuclear translocation and reprograms HIF-1α-mediated glucose metabolism.', Proceedings of the National Academy of Sciences of the United States of America. National Academy of Sciences, 111(1), pp. 279–84. doi: 10.1073/pnas.1311249111.

Wang, J. and Pantopoulos, K. (2011) 'Regulation of cellular iron metabolism.', The Biochemical journal. Portland Press Ltd, 434(3), pp. 365–81. doi: 10.1042/BJ20101825.

Wang, L., Gu, Z., Zhao, X., Yang, N., Wang, F., *et al.* (2016) 'Extracellular Vesicles Released from Human Umbilical Cord-Derived Mesenchymal Stromal Cells Prevent Life-Threatening Acute Graft-Versus-Host Disease in a Mouse Model of Allogeneic Hematopoietic Stem Cell Transplantation', Stem Cells and Development. Mary Ann Liebert, Inc. 140 Huguenot Street, 3rd Floor New Rochelle, NY 10801 USA , 25(24), pp. 1874–1883. doi: 10.1089/scd.2016.0107.

Warnecke, C., Griethe, W., Weidemann, A., Jurgensen, J. S., Willam, C., *et al.* (2003) 'Activation of the hypoxia-inducible factor pathway and stimulation of angiogenesis by application of prolyl hydroxylase inhibitors', The FASEB Journal, 17(9), pp. 1186–8. doi: 10.1096/fj.02-1062fje.

Warnecke, C., Weidemann, A., Volke, M., Schietke, R., Wu, X., *et al.* (2008) 'The specific contribution of hypoxia-inducible factor-2α to hypoxic gene expression in vitro is limited and modulated by cell type-specific and exogenous factors'. doi: 10.1016/j.yexcr.2008.03.003.

Wartenberg, M., Ling, F. C., Müschen, M., Klein, F., Acker, H., *et al.* (2003) 'Regulation of the multidrug resistance transporter P-glycoprotein in multicellular tumor spheroids by hypoxia-inducible factor-1 and reactive oxygen species', The FASEB Journal, 17(3), pp. 503–5. doi: 10.1096/fj.02-0358fje.

Watt, I. N., Montgomery, M. G., Runswick, M. J., Leslie, A. G. W. and Walker, J. E. (2010) 'Bioenergetic cost of making an adenosine triphosphate molecule in animal mitochondria.', Proceedings of the National Academy of Sciences of the United States of America. National Academy of Sciences, 107(39), pp. 16823–7. doi: 10.1073/pnas.1011099107.

Webster, K. A. (2012) 'Mitochondrial membrane permeabilization and cell death during myocardial infarction: roles of calcium and reactive oxygen species.', Future cardiology. NIH Public Access, 8(6), pp. 863–84. doi: 10.2217/fca.12.58.

Wei, Q., Bian, Y., Yu, F., Zhang, Q., Zhang, G., *et al.* (2016) 'Chronic intermittent hypoxia induces cardiac inflammation and dysfunction in a rat obstructive sleep apnea model.', Journal of biomedical research. Education Department of Jiangsu Province, 30(6), pp. 490–495. doi: 10.7555/JBR.30.20160110.

Werth, N., Beerlage, C., Rosenberger, C., Yazdi, A. S., Edelmann, M., *et al.* (2010) 'Activation of Hypoxia Inducible Factor 1 Is a General Phenomenon in Infections with Human Pathogens'. doi: 10.1371/journal.pone.0011576.

Westphal, D., Dewson, G., Czabotar, P. E. and Kluck, R. M. (2011) 'Molecular biology of Bax and Bak activation and action', Biochimica et Biophysica Acta (BBA) - Molecular Cell Research, 1813(4), pp. 521–531. doi: 10.1016/j.bbamcr.2010.12.019.

Wheaton, W. W. and Chandel, N. S. (2011) 'Hypoxia. 2. Hypoxia regulates cellular metabolism', AJP: Cell Physiology, 300(3), pp. C385–C393. doi: 10.1152/ajpcell.00485.2010.

Widowati, W., Wijaya, L., Murti, H., Widyastuti, H., Agustina, D., *et al.* (2015) 'Conditioned medium from normoxia (WJMSCs-norCM) and hypoxia-treated WJMSCs (WJMSCs-hypoCM) in inhibiting cancer cell proliferation', Biomarkers and Genomic Medicine, 7(1), pp. 8–17. doi: 10.1016/j.bgm.2014.08.008.

Wiesener, M. S., Turley, H., Allen, W. E., Willam, C., Eckardt, K.-U., *et al.* (1998) 'Induction of Endothelial PAS Domain Protein-1 by Hypoxia: Characterization and Comparison With Hypoxia-Inducible Factor-1α', Blood, 92(7).

Wigerup, C., Påhlman, S. and Bexell, D. (2016) 'Therapeutic targeting of hypoxia and hypoxia-inducible factors in cancer', Pharmacology & Therapeutics, 164, pp. 152–169. doi: 10.1016/j.pharmthera.2016.04.009.

Williams, A. R. and Hare, J. M. (2011) 'Mesenchymal stem cells: biology, pathophysiology, translational findings, and therapeutic implications for cardiac disease.', Circulation research, 109(8), pp. 923–40. doi: 10.1161/CIRCRESAHA.111.243147.

Willis, S. N., Fletcher, J. I., Kaufmann, T., van Delft, M. F., Chen, L., *et al.* (2007) 'Apoptosis Initiated When BH3 Ligands Engage Multiple Bcl-2 Homologs, Not Bax or Bak', Science, 315(5813). Available at: http://science.sciencemag.org/content/315/5813/856 (Accessed: 25 July 2017).

Wiltshire, C., Gillespie, D. A. F. and May, G. H. W. (2004) 'Sab (SH3BP5), a novel mitochondria-localized JNK-interacting protein', Biochemical Society Transactions, 32(6), pp. 1075–1077. doi: 10.1042/BST0321075.

Wu, Y., Lin, J. C., Piluso, L. G., Dhahbi, J. M., Bobadilla, S., *et al.* (2014) 'Phosphorylation of p53 by TAF1 inactivates p53-dependent transcription in the DNA damage response.', Molecular cell. NIH Public Access, 53(1), pp. 63–74. doi: 10.1016/j.molcel.2013.10.031.

Xicoy, H., Wieringa, B. and Martens, G. J. M. (2017) 'The SH-SY5Y cell line in Parkinson's disease research: a systematic review', Molecular Neurodegeneration, 12(1), p. 10. doi: 10.1186/s13024-017-0149-0.

Xu, E., Sun, W., Gu, J., Chow, W.-H., Ajani, J. A. *et al.* (2013) 'Association of mitochondrial DNA copy number in peripheral blood leukocytes with risk of esophageal adenocarcinoma', Carcinogenesis, 34(11), pp. 2521–2524. doi: 10.1093/carcin/bgt230.

Xu, L., Huang, J., Deng, F., Wang, L., Xiang, X.-R., *et al.* (2011) 'Effects of Hypoxia on Mesenchymal Stem Sells Hypoxia Induces Osteogenesis-Related Activities and Expression of Core Binding Factor α1 in Mesenchymal Stem Cells', Tohoku J. Exp. Med, pp. 7–12. doi: 10.1620/tjem.224.7.

Yamamoto, T., Ebisuya, M., Ashida, F., Okamoto, K., Yonehara, S. *et al.* (2006) 'Continuous ERK Activation Downregulates Antiproliferative Genes throughout G1 Phase to Allow Cell-Cycle Progression', Current Biology, 16(12), pp. 1171–1182. doi: 10.1016/j.cub.2006.04.044.

Yang, D.-C., Tsai, C.-C., Liao, Y.-F., Fu, H.-C., Tsay, H.-J., *et al.* (2011) 'Twist controls skeletal development and dorsoventral patterning by regulating runx2 in zebrafish.', PloS one. Public Library of Science, 6(11), p. e27324. doi: 10.1371/journal.pone.0027324.

Yang, H., Mu, J., Chen, L., Feng, J., Hu, J., *et al.* (2015) 'S-nitrosylation positively regulates ascorbate peroxidase activity during plant stress responses.', Plant physiology. American Society of Plant Biologists, 167(4), pp. 1604–15. doi: 10.1104/pp.114.255216.

Yang, W.-W., Shu, B., Zhu, Y. and Yang, H.-T. (2008) 'E2F6 inhibits cobalt chloride-mimetic hypoxia-induced apoptosis through E2F1.', Molecular biology of the cell. American Society for Cell Biology, 19(9), pp. 3691–700. doi: 10.1091/mbc.E08-02-0171.

Yao, L.-M., He, J.-P., Chen, H.-Z., Wang, Y., Wang, W.-J., *et al*. (2012) 'Orphan receptor TR3 participates in cisplatin-induced apoptosis via Chk2 phosphorylation to repress intestinal tumorigenesis', Carcinogenesis, 33(2), pp. 301–311. doi: 10.1093/carcin/bgr287.

Yousefifard, M., Nasirinezhad, F., Manaheji, H. S., Janzadeh, A., Hosseini, M. *et al*. (2016) 'Human bone marrow-derived and umbilical cord-derived mesenchymal stem cells for alleviating neuropathic pain in a spinal cord injury model'. doi: 10.1186/s13287-016-0295-2.

Yu, W., Sanders, B. G. and Kline, K. (2003) 'RRR-alpha-tocopheryl succinate-induced apoptosis of human breast cancer cells involves Bax translocation to mitochondria.', Cancer research, 63(10), pp. 2483–91. Available at: http://www.ncbi.nlm.nih.gov/pubmed/12750270 (Accessed: 26 July 2017).

Yuan, G., Khan, S. A., Luo, W., Nanduri, J., Semenza, G. L. *et al*. (2011) 'Hypoxia-inducible factor 1 mediates increased expression of NADPH oxidase-2 in response to intermittent hypoxia.', Journal of cellular physiology. NIH Public Access, 226(11), pp. 2925–33. doi: 10.1002/jcp.22640.

Yuan, Q., Bleiziffer, O., Boos, A. M., Sun, J., Brandl, A., *et al*. (2014) 'PHDs inhibitor DMOG promotes the vascularization process in the AV loop by HIF-1a up-regulation and the preliminary discussion on its kinetics in rat.', BMC biotechnology. BioMed Central, 14, p. 112. doi: 10.1186/s12896-014-0112-x.

Yung, H. W. and Tolkovsky, A. M. (2003) 'Erasure of kinase phosphorylation in astrocytes during oxygen-glucose deprivation is controlled by ATP levels and activation of phosphatases', Journal of Neurochemistry. Blackwell Science Ltd, 86(5), pp. 1281–1288. doi: 10.1046/j.1471-4159.2003.01946.x.

Zeng, H.-L., Zhong, Q., Qin, Y.-L., Bu, Q.-Q., Han, X.-A., *et al*. (2011) 'Hypoxia-mimetic agents inhibit proliferation and alter the morphology of human umbilical cord-derived mesenchymal stem cells'. doi: 10.1186/1471-2121-12-32.

Zeno, S., Veenman, L., Katz, Y., Bode, J., Gavish, M. *et al*. (2012) 'The 18 kDa Mitochondrial Translocator Protein (TSPO) Prevents Accumulation of Protoporphyrin IX. Involvement of Reactive Oxygen Species (ROS)', Current Molecular Medicine, 12(4), pp. 494–501. doi: 10.2174/156652412800163424.

Zetterberg, A., Larsson, O. and Wiman, K. G. (1995) 'What is the restriction point?', Current opinion in cell biology, 7(6), pp. 835–42. Available at: http://www.ncbi.nlm.nih.gov/pubmed/8608014 (Accessed: 25 July 2017).

Zhang, J., Huang, X., Wang, H., Liu, X., Zhang, T., *et al*. (2015) 'The challenges and promises of allogeneic mesenchymal stem cells for use as a cell-based therapy.', Stem cell research & therapy. BioMed Central, 6, p. 234. doi: 10.1186/s13287-015-0240-9.

Zhang, N., Fu, Z., Linke, S., Chicher, J., Gorman, J. J., *et al*. (2011) 'essential regulator of metabolism', 11(5), pp. 364–378. doi: 10.1016/j.cmet.2010.03.001.

Zhang, T., Shen, S., Qu, J., Correspondence, S. G. and Ghaemmaghami, S. (2016) 'Global Analysis of Cellular Protein Flux Quantifies the Selectivity of Basal Autophagy', Cell Reports, 14, pp. 2426–2439. doi: 10.1016/j.celrep.2016.02.040.

Zhang, X., Qin, J., Zou, J., Lv, Z., Tan, B., *et al*. (2016) 'Extracellular ADP facilitates monocyte recruitment in bacterial infection via ERK signaling', Cellular & Molecular Immunology. Nature Publishing Group. doi: 10.1038/cmi.2016.56.

Zhang, X., Tang, N., Hadden, T. J. and Rishi, A. K. (2011) 'Akt, FoxO and regulation of apoptosis', Biochimica et Biophysica Acta (BBA) - Molecular Cell Research, 1813(11), pp. 1978–1986. doi: 10.1016/j.bbamcr.2011.03.010.

Zhang, Y., Zhai, W., Zhao, M., Li, D., Chai, X., *et al*. (2015) 'Effects of Iron Overload on the Bone Marrow Microenvironment in Mice', PLOS ONE. Edited by E. Mezey. Public Library of Science, 10(3), p. e0120219. doi: 10.1371/journal.pone.0120219.

Zhang, Z., Lotti, F., Dittmar, K., Younis, I., Wan, L., *et al*. (2008) 'SMN deficiency causes tissue-specific perturbations in the repertoire of snRNAs and widespread defects in

splicing.', Cell. Howard Hughes Medical Institute, 133(4), pp. 585–600. doi: 10.1016/j.cell.2008.03.031.

Zhang, Z., Yang, M., Wang, Y., Wang, L., Jin, Z., *et al*. (2016) 'Autophagy regulates the apoptosis of bone marrow-derived mesenchymal stem cells under hypoxic condition via AMP-activated protein kinase/mammalian target of rapamycin pathway', Cell Biology International, 40(6), pp. 671–685. doi: 10.1002/cbin.10604.

Zheng, H., Nong, Z. and Lu, G. (2015) 'Correlation Between Nuclear Factor E2-Related Factor 2 Expression and Gastric Cancer Progression.', Medical science monitor: international medical journal of experimental and clinical research. International Scientific Literature, Inc., 21, pp. 2893–9. doi: 10.12659/MSM.894467.

Zhong, H., De Marzo, A. M., Laughner, E., Lim, M., Hilton, D. A., *et al*. (1999) 'Overexpression of hypoxia-inducible factor 1alpha in common human cancers and their metastases.', Cancer research, 59(22), pp. 5830–5. doi: 10.1016/s0968-0004(98)01344-9.

Zhou, D., Shao, L. and Spitz, D. R. (2014) 'Reactive oxygen species in normal and tumor stem cells.', Advances in cancer research. NIH Public Access, 122, pp. 1–67. doi: 10.1016/B978-0-12-420117-0.00001-3.

Zhou, F., Yang, Y. and Xing, D. (2011) 'Bcl-2 and Bcl-xL play important roles in the crosstalk between autophagy and apoptosis', FEBS Journal. Blackwell Publishing Ltd, 278(3), pp. 403–413. doi: 10.1111/j.1742-4658.2010.07965.x.

Zhu, W., Chen, J., Cong, X., Hu, S. and Chen, X. (2006) 'Hypoxia and Serum Deprivation-Induced Apoptosis in Mesenchymal Stem Cells', Stem Cells, 24(2), pp. 416–425. doi: 10.1634/stemcells.2005-0121.

Zhulin, I. B., Taylor, B. L. and Dixon, R. (1997) 'PAS domain S-boxes in Archaea, Bacteria and sensors for oxygen and redox.', Trends in biochemical sciences, 22(9), pp. 331–3. Available at: http://www.ncbi.nlm.nih.gov/pubmed/9301332 (Accessed: 20 January 2017).

Zorov, D. B., Juhaszova, M. and Sollott, S. J. (2014) 'Mitochondrial reactive oxygen species (ROS) and ROS-induced ROS release.', Physiological reviews. American Physiological Society, 94(3), pp. 909–50. doi: 10.1152/physrev.00026.2013.

Zorzano, A. and Claret, M. (2015) 'Implications of mitochondrial dynamics on neurodegeneration and on hypothalamic dysfunction.', Frontiers in aging neuroscience. Frontiers Media SA, 7, p. 101. doi: 10.3389/fnagi.2015.00101.